Synthesis and Characterisation of Novel Aryl Carbazole Based Conjugated Polymers for Applications in Electroluminescent Devices

Thesis Submitted for The Degree of Doctor of Philosophy

April 2007

Akbar Kulasi

The Department of Chemistry
Polymer Centre
The University of Sheffield
Sheffield, UK

1.1 Declaration

This thesis is submitted for the degree of doctorate of philosophy (P.hD) at The University of Sheffield, having been submitted for no other degree. It records the research carried out at The University of Sheffield from October 2003 to April 2007. It is entirely my original work, unless where referenced.

Signed .....
AKBAR. KULASI.

Date 26th July 2007

1.2 Acknowledgments

I would like to express my warmest gratitude to Dr. Ahmed Iraqi of the department chemistry for his guidance and supervision through out this project. I would like to thank Dr. David Lidzey of the physics department for his supervisory work in the device manufacture and the characterisation of the polymers devices.

I would like to thank the secretarial staff, Elaine Fisher, Pat Mellor, Michelle Bates, Helen Fairley and Carole Gracanin and the accounting staff Denise Richards, Louise Brown-Leng and Rita Dunman for their kind support, Dr. B. Taylor and Mrs S. Bradshaw for NMR spectra measurements, Mr A. Jones for micro elemental analysis, Mr S. Thorpe for mass spectrometry analysis, Dr B. Hunt and Miss M. Hannah for GPC, TGA analysis, Dr R. Hanson for DSC and spectroscopy/chromatography analysis, Mr M. Manterfield for computer services, Mr P Farran, Mr N Smith and Mr K. Owen from chemical stores and Mr A. Yates for the health and safety advice.

I would also like to thank all members of staff at The Department of Chemistry, University of Sheffield and everyone at the polymer centre, with special mention to the Iraqi group for a pleasant working environment.

1.3 Abstract

There has been significant interest in the development of wide band gap conjugated polymers for application in light-emitting diodes both as blue emitters as well as hosts for lower band gap fluorophores and phosphorescent dyes.

Previous work has seen the development route to two families of carbazole main chain conjugated polymers which have been alkylated at the 9 position of the carbazole ring in an aid to improve solubility and process ability of these compounds. The carbazole repeat units have either been polymerised through the 2,7-positions giving poly(9-alkyl-carbazole-2,7-diyl)s or the 3,6 positions giving poly(9-alkyl-carbazole-3,6-diyl)s.

These polymers have shown quantum efficiencies of $\Phi_{fl} = 0.80 \pm 0.08$ in dichloromethane for poly(9-alkyl-carbazole-2,7-diyl)s and quantum efficiencies of $\Phi_{fl} = 0.065 \pm 0.006$ in dichloromethane for poly(9-alkyl-carbazole-3,6-diyl)s. Also these polymers have exhibited ionisation potentials of ~ 5.2-5.5 eV respectively.

The introduction of aryl groups at the 9-position should ensure that the materials obtained would have low ionisation potentials. This is important for the injection of holes from the ITO electrode into polymer films during LED device operation and should lead to devices with low turn on voltages. It is also hoped that this would allow the exploitation of the energy transfer donor properties of these wide band gap polymers by the variation of aryl substituent. In addition to this, these polymers would also contain alkoxy solubilising groups, which should ensure good process ability of the resulting materials.

This thesis provides an efficient method for the formation to a new class of poly-aryl-carbazoles. It has shown that the formation of arylated-carbazoles can not be produced via conventional copper (I) catalysed reaction methods that were intended for polymerisation through Suzuki and Kumada type polymerisations. It shows that the formation of arylated-carbazoles have been successfully achieved though nucleophilic aromatic substitution reactions, and has opened the path to high yielding arylated carbazole polymers.

Poly(9-(bis-[4-(2-butyl-octyloxy)-phenyl]-amino-phen-4-yl)-carbazole-3,6-diyl) P3.AK and various co-polymers were prepared through a Suzuki coupling polymerisation route. The polymers have been characterized by ^{1}H NMR, ^{13}C NMR, IR absorption, elemental analysis, thermo-gravimetric analysis (TGA) and differential scanning calorimetry (DSC). Their photophysical and electrochemical properties have been characterised by UV-vis spectroscopy, photoluminescence spectroscopy, cyclic voltammetry (CV) and their molecular weights were estimated using gel permeation chromatography. Polymer P3.AK had one of the highest average molecular weights reported for 3,6-linked carbazole main chain conjugated polymers. The fluorescence quantum yields of the polymers were also determined to show quantum efficiencies of $\Phi_{fl} = 0.164 \pm 0.006$ in dichloromethane. Cyclic voltammetric studies on these polymers reveal reversible oxidation waves up to 0.9 V (vs Ag/Ag+) and ionisation potentials in the region of ~ 5.0 - 5.1 eV for the polymers. These low ionisation potentials were a result of their *N*-substitution with the tri-arylamine substituents.

1.1 **Declaration** i

1.2 **Acknowledgments** ii

1.3 **Abstract** iii

2.0 **Introduction** 1
2.1 Conjugated Polymers 1
2.2 Conduction in conjugated polymers 3
2.3 Conjugated polymer backbone: degenerate and non degenerate ground states 6
2.4 Transport of charge in conducting polymers 8
2.5 Stability of conjugated polymers 9
2.6 Application of conjugated polymers 10
2.6.1 Field effect transistors 10
2.6.1.1 Metal Oxide Semiconductors 11
2.6.1.2 Thin film transistors 12
2.6.1.3 Inorganic field effect transistors vs Organic field effect transistors 13
2.6.2 Photovoltaics 13
2.7 Polymerisation of conjugated polymers 16
2.7.1 Electrochemical route 16
2.7.2 Metal catalysed route 17
2.7.2.1 Kumada Type Cross Coupling 17
2.7.2.2 Stille Type Cross Coupling 19
2.7.2.3 Suzuki Type Cross Coupling 20
2.8 Photoluminescence 22
2.8.1 Fluorescence 23
2.8.2 Photochemistry 23
2.8.3 Fluorescence Quantum Yield 24
2.8.4 Phosphorescence 24
2.9 Electroluminescence 24
2.10 Mechanism of Electroluminescence 26
2.11 Band Gap 27
2.11.1 Bond length alteration 28
2.11.2 Donor Acceptor System 29
2.12 Band gap tuning in polymers for light emitting diodes 30
2.13 Device efficiency 31
2.14 Blue light emitting devices 32
2.15 Carbazole based polymers 33
2.15.1 Poly(3,6-carbazole)s 34
2.15.2 Poly(2,7-carbazole)s 37

2.2 References 40

3.0 **Aims and Objectives** 47

4.0 **Experimental** 49

4.1 Materials 49

4.2 Measurements & instruments 49

4.3 Synthesis of 2,7-dibromo-*9H*-carbazole (3) 53
4.3.1 4,4'-Dibromo-2,2'dinitrobiphenyl (1) 53
4.3.2 2,2'-Diamino-4,4'-dibromobiphenyl (2) 53
4.3.3 2,7-Dibromo-*9H*-carbazole (3) 54

4.4 Synthesis of 2,7-dibromo-3,6-dimethyl-*9H*-carbazole (7) 55
4.4.1 2,5-Dibromo-4-nitro-toluene (4) 55
4.4.2 4,4'-Dibromo-2,2'-dinitro-5,5'-dimethylbiphenyl (5) 55
4.4.3 4,4'-Diamino-2,2'-dibromo-5,5'-dimethylbiphenyl (6) 56
4.4.4 2,7-Dibromo-3,6-dimethyl-*9H*-carbazole (7) 57

4.5 Synthesis of 3,6-dibromo-*9H*-carbazole (8) 58

4.6 Attempted synthesis of aryl substituted carbazole derivatives 59
4.6.1 1-Iodo-3,5-dimethoxybenzene (9) 59
4.6.2 1-Iodo-3,5-dimethoxybenzene from 3,5-dimethoxy-phenyl-amine (10) 60
4.6.3 5-Iodoresorcinol (11) 60
4.6.4 1,3-Bis-(2-ethyl-hexyloxy)-5-iodobenzene (12) 61
4.6.5 Attempted synthesis of 2,7-dibromo-9-[3,5-bis(2-ethyl-hexyloxy)-phenyl]-*9H*-carbazole (13) 61
4.6.6 Attempted synthesis of 2,7-dibromo-3,6-dimethyl-9-[3,5-bis(2-ethyl-hexyloxy)-phenyl]-*9H*-carbazole (14) 64
4.6.7 Attempted synthesis of 2,7-dibromo-3,6-dimethyl-9-[3,5-dimethoxy-phenyl]-*9H*-carbazole (15) 64
4.6.8 9-[3,5-(Dimethoxy)-phenyl]-*9H*-carbazole (16) 65
4.6.9 Attempted synthesis of 3,6-dibromo-9-[3,5-dimethoxy-phenyl]-*9H*-carbazole (17) 65
4.6.10 Attempted synthesis of 3,6-diiodo-9-[3,5-dimethoxy-phenyl]-*9H*-carbazole (18) 66
4.6.11 9-(3,5-Dihydroxy-phenyl)-*9H*-carbazole (19) 66
4.6.12 Attempted synthesis of 9-(3,5-bis(2,2,2-trifluoro-acetoxy)-phenyl)-*9H*-carbazole (20) 67

4.7 Synthesis of tri-arylamino substituted carbazole derivatives 68
4.7.1 3,6-Dibromo-9-(4-nitro-phenyl)-*9H*-carbazole (21) 68
4.7.2 3,6-Dibromo-9-(4-amino-phenyl)-*9H*-carbazole (22) 68
4.7.3 4-(2-Butyl-octyloxy-)-1-iodobenzene (23) 69

4.7.4 3,6-Dibromo-9-(bis-[4-(2-butyl-octyloxy)-phenyl]-amino-phen-4-yl)-carbazole (24) 69
4.7.5 3,6-Dibromo-9-(bis-[3,5-bis-(2-ethyl-hexyloxy)-phenyl]-amino-phen-4-yl)-carbazole (25) 70
4.7.6 Attempted synthesis of 3,6-Bis-(4,4,5,5-tetramethyl-[1,3,2]dioxaborolan-2-yl)-9-(bis-[3,5-bis-(2-ethyl-hexyloxy)-phenyl]-amino-phen-4-yl)-carbazole (26) 71
4.7.7 3,6-Bis-(4,4,5,5-tetramethyl-[1,3,2]dioxaborolan-2-yl)-9-(bis-[4-(2-butyl-octyloxy)-phenyl]-amino-phen-4-yl)-carbazole (27) 72

4.8 Other Compounds Used 73
4.8.1 Preparation of the palladium scavenger N,N-diethyl-phenyl-azo-thio-formamide (28) 73
4.8.2 Activated magnesium (29) 74
4.8.3 2,5-Bis-(4-bromo-phenyl)-[1,3,4]-oxadiazole (30) 74
4.8.4 4,7-Dibromobenzo[c][1,2,5]thiadiazole (31) 74
4.8.5 2,7-Dibromo-9,9-dioctyl-*9H*-fluorene (32) 74
4.8.6 2,7-Bis(trimethylene boronate)-9,9-dioctyl-*9H*-fluorene (33) 74

4.9 Preparation of the Polymers 75

4.9.1 Attempted synthesis of poly(9-(bis-[3,5-bis-(2-ethyl-hexyloxy)-phenyl]-amino-phen-4-yl)-carbazole-3,6-diyl) (34) **kumada** 75
4.9.2 Attempted synthesis of poly(9-(bis-[4-(2-butyl-octyloxy)-phenyl]-amino-phen-4-yl)-carbazole-3,6-diyl) (35) **kumada** 75
4.9.3 Poly(9-(bis-[4-(2-butyl-octyloxy)-phenyl]-amino-phen-4-yl)-carbazole-3,6-diyl) (36) **Suzuki (a)** 76
4.9.4 Poly{[9-(bis-[4-(2-butyl-octyloxy)-phenyl]-amino-phen-4-yl)-carbazole-3,6-diyl] -*alt*-[2,5-bis(*p*-phenylene)-1,3,4-oxadiazole]} (37) **Suzuki (a)** 77
4.9.5 Poly{[9-(bis-[4-(2-butyl-octyloxy)-phenyl]-amino-phen-4-yl)-carbazole-3,6-diyl] -*alt*-[2,5-bis(*p*-phenylene)-1,3,4-oxadiazole]} (38) **Suzuki (b)** 78
4.9.6 Poly{[9-(bis-[4-(2-butyl-octyloxy)-phenyl]-amino-phen-4-yl)-carbazole-3,6-diyl] -*alt*-[benzo-2,1,3-thiadiazol-4,7-diyl]} (39) **Suzuki (a)** 80
4.9.7 Poly-(9,9'-dioctyl-fluorene-2,7-diyl) (40) **Suzuki (a)** 81
4.9.8 Poly-(9,9'-dioctyl-fluorene-2,7-diyl) (41) **Suzuki (b)** 82

4.10 References 84

5.0 Results and Discussion 86

5.1 Synthesis of 2,7-dibromo-*9H*-carbazole (3) 86
5.1.1 4,4'-Dibromo-2,2'dinitrobiphenyl (1) 87
5.1.2 2,2'-Diamino-4,4'-dibromobiphenyl (2) 90
5.1.3 2,7-Dibromo-*9H*-carbazole (3) 93

5.2 Synthesis of 2,7-dibromo-3,6-dimethyl-*9H*-carbazole (7) 96
5.5.1 2,5-Dibromo-4-nitro-toluene (4) 97
5.5.2 4,4'-Dibromo-2,2'-dinitro-5,5'-dimethylbiphenyl (5) 100
5.5.3 4,4'-Diamino-2,2'-dibromo-5,5'-dimethylbiphenyl (6) 102
5.5.4 2,7-Dibromo-3,6-dimethyl-*9H*-carbazole (7) 104

5.3 Synthesis of 3,6-dibromo-*9H*-carbazole (8) 106

5.4 Attempted synthesis of aryl substituted carbazole derivatives 108
5.4.1 1-Iodo-3,5-dimethoxybenzene (9) 108
5.4.2 1-Iodo-3,5-dimethoxybenzene from 3,5-dimethoxy-phenyl-amine (10) 109
5.4.3 5-Iodoresorcinol (11) 111
5.4.4 1,3-Bis-(2-ethyl-hexyloxy)-5-iodobenzene (12) 115
5.4.5 Attempted synthesis of 2,7-dibromo-9-[3,5-bis(2-ethyl-hexyloxy)-phenyl]-*9H*-carbazole (13) 120
5.4.6 Attempted synthesis of 2,7-dibromo-3,6-dimethyl-9-[3,5-bis(2-ethyl-hexyloxy)-phenyl]-*9H*-carbazole (14) 127
5.4.7 Attempted synthesis of 2,7-dibromo-3,6-dimethyl-9-[3,5-dimethoxy-phenyl]-*9H*-carbazole (15) 129
5.4.8 9-[3,5-(Dimethoxy)-phenyl]-*9H*-carbazole (16) 132
5.4.9 Attempted synthesis of 3,6-dibromo-9-[3,5-dimethoxy-phenyl]-*9H*-carbazole (17) 135
5.4.10 Attempted synthesis of 3,6-diiodo-9-[3,5-dimethoxy-phenyl]-*9H*-carbazole (18) 136
5.4.11 9-(3,5-dihydroxy-phenyl)-*9H*-carbazole (19) 137
5.4.12 Attempted synthesis of 9-(3,5-bis(2,2,2-trifluoro-acetoxy)-phenyl)-*9H*-carbazole (20) 140

5.5 Synthesis of tri-arylamino substituted carbazole derivatives 142
5.5.1 3,6-Dibromo-9-(4-nitro-phenyl)-*9H*-carbazole (21) 142
5.5.2 3,6-Dibromo-9-(4-amino-phenyl)-*9H*-carbazole (22) 145
5.5.3 4-(2-Butyl-octyloxy-)-1-iodobenzene (23) 148
5.5.4 3,6-Dibromo-9-(bis-[4-(2-butyl-octyloxy)-phenyl]-amino-phen-4-yl)-carbazole (24) 151
5.5.5 3,6-Dibromo-9-(bis-[3,5-bis-(2-ethyl-hexyloxy)-phenyl]-amino-phen-4-yl)-carbazole (25) 156
5.5.6 Attempted synthesis of 3,6-Bis-(4,4,5,5-tetramethyl-[1,3,2]dioxaborolan-2-yl)-9-(bis-[3,5-bis-(2-ethyl-hexyloxy)-phenyl]-amino-phen-4-yl)-carbazole (26) 159
5.5.7 3,6-Bis-(4,4,5,5-tetramethyl-[1,3,2]dioxaborolan-2-yl)-9-(bis-[4-(2-butyl-octyloxy)-phenyl]-amino-phen-4-yl)-carbazole (27) 162

5.6 Other Compounds Used 166
5.6.1 Preparation of the palladium scavenger N,N-diethyl-phenyl-azo-thio-formamide (28) 166

5.7 Preparation of the Polymers 168

5.7.1 Attempted synthesis of poly(9-(bis-[3,5-bis-(2-ethyl-hexyloxy)-phenyl]-amino-phen-4-yl)-carbazole-3,6-diyl) **(34) kumada** 168

5.7.2 Attempted synthesis of poly(9-(bis-[4-(2-butyl-octyloxy)-phenyl]-amino-phen-4-yl)-carbazole-3,6-diyl) **(35) kumada** 170

5.7.3 Poly(9-(bis-[4-(2-butyl-octyloxy)-phenyl]-amino-phen-4-yl)-carbazole-3,6-diyl) **(36) Suzuki (a)** 172

5.7.4 Poly{[9-(bis-[4-(2-butyl-octyloxy)-phenyl]-amino-phen-4-yl)-carbazole-3,6-diyl] -*alt*-[2,5-bis(*p*-phenylene)-1,3,4-oxadiazole]} **(38) Suzuki (b)** 189

5.7.6 Poly{[9-(bis-[4-(2-butyl-octyloxy)-phenyl]-amino-phen-4-yl)-carbazole-3,6-diyl] -*alt*-[benzo-2,1,3-thiadiazol-4,7-diyl]} **(39) Suzuki (a)** 207

5.7.7 Poly-(9,9'-dioctyl-fluorene-2,7-diyl) **(41) Suzuki (b)** 224

5.8 References 237

6.0 Conclusion 239

7.0 Future Work 242

8.0 Appendix I – List of Schemes 244

9.0 Appendix II – List of Figures 247

10.0 Appendix III – List of Mechanisms 249

11.0 Appendix IV – List of Tables 250

2.0 Introduction

2.1 Conjugated Polymers

Conjugated polymers are organic macromolecules which consist of at least one backbone chain of alternating double and single carbon-carbon (sometimes carbon-nitrogen) [1] bonds, depending upon the monomer units used to build the polymer. [2] Single bonds are referred to as σ-bonds, and double bonds contain both σ-bonds and π-bonds. All conjugated polymers have an σ-bond backbone of overlapping sp^2 hybrid orbitals. The remaining out-of-plane p_z orbital on the carbon atoms overlap with neighbouring p_z orbitals to give π-bonds as shown below in figure 1.1. This extensive delocalization of π-electrons is known to be responsible for many characteristics that these polymers can exhibit. These properties can include electronic conductivity, optical and mechanical properties. [3-5]

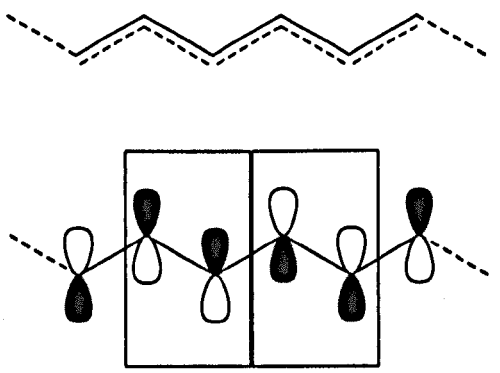

Figure 1.1, Diagram showing conjugation of π orbitals

Conjugated polymers are organic semiconductors that with respect to electronic energy levels hardly differ from inorganic semiconductors. Both have their electrons organised in bands rather than in discrete levels and both have their ground state energy bands either completely filled or completely empty. [6,7] The band structure of a conjugated polymer originates from the interaction of the π-orbitals of the repeating units throughout the chain. This is exemplified below in figure 1.2 with the energy levels of oligo-thiophenes and poly-thiophene which are shown as a function of oligomer length. [8]

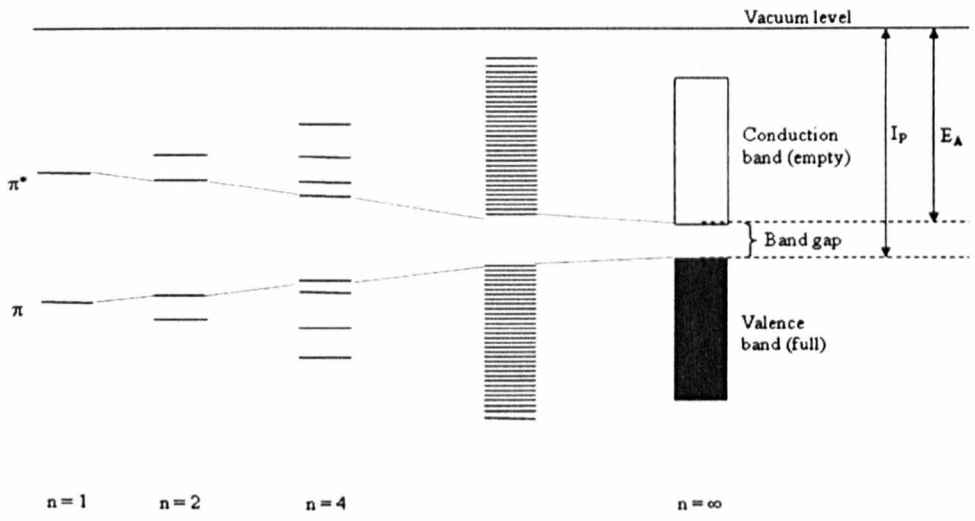

Figure 1.2, Energy level diagram

The addition of every new thiophene unit causes hybridization of the energy levels yielding more and more levels until a point is reached at which there are bands rather than discrete levels. The highest occupied band is called the valence band, while the lowest unoccupied band is called the conduction band. The difference in energy *Eg* between these levels is called the band gap. Since conjugated polymers allow virtually endless manipulation of their chemical structure, control of the band gap of these semiconductors is a research issue of ongoing interest. Band gap engineering may give the polymer its desired electrical and optical properties, and allow the reduction of the band gap to approximately zero which would afford an intrinsically conducting polymer. [9-11]

MacDiarmid, Shirakawa, and Heeger [12] brought some of these unique properties of conjugated polymers to the fore in 1977, when they discovered that chemical doping of polyacetylene resulted in an increase in electronic conductivity over several orders of magnitude. Since then, electronically conducting materials based on conjugated polymers have been applied in diverse items such as sensors, biomaterials, light-emitting diodes, photovoltaic cells, lasers and field-effect transistors. [13-16]

In the long run conjugated polymers should combine the physical properties of polymers with those of semiconductors to obtain unique and novel materials with numerous exciting applications. Examples of such an application is organic polymer light emitting diodes that can emit light in virtually any part of the visible spectrum. (17-19)

These attractive properties of conjugated polymers have lead to one of the most widely investigated applications for these materials. This is the incorporation into electroluminescent (EL) devices, which allows its application into the world wide market of display and lighting products. For these materials to be processed into electronic devices they need to be manufactured into thin films. However conjugated polymer adopt a planar configuration [20] (often rigid, rod-like structures) which results in materials with high melting points and low solubility in common organic solvents. It is important to overcome this hurdle; conjugated polymers can be functionalised with solubilising side chains typically alkyl and/or alkoxy groups. These are designed not to affect the conjugation in the polymer but aid solubility so the polymer can be processed from solutions into thin films by wet processes such as spin-coating and ink-jet printing.

2.2 Conduction in Conjugated Polymers

Polymers are considered electrically insulating, until they have been exposed to suitable electron acceptors or donors (oxidising and reducing agents respectively). [21] This phase of so called charge transfer agents (doping) cause the key transformations from an insulator to a conductor.

Electron transfer within polymers [22] obtained through electron acceptors or donors (chemical oxidation or reduction) involves the formation of charged species within the polymer backbone (carbenium ions or carb-anions) and the formation of counter-ion that insures that charge is neutrality preserved as shown in figure 1.3.

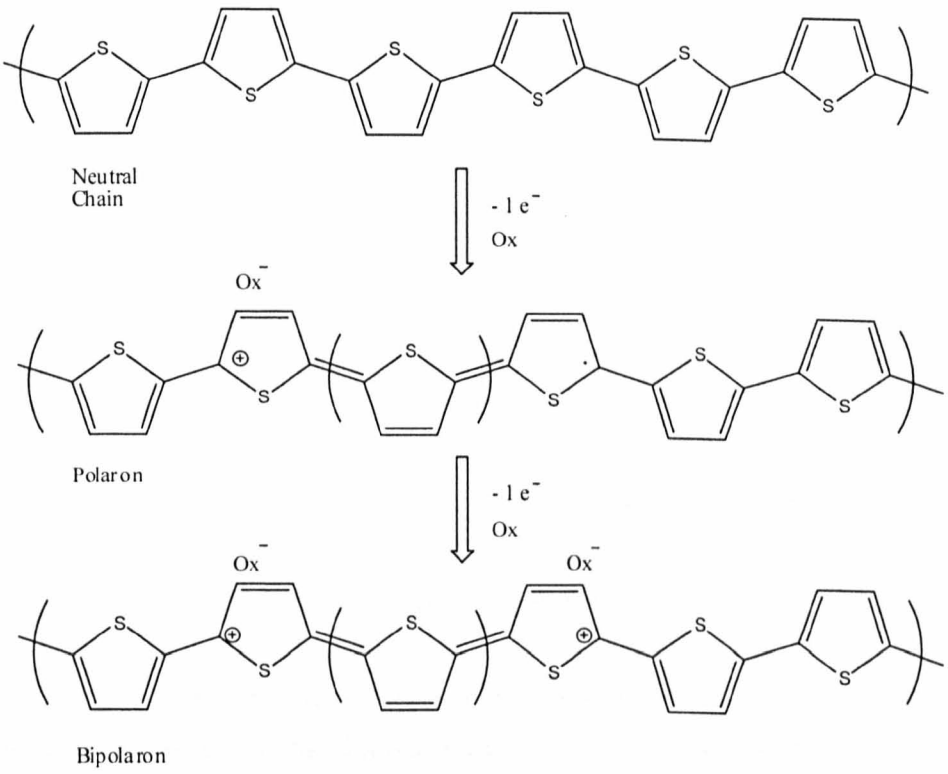

Figure 1.3, Electron transfer in a polymer

Exposure to charge transfer agents increase the conductivity of the polymer rapidly to a plateau where the conductivity reaches asome maximum point, dependent upon the characteristics of the polymer. These charge transfer agents influence the conductivity of the polymer in a number of ways, for example how homogeneously they are distributed throughout the polymer and whether or not they are capable of initiating side reactions that inhibit the polymer's ability to achieve high conductivity. [23]

Looking at this system, one might expect that oxidation of the polymer backbone simply removes electrons from within the valance band and therefore causing band type conduction due to the free unpaired electrons. Likewise, reduction of the polymer backbone can be seen as the addition of electrons to the empty conduction band. This brings the simple analogy that conduction occurs by the movement of free

spin of the unpaired electrons which would be formed from either the conduction or valance band. [24]

This process of charge transfer (doping) induced conductivity does not explain a important factor of conducting polymers, the aspect of free spin; in most conducting polymers the concentration of free spin is simply too small to justify the levels of conductivity found in the material. It is found that at low dopant levels the concentration of free spin increases with conductivity, but as doping is exhausted, saturation occurs which decrease the concentration of free spin to a negligible amount that is undetectable at high doping levels. [6] This brings the conclusion that doping regions of high conductivity occurs without the presence of unpaired electrons. This can be understood from the storage of charge on the polymer backbone and the influence this has on the band structure of the polymer.

Focusing on the oxidation process; the charge produced is transferred from the polymer's π-system to the doping agent. This new formed polymer cation and altered state of dopant (anionic counter ion) produces an ionic complex which establishes the basis of the p-type conduction band of the polymer. The providence of the cationic state produced on the polymer backbone is directed by the ability of the polymer to support the charged state in an energetically favourable manner. Delocalisation of the charge over the polymer backbone would be the same as the removal of an electron from the valence band, hence creating a partially filled band and more so metallic-like conductivity. When charged localisation moves through the polymer backbone it forces the shifting of bonding configuration in the neighbouring environment of the charge which leads to the polymer backbone to gain in elastic energy. This distortion of bonding configuration permits the support of the localised charge, and also lowers the ionisation energy of the chain which in turn allows further oxidation and more suitable environments to withstand further charge formation on the polymer backbone. [25]

2.3 Conjugated polymer backbones: degenerate and non degenerate ground states

The structural relaxations of the lattice, surrounding the charged site are due to the one dimensional polymeric system. This kind of nature would not be expected to be seen in 3D structures where electrons and holes are dominated. There are two main forms of conjugated polymer backbones that can be disclosed; degenerate ground states and non degenerate ground states. [26]

The ground state geometry of trans-polyacetylene is degenerate [27], since the order in which the carbon-carbon single and double bonds alternate leads to the same ground state energy. This in turn means that the ground state energy also is degenerate, with the polymer having two possible bond alternation patterns as shown in figure 4.

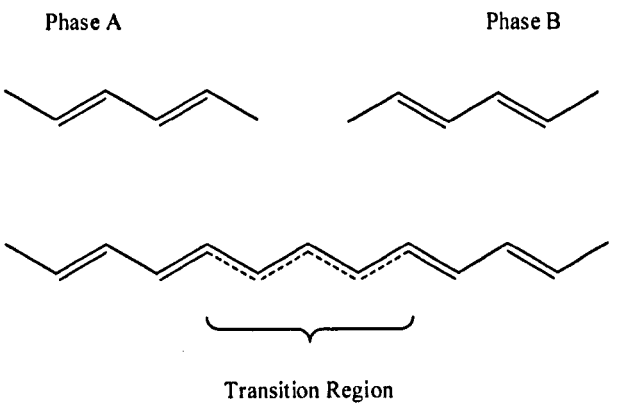

Figure 1.4, Example of a degenerate polymer

In these systems bond alternation can occur, the order of carbon-carbon single and double bonds are changed over a finite length of the polymer chain, creating a transition region where the bond alternation is suspended with the bonds being roughly of the same length.

A bond alternation defect (transition region) will thus cause the isolation of an unpaired electron. These types of defects are called solitons, due to the mathematics describing their properties. [28] Since the polymer remains neutral, the solitons

behave like charge-less unpaired spin-carriers. Neutral solitons have both experimentally and theoretically been determined to be spread out over about 10-14 carbon atoms. With the trans-polyacetylene chains being terminated by double bonds, solitons are always created in pairs, forming a soliton and an anti-soliton. These pairs can be separated with the individual solitons moving freely along the polymer chain, since the two bond alternation conformations are equal in energy. [29]

The vast majority of conjugated polymers, however, have a non-degenerate ground state. For this class of polymers, charge transfer agent injection, also cause a reversal of the bond alternation, though of a different type than that of the case for degenerate ground state polymers. These bond alternation reversals are created in pairs, i.e. a transition back to the original bond alternation conformation will occur along the chain.

Since the ground state is non-degenerate, the area between the reversed ones will have higher energy than the ground state conformation. This will lead to an attraction between the defects, minimizing the region of higher energy. The resulting pair of bond alternation transitions is therefore viewed as one unit. The size of these units is of the same order as for the solitons.

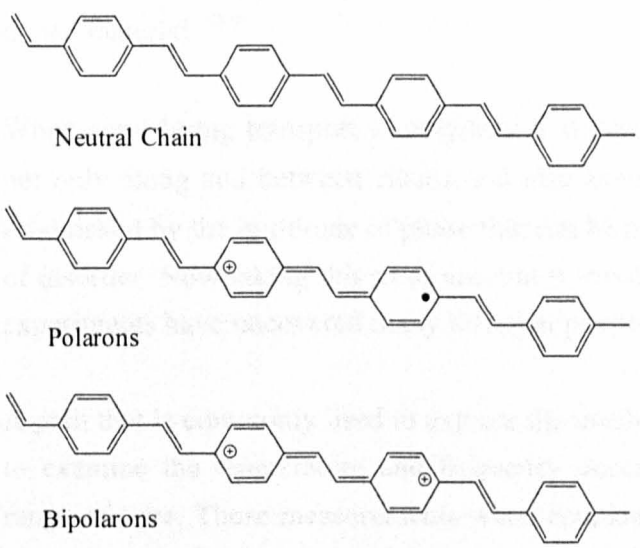

Figure 1.5, Example of non-degenerate polymer

2.4 Transport of charge in conducting polymers

This is a complex area that has been studied in an attempt to understand the many conduction mechanisms that have been put forth to explain the transport in conducting polymers.

The main difficulty in understanding the mechanism of transport arises when attempts are made to trace the path of a charge carrier through a bulk of polymeric matrix. It is widely believed that solitons and bipolarons are the primary source of charge carriers in conducting polymers.

When tracing crystalline materials or semiconducting lattices there is not much complication in following solitons / bipolarons due to the well ordered state of the material. But when one looks at a polymer, it comprises both crystalline and amorphous regions which adds to a factor of disorder within the material. This factor is increased by the diffusion of counterions during the doping process essentially insuring that the electrically conductive form of a conjugated polymer will be dominated by the effects of disorder. This is further more complicated by the fact that many doping process do not produce a homogeneously doped material, but instead create regions of highly doped material coexisting with regions of un-doped or lightly doped material. [30]

When considering transport in polymers it is necessary to take into account charges not only along and between chains, but also across the complex domain boundaries established by the multitude of phase that can be present in the material due to factors of disorder. Now taking this in to account it should not be too surprising to find that experiments have uncovered many different possible conductions mechanisms. [6]

A path that is commonly used to explore the mechanism of conduction in materials is to examine the temperature and frequency dependence of the conductivity over a range of time. These measurements when coupled with magnetic and optical studies can provide information on the nature of the charge carriers, their mobility and the activation energies associated with charge transport.

In highly ordered materials conduction is primarily determined by the number and mobility of the charge carriers present in the band. A signature of true metallic conduction is the existence of a linear increase in conductivity with a decrease in temperature which is independent of frequency. The situation when dealt with in conducting polymers is slightly different. With low levels of doping, charge defects on the polymer chain do not exist within extended states, they are rather confined to localised states. As the level of doping increases the localised states can overlap, which can allow formation of soliton or bipolaron bands. These bands, however, will either be completely filled existing as n-type, or completely empty and therefore existing as p-type. Only after extensive doping levels are reached will these bands merge to produce a true metallic-like conductivity.

Transport in conducting polymers is dominated by thermal activated hopping or tunnelling processes, meaning simply where the charge either hops across or tunnels through barriers created by the presence of isolated states. A review of the literature reveals large numbers of transport models based on the tunnelling and hopping affects. [6,31-33]

2.5 Stability of conducting polymer

The stability of a conducting polymer [34-36] can be found due to different factors which are both intrinsic and extrinsic in nature. Extrinsic stability is related to the polymer's vulnerability to external environmental agents such as water vapour and oxygen. In this case, the susceptibility of the changed sites along the polymer chain, i.e. carbenium ions, carbanions or free radicals, to be attacked by a nucleophiles, electrophiles or free radicals determines the stability of the system. When poor stability is dominated by extrinsic effects, it is possible to encapsulate the polymer in suitable barrier materials or to prepare denser morphologies both of which inhibit the diffusion of the chemical agent to the active sites within the polymer and thereby improving the polymer's stability.

Many conducting polymers, however, are also intrinsically unstable. This effect is thermodynamic in origin and often reflects irreversible chemical reactions that take place between the charged sites of the polymer chain and either the dopant counter-ions of the conjugated system of an adjacent neutral chain. The net effect of these reactions is to introduce defects along the polymer chain that break conjugation and decrease conductivity. Intrinsic instability can also take the form of a thermally driven undoping process in which conformational changes in the polymer backbone activated at elevated temperatures destabilise the charge sites created by oxidation and completely reverse the doping process.

In short, the stability of a conducting polymer depends on a number of factors including its susceptibility and accessibility to external chemical species, the nature and type of counter ion present in the material, the reactivity of its doped sites to surrounding chains, and the flexibility and conformational states of its backbone.

2.6 Applications of conjugated polymers

Since the discovery of the semi-conductive properties of conjugated polymers, research has been directed towards incorporating them into various electronic devices. Some of these devices have been discussed below.

2.6.1 Field effect transistors (FETs)

The field-effect transistor (FET) is a transistor that relies on an electric field to control the shape and hence the conductivity of a channel in a semiconductor material. FETs are sometimes used as voltage-controlled resistors. This is an important area of electronics as they make up an integral part of the circuitry used in computer chips and are used to drive other electronic devices, such as LEDs.

The FET can be constructed from a wide range of materials. [37] The channel region of any FET is either doped to produce an n-type or a p-type semiconductor device. The doping determines the polarity of gate operation. The different types of field-

effect transistors can be distinguished by the method of insulation between channel and gate.

2.6.1.1 Metal-oxide-semiconductor field-effect transistor (MOSFET)

The metal-oxide-semiconductor field-effect transistor [38], is by far the most common field-effect transistor in both digital and analoge circuits. The MOSFET is composed of a channel of n-type or p-type semiconductor material, and is accordingly called an NMOSFET or a PMOSFET.

Usually the semiconductor of choice is silicon, but mixtures of silicon and germanium (SiGe) in MOSFET channels are more commonly known. Unfortunately, many semiconductors with better electrical properties than silicon, such as gallium arsenide, do not form good gate oxides and thus are not suitable for MOSFETs.

A Metal–Oxide–Semiconductor structure is obtained by depositing a layer of dielectric (SiO_2) and a layer of conductor (Si) on top of a semiconductor substrate. Its structure is equivalent to that of a plane capacitor with one of the electrodes replaced by a semiconductor.

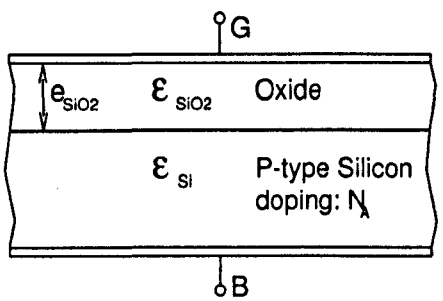

Figure 1.6, Diagrammatic representation of Metal Oxide Semiconductor

When a voltage is applied across a MOS structure, it modifies the distribution of charges in the semiconductor.

2.6.1.2 Thin film transistor (TFT)

A thin film transistor (TFT) [39] is a special kind of field effect transistor made by depositing thin films for the metallic contacts, semiconductor active layer, and dielectric layer. The channel region of a TFT is a thin film that is deposited onto a substrate (often glass, since the primary application of TFTs is in liquid crystal displays). Most TFTs are not transparent themselves, but their electrodes and interconnects can be coloured.

The best known application of thin-film transistors is in TFT LCDs, a variant of LCD technology, especially for use in cellular phone display. Transistors are embedded within the panel itself, reducing crosstalk between pixels and improving image stability.

Figure 1.7, Diagrammatic representation of TFT LCD display

2.6.1.3 Inorganic field effect transistors vs. Organic field effect transistors

One method to compare inorganic field effect transistor and organic field effect transistors would be to consider their charge carrier mobility. This can be termed a good indication to the performance and efficiency of such a device. Inorganic field effect transistor are fabricated from single crystals of silicon or germanium and have charge carrier mobilitics in the region of 1500 $cm^2 V^{-1} s^{-1}$.

Organic field effect transistors [40] is an area where research is being concentrated but at the current moment the best charge carrier mobility in conjugated polymer devices is about 0.2 $cm^2 V^{-1} s^{-1}$. So it appears clear that polymer field effect transistors at the moment will not reach the performance, or for that matter the lifetimes, of these inorganic field effect transistors. But, conjugated polymer based organic field effect transistors do have advantages over their inorganic counterparts; device fabrication costs are lower and also more flexible and robust devices are possible. This has led to interest in polymer field effect transistors having applications where inorganic field effect transistors are not viable, for example large-area and/or low cost disposable electronic products such as identification tags, smart cards and electronic paper. Inferior lifetime and performance can be sacrificed for the economical advantages that polymer field effect transistors possess.

2.6.2 Photovoltaics

Photovoltaics, or PV for short, is a solar power technology that uses solar cells or solar photovoltaic arrays to convert energy from the sun into electricity. Solar cells produce DC electricity from the sun's rays, which in total can be used to power electrical devices.

As global warming continues to rise, the need for a compromise in conventional methods in which we create, store and transport electricity needs to be considered. Photovoltaic cells satisfy these criteria, but in order to gain widespread acceptance as

a source of clean renewable energy, the factor of cost in solar energy must be reduced.

Solar power systems installed in the areas defined by the dark disks could provide a little more than the world's current total primary energy demand (assuming a conversion efficiency of 8%). That is, all energy currently consumed, including heat, electricity, fossil fuels, etc., would be produced in the form of electricity by solar cells.

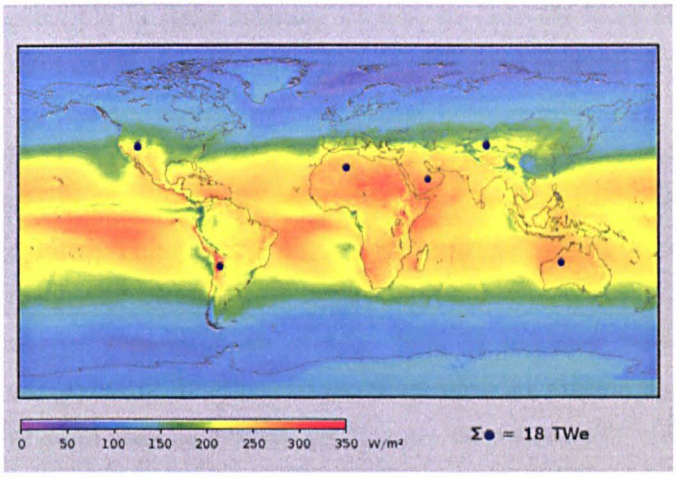

Figure 1.8, The solar irradiance averaged over three years from 1991 to 1993

Many institutions are currently developing ways to increase the practicality of solar power. [41] The most important issue with solar panels is cost. Common PV cells are inorganic based and the high cost comes from manufacturing crystalline silicon. Which in turn means; PV cells are not capable of competing with conventional grid electricity.

Conjugated polymer based PV cells provide a potential alternative to the current crystalline silicon technology. They can be easily processed onto flexible substrates over large areas using wet processing techniques, thus decreasing the device cost. If they can achieve reasonable power efficiency and lifetimes they could become desirable alternatives to inorganic PV cells.

Conjugated polymer based PV cells are built from thin films of organic semiconductors such as polymers and small-molecule compounds like polyphenylene vinylene and carbon fullerenes. [42,43] Energy conversion efficiencies achieved to date using conductive polymers are low, but current research is pushing these bounderies and linked with the processability, mechanical flexibility and disposability of these materials makes them great contenders for the future of PV cells.

The underlying principle of a light-harvesting organic PV cell is the reverse of the principle in light emitting diodes. In light emitting diodes, electricity is converted into light whereas in PV cells light is converted into electricity.

In an organic PV cell when light is absorbed an electron is promoted from the highest occupied molecular orbital to the lowest unoccupied molecular orbital, forming an exciton. This process must then be followed by exciton dissociation – the electron must reach one electrode whilst the hole must reach the other electrode. In order to achieve charge separation an electric field is required, which is provided by the ionization energy/work functions of the electrodes. As exciton dissociation does not occur readily in organic materials many devices are fabricated with a heterojunction, using two materials with different electron affinities and ionisation potentials. This will favour exciton dissociation; the electron will be accepted by the material with the larger electron affinity and the hole by the material with the lower ionisation potential. This will result in increased device efficiency.

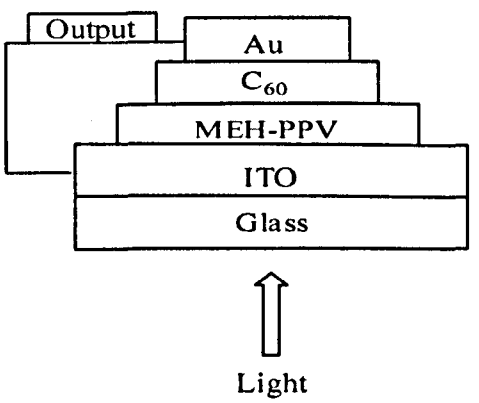

Figure 1.9, Device structure of a hetero-junction PV cell [44]

2.7 Polymerisation of conjugated polymers

Conjugated polymers have been synthesised for many years through a number of different techniques, like condensation polymerisations, radical addition polymerisation, step reaction polymerisations and photo induced polymerisation. There are two common methods that have been employed for organic conjugated polymers, the electrochemical route and the metal catalysis route.

2.7.1 Electrochemical Route to Conjugated Polymers

The electrochemical route was found to have great importance when the electrochemical synthesis of a flexible and stable polypyrrole was carried out. [45] As a result of its electro activity, high electrical conductivity and stability it is frequently used in commercial applications such as sensors, batteries, molecular devices and membranes. Research has been focused on conductive polymers synthesised by electrochemical methods since they have some advantages like simplicity, reproducibility and thickness control. A wide spectrum of applications was proposed, mainly related to the conductive properties of the material. However, some difficulties appear in processing conducting polymers since they have poor mechanical and physical properties.

Properties of such electrochemically deposited conducting polymers can be followed by cyclic voltammetry (CV), quartz microbalance (QMB) and electrochemical impedance spectrometry (EIS). Actually, these techniques allow the investigation of the cation/anion doping/de-doping phenomena, which accompanies the oxidation state variations of the polymer.

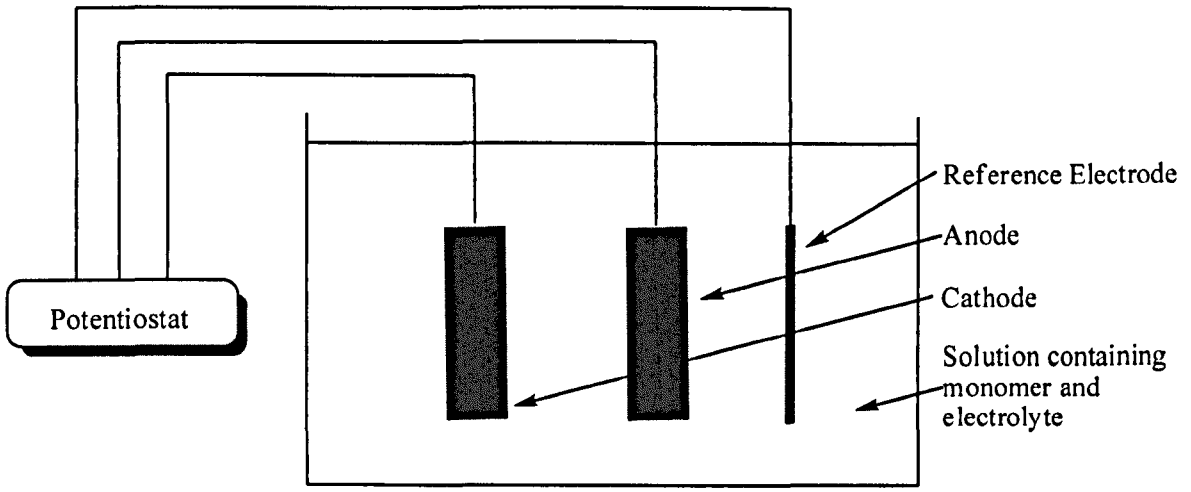

Figure 1.10, Diagram of a typical electrochemical cell

Anodic polymerisation is most commonly used. It involves the oxidation of a monomer in solution leading to deposition of polymers as coating on electrode. [46] It is generally done in a classical three-electrode cell which is shown in figure 1.10 above.

2.7.2 Metal-Catalysed Routes to Conjugated Polymers.

2.7.2.1 Kumada Type cross-coupling

In these reactions, bi-functional monomers comprising both halo- and halomagnesio-functionalities are used. The reaction is normally catalysed with the use of either nickel or palladium.

The phosphine/nickel complex catalyses the cross-coupling of a number of functionalities, for instance alkyl, alkenyl, aryl, and heteroaryl Grignard reagents can be readily reacted with aryl, heteroaryl, and alkenyl halides. [47] This method can thus be seen to have a wide scope of application. Alkyl halides also exhibit considerable reactivity, but give a complex mixture of products. A labile diorgano-nickel complex involving the two organic groups originating from the Grignard reagent and from the

organic halide, respectively, has been proposed as a reaction intermediate. The fact that simple alkyl Grignard reagents with hydrogen-bearing β-carbon atoms react with equal efficiency is one of the most remarkable features of this present method, considering the great tendency with which transition metal alkyls undergo a β-elimination reaction, forming alkenes and metal hydrides. [48-51] Although the β-elimination may be responsible for the side products formed during the coupling, an appropriate choice of phosphine ligand for the nickel catalyst minimises this side reaction. The catalytic activity of the phosphine / nickel complex depends not only on the nature of the phosphine ligand but also on the combination of the Grignard reagent and organic halide.

The mechanism for a Kumada cross-coupling reaction is be believed to take place as shown below in figure 1.11.

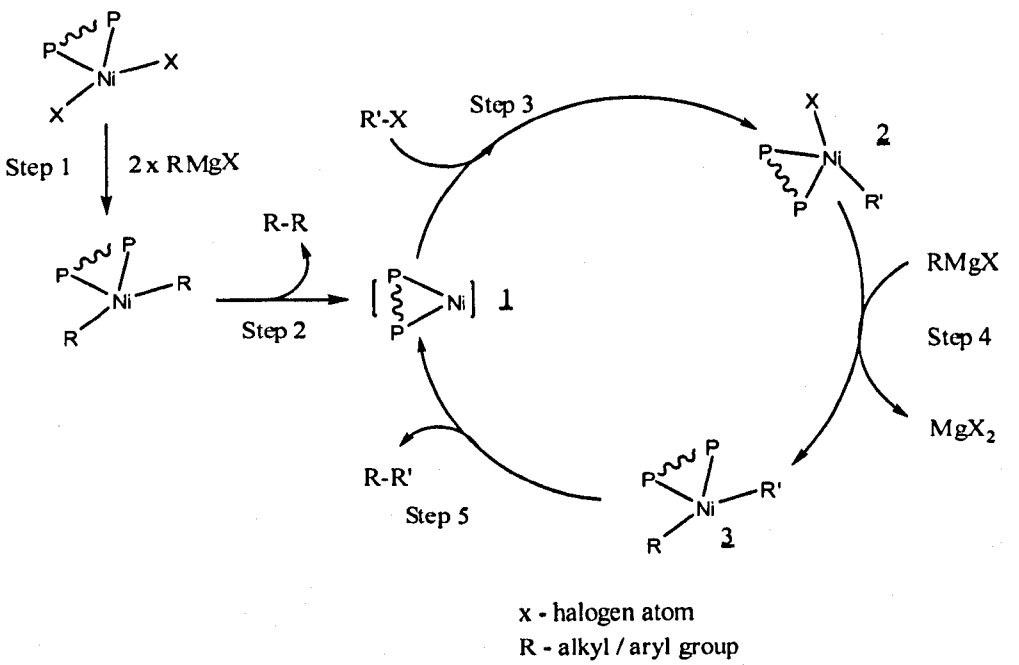

Figure 1.11, Mechanism for Kumada cross-coupling reaction

2.7.2.2 Stille Type Cross-coupling

In these reactions, functional monomers comprising halo- and/or organitin-functionalities are used. The Stille cross-coupling reactions are similar to Kumada-type cross-coupling reactions, apart that organotin-derivatives are used instead of Grignard-derivatives. The Stille reaction tolerates a variety of functional groups on the coupling partners as opposed to reactions involving organo-magnesium or organo-zinc derivatives. [52, 53]

The Stille reaction was discovered in 1977 by John K. Stille and co-workers. This type of reaction continues to be exploited in industry, especially for the pharmaceuticals industry. The reaction is usually performed under inert atmosphere using dehydrated and degassed solvent. This is because oxygen causes the oxidation of the palladium catalyst and promotes homo coupling of organic stannyl compounds, and these side reactions lead to a decrease in the yield of the cross coupling reaction.

As the organic tin compound, a trimethylstannyl or tributylstannyl compound is normally used. Although trimethylstannyl compounds show higher reactivity compared with tributylstannyl compounds, the toxicity of the former is about 1000 times larger than that of the latter. Therefore it is better to avoid using trimethylstannyl compounds unless necessary.

The reaction mechanism of the Stille reaction has been well studied. [54] The first step in this catalytic cycle is the reduction of the palladium catalyst (**1**) to the active Pd(0) species (**2**). The oxidative addition of the organohalide (**3**) gives a *cis* intermediate which rapidly isomerises to the *trans* intermediate (**4**). [55] Transmetalation with the organostannane (**5**) forms intermediate (**7**), which produces the desired product (**8**) and the active Pd(0) species (**2**) after reductive elimination. The oxidative addition and reductive elimination retain the stereo chemical configuration of the respective reactants as shown below in figure 1.12.

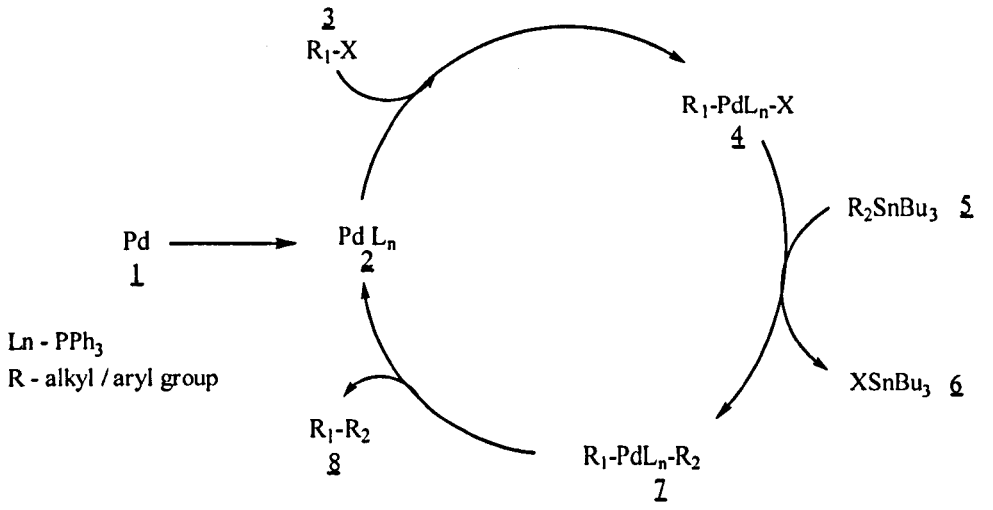

Figure 1.12, Mechanism for Stille cross-coupling reaction

2.7.2.3 Suzuki Type cross-coupling

The Suzuki cross coupling reaction is the organic reaction of an aryl- or vinyl-boronic acid / ester with an aryl- or vinyl-halide catalyzed by a palladium(0) complex. [56, 57] This is a powerful synthetic tool as it represents one of the most valuable methods for carbon-carbon bond formation, not least because of its tolerance of a broad range of functional groups and its non-toxic bi-products. The boronic acid is also thermally stable and inert to air and water which allows easy handling without special precautions. The presence of a mineral base seems to be fundamental for the success of the cross-coupling reaction.

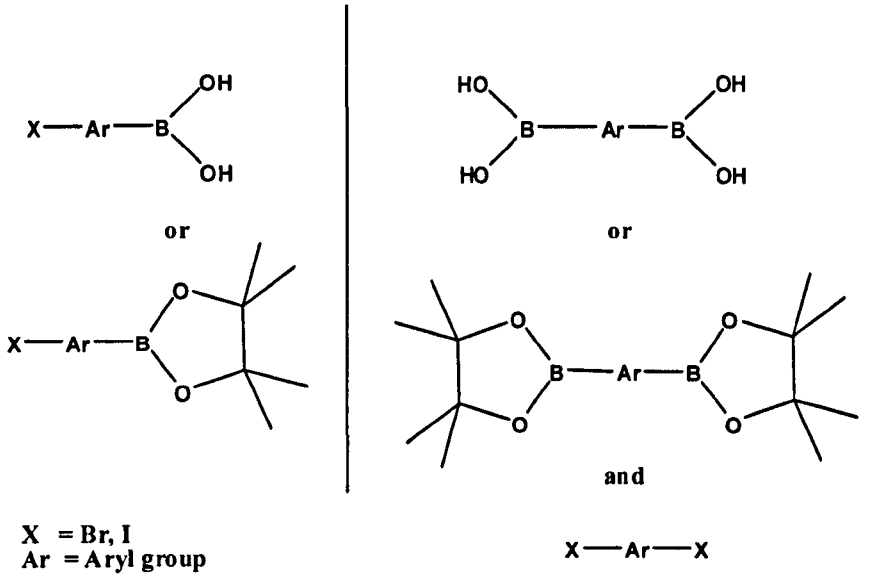

Figure 1.13, Structure of boronic counterparts for Suzuki cross-coupling reaction

The mechanism of the Suzuki reaction is best viewed from the perspective of the palladium catalyst. The first step is the oxidative addition of palladium to the halide (**2**) to form the organo-palladium species (**3**). Reaction with base gives intermediate (**4**), which via transmetallation [58] with the boron-ate complex (**6**) forms the organopalladium species (**8**). Reductive elimination of the desired product (**9**) restores the original palladium catalyst (**1**) as shown below in figure 1.14.

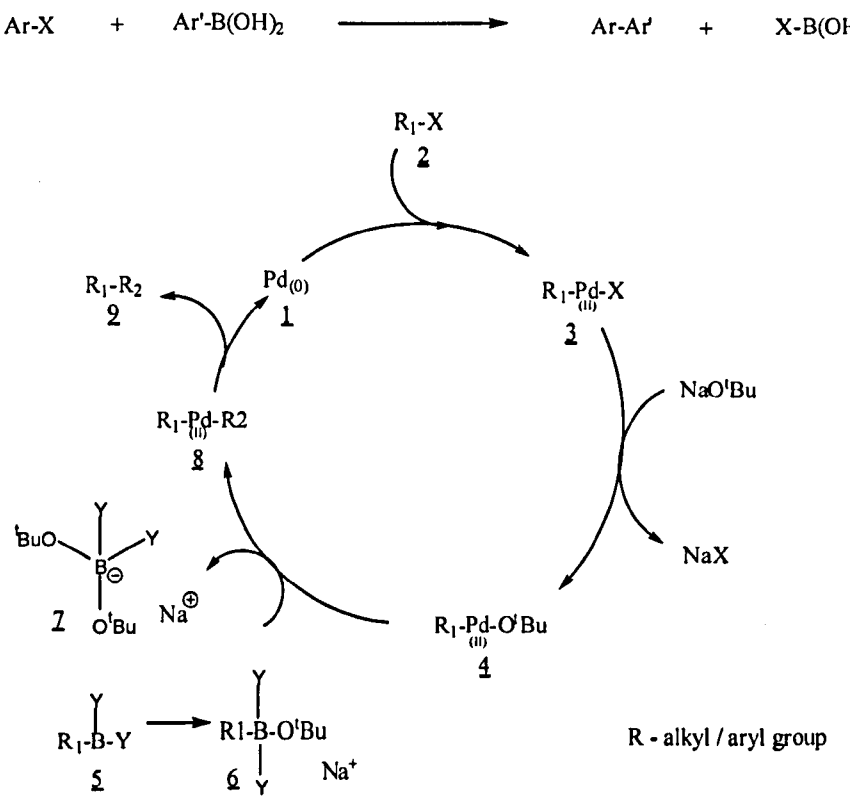

Figure 1.14, Mechanism for Suzuki cross-coupling reaction

2.8 Photoluminescence

Photoluminescence is a process in which a chemical compound absorbs a photon, this photon excites an electron to a higher electronic energy state, and then the electron radiates the photon back out, returning the electron to the lower energy state. The period between absorption and emission is typically extremely short, in the order of 10 nanoseconds.

The simplest photoluminescent processes are resonant radiations, in which a photon of a particular wavelength is absorbed and an equivalent photon is immediately emitted. This process involves no significant internal energy transitions of the chemical substrate between absorption and emission.

2.8.1 Fluorescence

Fluorescence is where the molecular absorption of a photon triggers the emission of another photon with a longer wavelength. The energy difference between the absorbed and emitted photons ends up as molecular vibrations or heat. Usually the absorbed photon is in the ultraviolet range, and the emitted light is in the visible range, but this depends on the absorbance curve and Stokes shift of the particular fluorophore.

2.8.2 Photochemistry

Fluorescence occurs when a molecule relaxes to its ground state after being electronically excited.

Excitation: $S_o + h\upsilon \rightarrow S_1$ Equation 1

Fluorescence (emission): $S_1 \rightarrow S_0 + h\upsilon$ Equation 2

$h\nu$ is a generic term for photon energy where: h = Planks Constant and ν = frequency of light. State S_0 is called the ground state of the fluorophore and S_1 is its first excited state.

A molecule in its excited state, S_1, can relax by various competing pathways. It can undergo 'non-radiative relaxation' in which the excitation energy is dissipated as heat to the solvent. Excited organic molecules can also relax via conversion to a triplet state which may subsequently relax via phosphorescence or by a secondary non-radiative relaxation step.

Relaxation of an S_1 state can also occur through interaction with a second molecule through fluorescence quenching. Molecular oxygen is an extremely efficient quencher of fluorescence because of its unusual triplet ground state.

2.8.3 Fluorescence Quantum Yield

The fluorescence quantum yield gives the efficiency of the fluorescence process. It is defined as the ratio of the number of photons emitted to the number of photons absorbed. The maximum fluorescence quantum yield is 1.0, every photon absorbed results in a photon emitted. Compounds with quantum yields of 0.10 are still considered quite fluorescent.

Fluorescence quantum yields are measured by comparison to a standard with known quantum yield; quinine sulphate, in a sulphuric acid solution is a common fluorescence standard.

2.8.4 Phosphorescence

Phosphorescence is a process in which energy absorbed by a substance is released relatively slowly in the form of light, the re-emission are associated with forbidden energy states. Unlike the relatively swift reactions in a common fluorescent tube, phosphorescent materials used in these materials absorb the energy and store it.

The absorbed photon energy undergoes an unusual intersystem crossing into an energy state of higher spin multiplicity, a triplet state. As a result, the energy can become trapped in the triplet state with only quantum mechanically forbidden transitions available to return to the lower energy state. These transitions, although, will occur but are kinetically un-favoured and thus progress at significantly slower time scales.

2.9 Electroluminescence

There are two main ways of producing light: incandescence and luminescence. In incandescence, electric current is passed through a filament whose resistance to the passage of current produces heat. The greater the heat of the filament, the more light

it produces. Luminescence, in contrast, is the name given to all forms of visible radiant energy due to causes other than temperature.

There are a number of different types of luminescence, including: electroluminescence, cathodoluminescence, and photoluminescence.

Electroluminescence is the production of visible light by a substance exposed to an electric field without thermal energy generation. Photoluminescence is emission of light as a result of being exposed to ambient light. As the material absorbs light rays, it stores energy. Upon removal of the light source, the stored light is gradually released, producing a visible glow that fades over a period of time.

An electroluminescent device is similar to a laser in that photons are produced by the return of an excited substance to its ground state, but unlike lasers electroluminescent devices require much less energy to operate. Electroluminescent devices are discrete devices that produce light when a current is applied to a doped p-n junction of a semiconductor.

All electroluminescent displays have the same basic structure. There are at least six layers to the device. The first layer is a base-plate (glass substrate), the second is a conductor (electrode), the third is an insulator, the fourth is a layer of phosphors, and the fifth is an insulator, and the sixth is another conductor.

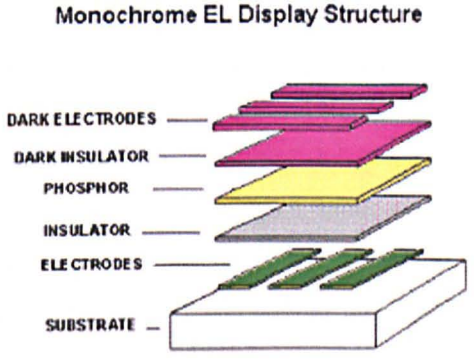

Figure 1.15, a simple monochrome EL device.

EL devices are quite similar to capacitors except for the phosphor layer. You can think of it as, if the device becomes electrically charged and then loses its energy in the form of light. The insulator layers are necessary to prevent arcing between the two conductive layers.

EL devices have a number of advantages over current market leading display technologies such as cathode-ray tubes and liquid crystal displays. These modern EL devices have shown to be lighter in weight, smaller in size, possess great viewing angles and require lower driving voltages.

It was in early 1960s when EL was first observed for organic materials. This was when a single anthracene crystal was placed between liquid electrolytic electrodes, and a voltage was applied and light was emitted from the crystal. [59-61] But it was not until 1987 when Van Slyke [62] demonstrated an efficient small-molecule based organic electroluminescent device, this drew great interest to the area, shortly after Burroughes *et al.* [63] and Nakano *et al.* [64,65] both demonstrated conjugated polymer could be used in the production of electroluminescent devices. There have become two main areas of research for organic electroluminescent device, one incorporating small molecule organics the other incorporating conjugated polymers.

2.10 Mechanism of Electroluminescence

The basic mechanism for EL was electron injection from the cathode into the polymer and removal of the electron by the anode. The oppositely charged species produced in the polymer then migrate along the polymer chain and recombine. The recapture of these oppositely charged species results in an excited state, which can decay radioactively to produce a photon and hence light emission, the colour of which will depend upon the band gap of the material.

There are two types of exciton states created when electrons and holes recombine, triplet and singlet excited states. The singlet-excited states are capable of radiative

decay to produce fluorescent electroluminescence. The triplet-excited states will decay radioactively, to produce phosphorescent EL, but in very low yields. Due to the ratio of the singlet to triplet state there is generally a loss of ¾ which will decay non-radioactively releasing heat and vibrational/kinetic energy.

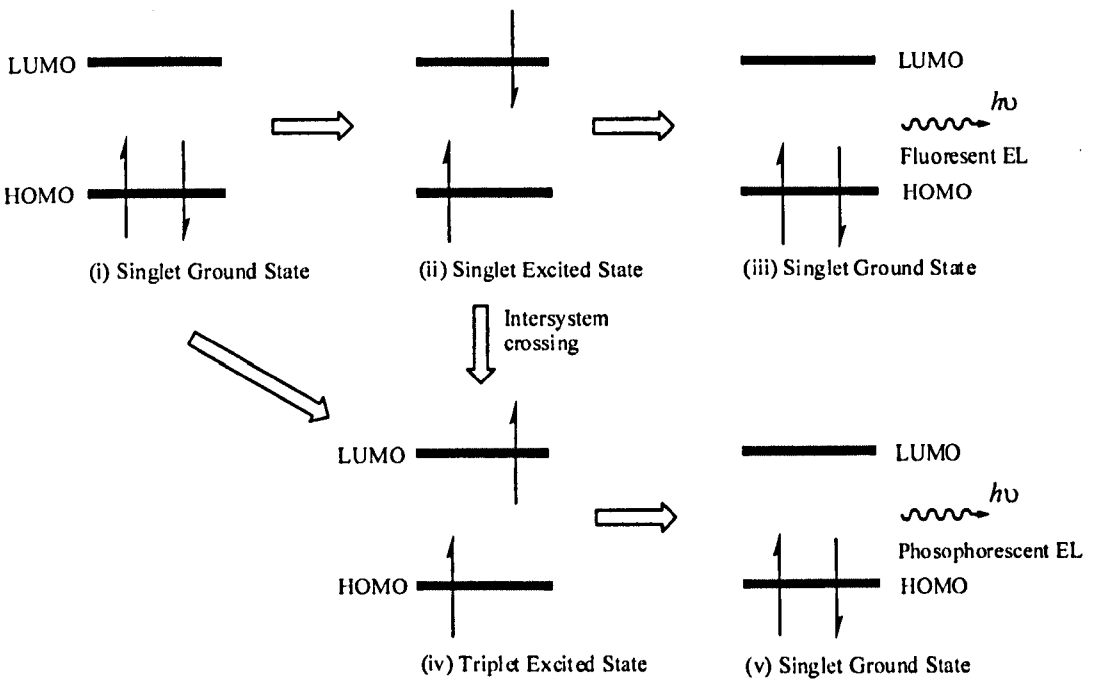

Figure 1.16, The mechanism of EL for a conjugated polymer [66]

2.11 Band gap

There are two main areas that have been considered to cause dramatic decrease in the band gap of conjugated polymers: cancellation of bond-length alternation and the donor-acceptor repeating unit strategy.

2.11.1 Bond-length alternation

The simplest representative of a conjugated polymer is trans-polyacetylene. Its first successful synthesis was described in 1974. [67] Polyacetylene would be a metallic conductor if the distance between all carbon atoms was identical. In this situation, the double bonds are really delocalized along the polymer chain. Finding a band gap as the energy difference between a "bonding" ground state and an "anti-bonding" excited state is impossible due to the equivalence (degeneracy) for an infinite chain of both structures, resulting in a metal-like half-filled band.

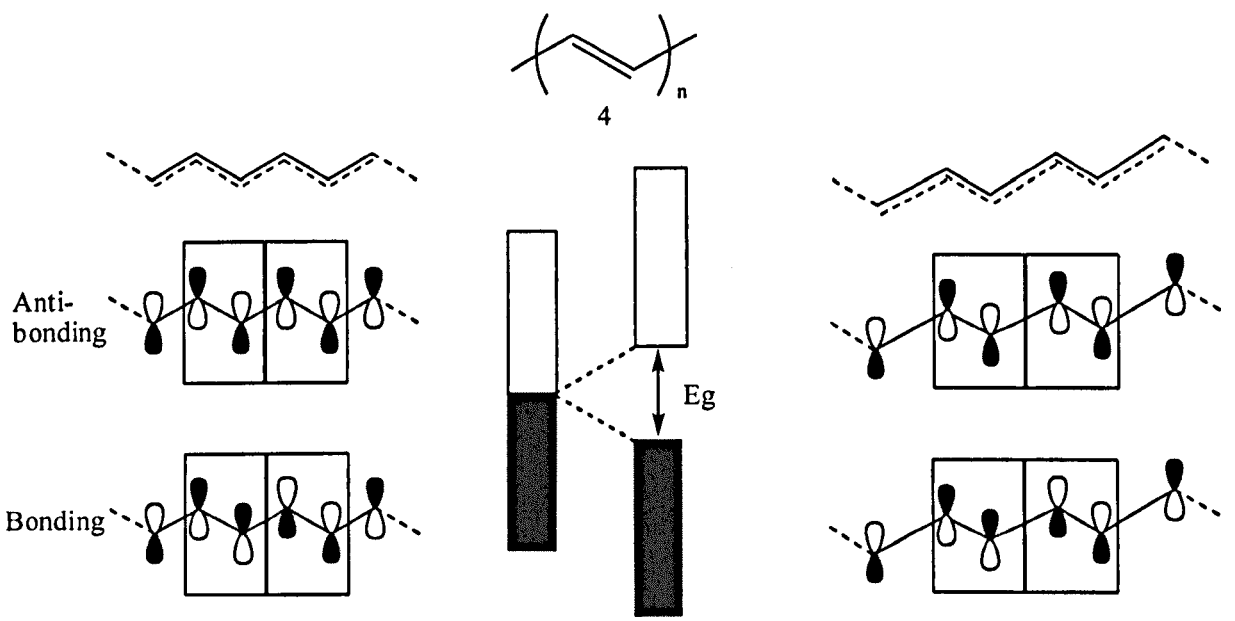

Figure 1.17, Effect of bond length alternation [67,68]

However, the equidistant linear chain structure is unstable towards a structural deformation of alternating shorter double and longer single bonds, and the result is a finite band gap Eg. This "bond length alternation" is due to a gain in electronic energy that overcompensates the loss of "elastic" energy, and is known as Peierls effect. [69] Minimizing the bond length alternation along the backbone of a conjugated polymer is an important guideline in band gap-reduction.

2.11.2 Donor-Acceptor System.

It was shown in polyisothianaphthene [70] that reduction of bond-length alternation by increasing the double-bond character between the repeating units of a conjugated polymer, results in a decreased band gap. The driving force for such a process is the gain in aromaticity of the fused ring systems. The interaction between a strong electron-donor and a strong electron-acceptor may also give rise to an increased double bond character between these units. Hence, a conjugated polymer with an alternating sequence of the appropriate donor- and acceptor-units in the main-chain may have a decreased band gap.

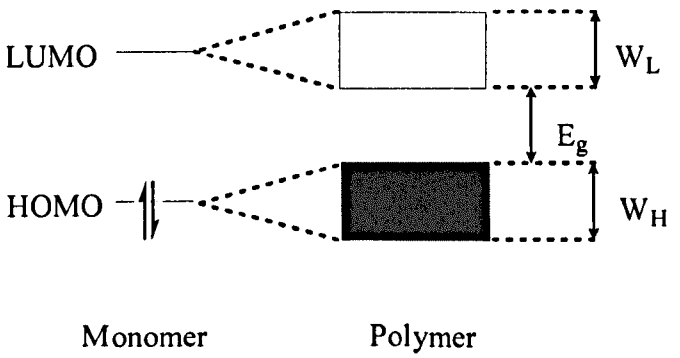

Figure 1.18, Energy level diagram

The highest occupied molecular orbital (HOMO) and lowest unoccupied molecular orbital (LUMO) levels of the repeating unit disperse into a valence- and conduction band upon chain extension. The degree with which this happens; also called the bandwidth shown in the figure 1.18 above is represented by W_L and W_H. The magnitudes of W_L and W_H are strongly dependent on the degree of overlap between the atomic orbitals in the coupling positions of the consecutive units. The maximal values for W_L and W_H are only reached in the case of an unobstructed overlap. Deviation from this ideal situation can occur when i) steric hindrance forces the consecutive units out of plane, or ii) when the size of the atomic orbitals at the coupling positions is diminished.

2.12 Band gap tuning in polymers for light emitting diodes

Many other factors, besides the main-chain chemical constitution, can influence the band gap, for example the nature of side-chains or the conformation of the main chain.

In the field of polymer light emitting diodes [71] tuning of the band gap is an important issue since it can effect the emission colour. An example is the influence of various side-chains on the (photo- and electro-) luminescence of substituted poly-thiophene. [72] The luminescence of this set of polymers covers nearly the whole visible spectrum as shown in figure 1.19 below.

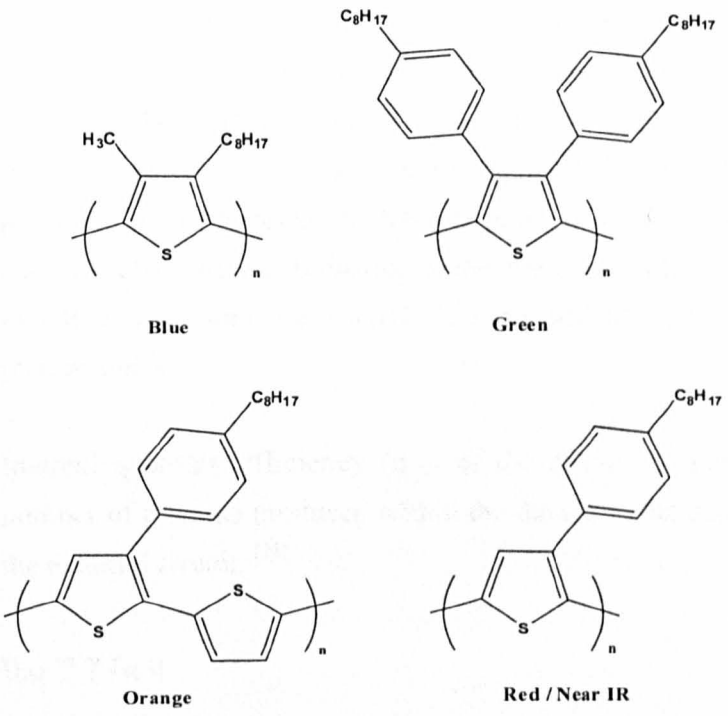

Figure 1.19, Example of emission of colours achieved by polymers

A trend seen is that with increasing size of the solubilising group, there is a larger deviation from co-planarity of the subsequent thiophene units. This causes a diminished extended conjugation and, hence, a hypsochromic shift in the luminescence spectra, while the application of a phenyl ring in the solubilising group

enlarges the conjugated systems causing a bathochromic shift in the luminescence spectra.

The band gap of a conjugated polymer can be tuned by limiting the conjugation length to a certain degree, for example the introduction of side-chains or main-chain subunits with a varying degree of steric crowding. However, the electronic effects of such substitutions are also of great influence on the band gap, which implies that band gap engineering following this approach may be a matter of trial and error.

2.13 Device efficiency

In order to obtain an efficient electroluminescent device it is necessary to meet the following criteria. A good charge injection from the electrode, which can be achieved by tuning the work function of the anode to the ionisation potential of the polymer. Also tuning the work function of the cathode with the electron affinity of the polymer. It is important to have a good balance between the electron and hole currents, efficient recombination of electrons and holes in the emissive layer, stronger radiative transitions for singlet excitons and efficient decay of these excitons to photon states.

Internal quantum efficiency (η_{int}) of the device is determined as the ratio of the number of photons produced within the device to the number of electrons flowing in the external circuit. [73]

$$\eta_{int} = \gamma\, r_{st}\, q \qquad \text{Equation 3}$$

Internal quantum efficiency

Where γ is the ratio of the number of exciton formation events within the device to the number of electrons flowing through the external circuit. r_{st} is the fraction of excitons formed in the singlet state and q is the efficiency of decay of these singlet excitons.

External quantum efficiency (η_{ext}) of electroluminescent device is determined as the ratio of the number of photons that escape the device to the number of electrons injected.

$$\eta_{ext} = \chi \eta_{int} \qquad \text{Equation 4}$$

External quantum efficiency

Where χ is the number of emitted photons that escape the device. From this equation the internal quantum efficiency of the electroluminescent device η_{int} could be directly calculated from the external quantum efficiency η_{ext}, which can be directly measured.

2.14 Blue light emitting diodes

Over the past two decades the active materials used in commercial light emitting diodes were, and mainly still are inorganic semiconductors. An experiment carried out using a single anthracene crystal showed that molecular organic materials could be used to produce electroluminescence. [59]

There are many organic molecules that are used to produce light emitting in various parts of the visible spectrum[62] based on their fluorescence properties and ability to transport charge over there structural back bone. But the only property which was benefited was their structural stability compared to their inorganic counterparts.

Conjugated polymers were shown to yield electroluminescent character when research was carried out on poly-*p*-phenylene vinylene. [63] The ease in which the band gap could be adjusted to colour emission made conjugated polymers very attractive for their use in light emitting diodes, which is reflected in the immense research effort performed in this area over the past decade. [16,72] One of the first blue light-emitting polymer device was made by Yoshino, *et al.* in 1987 forming poly(9,9-dihexylfluorene-2,7-diyl)s. [74] This was due to their good processibility, ease of

synthesis, thermal and chemical stability and high quantum yields of fluorescence (Φ_{fl} between 0.6 and 0.8). [75, 76]

There is an ongoing search for the ideal active material, which can be used as a stable blue light-emitting polymer diode. This illustrates the importance of producing a polymer that has a concise band gap. Since blue light emission is around 450 nm, a conjugated polymer requires a large band gap of about 2.7 - 3.0 eV. Indeed, blue light-emitting polymers have been made from the large-band gap polymers for example poly-*p*-phenylene (PPP). [77]

At present approaches towards high-band gap systems for blue-light emitting diodes consist of: (i) limiting the conjugation length by the introduction of 1,3-phenylene Linkages,[78-80] (ii) silicon sp^3 linkages, [81-84] or (iii) the use of non-conjugated polymers with a blue luminescent chromophore in the side chain[85,86] or the main-chain. [87-89]

The disadvantage of reducing the conjugation in these drastic ways is a major decrease in semiconducting properties, which for instance results in the need for high onset voltages. Although the use of a fully conjugated polymer may result in enhanced semiconducting properties, keeping the photo- and electroluminescence of these polymers within the blue part of the visible spectrum is difficult due to their extended conjugation and, hence, decreased band gaps. [90-92]

2.15 Carbazole Based Polymers

In the recent years we have seen an increase in research into conjugated polymers that have been designed for the use in electrical devices, and these have been thoroughly investigated. For example poly(*p*-phenylene)s, [93] poly(*p*-phenylenevinylene)s, [63] polythiophenes, [94-96] and polyfluorenes. [97-100]

Polycarbazole is also a material which has seen much interest. The 9H-carbazole molecule is favourable for a number of reasons, firstly it is commercially cheap to

buy. The molecule is fully aromatic which allows better chemical stability; it is easily functionalised at the nitrogen atom which can open a number of positions to tailor the physical properties of the molecule. Also the carbazole molecule can be substituted in two different positions which can effectively lead to two different products with different properties and potential applications.

2.15.1 Poly-(3,6-carbazole)

Poly(N-vinylcarbazole)s have been the subject of extensive research due to their photoconductive properties and their ability to form charge-transfer complexes arising from the electron donating character of the carbazole moiety. [101-105] There have been attempts to prepare conjugated polymers by electrochemical methods. The formation of preparing polymers in this way has allowed thin films to be prepared in one step from the monomer material. With regards to the carbazole [106-109] molecule, the electrochemical oxidation has seen to have been one of the first soluble oligomers to be formed. [110-111]

It was found that the 3,6 and 9 positions were extremely reactive and the electrochemical oxidation of the carbazole ring allows coupling to occur which lead to the formation of the carbazole radical cation. The stabilisation of the bicarbazylium radical cations was found due to their ability to delocalise the charge through out the π-conjugation extended between the two nitrogen atoms as shown below in figure 1.20.

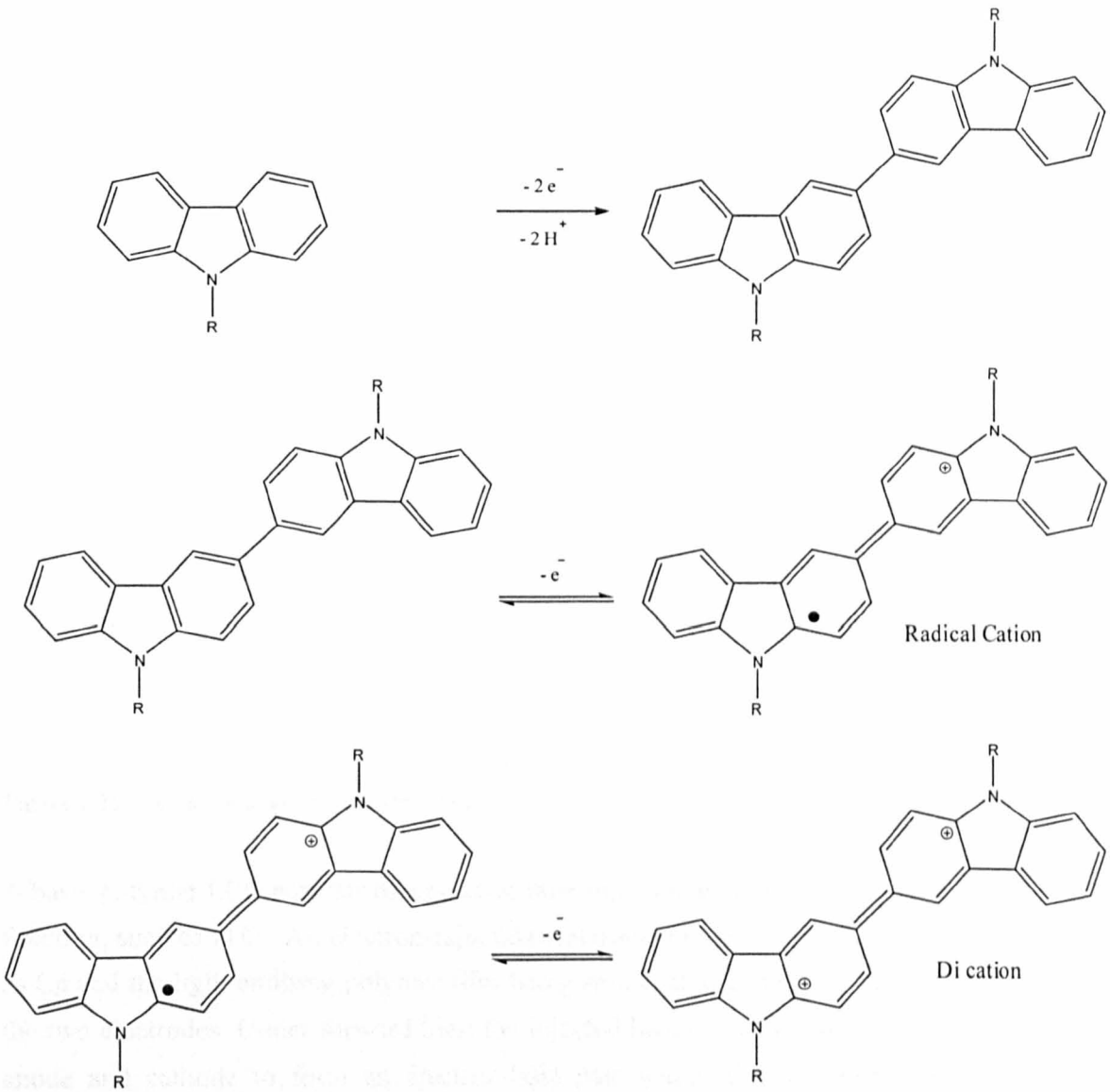

Figure 1.20, Electrochemical oxidation of N-alkylcarbazole

There have been generally three methods which have been applied to the formation of poly(3,6-carbazole)s. These have been electrochemical oxidation, [112-118] reductive polymerisations from Grignards [119-121] and coupling reactions with the use of palladium or nickel catalysts. [122-124]

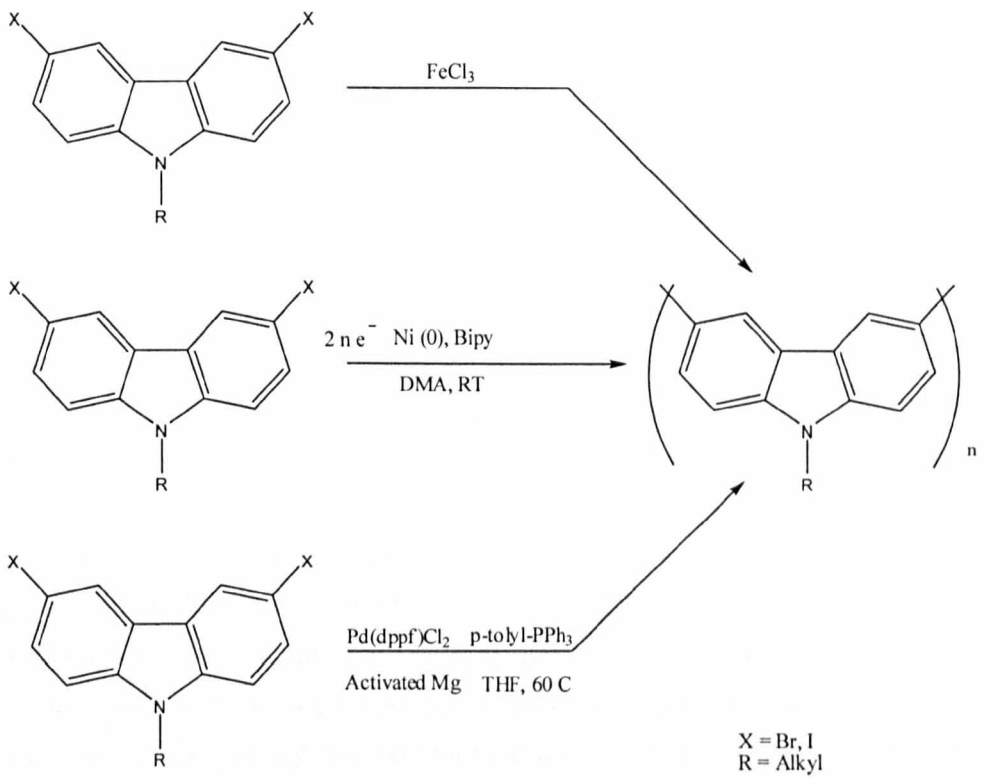

Figure 1.21, Formation of poly(3,6-carbazole)s

A basic polymer LED consists of a positive hole-injecting electrode, with a high work function, such as ITO. An electron-injecting electrode with a low work function such as Ca and the light emitting polymer film being spin coated and sandwiched between the two electrodes. Under forward bias, the injected holes and electrons migrate from anode and cathode to form an electron-hole pair within the polymer layer. This recombination results in the emission of a photon. This release of energy is dependent on the chemical structure of the polymer and on the energy of its band-gap.

Particular attention is paid to blue light [125] since the construction of blue light has been difficult to grasp in both inorganic and organic materials. Also the formation of a blue light emitting material will allow the fundamental generation of the green and red colours, whereas the reverse cannot be achieved. Blue light emission requires a high energy band gap, from the highest occupied molecular orbital to the lowest unoccupied molecular orbital.

The high molecular weight polymers formed by oxidative polymerisations are based around the 3,6-cabazole unit. [126] Due to the steric hindrance of the monomer units; this forced a chain twisting to occur which prevented π-conjugation from taking place. Electrochemical studies of these polymers showed that there was only one irreversible oxidation process. Studies were carried out in which the 3,6-carbazole monomers were co-polymerised; [127, 128] these gave polymers which exhibited redox properties that were dependent on the co-monomer structure.

The syntheses of poly(N-alkyl-carbazole-3,6-diyl)s have also been achieved via coupling reactions with the use of metal catalyst and have been applied as blue polymer light emitters. This along with their hole-transporting abilities, together with their short π-conjugation lengths and their good film-forming properties made them potential candidates as blue-light emitters in PLEDs. The polymers were applied as the hole-transporting and light emitting layer in a single layer device with ITO and Al as the anode and cathode respectively. Diodes yielded blue emission with a low EL intensity. Unfortunately, the polymer exhibited broad excimer emission in the solid state (dimerised units in the excited state emitting at lower energies), spoiling the blue emission and the device's performance. In such a PLED, the current was found to be limited by the hole carrier injection at the ITO/polymer contact. [129]

2.15.2 Poly(2,7-carbazole)

The syntheses and properties of 2,7-carbazole-based organic materials could be very interesting for electro active and photoactive devices, since carbazole units linked at the 2- and 7-positions should lead to materials having a longer conjugation length. [130-132] However, the synthesis of 2,7-carbazole-based materials is not as straightforward as that of 3,6-carbazole- based materials. Indeed, both the 2- and 7-positions are in the meta position of the amino group of the carbazole unit. These positions cannot be directly functionalised by standard electrophilic aromatic substitution. Therefore, different strategies involving precursor biphenyl units have been developed to synthesise 2,7-functionalised carbazoles.

It can be understood that poly(9-alkyl-*9H*-carbazole-2,7-diyl)s have shown similar properties to those demonstrated by poly(9,9-dialkyl-*9H*-fluorene-2,7-diyl)s. But poly(9,9-dialkyl-*9H*-fluorene-2,7-diyl)s have exhibit a red shifted emission in the solid state due to excimer emission, which is less proninate in poly(9-alkyl-*9H*-carbazole-2,7-diyl)s suggesting them to be more stable.

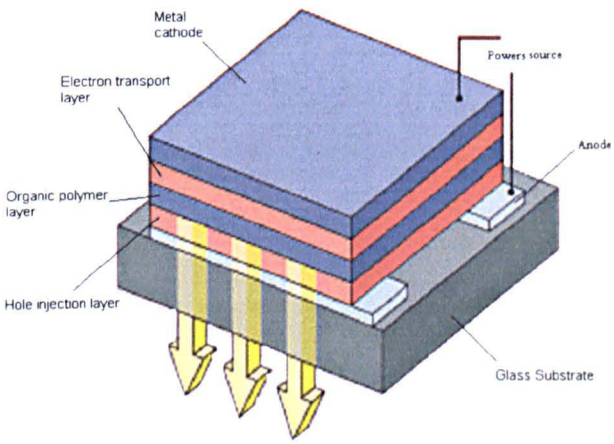

Figure 1.22, OLED / PLED device layout

Poly(9-alkyl-*9H*-carbazole-2,7-diyl)s have the advantage of being less susceptible to emission from excimer formation. Also, the carbazole rings are more electron rich than the fluorene rings found on the main chain of the polymers. These poly(9-alkyl-*9H*-carbazole-2,7-diyl)s have shown good quantum efficiencies ($E_g \approx 2.8eV$, $\Phi_F \approx 0.8$) as they have planar structure, affording a greater degree of conjugation. This difference imparts poly(9-alkyl-*9H*-carbazole-2,7-diyl)s with good hole transporting properties, therefore allowing fabrication of EL devices without the inclusion of a hole transporting layer thus solving the problem faced by the use of poly(9,9-dialkyl-*9H*-fluorene-2,7-diyl)s.

Whilst these polymers showed good PL with high quantum yield of fluorescence and good thermal stability, electrochemical studies have showed the stability of the materials was questionable. The instability can be seen to originate from the reactive 3,6 positions that are very susceptible to oxidation, which results in cross-linking within the polymer.

Although some cross-linking is thought to increase device efficiency, it is thought that these sites are so susceptible to oxidation that it would produce too much cross-linking and this would be severely detrimental to the stability and effective lifetime of the EL device, in fact rendering the polymer electrically inactive.

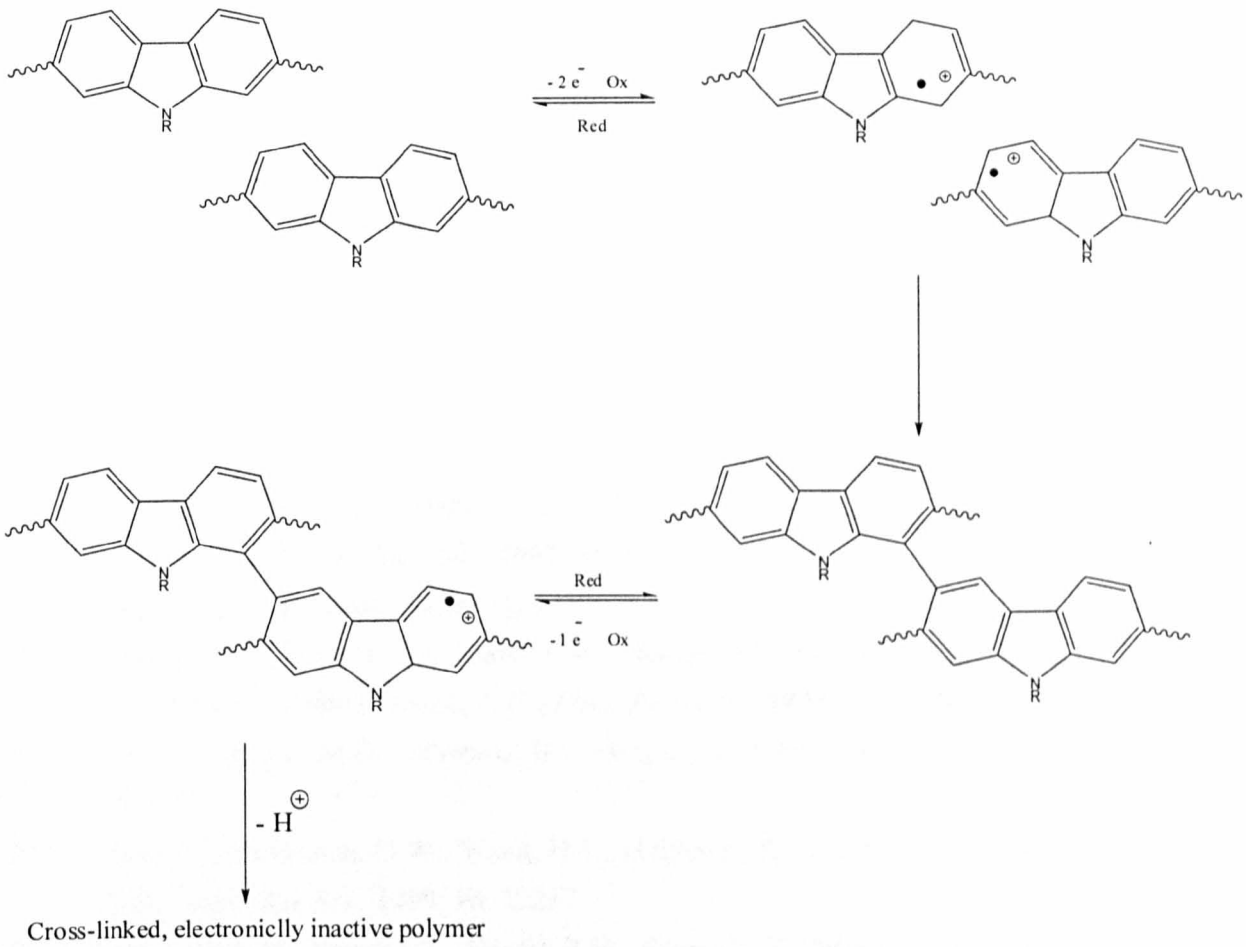

Figure 1.23, Electrochemical instability of poly(9-alkyl-*9H*-carbazole-2,7-diyl)s [133]

2.2 References

1. Yong, C., Smith, P., Heeger, A.J.; *Synth. Met.*, **1992**, *48*, 91.
2. Wallace, G.G., Dastoor, P.C., Officer, D.L., Too, C.O.; *Chem. Innovation.*, **2000**, *30*, 14.
3. Osaheni, J.A., Jenekhe, S.A.; *Chem. Mater.*, **1992**, *4*, 1282.
4. Roberts, M.F., Jenekhe, S. A.; *Chem. Mater.*, **1994**, *6*, 135.
5. Dotrong, M., Meheta, R., Balchin, G.A., Tomlinson, R.C., Sinksky, M., Lee, C.Y.-C., Evers, R.C.; *J. Poly. Sci. Part A.*, **1993**, *31*, 723
6. Skotheim, T.A., Elsenbaumer, R.L., Reynolds, J.R.; Ed. Marcel Dekker.; *Handbook of Conducting Polymers; 2 Ed.*, New York, **1998**.
7. Nalwa, H.S. Ed.; *Organic Conductive Molecules and Polymers*; John Wiley & Sons, **1997**.
8. Salzner, U., Lagowski, J.B., Pickup, P.G., Poirier, P.A.; *Synth. Met.*, **1998**, *96*, 177.
9. Roncali, J.; *Chem. Rev.*, **1997**, *97*, 173.
10. Higgins, S.J.; *Chem. Soc. Rev.*, **1997**, *26*, 247.
11. Bäuerle, P.; *Adv. Mater.*, **1993**, *5*, 879.
12. Chiang, C.K., Fincher, C.R., Park, Y.W., Heeger, A.J., Shirakawa, H., Louis, E.J., Gau, S.C., MacDiarmid, A.G.; *Phys. Rev. Lett.*, **1977**, *39*, 1098.
13. Hide, F., Garcia, M.D., Schwartz, B.J., Heeger, A.J.; *Acc. Chem. Res.*, **1997**, *30*, 430.
14. Chen, L., McBranch, D.W., Wang, H-L., Helgeson, R., Wudl, F., Whitten D.G.; *Appl. Bio. Sci.*, **1999**, *96*, 12287.
15. Sirringhaus, H., Kawase, T., Friend, R.H., Shimoda, T., Inbasekaran, M., Wu, W., Woo, E.P.; *Science*, **2000**, *290*, 2123.
16. Kraft, A., Grimsdale, A.C., Holmes, A.B.; *Ange. Chem. Inter. Ed.*, **1997**, *37*, 402.
17. Kido, J., Kimura, M., Nagai, K.; *Science*, **1995**, *267*, 1332.
18. Han, S., Huang, C., Lu, Z-H.; *J. Appl. Phys.*, **2005**, *97*, 5.
19. Burrows, P.E., Gu, G., Bulovic, V., Shen, Z., Forrest, S.R., Thompson, M.E.; *Electron Devices, IEEE Transactions*, **1997**, *44*, 1188.

20. Zheng, G., Clark, S.J., Brand, S., Abram, R.A.; *J. Phys.: Condens. Matter.*, **2004**, *16*, 8609.
21. Baughman, R.H., J. L. Breadas,J.L., Chance, R.R., Elsenbaumer, R.L., L. W. Shacklette, L.W.; *Chem. Rev.*, **1982**, *82*, 209.
22. Xie, S-J., Mei, L-M.; *J. Phys.: Condens. Matter.*, **1994**, *6*, 3909.
23. Lewis, T.J.; *Chem. Soc.*, **1989**, *88*, 189.
24. Proctor, P.; *Physiol Chem. & Phys.*, **1970**, *4*, 349.
25. Bredas, J.L., Street, G.B.; *Acc. Chem. Res.*, **1985**, *18*, 309.
26. Wudll, F.; *J. Mater. Chem.*, **2002**, *12*, 1959.
27. Stafström, S.; *Phys. Rev.*, **1985**, *B32*, 4060.
28. Drazin, P.D., Johnson R.S.; *Solitons: an introduction.* Cambridge University Press; **1989**.
29. Zabusky, N.J., Kruskal, M.D.; *Phys. Rev. Lett.*, **1965**, *15*, 240.
30. Sichel, E.K., Rubner, M.F., Tripathy, S.K.; *Phys. Res. B.*, **1982**, *26*, 6719.
31. Kivelson, S.; *Phys. Res. B.*, **1982**, *25*, 3798.
32. Chance, R.R., Bredas, J.L., Silbey, R.; *Phys. Res. B.*, **1984**, *29*, 4491.
33. Sheng, P., Abeles, B., Arie, Y.; *Phys. Res. Lett.*, **1973**, *31*, 44.
34. Wang, G., Yaun, C., Wu, H., Wei, Y.J.; *J. App. Phys.*, **1995**, *78*, 2679.
35. Hu, B., Yang, Z., Karasz, F.E.; *J. App. Phys.*, **1994**, *76*, 2419.
36. Zhang, C., Von-Seggern, H., Pakbaz, K., Kraabel, B., Schmidt, H.W., Heeger, A.J.; *Synth. Met.* **1994**, *62*, 35.
37. Martel, R., Schmidt, T., Shea, H.R., Hertel, T., Avouris P.; *Appl. Phys. Lett.*, **1998**, *73*, 2447.
38. Wang, C., Snyder, J.P., Tucker, J.R.; *Appl. Phys. Lett.*, **1999**, *74*, 1174.
39. Sheraw, C.D., Zhou, L., Huang, J.R., Gundlach, D.J., Jackson, T.N.; *Appl. Phys. Lett.*, **2001**, *80*, 1088.
40. Horowitz, G.; *Adv. Mater.*, **1999**, *10*, 365.
41. Coakley, K.M., McGehee, M.D.; *Chem. Mater.*, **2004**, *16*, 4533.
42. Peumans, P., Forrest, S.R.; *Appl. Phys. Lett.*, **2001**, *79*, 126.
43. Brabec, C.J., Sariciftci, N.S., Hummelen, J.C.; *Adv. Funct. Mater.*, **2001**, *11*, 15.
44. Halls, J.J.M., Pichler, K., Friend, R.H., Moratti, S.C., Holmes, A.B.; *Synth. Met.*, **1996**, *77*, 277.

45. Dall'olio, A., Dascola, G., Bocchi, V., Varacca, V.; *Compt. Rendu. Aca. Sci. Paris ser.*, **1968**, *C267*, 443.
46. Kulikov, V., Mirsky, V.M.; *Meas. Sci. Technol.*, **2004**, *15*, 49.
47. Babudri, F., Colangiuli, D., Farinola, G.M., Naso, F.; *Eur. J. Org. Chem.*, **2002**, 2785.
48. Mowat, W., Shortland, A., Yagupsky, G., Hill, N.J., Yagupsky, M., Wilkinson, G.; *J. Chem. Soc., Dalton Trans.*, **1972**, 533.
49. Braterman, P.S., Cross, R.J.; *Chem. Soc. Rev.*, **1973**, *2*, 271.
50. Tamao, K., Kiso, Y., Sumitani, K., Kumada, M.; *J. Am. Chem. Soc.*, **1972**, *94*, 9268.
51. Kiso, Y., Tamao, K., Kumada, M.; *J. Org. Met. Chem.*, **1973**, *C12*, 50.
52. Kosugi, M., Sasazawa, K., Shimizu, Y., Migita, T.; *Chem. Lett.*, **1977**, 301.
53. Milstein, D., Stille, J.K.; *J. Am. Chem. Soc.*, **1978**, *100*, 3636.
54. Casado, A. L., Espinet, P.; *J. Am. Chem. Soc.*, **1998**, *120*, 8978.
55. Casado, A. L., Espinet, P.; *Organometallic*, **1998**, *17*, 954.
56. Miyaura, N., Yamada, K., Suzuki, A.; *Tetra. Lett.*, **1979**, 3437.
57. Miyaura, N., Suzuki, A.; *Chem. Commun.*, **1979**, 866.
58. Matos, K., Soderquist, J. A.; *J. Org. Chem.*, **1998**, *63*, 461.
59. Helfrich, W., Schneider, W.G.; *Phys. Rev. Lett.*, **1965**, *14*, 229.
60. Helfrich, W., Schneider, W.G.; *J. Chem. Phys.*, **1965**, *44*, 2902.
61. Pope, M., Kallmann, H.P., Magnate, P.; *J. Chem. Phys.*, **1963**, *38*, 2042.
62. Tang, C.W., Van Slyke, S.A.; *Appl. Phys. Lett.*, **1987**, *51*, 913.
63. Burroughes, J.H., Bradley, D.D.C., Brown, A.R., Marks, R.N., Mackay, K., Friend, R.H., Burns, P.L., Holmes, A.B.; *Nature*, **1990**, *347*, 539.
64. Nakano, T., Doi, S., Noguchi, T., Ohnishi, T.; *Electron Devices, IEEE Transactions*, **1991**, *8*, 1253.
65. Nakano, T., Doi, S., Noguchi, T., Ohnishi, T., Iyechika, Y.; *In. Eur. Pat. Appl.*; Sumitomo Chemical Co., Ltd., Japan. Ep, **1991**, 19.
66. Rothberg, L.J., Lovinger, A.J.; *J. Mater. Res.*, **1996**, *11*, 3174.
67. Ito, T., Shirakawa, H., Ikeda, S.; *J. Poly. Sci., Poly. Chem.*, **1974**, *12*, 11.
68. Albright, T.A., Burdett, J.K., Whangbo, M.H.; *In Orbital Interactions in Chemistry*; John Wiley & Sons: New York, **1985**.

69. Peierls, R.E.; *Quantum Theory of Solids*; Oxford University Press: London, **1956**.
70. Tolbert, L.M.; *Acc. Chem. Res.*, **1992**, *25*, 561.
71. Wudl, F., Kobayashi, N., Heeger, A.J.; *J. Org. Chem.*, **1984**, *49*, 3381.
72. Segura, J.L.; *Acta. Polym.*, **1998**, *49*, 319.
73. Friend, R.H., Gymer, R.W., Holmes, A.B., Burroughes, J.H., Marks, R.N., Taliana, C., Bradley, D.D.C., Dos Santos, D A., Bredas, J.L., Logdlund, M., Salaneck, W.R.; *Nature,* **1999**, *397*, 121.
74. Yoshino, K., Nakajima, S., Fujii, M.,Sugimoto, R.; *Poly. Commun.*, **1987**, *28*, 309.
75. Zlemelis, K.; *Nature,* **1999**, *399*, 408.
76. Klärner, G., Davey, M.H., Chen, W.-D., Scott, J.C., Miller, R.D.; *Adv. Mater.*, **1998**, *10*, 993.
77. Grem, G., Leditzky, G., Ullrich, B., Leising, G.; *Adv. Mater.*, **1999**, *4*, 36.
78. Cho, H.N., Kim, J.K., Kim, D.Y., Kim, C.Y., Song, N.W., Kim, D.; *Macromolecules,* **1999**, *32*, 1476.
79. Cho, H.N., Kim, D.Y., Kim, Y.C., Lee, J.Y., Kim, C.Y.; *Adv. Mater.*, **1997**, *9*, 326.
80. Ahn, T., Jang, M.S., Shim, H.K., Hwang, D.-H., Zyung, T.; *Macromolecules,* **1999**, *32*, 3279.
81. Satoh, S., Suzuki, H., Kimata, Y., Kuriyama, A.; *Synth. Met.*, **1996**, *79*, 97.
82. Cimrova, V., Neher, D., Remmers, M., Kminek, I.; *Adv. Mater.*, **1998**, *10*, 676.
83. Garten, F., Cacialli, F., Hilberer, A., Esselink, F.J., Van Dam, Y., Schlatmann, A.R., Friend, R. H., Klapwijk, T.M., Hadziioannou, G.; *Adv. Mater.*, **1997**, *9*, 127.
84. Garten, F., Hilberer, A., Cacialli, F., Esselink, F.J., Van Dam, Y., Schlatmann, A.R., Friend, R.H., Klapwijk, T.M., Hadziioannou, G.; *Synth. Met.*, **1997**, *85*, 1253.
85. Bouché, C.-M., Berdagué, P., Facoetti, H., LeBarny, P., Schott, M.; *Synth. Met.* **1996**, *81*, 191.
86. Boyd, T.J., Geerts, Y., Lee, J.-K., Fogg, D.E., Lavoie, G.G., Schrock, R.R., Rubner, M.F.; *Macromolecules,* **1997**, *30*, 3553.

87. Cumming, W., Gaudiana, R.A., Hutchinson, K., Kolb, E., Mehta, P., Minns, R.A., Petersen, C.P., Waldman, D.; *J.M.S; -P. Appl. Chem.*, **1996**, *A331*, 1301.
88. Kim, Y., Kwon, S., Yoo, D., Rubner, M.F., Wrighton, M.S.; *Chem. Mater.* **1997**, *9*, 2699.
89. Pyo, S.M., Kim, S.I., Shin, T.J., Park, H.K., Ree, M., Park, K.H., Kang, J.S.; *Macromolecules,* **1998**, *31*, 4777.
90. Hsieh, B.R., Yu, Y., Forsythe, E.W., Schaaf, G.M., Feld, W.A.; *J. Am. Chem. Soc.* **1998**, *120*, 231.
91. Huang, W., Meng, H., Yu, W.L., Gao, J., Heeger, A.J.; *Adv. Mater.* **1998**, *10*, 593.
92. Grice, A.W., Tajbakhsh, A., Burn, P.L., Bradley, D.C.; *Adv. Mater.* **1997**, *9*, 1174.
93. Rehahn, M., Schluter, A.D., Wegner, G., Feast, W.J.; *Polymer,* **1989**, *30*, 1054.
94. Leclerc, M., Faid, K.; *Adv. Mater.*, **1997**, *9*, 1087.
95. McCullough, R.D.; *Adv. Mater.*, **1998**, *10*, 93.
96. Leclerc, M.; *Adv. Mater.*, **1999**, *11*, 1491.
97. Leclerc, M.; *J. Polym. Sci. Polym. Chem.*, **2001**, *39*, 2867.
98. Yang, Y., Pei, Q., Heeger, A.J.; *Synth. Met.*, **1996**, *78*, 263.
99. Ranger, M., Rondeau, D., Leclerc, M.; *Macromolecules,* **1997**, *30*, 7686.
100. Neher, D.; *Macromol. Rapid Commun.*, **2001**, *22*, 1366.
101. Grazulevicius, J.V., Strohriegl, P., Pielichowski, J., Pielichowski, K.; *Prog. Polym. Sci.*, **2003**, *28*, 1297.
102. Pearson, J.H., Stolka, M.; M.B. Huglin Ed., *Polymer Monographs,* Vol. 6, Gordon and Breach, New York, **1981**.
103. Stolka, M.; *En. Poly. Sci. Eng.*, Vol. 11, Wiley, New York, **1988**.
104. Narmann, H., Strohriegl, P.; *Handbook of Polymer Synthesis,* M. Dekker, New York, **1992**.
105. Borsenberger, P.M., Weiss, D.; *Organic Photoreceptors for Xerography,* M. Dekker, New York, **1998**.
106. Desbene-Monvernay, A., Lacaze, P.C., Dubois, J.E., *J. Electroanal. Chem.*, **1981**, *129*, 229.

107. Mengoli, G., Musiani, M.M., Schreck, B., Zeccin, S.; *J. Electroanal. Chem.*, **1988**, *246*, 73.
108. Cattarin, S., Mengoli, G., Musiani, M.M., Schreck, B.; *J. Electroanal. Chem.*, **1988**, *246*, 87.
109. Marrec, P., Dano, C., Gueguen-Simonet, N., Simonet, J.; *Synth. Met.*, **1997**, *89*, 171.
110. Ambrose, J.F., Nelson, R.F., *J. Electrochem. Soc. Electrochem. Sci.*, **1967**, *115*, 1159.
111. Ambrose, J.F., Carpenter, L.L., Nelson, R.F.; *J. Electrochem. Soc. Electrochem. Sci. Techn.*, **1975**, *122*, 876.
112. Siove, A., Ade`s, D., Chevrot, C., Froyer, G.; *Macromol. Chem.*, **1989**, *190*, 1361.
113. Ngbilo, E., Ade`s, D., Chevrot, C., Siove, A.; *Polym. Bull.*, **1990**, *24*, 17.
114. Siove, A., Ade`s, D., Ngbilo, D., Chevrot, C.; *Synth. Met.*, **1990**, *38*, 331.
115. Helary, G., Chevrot, C., Sauvet, G., Siove, A.; *Polym. Bull.*, **1991**, *26*, 131.
116. Faid, K., Ade`s, D., Chevrot, C., Siove, A.; *Macromol. Chem. Macromol. Symp.*, **1991**, *47*, 377.
117. Aboulkassim, A., Faid, K., Siove, A.; *Macromol. Chem.*, **1993**, *194*, 29.
118. Siove, A., Aboulkassim, A., Faid, K., Ade`s, D.; *Polym. Int.*, **1995**, *37*, 171.
119. Wellinghoff, S.T., Deng, Z., Reed, J.F.; *J. Racchini, Polym. Prepr.*, **1984**, *25*, 238.
120. Jenekhe, S.A., Wellinghoff, S.T., Reed, J.F.; *Mol. Cryst. Liq. Cryst.*, **1984**, *105*, 175.
121. Wellinghoff, S.T., Deng, Z., Reed, J.F., Jenekhe, S.A.; *Mol. Cryst. Liq. Cryst.*, **1985**, *118*, 403.
122. Geissler, U., Hallensleben, M.L., Rienecker, A., Rohde, N.; *Polym. Adv. Technol.*, **1997**, *8*, 87.
123. Iraqi, A., Wataru, I.; *Synth. Met.*, **2001**, *119*, 159.
124. Iraqi, A., Wataru, I.; *J. Polym. Sci., A: Polym. Chem. Ed.*, **2004**, *42*, 6041.
125. Kim, D.Y., Cho, H.N., Kim, C.Y.; *Prog. Polym. Sci.*, **2000**, *25*, 1089.
126. Siove, A., Ade`s, D.; *Polymer.*, **2004**, *45*, 4045.
127. Gaupp, C.L., Reynolds, J.R.; *Macromolecules*, **2003**, *36*, 6305.

128. Sotzing, G.A., Reddinger, J.L., Katritzky, A.R., Soloducho, J., Musgrave, R., Reynolds, J.R.; *Chem. Mater.*, **1997**, *9*, 1578.
129. Limouni, K., Legrand, C., Chapoton, A.; *Synth. Met.*, **1998**, *97*, 151.
130. Belletete, M., Bedard, M., Leclerc, M., Durocher, M.; *J. Mol. Struct.*, **2004**, *679*, 9.
131. Belletete, M., Bedard, M., Bouchard, J., Leclerc, M., Durocher, M.; *Can. J. Chem.*, **2004**, *82*, 1280.
132. Briere, J-F., Cote, M.; *J. Phys. Chem. B.*, **2004**, *108*, 3123.
133. Zotti, G., Schiavon, G., Zecchin, S., Morin, J.-F., Leclerc, M.; *Macromolecules*, **2002**, *35*, 2122.

3.0 Aims and objectives

The aim of this project is to develop and characterise novel blue light emitting polymers for application in electroluminescent devices. Currently there is a considerable drive to develop highly fluorescent blue light emitting polymers. Such polymers are not only required for efficient emission in the blue part of the electromagnetic spectrum but could also serve as energy transfer donors when used in conjunction with added lower bandgap fluorophores.

Previous work has seen the development route to two families of carbazole main chain conjugated polymers in which the carbazole repeat units are either linked through the 2,7-positions giving poly(9-alkyl-carbazole-2,7-diyl)s (**1**) or the 3,6 positions giving poly(9-alkyl-carbazole-3,6-diyl)s (**2**).

The poly(9-alkyl-carbazole-2,7-diyl)s have been prepared via a palladium catalysed Suzuki cross-coupling reaction, and the poly(9-alkyl-carbazole-3,6-diyl)s have been synthesised via a palladium catalysed Grignard type reaction. Both set of polymers have been fully characterised. While the electronic conjugation has been limited to about two carbazole repeat units in the case of poly(9-alkyl-carbazole-3,6-diyl)s, it is further extended in the case of poly(9-alkyl-carbazole-2,7-diyl)s. These polymers have shown quantum efficiencies for poly(9-alkyl-carbazole-2,7-diyl)s – fluorescence quantum yield Φ_{fl} = 0.800 ± 0.08 in dichloromethane and a fluorescence quantum yield of Φ_{fl} = 0.065 ± 0.006 in dichloromethane for poly(9-alkyl-carbazole-3,6-diyl)s

Further work has been carried out on the poly(9-alkyl-carbazole-2,7-diyl)s to protect the 3,6-positions in order to impart better electrochemical stability towards oxidation producing poly(9-alkyl-3,6-dimethyl-carbazole-2,7-diyl)s (**3**) which has also been full characterised. Also a series of co-polymer have been produced with all three of these carbazole polymers in order to improve their electrochemical and physical properties.

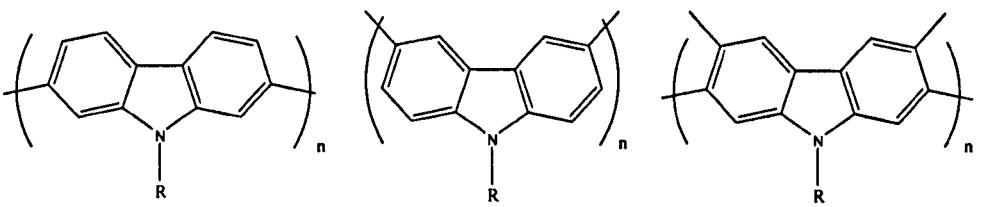

(1) (2) (3) R - alky group

This project concerns the development of a new method for the formation to a new class of poly-carbazoles. It is in order to develop arylated side groups that will be coupled to the 9-position of the carbazole moieties forming poly(9-aryl-carbazole-2,7-diyl)s and poly(9-aryl-carbazole-3,6-diyl)s. It is hoped that these new compounds will develop stable blue light emitting materials consisting of new main chain carbazole polymers with aryl substituents.

The introduction of aryl groups at the 9-position should ensure that the materials obtained would have low ionisation potentials. This is important for the injection of holes from the ITO electrodes into polymer films during LED device operation and should lead to devices with low turn on voltages. It is also hoped that this would allow the exploitation of the energy transfer donor properties of these wide band gap polymers by the variation of aryl substituents. In addition to this these polymers would also contain alkoxy solubilising groups, which should ensure good processibility of the resulting materials.

These materials are intended for studies of their physical and electrochemical properties as well as their blends with various other monomers and fluorophores in order to develop LED devices with enhanced charge mobilities, high external quantum efficiencies, low turn-on voltages and extended lifetimes.

4.0.0 Experimental

4.1.0 Materials

1-Chloro-3,5-dimethoxybenzene, 3,5-dimethoxy-phenyl-amine, potassium hydroxide (flakes/pellets/powder), potassium tri phosphate, 18-crown-6 ether, ethylenediamine, copper (I) chloride, copper (I) iodide, ethylene diamine, dimethyl ethylenediamine were ordered from Lancaster Synthesis and used as received.

2,5-Dibromo-nitrobenzene, 2,5-dibromo-toluene, 2-butyl-octylbromide, 2-ethyl-hexylbromide, dichloro-palladium(II)-(2,2'-bipyridine), palladium acetate, palladium dba, tert-butyl-lithium, borolane, bis-pinacolate, dodecylbenzenesulphonic acid, tetrabutylammonium hydrogensulfate, tetrabutylammonium hydroxide, 4-iodo-anisole, *9H*-carbazole, N-bromosuccinimide, 5-tert-butyl–*m*-xylene, 1,10-phenthroline, copper powder, tin powder, 4,4'-(9,9-dioctyl-*9H*-fluorene-2,7-diyl)bis(1,2,4-dioxaborolane), 2,7-dibromo-9,9-dioctyl-9H-fluorene, chloroform-d_1, acetone-d_6, boron tribromide were ordered from Aldrich Chemicals Ltd and where necessary received and stored under an inert atmosphere.

Magnesium (flakes), iodine (crystals), 37% hydrochloric acid, 57% hydroiodic acid, potassium hydroxide (pellets), anhydrous potassium carbonate, sodium chloride, magnesium sulphate were used as received from internal stores. N,N-dimethylformaide, toluene, dichloromethane, carbon disulphide, diethylamine, tetrahydrofuran, dioxane, acetone (HPLC), ethanol (HPLC) methanol (HPLC), petroleum ether (40-60), hexane, ethyl acetate were obtained from commercial stores, dried and distilled before use. Diethyl ether were used as received from internal stores via Grubbs Dry Solvent dispenser.

4.2.0 Measurements & Instruments

NMR spectra were obtained using the Bruker 250 MHz, AMX400 400 MHz or DRX500 500MHz NMR spectrometers at 22°C in chloroform-*d*1 or acetone-*d*6 solutions. Coupling constants are measured in Hertz and chemical shifts in ppm.

IR absorption spectra were recorded on the Nicolet Model 205 FT-IR Spectrometer. Liquid samples were analysed neat, using NaCl–plate method and solid samples were analysed using the Diamond ATR attachment for solid samples.

Melting points were obtained using Gallenkamp Melting Point Apparatus. GC-MS spectra were recorded on Perkin Elmer Turbomass Mass Spectrometer equipped with a Perkin Elmer Autosystem XL Gas Chromatograph.

Mass spectra were obtained by the electron impact method (EI) or the chemical ionisation method (CI).

GPC curves were recorded on the equipment consisting of Waters Model 515 HPLC Pump, GILSON Model 234 Autoinjector, MILLIPORE Waters Lambda-Max Model 481 LC Spectrometer, Erma ERC-7512 RI Detector, PLgel 5m 500^{a} Column, and PLgel 10m MIXED-B Column using THF as the eluent at a rate of 1 cm^3 $minute^{-1}$. Polymer solutions in THF (2.5 mg cm^{-3}) were used as samples for GPC analysis. The GPC curves were obtained by the RI-detection method, which was calibrated with a series of polystyrene narrow standards (Polymer Laboratories).

Elemental analyses were carried out by the Perkin Elmer 2400 CHN Elemental Analyser for CHN analysis and by the Schöniger oxygen flask combustion method for anion analysis.

UV-visible absorption spectra were measured by Hitachi U-2010 Double Beam UV / Visible Spectrophotometer. The absorbance of monomers and polymers was measured in a solution of spectrophotometric solvents at ambient temperature using rectangular quartz cuvettes (light path length = 10 mm) purchased from Sigma-Aldrich. Samples of pristine polymer thin films for UV-visible absorption spectra measurements were prepared by dip coating quartz slides in solutions and were carried out at ambient temperature.

PL spectra were obtained using the Hitachi F-4500 Fluorescence Spectrophotometer equipped with Hamamatsu Photonics R928F Photomultiplier Tube (PMT). PL solution measurements were carried out using the Quartz Fluorescence Cuvette (light path length = 10 mm) purchased from Sigma-Aldrich. All measurements were carried out in a dilute solution of spectrophotometric solvents at ambient temperature without the presence off air. The UV-vis absorbance of the samples was kept below 0.05 in order to obtain PL spectra free from inner–filter effects. Samples of pristine polymer thin films for PL spectra measurements were prepared by dip coating quartz plates into 0.1 mg cm^{-3} polymer solutions in toluene (spectroscopic grade), and the measurements were carried out at ambient temperature in the air.

Harmine and quinine sulfate dihydrate in 0.05 and 0.5 mol dm^{-3} sulfuric acid, respectively, were employed as fluorescence standards. The quantum yields in diluted solutions were obtained by comparison with a fluorescence standard of a known quantum yield using the following equation:

$$\Phi_x = \Phi_s \times \left(\frac{A_s}{S_s}\right) \times \left(\frac{S_x}{A_x}\right) \times \left(\frac{n_x^2}{n_s^2}\right) \qquad \text{Equation 5}$$

where the subscripts s and x refer to the standard and the unknown sample solutions, Φ is the quantum yield, A is the absorbance at used excitation wavelength, S is the integral intensity of the corrected photoluminescence spectra, and n is the refractive index of the solvent. The fluorescence standard solution and the unknown sample solution were excited at the same wavelength. Quinine sulfate dihydrate solution in 0.5 mol dm^{-3} sulfuric acid (Φs = 0.546) was employed as the fluorescence standard solution. With regard to the refractive indexes of the solvents, 1.339, 1.334, and 1.424 were employed for, respectively, 0.5 mol dm^{-3} sulfuric acid, 0.05 mol dm^{-3} sulfuric acid, and dichloromethane. (S/A) values of each sample in solution could be obtained by simply dividing the integral intensities of the spectra by the absorbances at used excitation wavelengths using a sample solution of a certain concentration.
To minimize experimental error, the final (S/A) values used in the calculations for each sample were obtained from the plots of the integral intensities of the spectra vs the absorbances at used excitation wavelengths using sample solutions of various

concentrations. Reliability of our measurements was confirmed upon measurement of the quantum yield of harmine using quinine sulfate dihydrate as a standard. The experimental value obtained was identical to that reported in the literature [28] (Φs = 0.45).

Thermo Gravimetric Analysis - TGA curves were obtained by using the Perkin Elmer Pyris 1 Thermo gravimetric Analyzer at the scan rate of 20°C minute^{-1} under an inert nitrogen atmosphere. The weights of the samples were ca. 5 mg.

DSC curves were recorded on the Perkin Elmer Pyris 1 Differential Scanning Calorimeter equipped with Perkin Elmer CCA 7 Subambient Accessory at the scan rate of 10°C minute^{-1} under inert nitrogen atmosphere.

Cyclic voltammograms were recorded with the equipment consisting of Princeton Applied Research Model 263A Potentiostat/Galvanostat and K0264 Micro Cell Kit of which the reference electrode was transformed from Ag / AgCl reference electrode into Ag/ Ag^+ reference electrode. Measurements were carried out under an inert argon atmosphere at ambient temperature. 10 cm^3 of tetrabutylammonium perchlorate solution in acetonitrile (HPLC grade) (0.1 mol dm^{-3}) was used as the electrolyte solution. A three electrode system was used consisting of Ag / Ag^+ reference electrode (silver wire in 0.01 mol dm^{-3} silver nitrate solution in the electrolyte solution), platinum working electrode (2mm-diameter smooth platinum disc), and platinum counter electrode (platinum wire). Polymer thin films were formed by drop casting 1.0 mm^3 of polymer solutions in dichloromethane (HPLC grade) (1 mg cm^{-3}) onto the working electrode, then dried in the air. Ferrocene was employed as a reference redox system according to IUPAC's recommendation. [29] Fresh reference electrodes were made before each series of measurements and calibrated against Fc/Fc^+. Polymer thin films were formed by drop-casting 1.0 mm^3 of polymer solutions in dichloromethane (analytical reagent, 1 mg cm^{-3}) onto the working electrode, and then dried in the air.

4.3.0 Synthesis of 2,7-dibromo-*9H*-carbazole (3)

4.3.1 4,4'-Dibromo-2,2'dinitrobiphenyl [1] (1)

Into a reaction vessel was placed 1,4-dibromo-nitrobenezene (99.93 g, 354 mmol), copper mesh (-100) powder (50.00 g, 788 mmol) and dry DMF (600 cm^3). The system was degassed and allowed to reflux for 2 hours with the aid of stirring under a nitrogen atmosphere. The mixture was then allowed to cool to room temperature; dry toluene (750 cm^3) was added to the mixture while stirring gently. The precipitate was filtered off leaving a dark brown solution. The filtrate was washed with saturated sodium chloride solution (3 x 600 cm^3). This left a bright clear yellow solution obtained as the organic layer which was dried over $MgSO_4$. The organic layer was filtered and the solvent removed under vacuum. The crude product was re-crystallised from ethanol (1500cm^3) separating a single product which was dried under vacuum. A yellow crystalline solid of mass 53.35 g, yielding 74% was obtained. The melting point of 147 – 149 °C was obtained which fell in to the literature barrier 146 – 148 °C [1]. GCMS: RT: 14.7 min.; CHN Br - $C_{12}H_6Br_2N_2O_4$ Expected; C, 35.85; H, 1.50; Br, 39.75; N, 6.97; O, 15.92.% Achieved; C, 37.95; H, 1.47; Br, 40.70; N, 6.89.%; I.R cm^{-1}(KBr): 3071, 2850, 1936, 1925, 1860, 1786, 1780, 1672, 1602, 1554, 1528, 1464, 1341, 1279, 1239, 1147, 1095, 999, 896, 865, 839, 782, 762, 729, 704, 677, 581, 553, 509.; Mass (EI); (m/z): 400, 402, 404 (M^+).; ^1H NMR: ($CDCl_3$) δ_H: 8.37 (2H, d, *J*=2Hz); 7.83 (2H, dd, *J*=8Hz); 7.17 (2H, d, *J*=8Hz).; ^{13}C NMR: ($CDCl_3$) δ_C: 147.5 (2C), 138 (2C), 132 (4C); 128 (2C); 123 (2C).:

4.3.2 2,2'-Diamino-4,4'-dibromobiphenyl [1] (2)

Into a reaction vessel was placed 4,4'-dibromo-2,2'-dinitrobiphenyl (53.35 g, 132.30 mmol), ethanol HPLC grade (800 cm^3), 37% hydrochloric acid (330 cm^3) and tin powder (-325 mesh) (58.97 g, 529 mmol). The vessel was degassed and refluxed for 1 hour under a nitrogen atmosphere. The vessel was allowed to cool to room temperature and a second portions of tin powder (-325 mesh) (58.97g, 526mmol) was added, and then the reaction vessel was further degassed and allowed to reflux for 1 hour under a nitrogen atmosphere. The vessel was once again cooled to room

temperature and the un-reacted tin powder was filtered off. The remaining yellow solution was poured into a large amount of ice and 10% sodium hydroxide solution (1500 cm^3). The solution converted to a white / cream precipitate which was filtered through sintered filter funnel lined with Celite® to aid filtration. The solution was then extracted with DCM (3 x 600 cm^3) and the organic layer washed consecutively with de-ionised water (3 x 300 cm^3). The extracts were combined and dried over $MgSO_4$, and the solvent were then removed under vacuum, resolving 41.78 g of crude solid. The crude solid was re-crystallised from ethanol (85 cm^3) to yield a single spot. The product was dried under vacuum. A yellow crystalline solid of mass 32.06, yielding 89% was obtained. The melting point of 101 – 103°C was obtained which fell in to the literature barrier 99 – 105 °C [1]. GCMS: RT: 14.6 min.; CHN Br – $C_{12}H_{10}Br_2N_2$ Expected; C, 42.14; H, 2.95; Br, 46.72; N, 8.19.% Achieved; C, 42.58; H, 2.35; Br, 47.80; N, 8.27.%; I.R cm^{-1}(KBr): 3396, 3289, 3186, 3073, 3006, 1881, 1866, 1694, 1639, 1579, 1558, 1491, 1474, 1402, 1289, 1272, 1253, 1153, 1135, 1084, 997, 931, 893, 868, 855, 832, 811, 767, 739, 709, 682, 667, 600, 581, 554, 527, 506, 467, 434.; Mass (EI); (m/z): 340, 342, 344 (M^+).; ^1H NMR: ($CDCl_3$) δ_H: 7.00 (2H, s), 6.97-6.82 (4H, m). 3.74 (4H, br s).; ^{13}C NMR: ($CDCl_3$) δ_C: 145 (2C) 132 (2C); 123 (2C); 122 (2C), 119 (2C); 118 (2C).:

4.3.3 2,7-Dibromo-*9H*-carbazole [1] (3)

Into a reaction vessel was placed 2, 2'-diamino-4, 4'dibromobiphenyl (32.00g, 93mmol), dodecylbenzenesulfonic acid (49.80g, 176mmol) and 5-*tert*-butyl-*m*-xylene (260 cm^3). The vessel was degassed and refluxed under a nitrogen atmosphere for 24 hours. The vessel was allowed to cool to room temperature and 5-*tert*-butyl-*m*-xylene was removed by distillation under vacuum to leave a residue. The residue was then run through a flash column using toluene / pet ether; 30 / 70 via a procedure by Harwood[2]. The solvent was removed invacuo to leave a solid which was further dried under vacuum to give 2,7-dibromocarbazole. An orange crystalline solid of mass 26.85 g, yielding 87% was obtained. The melting point of 217 – 220°C was obtained which was close to the literature barrier 233 – 234 °C [1]. GCMS: RT: 15.0 min.; CHN Br – $C_{12}H_7Br_2N$ Expected; C, 44.35; H, 2.17; Br, 49.17; N, 4.31.%; Achieved; C, 44.95; H, 2.67; Br, 49.97; N, 4.21.%; I.R cm^{-1}(KBr) 3400, 3100, 3074,

1889, 1705, 1625, 1600, 1481, 1461, 1448, 1424, 1349, 1329, 1315, 1256, 1241, 1203, 1139, 1058, 1005, 949, 897, 861, 805, 732, 662, 600, 534, 471.; Mass (EI); (m/z): 323, 325, 327 (M^+).; ^1H NMR: (Acetone-d_6) δ_H: 10.67 (1H, br s), 8.04 (2H, d, *J*=8Hz); 7.73 (2H, d, *J*=2Hz); 7.34 (2H, dd, *J*=8, 2Hz).; ^{13}C NMR: (Acetone-d_6) δ_C: 142 (2C); 124 (2C); 123 (2C); 122 (2C); 120 (2C), 115 (2C).:

4.4.0 Synthesis of 2,7-dibromo-3,6-dimethyl-*9H*-carbazole (7)

4.4.1 2,5-Dibromo-4-nitro-toluene [2] (4)

Into an oven dried flask was placed potassium nitrate (KNO_3) (10.1g, mmol) and sulphuric acid (H_2SO_4) (450 cm^3) under an inert nitrogen atmosphere. The reaction vessel was placed into an ice bath and water (150 cm^3) was added dropwise to the solution followed by 2,5-dibromotoluene (25 g, 100 mmol). The reaction was then heated in a water bath (40°C) for 3 hours. The reaction mixture was cooled to room temperature and poured onto water/ice (1500 cm^3), then followed by an extraction with DCM (3 x 100 cm^3). The organic layer was washed with water (3 x 50 cm^3) and dried over $MgSO_4$ before the solvent being removed invacuo. The crude product was re-crystallised from ethanol to give a solid compound which was dried under vacuum producing 26.35 g, 89% of product. The melting point of 158 – 160 °C was obtained. GCMS: RT: 14.39 min.; CHN Br – $C_7H_5NO_2Br_2$ Expected; C, 28.47; H, 1.69; N, 4.75; Br, 54.24.% Achieved C, 28.52; H, 1.50; N, 4.60; Br, 54.30.%; I.R cm^{-1}(KBr) 3090, 2973, 2854, 1769, 1562, 1511, 1456, 1386, 1332, 1281, 1258, 1212, 1135, 1055, 1028, 915, 892, 820, 749, 694, 640, 586, 574.; Mass (EI); (m/z): 293, 295, 297 (M^+).; ^1H NMR: ($CDCl_3$) δ_H: 8.02 (s, 1H), 7.55 (s, 1H), 2.39 (s, 3H).; ^{13}C NMR: ($CDCl_3$) δ_C: 147 (1C); 144 (1C); 136 (1C); 129 (1C); 123 (1C); 113 (1C); 22 (1C).:

4.4.2 4,4'-Dibromo-2,2'-dinitro-5,5'-dimethylbiphenyl [1] (5)

Into a reaction vessel was placed 2,5-dibromo-4-nitro-toluene (75 g, 254.2 mmol), copper mesh (-100) powder (37.50 g, 559.24 mmol) and DMF (450 cm^3). The system was degassed and allowed to reflux for 2 hours with the aid of stirring under a

nitrogen atmosphere. The complex was then allowed to cool to room temperature; toluene (550 cm^3) was added to the mixture while stirring gently. The precipitate was filtered leaving a dark brown solution. The filtrate was washed with saturated sodium chloride solution (3 x 400 cm^3). This left a bright clear yellow solution obtained as the organic layer which was dried over $MgSO_4$. The organic layer was filtered and the solvent removed invacuo. The crude product was re-crystallised from ethanol (1000 cm^3) separating a single product which was dried under vacuum. A yellow crystalline solid of mass 45.53 g, yielding 86% was obtained. The melting point of 241.0 – 243.9 °C was obtained which was close to the literature barrier 228 – 230 °C [1]. GCMS: RT: 11.04 min.; CHN Br – $C_{14}H_{10}N_2O_2Br_2$ Expected; C, 39.10; H, 2.34; N, 6.51; Br, 37.16.% Achieved; C, 39.20; H, 2.79; N, 5.60; Br, 36.67.%; I.R cm^{-1}(KBr): 3106, 2961, 1596, 1562, 1513, 1434, 1382, 1338, 1283, 1260, 1117, 1095, 1057, 1034, 1012, 913, 894, 881, 840, 798, 761, 738, 699, 684, 658, 630, 620, 569, 545.; Mass (EI); (m/z): 428, 430, 432 (M^+).; ^1H NMR: ($CDCl_3$) δ_H: 8.36 (s, 2H), 7.06 (s, 2H), 2.43 (s, 6H).; ^{13}C NMR: ($CDCl_3$) δ_C: 146 (2C), 145 (2C); 133 (2C); 132 (2C); 128 (2C); 124 (2C); 23 (2C).:

4.4.3 4,4'-Diamino-2,2'-dibromo-5,5'-dimethylbiphenyl [1] (6)

Into a reaction vessel was placed 4,4'-dibromo-2,2'-dinitro-5,5'-dimethylbiphenyl (45 g, 110 mmol), ethanol (HPLC grade) (800 cm^3), 37% hydrochloric acid (330 cm^3) and tin powder (-325 mesh) (52 g, 440 mmol). The vessel was degassed and refluxed for 1 hour under a nitrogen atmosphere. The vessel was allowed to cool to room temperature and a second portions of tin powder (-325 mesh) (52g, 440mmol) was added, and then the reaction vessel was further degassed and allowed to reflux for 1 hour under a nitrogen atmosphere. The vessel was once again cooled to room temperature and the un-reacted tin powder was filtered off. The remaining yellow solution was poured into a large amount of ice and 10% sodium hydroxide solution (1500 cm^3). The solution converted to a white / cream precipitate which was filtered through sintered filter funnel lined with Celite® to aid filtration. The solution was then extracted with DCM (3 x 600 cm^3) and wash consecutively with de-ionised water (3 x 300 cm^3). The extracts were combined and dried over $MgSO_4$, and the solvent were then removed invacuo. The crude solid was re-crystallised from ethanol

(65 cm^3) to yield a single product which was dried under vacuum. A yellow crystalline solid of mass 34.73 g, yielding 90% was obtained. The melting point of 122 – 123 °C was obtained. GCMS: RT: 12.86 min.; CHN Br – $C_{14}H_{14}N_2Br_2$ Expected; C, 45.44; H, 3.81; N, 7.57; Br, 43.18.% Achieved; C, 45.39; H, 3.84; N, 6.99; Br, 46.47.%; I.R cm^{-1}(KBr): 3402, 3294, 3092, 3015, 2960, 2869, 2017, 1967, 1918, 1848, 1789, 1715, 1615, 1584, 1474, 1438, 1349, 1324, 1291, 1268, 1194, 1135, 1102, 1074, 1002, 976, 925, 904, 880, 862, 823, 779, 718, 665, 652, 611, 594, 563, 534, 510.; Mass (EI); (m/z): 368, 370, 372 (M^+).; ^{1}H NMR: ($CDCl_3$) δ_H: 6.98 (s, 2H), 6.92 (s, 2H), 3.51 (br s, 4H), 2.29 (s, 6H).; ^{13}C NMR: ($CDCl_3$) δ_C: 142 (2C), 132 (2C); 127 (2C); 123 (2C); 119 (2C); 118 (2C); 21 (2C).:

4.4.4 2,7-Dibromo-3,6-dimethyl-*9H*-carbazole [1] (7)

Into a reaction vessel was placed 4,4'-diamino-2,2'-dibromo-5,5'-dimethylbiphenyl (30 g, 86 mmol), dodecylbenzenesulfonic acid (45.80 g, 160 mmol) and 5-*tert*-butyl-*m*-xylene (250 cm^3). The vessel was degassed and refluxed under a nitrogen atmosphere for 24 hours. The vessel was allowed to cool to room temperature and 5-*tert*-butyl-*m*-xylene was removed by distillation under vacuum to leave a residue. The residue was then run through a flash column using ethyl acetate / pet, ether; 20 / 80. The solvent was removed in-vacuo to leave a solid which was further dried under vacuum to give 2,7-dibromo-3,6-dimethyl-9H-carbazole; as dark orange crystalline solid of mass 23.50 g, yielding 82% was obtained. The melting point of 242.2 – 243.4 °C was obtained. GCMS: RT: 11.34 min.; CHN Br – $C_{14}H_{11}NBr_2$ Expected: C, 47.63; H, 3.14; N, 3.97; Br, 45.26. Achieved; C, 47.93; H, 3.30; N, 3.98; Br, 44.91.; I.R cm^{-1}(KBr): 3416, 2921, 2360, 1707, 1601, 1479, 1450, 1377, 1324, 1303, 1276, 1241, 1210, 1053, 1038, 995, 972, 903, 874, 856, 809, 777, 724, 669, 620, 598, 579, 570.; Mass (EI); (m/z): 351, 353, 355 (M^+).; ^{1}H NMR: ($CDCl_3$) δ_H: 7.86-7.85 (br m, 3H), 7.60 (s, 2H), 2.54 (s, 6H).; ^{13}C NMR: ($CDCl_3$) δ_C: 140 (2C) 128 (2C); 123 (2C); 122 (2C); 120 (2C); 115 (2C); 23 (2C).:

4.5.0 Synthesis of 3,6-dibromo-*9H*-carbazole [3] (8)

A mixture of *9H*-carbazole (1.10 g, 6.5 mmol), silica gel 60 (20 g) and N-bromosuccinimide (NBS) (2.32 g, 13 mmol) in DCM (150 cm^3) was stirred for 20 hours in the absence of light at room temperature. The precipitate was filtered off and washed with DCM (100 cm^3). The combined organic layer was washed with 10wt% NaOH aqueous solution (2 x 200 cm^3) followed by water (3 x 200 cm^3). The organic layer was dried over $MgSO_4$ and solvent removed invacuo. The crude product was re-crystallised from ethanol (30 cm^3) and dried under vacuum to give 3,6-dibromo-*9H*-carbazole 1.55 g in 74% yield. The melting point of 207 – 208 °C was obtained which fell in to the literature barrier 206 – 208 °C [3]. GCMS: RT: 14.64min.; CHN Br – $C_{12}H_7NBr_2$ Expected: C, 44.35; H, 2.17; N, 4.31; Br, 49.17.% Achieved; C, 44.12; H, 2.19; N, 4.38; Br, 49.91.%; I.R cm^{-1}(KBr); 3437, 3074, 1871, 1813, 1736, 1632, 1621, 1602, 1566, 1475, 1466, 1432, 1383, 1360, 1323, 1287, 1243, 1212, 1198, 1113, 1056, 1018, 989, 898, 866, 806, 757, 724.; Mass (EI); (m/z): 323, 325, 327 (M^+).; ^1H NMR: ($CDCl_3$) δ_H: 8.10 (1H, s), 7.50 (2H, dd, *J*=8, 2Hz), 7.30 (4H, d, *J*=8Hz).; ^{13}C NMR: ($CDCl_3$) δ_C: 138 (2C) 129 (2C); 124 (2C); 123 (2C); 112 (2C); 111 (2C).:

4.6.0 Attempted synthesis of aryl substituted carbazole derivatives

4.6.1 1-Iodo-3,5-dimethoxybenzene [4] (9)

Into an oven dried flask magnesium flakes (3.70 g, 154.00 mmol) was charged. The magnesium was heat activated under vacuum using a heating gun for 1 hour. 1-Chloro-3,5-dimethoxybenzene (20.00 g, 115.87 mmol) dissolved in dry THF (30 cm^3) was added and the system was degassed and allowed to reflux for 36 hours with the aid of stirring under a nitrogen atmosphere. The solution was cooled and under a nitrogen atmosphere a few small crystals of iodine were added and the solution was allowed to reflux for a further 12 hours. The mixture turned to a dark suspension which was cooled on an ice bath. Iodine (19.2 g, 151.18 mmol) dissolved in dry THF (60 cm^3) was added to the suspension dropwise over a 2 hour period with the aid of stirring. The suspension was allowed to stir over night at room temperature. The suspension turns to cream slurry which is hydrolysed by the addition of 1M hydrochloric acid (50 cm^3). Diethyl ether (2 x 40 cm^3) is used to extract the organic product. The organic layer is washed with 1M sodium hydrogen sulphite (30 cm^3) followed by water (30 cm^3). The organic layer was dried over $MgSO_4$ and the solvent removed invacuo. The product was run through a column using ethyl acetate pet, ether (10:90) to obtain a single spot by TLC of the product. The product was then crystallised from minimum amount of hot methanol and allowed to re-crystallise under a cool temperature to separate any dimethoxy-benzene formed. A white crystalline solid of mass 11.35 g, yielding 36% was obtained. The melting point of 74 – 75°C was obtained which fell in to the literature barrier 74 – 76 °C [4]. GCMS: RT: 12.29 min. CHN Br – $C_8H_9IO_2$ Expected; C, 36.39; H, 3.44; I, 48.06; O, 12.12.% Achieved: C: 36.94, H: 3.33, I: 47.68.%; I.R cm^{-1}: 3069, 3005, 2963, 2931, 2833, 1961, 1709, 1571, 1468, 1450, 1438, 1422, 1157, 1028, 984. Mass (EI); (m/z): 152, 153 (M^+). ^1H NMR: ($CDCl_3$) δ_H: 6.85 (2H, d, J=2.3Hz); 6.40 (1H, t, J=2.3Hz); 3.75 (6H, s); 13 C NMR: ($CDCl_3$) δ_C: 160 (2C) 115 (1C); 100 (2C); 94 (1C); 55 (2C).:

4.6.2 1-Iodo-3,5-dimethoxybenzene from 3,5-dimethoxy-phenyl-amine [5] (10)

Sodium nitrate (15.18 g, 220 mmol) dissolved in water (50 cm^3) was added drop wise to a solution of 3,5-dimethoxy-phenyl-amine (30 g, 200 mmol) in 37% hydrochloric acid (70 cm^3) and ice (100 g) over a period of 30 minutes. The reaction vessel was stirred vigorously and kept a 0C for a further 45 minutes. The reaction vessel was then allowed to warm to room temperature and potassium iodide (33.18 g, 200 mmol) dissolved in water (300 cm^3) was added dropwise. The reaction mixture was allowed to stand over night. The product was extracted from DCM (3 x 500 cm^3). The organic layer was washed first with sodium carbonated solution (500 cm^3) and then with water (3 x 300cm^3). Followed by sodium thiosulphate solution (2 x 500 cm^3) and then with water (3 x 300 cm^3). The organic layer was collected, dried over $MgSO_4$ and solvent removed invacuo. The crude product was purified by column chromatography using ethyl acetate: pet, ether 20:80 to yield a single product. A white crystalline solid of mass 25.35 g, yielding 76% was obtained. The melting point of 74 °C was obtained which fell in to the literature barrier 74 – 76 °C [5]. GCMS: RT: 12.29 min. CHN Br - $C_8H_9IO_2$ Expected; C, 36.39; H, 3.44; I, 48.06; O, 12.12 Achieved; C: 36.94, H: 3.33, I: 47.68. I.R cm^{-1}: 3069, 3005, 2963, 2931, 2833, 1961, 1709, 1571, 1468, 1450, 1438, 1422, 1157, 1028, 984. Mass (EI); (m/z): 152, 153 (M^+). ^1H NMR: ($CDCl_3$) δ_H: 6.85 (2H, d, J=2.3Hz); 6.40 (1H, t, J=2.3Hz); 3.75 (6H, s); 13 C NMR: ($CDCl_3$) δ_C: 160 (2C) 115 (1C); 100 (2C); 94 (1C); 55 (2C).:

4.6.3 5-Iodoresorcinol [4] (11)

A solution of 1-iodo-3,5-dimethoxybenzene (5.00 g, 18.90 mmol) was dissolved in dry DCM (60 cm^3) and was cooled to -78°C using carb-ice in acetone. Boron tribromide (37.8 cm^3, 37.8 mmol) was added dropwise while maintaining the temperature at -78°C. The solution was allowed to warm to room temperature overnight. The dark brown solution was cooled on an ice bath and water (100 cm^3) was added slowly. The precipitate was extracted and washed with DCM (2 x 80 cm^3). The organic layer was washed with sodium hydrogen sulphite (50 cm^3) followed by water (2 x 50cm^3). The organic layer was dried over $MgSO_4$ and the solvents removed invacuo. The product was purified via column chromatography and stored in

the dark as it is a light sensitive compound. A white crystalline solid of mass 3.80 g, yielding 76% was obtained. The melting point of 85 – 86 °C was obtained which fell in to the literature barrier 84 – 85 °C [4]. GCMS: RT: 16.69 min. CHN Br - $C_6H_5IO_2$ Expected; C, 30.53; H, 2.14; I, 53.77; O, 13.56.% Achieved; C: 31.53, H: 2.20, I: 50.79.%; I.R cm^{-1}: 3591, 3236, 3048, 2967, 1977, 1583, 1475, 1437, 1399, 1343, 1292, 989. Mass (EI); (m/z): 236, 238 (M^+). ^1H NMR: (Acetone-d_6) δ_H: 8.62 (1H, s, OH); 6.83 (2H, d, *J*=2.2Hz); 6.44 (1H, t, *J*=2.2Hz); 3.15 (1H, s, OH). ^{13}C NMR: (Acetone-d_6) δ_C: 160 (2C); 117 (1C); 103 (2C); 95 (1C).:

4.6.4 1,3-Bis-(2-ethyl-hexyloxy)-5-iodobenzene [6] (12)

Into a oven dried reaction vessel was placed 5-iodoresorcinol (3.24 g, 13.73 mmol), 2-ethyl-hexybromide (5.83 g, 30.19 mmol), 18-crown-6 ether (50 mg, 0.2 mmol), anhydrous potassium carbonate (3.98 g, 28.80 mmol) in HPLC grade acetone (35 cm^3) were degassed and set under a nitrogen atmosphere. The mixture was refluxed for a total of 36 hours while monitoring via TLC pet, ether neat. The solution was cooled and the solvents removed in-vacuo to leave a dark precipitate. This was extracted with DCM (3x30 cm^3) and washed with water (3x20 cm^3). The organic layer was collected and dried over $MgSO_4$ and the solvent removed to leave a light brown oil. The product was purified by column chromatography using pet, ether neat producing a clear oil of mass 4.30 g, yielding 69%. CHN Br - $C_{22}H_{37}IO_2$ Expected C, 57.39; H, 8.10; I, 27.56; O, 6.95.% Achieved C, 58.36; H, 8.00; I, 26.60.%; I.R cm^{-1}: 3088, 2926, 2601, 1593, 1568, 1433, 1381, 1326, 1275, 1170, 1050, 988. Mass (EI); (m/z): 460, 462 (M^+). ^1H NMR: ($CDCl_3$) δ_H: 6.75 (2H, d, *J*=2Hz); 6.35 (1H, t, *J*=3Hz); 3.70 (4H, d, *J*=4Hz); 1.62 (2H, m); 1.20-1.55 (16H, m); 0.70-0.90 (12H, m). ^{13}C NMR: ($CDCl_3$) δ_C: 160 (2C); 116 (1C); 101 (2C); 94 (1C); 76 (2C); 39 (2C); 29 (4C); 22 (4C); 14 (2C); 11 (2C).:

4.6.1 Attempted synthesis of 2,7-dibromo-9-[3,5-bis(2-ethyl-hexyloxy)-phenyl]-*9H*-carbazole [8,9] (13)

Into a oven dried reaction vessel 2,7-dibromo-*9H*-carbazole (0.487 g, 1.5 mmol), 1,3-Bis-(2-ethyl-hexyl-oxy)-5-iodo-benzene (0.460 g, 1 mmol), copper chloride (1.979

mg, 0.002 mmol), 1,10-phenathroline (0.0361 g, 0.02 mmol), tri-potassium phosphate (0.530 g, 2.5 mmol) in dry toluene (8 cm^3) was degassed and allowed to reflux for 48 hours under a argon atmosphere. The reaction was monitored via TLC using pet, ether neat for the consumption of 1,3-Bis-(2-ethyl-hexyl-oxy)-5-iodo-benzene. The reaction mixture was worked up by diluting with diethyl ether (3 x 50 cm^3) and washed with water (3 x 40 cm^3). The organic layer was collected and dried over $MgSO_4$ and the solvent removed invacuo. The product was first filtered through flash column using pet, ether neat and was then purified using column chromatography using pet, ether neat. A contaminated compound of mass 0.41, yielding 63% was obtained containing three spots by TLC with the major compound being the desired product as estimated from analysis of the compound. CHN Br- $C_{34}H_{43}Br_2NO_2$ Expected: C, 62.11; H, 6.59; Br, 24.30; N, 2.13; O, 4.87.% Achieved: C, 63.81; H, 6.95; N, 2.23; Br, 20.84.%; ^1H NMR: ($CDCl_3$) δ_H: 7.85 (2H, d, *J*=8Hz); 7.75 (2H, d, *J*=6Hz); 7.60 (2H, d, *J*=6Hz); 7.50 (2H, d, *J*=6Hz); 7.45 (2H, d, *J*=3Hz); 7.30 (2H, dd, *J*=8, 2Hz); 6.50 (3H, m); 3.75 (*4H*, d, *J*=8Hz); 3.70 (4H, d, *J*=8Hz); 1.62 (2H, q, *J*=2Hz); 1.20-1.55 (16H, m); 0.70-0.90 (12H, m).:

Earlier methods attempted in the synthesis of 2,7-dibromo-9-[3,5-bis(2-ethyl-hexyloxy)-phenyl]-*9H*-carbazole **(13).**

Method 1 [7]

A reaction vessel was equipped with a Dean-Stark and reflux condenser. The vessel was charged with 2,7-dibromo-9H-carbazole (0.325g, 1mmol) 1,3-Bis-(2-ethyl-hexyloxy)-5-iodobenzene (0.450g, 1mmol), cuprous I chloride (8.95mg, 0.067mmol), 1,10-phenanthroline (14.20mg, 0.078 mmol), potassium hydroxide (pellets) (0.530g, 9.51mmol) in dry toluene (30cm^3). The reaction was rapidly heated to reflux and the Dean-Stark filled to concentrate the reaction vessel (removal of 10cm^3). After 4 hours of refluxing tetrabutylammonium hydrogensulfate (0.240g, 0.71mmol) was added and the reaction allowed to reflux for a further 2 hours. The reaction was monitored via TLC. The solvent was removed under vac, and the crude residue diluted with ethyl acetate pet, ether (10:90) and run though a flash column to filter the product. These results are discussed in the appropriate results and discussion section.

Method 2 [7]

A reaction vessel was equipped with a Dean-Stark and reflux condenser. The vessel was charged with 2,7-dibromo-9H-carbazole (0.325g, 1mmol) 1,3-Bis-(2-ethyl-hexyl-oxy)-5-iodo-benzene (0.450g, 1mmol), cuprous chloride (8.95mg, 0.067mmol), 1,10-phenanthroline (14.20mg, 0.078mmol), potassium hydroxide (flakes) (0.530g, 9.51mmol), 18-crown-6 (5.30mg, 0.2mmol) in dry toluene ($30cm^3$). The reaction was rapidly heated to reflux and the Dean-Stark filled to concentrate the reaction vessel (removal of 10 cm^3). The reaction was monitored via TLC ethyl acetate pet ether (10:90). After 3 hours refluxing, the reaction was once again concentrated to leave (2 cm^3) of solvent in the system (making a 1M concentration). The reaction was allowed to reflux over night. The solvent was removed under vac, and the crude residue diluted with ethyl acetate pet, ether (10:90) and run though a flash column to filter the product. These results are discussed in the appropriate results and discussion section.

Method 3 [8,9]

Into a oven dried reaction vessel 2,7-dibromo-9H-carbazole (0.325g, 1mmol), 1,3-Bis-(2-ethyl-hexyl-oxy)-5-iodo-benzene (0.460g, 1mmol), copper chloride (0.989 mg, 0.001mmol), ethylene diamine (6.0mg, 0.01mmol), tri-potassium phosphate (0.581g, 2mmol) in dry dioxane ($2cm^3$) was allowed to reflux for 24 hours under a nitrogen atmosphere. The reaction was monitored via TLC using ethyl acetate pet, ether (5:95). The reaction mixture was worked up by diluting with diethyl ether (3x50 cm^3) and washed with water (3x40 cm^3). The organic layer was collected and dried over MgSO4 and the solvent removed under vac. The product was purified using column chromatography ethyl acetate pet, ether (5:95) to filter the product. These results are discussed in the appropriate results and discussion section.

4.6.2 Attempted synthesis of 2,7-dibromo-3,6-dimethyl-9-[3,5-bis(2-ethyl-hexyloxy)-phenyl]-*9H*-carbazole [8,9] (14)

Into a oven dried round bottom flask was placed 2,7-dibromo-3,6-dimethyl-*9H*-carbazole (0.250 g, 0.735 mmol), 1,3-bis-(2-ethyl-hexyloxy)-5-iodobenzene (0.230 g, 0.500 mmol), copper iodide (0.572 mg, 0.015 mmol), 1,10-phenathroline (0.270 g, 0.15 mmol), anhydrous potassium phosphate (0.368 g, 1.735 mmol) followed by dry toluene (5 cm^3). The reaction was purged with argon and allowed to reflux for 48 hours. The reaction was monitored by the consumption of 1,3-Bis-(2-ethyl-hexyloxy)-5-iodobenzene via TLC using pet. ether (neat). The solution was worked up by diluting with diethyl ether (3 x 5 cm^3) and washed with water (3 x 4 cm^3). The organic layer was collected and dried over $MgSO_4$ and the solvent removed invacuo. The product was first filtered through column using pet, ether neat. A compound of mass 0.41g, yielding 63% was obtained containing several spots by TLC with the desired product being present as estimated from analysis of the compound. CHN Br-$C_{36}H_{47}Br_2NO_2$ Expected: C, 63.07; H, 6.91; Br, 23.31; N, 2.04; O, 4.67.% Achieved: C, 65.12; H, 7.11; N, 2.18; Br, 19.43.%; ^1H NMR: ($CDCl_3$) δ_H: 7.90 (2H, s); 7.85 (2H, s); 7.55 (2H, d, *J*=6Hz); 6.50 (3H, m); 6.40 (3H, m); 3.75 (4H, d, *J*=8Hz); 3.70 (4H, d, *J*=8Hz); 2.55 (6H, m); 2.50 (6H, m); 1.62 (2H, q, *J*=2Hz); 1.20-1.55 (16H, m); 0.70-0.90 (12H, m).:

4.6.3 Attempted synthesis of 2,7-dibromo-3,6-dimethyl-9-[3,5-dimethoxy-phenyl]-*9H*-carbazole [8,9] (15)

Into a oven dried round bottom flask was placed 2,7-dibromo-3,6-dimethyl-*9H*-carbazole (2.00 g, 0.58 mmol), 1-iodo-3,5-dimethoxybenzene(3.06 g, 1.16 mmol), copper I iodide (0.044 g, 0.0232 mmol), 1,10 phenthroline (0.418 g, 0.0232 mmol), potassium phosphate (2.46 g, 1.16 mmol) in dry toluene (15 cm^3) and allowed to reflux for 24 hours. The reaction was monitored to completion via TLC; pet, ether/ ethyl acetate (90:10) for the consumption of the starting carbazole. The reaction mixture was extracted with DCM (30 cm^3) and washed with water (3 x 30 cm^3). The organic extracts were collected and the solvent removed invacuo. The crude material was re-crystallised from methanol (25 cm^3) to yield a compound of mass 1.81 g,

yielding 64% was obtained containing three spots by TLC with the desired product being present as estimated from analysis of the compound. CHN Br- $C_{22}H_{19}Br_2NO_2$ Expected: C, 54.01; H, 3.91; Br, 32.67; N, 2.86; O, 6.54.% Achieved: C, 55.72; H, 3.71; N, 2.78; Br, 28.43.%; ^{1}H NMR: ($CDCl_3$) δ_H: 7.90 (*2H*, s); 7.85 (2H, s); 7.80 (2H, d, *J*=6Hz); 7.50 (2H, s); 6.50 (3H, m); 3.75 (6H, s); 2.55 (6H, m); 2.50 (6H, m).:

4.6.4 9-[3,5-(Dimethoxy)-phenyl]-*9H*-carbazole [8,9] (16)

Into a oven dried reaction vessel was placed *9H*-carbazole (2.0 g, 12 mmol), 1,3-dimethoxy-iodo-benzene (3.2 g, 13 mmol), copper I chloride (0.084 g, 0.442 mmol), 1-10 phenathroline (0.79 g, 4.42 mmol), potassium phosphate (2.0 g, 26 mmol) in dry toluene (15 cm^3). The reaction vessel was degassed and allowed to reflux for 48 hours under a nitrogen atmosphere. The reaction vessel was cooled to room temperature. The reaction was worked up by diluting with water (25 cm^3) and extracted with DCM (3 x 25 cm^3). The organic extracts were combined and dried over $MgSO_4$ followed by the solvent being removed invacuo. The crude product was run through a column chromatography using ethyl acetate / pet, ether 5:95 to yield a single spot product of mass 1.31g, yielding 59%. GCMS: RT: 13.47 min. CHN Br - $C_{20}H_{17}NO_2$ Expected C, 79.19; H, 5.65; N, 4.62; O, 10.55.% Achieved C, 79.36; H, 5.30; N, 4.83.%; Mass (EI); (m/z): 303, 304 (M^+). ^{1}H NMR: ($CDCl_3$) δ_H: 8.10 (2H, d, *J*=8.2Hz); 7.40 (4H, dt, *J*=2.3, 2.3Hz); 7.20 (2H, dd, *J*=8.1, 2.6Hz); 6.60 (2H, m); 6.45 (1H, t, *J*=2.3Hz); 3.75 (6H, s).; ^{13}C NMR: ($CDCl_3$) δ_C: 155 (2C); 141 (1C); 140 (2C); 122 (2C); 121 (2C); 120 (2C); 118 (2C); 110 (2C); 98 (1C); 92 (2C); 55 (2C).:

4.6.5 Attempted synthesis of 3,6-dibromo-9-[3,5-dimethoxy-phenyl]-*9H*-carbazole [3] (17)

Into an oven dried reaction vessel was placed 9-[3,5-(dimethoxy)-phenyl]-*9H*-carbazole (0.71 g, 1.39 mmol) in dry DMF (10 cm^3) under a nitrogen atmosphere. The reaction vessel was kept at -20°C and in the absence of light. NBS (0.52g, 2.91mmol) in dry DMF (8cm^3) was added over a period of 1 hour via a dropping funnel. The solution was stirred at -20°C for a further 1 hour before being allowed to gradually warm to room temperature and then stir at room temperature for a further 5

hours. The reaction was worked up be the addition of water (50 cm^3) and the solution allowed to stir for 5 minutes, followed by the extraction with DCM (3 x 40 cm^3) followed by 1M potassium hydroxide solution (50 cm^3), and then with water (3 x 30 cm^3). The organic extracts were dried over $MgSO_4$ and the solvent removed invacuo. The crude product was run through column chromatography using ethyl acetate / pet, ether 4:96 to yield a compound of mass .0.54 g, yielding 60% was obtained.

4.6.6 Attempted synthesis of 3,6-diiodo-9-[3,5-dimethoxy-phenyl]-*9H*-carbazole [10] (18)

Into a oven dried reaction vessel was placed 9-[3,5-(dimethoxy)-phenyl]-*9H*-carbazole (0.1 g, 0.33 mmol) into acetic acid (2 cm^3) and heated under a nitrogen atmosphere until the carbazole had dissolved. To this hot solution was added potassium iodide (0.072 g, 0.435 mmol) and allowed to stir at reflux temperature for 10 minutes. The solution was cooled slightly and to this was added potassium periodated KIO_3 (0.105 g, 0.495 mmol) and the reaction vessel allowed to reflux for a further 15 minutes. The reaction was cooled to room temperature. The reaction was worked up by diluting with water (5 cm^3) and extracted with DCM (3 x 5 cm^3). The organic extracts were combined and dried over $MgSO_4$ followed by the solvent being removed invacuo. The crude product was run through a column chromatography using ethyl acetate / pet, ether 30: 70 to give a compound of mass 0.112 g, yielding 62% was obtained.

4.6.7 9-(3,5-dihydroxy-phenyl)-*9H*-carbazole [4] (19)

Into a oven dried reaction vessel was placed 9-[3,5-(dimethoxy)-phenyl]-*9H*-carbazole (5.0 g, 16.50 mmol) in dry DCM (60 cm^3) purged with nitrogen and cooled in an ice bath to 0°C. To this was added drop wise boron tri bromide (40 cm^3) and the vessel was allowed to stir for 96 hours at room temperature. The reaction was worked up by diluting with water (100 cm^3) and then extracted with DCM (3 x 100 cm^3). The collected organic layer was further washed with water (3 x 80 cm^3) before being dried over $MgSO_4$ and the solvent removed invacuo. The crude product was purified via column chromatography using ethyl acetate / pet, ether 40:60 to yield a single spot

product of mass 4.32 g, yielding 58% was obtained. GCMS: RT: 15.56 min. CHN Br - $C_{18}H_{13}NO_2$ Expected: C, 78.53; H, 4.76; N, 5.09; O, 11.62.% Achieved C, 78.26; H, 4.98; N, 5.00.%; Mass (EI); (m/z): 275, 276 (M^+). ^1H NMR: ($CDCl_3$) δ_H: 8.10 (2H, d, *J*=8.1Hz); 7.40 (4H, dt, *J*=2.3, 2.3Hz); 7.20 (2H, dd, *J*=8.1, 2.6Hz); 6.60 (2H, m); 6.45 (1H, t, *J*=2.3Hz); 5.50 (2H, br).; ^{13}C NMR: ($CDCl_3$) δ_C: 158 (2C); 141 (1C); 140 (2C); 122 (2C); 121 (2C); 120 (2C); 118 (2C); 111 (2C); 100 (1C); 95 (2C).:

4.6.8 Attempted synthesis of 9-(3,5-bis(2,2,2-trifluoro-acetoxy)-phenyl)-*9H*-carbazole [11-19] (20)

Into a oven dried reaction vessel was placed 9-(3,5-dihydroxy-phenyl)-*9H*-carbazole (0.50 g, 1.80 mmol), in dry THF (6 cm^3), tri fluoro acetic acid (1.135 g, 5.4 mmol) and tri ethylamine (0.55 g, 5.4 mmol). The system was degassed and set under nitrogen before being reflux for 5 hours. The reaction was cooled to room temperature and worked up by diluting with diethyl ether (10 cm^3) and water (15 cm^3). The product was extracted with diethyl ether (3 x 10 cm^3) and then washed with water (3 x 10 cm^3) before being dried over $MgSO_4$ and the solvent removed invacuo. The crude product was purified by running though column chromatography using ethyl acetate / pet ether / TEA (55:40:5). The desired compound was not acquired.
The reaction was also carried out with the use of di-isopropyl amine (0.54g, 5.4mmol) and DMAP (0.65g, 5.4mmol) respectively in place of tri ethylamine.

4.7.0 Synthesis of triaryl amino substituted Carbazole derivatives

4.7.1 3,6-Dibromo-9-(4-nitro-phenyl)-*9H*-carbazole [20] (21)

Into an oven dried round bottomed flask was placed 3,6-dibromo-cabazole (12.29 g, 37.81 mmol), potassium carbonate (26.13 g, 189.05 mmol) and 4-fluoronitrobenzene (21.34 g, 151.26 mmol) in dry DMF (200 cm^3). The solution was degassed and purged under a nitrogen atmosphere before being refluxed for 48 hours. The solution was cooled to room temperature and poured onto de-ionised water (1000 cm^3) which was kept at 40°C and allowed to stir for 1 hour forming a precipitate. The precipitate was filtered and dissolved with toluene before being purified by column chromatography using petroleum ether: toluene 3:2 to yield a single product as pale yellow crystals 13.50 g, 80% yield. m.p.: 125-126°C. GCMS: RT = 23.38 min. CHN Br - $C_{18}H_{10}N_2Br_2O_2$ Expected: C, 48.46; H, 2.26; Br, 35.82; N, 6.28; O, 7.17.% Achieved C: 48.51 H: 1.99 N: 6.30 Br: 35.89.%; IR (KBr) 3034, 1893, 1837, 1752, 1695, 1604, 1505, 1470, 1449, 1373, 1334, 1031, 923, 833, 763, 710, 692, 652, 623, 590 cm^{-1}; Mass (EI) 444, 446, 448 ([M+2]). ^1H NMR ($CDCl_3$) δ_H: 8.49 (2H, d, J = 8.9 Hz), 8.15 (2H, d, J = 1.5 Hz), 7.69 (2H, d, J = 8.9 Hz), 7.49 (2H, dd, J = 8.3, 1.5 Hz), 7.25 (2H, d, J = 8.9 Hz). ^{13}C NMR δ_C: 147 (1C); 144 (1C); 140 (2C); 125 (2C); 123 (2C); 122 (2C); 121 (4C); 117 (2C); 113 (2C).:

4.7.2 3,6-Dibromo-9-(4-amino-phenyl)-*9H*-carbazole [20] (22)

Into an oven dried round bottom flask was placed 3,6-dibromo-9-(4-nitro-phenyl)-*9H*-carbazole (12.50 g, 28.02 mmol) and $SnCl_2.2H_2O$ (31.61 g, 140.11 mmol) in EtOH (400 cm^3), the reaction vessel was degassed and purged with nitrogen before being refluxed for 48 hours. The reaction was cooled to room temperature and most of the EtOH was removed in-vacuo (leaving 60 cm^3 approximate 15%). A solution of sodium hydroxide (50.00 g) and water (100 cm^3) was poured into the reaction mixture slowly while the reaction vessel was cooled in an ice bath and stirred vigorously. A cream precipitate formed which was filtered and collected. The solid product was extracted with toluene (3*100 cm^3) the combined extracts were dried over $MgSO_4$, filtered and the solvent removed in-vacuo. The solid product was re-

crystallised from toluene (30 cm^3) to achieve the desired product as white ivory crystals 10.95 g, 94% yield, m.p.: 210-212°C. The purity of the product was confirmed by: GCMS: RT = 13.72 min. CHN Br - $C_{18}H_{12}N_2Br_2$ Expected C:51.96 H:2.91 N:6.73 Br:38.41.% achieved C:51.86 H:2.96 N:6.56 Br:38.57.%; IR; (KBr): 3420, 3329, 3034, 1893, 1893, 1752, 1695, 1604, 1505, 1470, 1449, 1373, 1334, 1023, 923,788 cm^{-1}; Mass (EI) 414, 416, 418 ([M+1]). ^1H NMR ($CDCl_3$) δ_H: 8.15 (2H, d, *J*=1.8Hz), 7.40 (2H, dd, *J*=8.5, 1.8Hz), 7.20 - 7.14 (m, 4H), 6.85 (2H, d, *J*=14.2Hz) 3.85 (br s, 2H). ^{13}C NMR δ_C: 145 (1C); 139 (2C); 131 (1C); 122 (4C); 121 (4C); 117 (2C); 116 (2C); 113 (2C).:

4.7.3 4-(2-Butyl-octyloxy-)-1-iodobenzene [6] (23)

Into a oven dried reaction vessel was placed 4-iodo-phenol (25.36 g, 115.27 mmol), 2-butyl-octylbromide (43.00 g, 172.90 mmol), 18-crown-6 ether (0.20 g, 0.8 mmol), anhydrous potassium carbonate (31.74 g) in dry DMF (200 cm^3) were degassed and set under a nitrogen atmosphere. The mixture was refluxed for a total of 12 hours while monitoring via TLC pet, ether neat. The solution was cooled and the solvents removed invacuo to leave a precipitate. This was extracted with DCM (3 x 300 cm^3) and washed with water (3x200 cm^3). The organic layer was collected and dried over $MgSO_4$ and the solvent removed to leave a light oil. The product was purified by column chromatography using pet, ether neat producing a clear oil of mass 36.66 g, yielding 82 %. Mass (EI); (m/z): 388, 390 (M^+). ^1H NMR: ($CDCl_3$) δ_H: 7.53 (2H, d, *J*=8Hz); 6.54 (2H, d, *J*=8Hz); 3.78 (2H, d, *J*=6Hz); 1.75 (1H, q, *J*=1.5Hz); 1.15–1.45 (16H, m); 0.75-0.95 (6H, d). ^{13}C NMR: ($CDCl_3$) δ_C: 159 (1C); 138 (2C); 116 (2C); 82 (1C); 71 (1C); 37 (1C); 36 (1C); 35 (1C); 31 (4C); 27 (2C); 14 (2C).:

4.7.4 3,6-Dibromo-9-(bis-[4-(2-butyl-octyloxy)-phenyl]-amino-phen-4-yl)-carbazole [7] (24)

Into a oven dried flask was placed 3,6-dibromo-9-(4-amino-phenyl)-*9H*-carbazole (3.00 g, 7.21 mmol), 4-(2-butyl-octyloxy)-iodobenzene (5.87 g, 15.14 mmol), copper I chloride (0.12 g, 1.26 mmol), 1-10 phenthroline (0.22 g, 1.26 mmol) and KOH

flakes (3.26 g, 57.65 mmol) in dry toluene (110 cm^3). The reaction vessel was degassed and purged with nitrogen before being refluxed 48 hours. On completion of the reaction, the vessel was cold to room temperature and diluted with water (150 cm^3) added. The mixture was extracted with DCM (3 x 200 cm^3) and washed with water (3 x 200 cm^3) before being dried over $MgSO_4$, filtered and the solvent removed in vacuo. The product was purified by column chromatography using petroleum ether: ethyl acetate 9:1 to yield a single product as a brown oil/solid of 4.97 g, 74% yield. The purity of the product was confirmed by: CHN Br - $C_{54}H_{68}N_2Br_2O_2$ Expected C:69.22 H:7.32 N:2.99 Br:17.06 O: 3.42.% achieved C:68.47 H:7.19 N:2.96 Br:17.38.%; IR (KBr) 3054, 3032, 2987, 2685, 2410, 1893, 1752, 1695, 1604, 1591, 1505, 1470, 1449, 1373, 1334, 1170, 1023, 923, 742 cm^{-1}; Mass (EI) 936, ([M+1]). ^1H NMR ($CDCl_3$) δ_H: 8.15 (2H, d, *J*=2.1Hz), 7.45 (2H, dd, *J*=8.8, 2.1Hz), 7.25 (2H, dd, *J*=8.6, 1.5Hz), 7.20 (2H, dd, *J*=6, 2Hz), 7.1 (4H, dd, *J*=8.6, 1.6Hz), 7.05 (2H, d, *J*=8.8Hz), 6.85 (4H, d, *J*=8.8Hz) 3.75 (4H, d, *J*=4.9Hz), 1.75 (2H, q, *J*=1.5Hz), 1.55 – 1.15 (m, 32H), 0.85 (m, 12H).; ^{13}C NMR δ_C: 156 (2C), 140 (1C), 139 (4C), 129 (2C), 128 (4C), 127 (1C), 126 (2C), 123 (4C), 119 (2C), 116 (4C), 113 (2C), 111(2C), 71 (2C); 38 (2C); 31 (2C); 29 (4C); 27 (6C); 23 (4C), 14 (4C).:

4.7.5 3,6-Dibromo-9-(bis-[3,5-bis-(2-ethyl-hexyloxy)-phenyl]-amino-phen-4-yl)-carbazole [7] (25)

Into a oven dried flask was placed 3,6-dibromo-9-(4-amino-phenyl)-*9H*-carbazole (1.26 g, 3.03 mmol), 1,3-bis-(2-ethyl-hexyloxy)-5-iodo-benzene (2.92 g, 6.36 mmol), copper I chloride (0.06 g, 0.54 mmol), 1-10 phenthroline (0.1 g, 0.54 mmol) and KOH flakes (2.78 g, 49.65 mmol) in dry toluene (40 cm^3). The reaction vessel was degassed and purged with nitrogen before being refluxed 48 hours. On completion of reaction the vessel was cooled to room temperature and diluted with water (50 cm^3), extracted with DCM (3 x 60 cm^3) and washed further with water (3 x 40 cm^3). The organic extracts were collected and dried over $MgSO_4$, filtered and the solvent removed in-vacuo. The product was purified by column chromatography (petroleum ether: ethyl acetate 9:1) to yield a single product as a brown oil 2.19g, 64% yield. The

purity of the product was confirmed by: CHN Br – $C_{62}H_{84}N_2Br_2O_4$ Expected: C, 68.88; H, 7.83; Br, 14.78; N, 2.59; O, 5.92.% Achieved C: 68.72, H: 7.98, N: 3.01, Br: 14.89.%; IR (KBr) 3185, 3056, 3017, 1831, 1794, 1651, 1594, 1581, 1515, 1470, 1469, 1373, 1334, 1170, 1028, 931, 776 cm^{-1}.; ^1H NMR ($CDCl_3$) δ_H: 8.15 (d, 2H, *J*=1.2Hz), 7.45 (dd, 2H, *J*=8.8, 1.8Hz), 7.30 – 7.05 (m, 6H), 6.30 (d, 4H, *J*=2.2Hz), 6.10 (t, 2H, *J*=2.1Hz), 3.75 (d, 8H, *J*=6.1Hz), 1.65 (q, 4H, *J*=6.8Hz), 1.55 – 1.15 (m, 32H), 0.85 (m, 24H).; ^{13}C NMR δ_C: 159 (4C); 143 (1C); 139 (2C); 131 (1C); 122 (4C); 121 (4C); 117 (2C); 116 (6C); 113 (2C) 111 (4C); 77 (4C); 76 (4C); 70 (4C); 39 (4C); 29 (4C); 22 (4C); 14 (8C).:

4.7.6 Attempted synthesis of 3,6-Bis-(4,4,5,5-tetramethyl-[1,3,2]dioxaborolan-2-yl)-9-(bis-[3,5-bis-(2-ethyl-hexyloxy)-phenyl]-amino-phen-4-yl)-carbazole [21] (26)

Under a nitrogen atmosphere into a oven dried flask was placed 3,6-Dibromo-9-(bis-[3,5-bis-(2-ethyl-hexyloxy)-phenyl]-amino-phen-4-yl)-carbazole (4.0 g, 3.12 mmol) which was dissolved into dry THF (120 cm^3). The reaction vessel was attached with a dropping funnel to which *t*-butyllithium (7.65 cm^3, 13 mmol, 1.7 M in pentane) was added. The vessel was cooled to -78°C and the *t*-butyllithium was allowed to be added drop wise to the stirred solution over a period of 4 hours. 2-isopropoxy-4,4,5,5-tetramethyl-1,3,2-dioxaborolane (8.05 g, 4.34 mmol) was then added dropwise to the solution at -78 °C and the reaction mixture was stirred at -78 °C for a further 3 hours. The reaction mixture was then allowed to warm up to ambient temperature and stirred for another 36 hours. The reaction mixture was then poured onto water (200 cm^3) and extracted with diethyl ether (3* 200 cm^3). The combined organic extracts were washed with water (3 x 150 cm^3), dried over $MgSO_4$ and the solvent removed invacuo. The residue was purified by flash vacuum chromatography eluting first with hexane, to remove starting material and then with DCM / Pet ether / TEA (49:50:1) to obtain a compound.

4.7.7 3,6-Bis-(4,4,5,5-tetramethyl-[1,3,2]dioxaborolan-2-yl)-9-(bis-[4-(2-butyl-octyloxy)-phenyl]-amino-phen-4-yl)-carbazole [22] (27)

Into a oven dried reaction vessel 3,6-dibromo-9-(bis-[4-(2-butyl-octyloxy)-phenyl]-amino-phen-4-yl)-carbazole (1.5 g, 1.6 mmol), bis(pinacolate)diboron (1.46 g, 5.76 mmol) KOAc (0.94 g, 9.6 mmol), $Pd(dppf)Cl_2$ (0.082 g, 0.1 mmol) in DMF (30 cm^3). The reaction was degassed and purged with argon and allowed to stir overnight at 60°C. The reaction was cooled to room temperature diluted with water (50 cm^3), extracted with diethyl ether (3 x 50 cm^3) and washed with water (3 x 80 cm^3) before being dried over $MgSO_4$, filtered and the solvent removed invacuo. The product was purified by column chromatography using petroleum ether: toluene: pyridine 50:50:2 to yield a light brown oil/solid 1.55 g, 94% yield. m.p.: 56 - 57°C; CHN Br - $C_{66}H_{92}N_2Br_2O_2$ Expected C:76.88 H:8.99 N:2.72 Br:2.10 O:9.31.% Achieved C:77.01 H:9.03 N:2.37.%; IR (KBr) 2943, 2924, 2852, 1962, 1623, 1551, 1503, 1458, 1437, 1370, 1326, 1271, 1246, 1207, 931, 858, 792, 738, 701 cm^{-1}; Mass (EI) 1031, 1032 ([M+1]). ^1H NMR ($CDCl_3$) δ_H: 8.70 (d, 2H, *J*=1.7Hz), 7.85 (dd, 2H, *J*=8.2, 1.2Hz), 7.40 (dd, 2H, *J*=9.0, 1.4Hz), 7.25 (m, 2H), 7.15 (dd, 4H, *J*=6.7, 1.6Hz), 7.05 (d, 2H, *J*=9.4Hz), 6.85 (d, 4H, *J*=8.6Hz), 3.75 (d, 4H, *J*=5.8Hz), 1.75 (m, 2H), 1.55 – 1.15 (m, 56H), 0.85 (m, 12H). ^{13}C NMR δ_C: 156 (2C), 143 (1C), 140 (4C), 132 (1C), 128 (2C), 127 (2C), 126 (2C), 123 (4C), 119 (2C), 116 (4C), 113 (2C), 111 (2C), 83 (2C), 71 (2C); 38 (2C); 31 (2C); 29 (4C); 27 (8C); 24 (12C), 23 (4C), 14 (2C).:

4.8.0 Other Compounds Used

4.8.1 Preparation of the palladium scavenger N,N-di ethyl phenyl azo thio formamide [23] (28)

Into a oven dried round bottom flask (2 Litre, 3 neck) was placed ethanol (750 cm^3). The ethanol was degassed with argon for 30 minutes. Phenylhydrazine (39.36 cm^3, 0.40 mol) was added and the solution was stirred under argon with a mechanical stirrer. Carbon disulphide (27.60 cm^3, 0.45 mol) was added dropwise over a 15 minute period with stirring, a thick colourless precipitate formed. The mixture was stirred for 30 minutes, potassium hydroxide (27 g) in ethanol (200 cm^3) (15 % excess) was added. The precipitate changed from a colourless solution to orange, the solution was stirred for a further 30 minutes and the orange precipitate dissolved and a thick colourless precipitate once again formed. Methyl iodide (27 cm^3) was added quickly and nearly all the precipitate re-dissolved. The solution was stirred over a 30 minute period where colour of the precipitate was observed to change to a dark red colour moving to a light yellow coloured solution. The solvent was removed by evaporation and diethylamine (300 cm^3) was added. The solution was then allowed to reflux for 3 days after which the reaction was cooled to room temperature and air was bubbled rapidly through the solution through a glass frit for 24 hours. The colour of the solution changed quickly to dark red. The solvent was removed by evaporation to leave a dark red oil. This was dissolved in ethyl acetate (300 cm^3) and the organic phase was washed with brine (3 x 250 cm^3) and dried over $MgSO_4$ before being filtered and the solvent removed. The crude product was run through a column using pet, ether and ethyl acetate (90:10) producing a single spot product. The product was collected and evaporated to dryness and re-crystallised once from hexane / ethyl acetate (20:1) to yield the desired product in 38g; 44% as orange crystals. CHN Br-$C_{11}H_{15}N_3S$ Expected: C, 59.69; H, 6.83; N, 18.99; S, 14.49.% Achieved: C, 59.53; H, 6.56; N, 17.67; S, 15.66.%; Mpt: 57.5 °C.; ^{1}H NMR: ($CDCl_3$) δ_H: 7.95 - 7.81 (2H, m); 7.62 – 7.44 (3H, m); 4.02 (2H, q); 3.51 (2H, q); 1.41 (3*H*, t); 1.18 (3H, t).; ^{13}C NMR: ($CDCl_3$) δ_C: 194 (1C); 151 (2C); 132 (2C); 129 (1C); 123 (1C); 48 (1C); 45 (1C); 13 (1C); 11 (1C).:

4.8.2 Activated magnesium (29)

Magnesium turnings (10 g) were taken and washed with 1M HCl (50 cm^3) followed by ethanol (50 cm^3) and diethyl ether (50 cm^3) successively three times before being heated with a heat gun under vacuum. The dry washed magnesium was allowed to crash stir under a nitrogen atmosphere for 1 week which created a black powder which was used for kumada polymerisations.

4.8.3 2,5-Bis-(4-bromo-phenyl)-[1,3,4]-oxadiazole [24] (30)

2,5-bis(4-bromo-phenyl)-[1,3,4]-oxadiazole was prepared by D Pickup and T Leese of the Iraqi group according to a modified procedure by Zhan *et al* [24]

4.8.4 4,7-dibromobenzo[c][1,2,5]thiadiazole [25] (31)

4,7-dibromobenzo[c][1,2,5]thiadiazole was synthesised by T. Simmence of the Iraqi group according to a modified procedure by Pilgram *et al* [25]

4.8.5 2,7-dibromo-9,9-dioctyl-*9H*-fluorene (32)

Purchased and used under a specific conditions.

4.8.6 2,7-Bis(trimethylene boronate)-9,9-dioctyl-*9H*-fluorene (33)

Purchased and used under a specific conditions.

4.9.0 Preparation of the Polymers

4.9.1 Attempted Synthesis of poly(9-(bis-[3,5-bis-(2-ethyl-hexyloxy)-phenyl]-amino-phen-4-yl)-carbazole-3,6-diyl) [26] (34) kumada P1.AK

Into an oven dried sealed tube was placed 3,6-dibromo-9-(bis-[3,5-bis-(2-ethyl-hexyloxy)-phenyl]-amino-phen-4-yl)-carbazole (0.6 g, 0.56 mmol), activated Mg, (14.64 mg, 0.61 mmol), (2,2'-bipyridine) dichloropalladium (II) (0.036g, 0.01mmol), dry THF (8 cm^3). The mixture was degassed before being set under argon atmosphere and the system was refluxed for 1 week. The reaction was cooled to room temperature and the polymer precipitated into methanol (500 cm^3) and allowed to stir overnight. The precipitate was filtered off using a micro pore filtration system, and then dissolved in chloroform (200 cm^3). The insoluble materials in the chloroform solution were filtered off using the micro pore filtration system, and then the filtrate was concentrated in-vacuo. The concentrated chloroform solution (~10 cm^3) was poured onto methanol (500 cm^3) and allowed to stir over night. The precipitate was filtered off using a micro pore filtration system and dried under vacuum giving the polymer mass 0.37 g, yielding 72%.
CHN Br - Expected: C: 80.65, H: 9.39, N: 3.03, O: 6.93, Br: 0.00.% Achieved: C: 69.88, H: 7.53, N: 2.65, Br: 6.92.%; ^1H NMR: ($CDCl_3$) δ_H: 8.15 (br, 2H), 7.45 - 7.05 (br m, 8H), 6.30 (br d, 4H), 6.10 (br s, 2H), 3.75 (br d, 8H), 1.65 (br, 4H), 1.55 – 1.15 (br, 32H), 0.85 (br, 24H).: GPC: Mn 2,900 / Mw 3,250 / PDI 1.13

4.9.2 Attempted Synthesis of poly(9-(bis-[4-(2-butyl-octyloxy)-phenyl]-amino-phen-4-yl)-carbazole-3,6-diyl) [26] (35) kumada P2.AK

Into an oven dried sealed tube was placed 3,6-dibromo-9-(bis-[4-(2-butyl-octyloxy)-phenyl]-amino-phen-4-yl)-carbazole (0.6 g, 0.64 mmol), activated Mg, (16.92 mg, 0.70 mmol), (2,2'-bipyridine) dichloropalladium (II) (0.042 g, 0.012 mmol), dry THF (8 cm^3). The mixture was degassed before being set under argon atmosphere and the system was refluxed for 1 week. The reaction was cooled to room temperature and the polymer precipitated into methanol (500 cm^3) and allowed to stir over night. The precipitate was filtered off using a micro pore filtration system, and then dissolved in

chloroform (200 cm^3). The insoluble materials in the chloroform solution were filtered off using the micro pore filtration system, and then the filtrate was concentrated invacuo. The concentrated chloroform solution (~10 cm^3) was poured onto methanol (500 cm^3) and allowed to stir over night. The precipitate was filtered off using a micro pore filtration system and dried under vacuum giving the polymer mass 0.33 g, yielding 66%.

CHN Br - Expected: C, 83.15; H, 8.86; N, 3.73; O, 4.26, Br, 0.00.% Achieved C, 68.78; H, 7.44; N, 2.78; Br, 16.72.%; ^1H NMR: ($CDCl_3$) δ_H: 8.15 (d, 2H), 7.45 (dd, 2H), 7.25 - 7.10 (br m, 8H), 6.95 (br, 2H), 6.85 (br, 4H) 3.75 (br d, 4H), 1.75 (br, 2H), 1.55 – 1.15 (br, 32H), 0.85 (br, 12H).:

GPC: Mn 900 / Mw 1,250 / PDI 1.50

4.9.3 Poly(9-(bis-[4-(2-butyl-octyloxy)-phenyl]-amino-phen-4-yl)-carbazole-3,6-diyl) [27] (36) Suzuki (a) P3.AK

Into a oven dried flask was placed $Pd_2(dba)_3$ (5 mg, 0.0054 mmol), tri-*p*-tolyl phosphine (11.8 mg, 0.0045 mmol) and dry THF (10 cm^3). The reaction vessel was degassed and set under an argon atmosphere before being allowed to stir at 60°C for 30 minutes. The solution was cooled and a solution of 3,6-dibromo-9-(bis-[4-(2-butyl-octyloxy)-phenyl]-amino-phen-4-yl)-carbazole (317 mg, 0.339 mmol), 3,6-bis-(4,4,5,5-tetramethyl-[1,3,2]dioxaborolan-2-yl)-9-(bis-[4-(2-butyl-octyloxy)-phenyl]-amino-phen-4-yl)-carbazole (350 mg, 0.339 mmol) in dry THF (15 cm^3) was added via syringe and allowed to stir for 10 minutes. Then to this was added sodium hydrogen carbonate (1 g, 11.9 mmol) and water (10 cm^3) (de-oxygenated by bubbling argon through for 3-4 hours). The system was degassed and set to reflux for 24 hours. The solution was cooled and end capped first with bromo-*m*-xylene (0.1 cm^3) and allowed to reflux for 1 hour @ 120°C and then allowed to cool, followed by the addition of 3,5-dimethyl phenyl boronic acid (0.12 g) and allowed to reflux for 1 hour @ 120°C. The reaction was cooled and the polymer solution was treated in the following manner; the solution was reduced to approximately ~ 10 cm^3, this solution was precipitated into distilled methanol (500 cm^3) and allowed to stir over night. The precipitate was filtered off using a micro pore filtration system under an argon

atmosphere, and then dissolved in chloroform (200 cm^3). The insoluble materials in the chloroform solution were filtered off using the micro pore filtration system under an argon atmosphere, and then the filtrate was concentrated invacuo. The concentrated chloroform solution (~10 cm^3) was once again precipitated into distilled methanol (500 cm^3) and allowed to stir over night. The precipitate was filtered off using a micro pore filtration system and dried under vacuum.

The compound was then placed into a round bottom flask and treated with N,N-diethylphenylazothioformamide as follows: The polymer was dissolved in THF (~ 1 cm3 for each 20 mg of sample) under an argon atmosphere and N,N-diethylphenylazothioformamide was added (~ 10 time excess with respect to the amount of Pd in the catalyst used) and allowed to stir at reflux for 3 hours and after this the solution was cooled and allowed to stir at room temperature for a further 3 hours. The polymer solution was then concentrated to approximately ~ 10 cm^3 and the above precipitated and filtrated giving the polymer mass 0.50 g, yielding 96%.
CHN – ($C_{54}H_{68}N_2O_2$) Expected: C, 83.24; H, 9.06; N, 3.45; O, 4.11, Br, 0.00.% Achieved: C, 82.42; H, 8.91; N, 3.45; Br 0.00.%; IR (KBr) 3046, 2919, 2853, 1603, 1501, 1464, 1280, 1235, 1106, 794.; ^{1}H NMR: ($CDCl_3$) δ_H: 8.50 (br m, 2H), 7.72 (br m, 2H), 7.45 (br m, 2H), 7.35 (br m, 2H) 7.00-7.20 (br m, 6H), 6.85 (br m, 4H), 3.75 (br m, 4H) 1.75 (br m, 2H), δ 1.55 – 1.15 (br m, 32H), δ 0.85 (br m, 12H), ^{13}C NMR: ($CDCl_3$) δ_C: 156 (2C), 141 (1C), 140 (2C), 128 (1C), 127 (4C), 125 (4C), 123 (2C), 120 (4C), 118 (2C), 115 (6C), 110 (2C), 71 (2C), 38 (2C); 31 (2C); 29 (4C); 26 (2C); 24 (2C), 23 (2C), 21 (2C), 14 (4C) .:GPC: Mn 19,900 / Mw 31,500 / PDI 1.58

4.9.3 Poly{[9-(bis-[4-(2-butyl-octyloxy)-phenyl]-amino-phen-4-yl)-carbazole-3,6-diyl] -*alt*-[2,5-bis(*p*-phenylene)-1,3,4-oxadiazole]} [27] (37) Suzuki (a)

Into a oven dried flask was placed $Pd_2(dba)_3$ (5 mg, 0.0054 mmol), tri-*p*-tolyl phosphine (11.8 mg, 0.0045 mmol) and dry THF (10 cm^3). The reaction vessel was degassed and set under an argon atmosphere before being allowed to stir at 60°C for 30 minutes. The solution was cooled and a solution of 2,5-bis-(4-bromo-phenyl)-[1,3,4]-oxadiazole (128 mg, 0.339 mmol), 3,6-bis-(4,4,5,5-tetramethyl-[1,3,2]dioxaborolan-2-yl)-9-(bis-[4-(2-butyl-octyloxy)-phenyl]-amino-phen-4-yl)-

carbazole (350 mg, 0.339 mmol) in dry THF (15 cm^3) via syringe and allowed to stir for 10 minutes. Then to this was added sodium hydrogen carbonate (1 g, 11.9 mmol) and water (10 cm^3) (de-oxygenated by bubbling argon through for 3-4 hours). The system was degassed and set to reflux for 24 hours. The solution was cooled and end capped first with bromo-m-xylene (0.1 cm^3) and allowed to reflux for 1 hour @ 120°C and then allowed to cool, followed by the addition of 3,5-dimethyl phenyl boronic acid (0.12 g) and allowed to reflux for 1 hour @ 120°C. The reaction was cooled to room temperature and the polymer solution was treated in the following manner; the solution was reduced on to approximately ~ 10 cm^3, this solution was precipitated into distilled methanol (500 cm^3) and allowed to stir overnight. The precipitate was filtered off using a micro pore filtration system under an argon atmosphere, and then dissolved in chloroform (200 cm^3). The insoluble materials in the chloroform solution were filtered off using the micro pore filtration system under an argon atmosphere, and then the filtrate was concentrated invacuo. The concentrated chloroform solution (~10 cm^3) was once again precipitated into distilled methanol (500 cm^3) and allowed to stir over night. The precipitate was filtered off using a micro pore filtration system and dried under vacuum.

The compound was then placed into a round bottom flask and treated with N,N-diethylphenylazothioformamide as follows: The polymer was dissolved in THF (~ 1 cm3 for each 20 mg of sample) under an argon atmosphere and N,N-diethylphenylazothioformamide was added (~ 10 time excess with respect to the amount of Pd catalyst used) was allowed to stir at reflux for 3 hours and after this the solution was cooled and allowed to stir at room temperature for a further 3 hours. The polymer solution was then concentrated to approximately ~ 10 cm^3 and the above precipitated and filtrated process was repeated.

4.9.4 Poly{[9-(bis-[4-(2-butyl-octyloxy)-phenyl]-amino-phen-4-yl)-carbazole-3,6-diyl] -*alt*-[2,5-bis(*p*-phenylene)-1,3,4-oxadiazole]} [27] (38) Suzuki (b) P4.AK

Into a sealed tube was placed palladium (II) acetate (3.8 mg, 6.4 μmol), tri-p-tolyl phosphine (15.9 mg, 52.2 μmol) in toluene (3 cm^3). The reaction vessel degassed and

placed under an argon atmosphere. The tube was heated for 30 minutes at 50°C before being cooled to room temperature. To this was added a solution of 2,5-bis-(4-bromo-phenyl)-[1,3,4]-oxadiazole (128 mg, 0.339 mmol), 3,6-bis-(4,4,5,5-tetramethyl-[1,3,2]dioxaborolan-2-yl)-9-(bis-[4-(2-butyl-octyloxy)-phenyl]-amino-phen-4-yl)-carbazole (350 mg, 0.339 mmol) in dry toluene (15 cm^3) via syringe and allowed to stir for 10 minutes. Then to this was added tertra ethyl ammonium hydroxide ($20^W/_W$) (6 cm^3) (de-oxygenated by bubbling argon through for 3-4 hours). The system was degassed and set to reflux for 72 hours. The solution was cooled and end capped first with bromo-m-xylene (0.1 cm^3) and allowed to reflux for 1 hour @ 120°C and then allowed to cool, followed by the addition of dimethyl phenyl boronic acid (0.21 g) and allowed to reflux for 1 hour @ 120°C. The reaction was cooled to room temperature and the polymer solution was treated in the following manner; the solution was reduced on to approximately ~ 10 cm^3, this solution was precipitated into distilled methanol (500 cm^3) and allowed to stir overnight. The precipitate was filtered off using a micro pore filtration system under an argon atmosphere, and then dissolved in chloroform (200 cm^3). The insoluble materials in the chloroform solution were filtered off using the micro pore filtration system under an argon atmosphere, and then the filtrate was concentrated invacuo. The concentrated chloroform solution (~10 cm^3) was once again precipitated into distilled methanol (500 cm^3) and allowed to stir overnight. The precipitate was filtered off using a micro pore filtration system and dried under vacuum.

The compound was then placed into a round bottom flask and treated with N,N-diethylphenylazothioformamide as follows: The polymer was dissolved in THF (~ 1 cm3 to each 20 mg of sample) under an argon atmosphere and N,N-diethylphenylazothioformamide was added (~ 10 time excess with respect to the amount of Pd catalyst used) and allowed to stir at reflux for 3 hours and after this the solution was cooled and allowed to stir at room temperature for a further 3 hours. The polymer solution was then concentrated to approximately ~ 10 cm^3 and the above precipitated and filtrated giving the polymer mass 0.63 g, yielding 96%.

CHN – $(C_{68}H_{78}N_4O_3)\eta$ Expected: C, 81.72; H, 7.87; N, 5.41; O, 4.80, Br, 0.00.% Achieved: C, 79.65; H, 7.58; N, 4.72; Br 0.00.%; IR (KBr) 3046, 2931, 2853, 1640, 1603, 1501, 1313, 1271, 1235, 1006, 812, 728.; ^1H NMR: ($CDCl_3$) δ_H: 7.90 (br m, 4H), 7.72 (br m, 2H), 7.60 (br m, 4H), 7.50 (br m, 2H), 7.45 (br m, 2H), 7.35-6.90 (br

m, 8H), 6.85 (br m, 4H), 3.75 (br m, 4H) 1.75 (br m, 2H), δ 1.55 – 1.15 (br m, 32H), δ 0.85 (br m, 12H); ^{13}C NMR: ($CDCl_3$) δ_C: 159 (2C), 156 (2C), 149 (2C), 141 (1C), 140 (2C), 134 (2C) 128 (1C), 127 (8C), 125 (6C), 123 (4C), 120 (4C), 118 (2C), 115 (6C), 110 (2C), 71 (2C), 60 (2C); 38 (2C); 31 (2C); 29 (4C); 26 (2C); 24 (2C), 23 (2C), 21 (2C), 14 (4C).:
GPC: Mn 4,900 / Mw 7,900 / PDI 1.63

4.9.5 Poly{[9-(bis-[4-(2-butyl-octyloxy)-phenyl]-amino-phen-4-yl)-carbazole-3,6-diyl] -*alt*-[benzo-2,1,3-thiadiazol-4,7-diyl]} [27] (39) Suzuki (a) P6.AK

Into a sealed tube was placed palladium (II) acetate (3.8 mg, 6.4 μmol), tri-p-tolyl phosphine (15.9 mg, 52.2 μmol) in toluene (4 cm^3). The reaction vessel degassed and placed under an argon atmosphere. The tube was heated for 30 minutes at 50°C before being cooled to room temperature. To this was added a solution of 4,7-dibromobenzo[c][1,2,5]thiadiazole (98.6 mg, 0.339 mmol), 3,6-bis-(4,4,5,5-tetramethyl-[1,3,2]dioxaborolan-2-yl)-9-(bis-[4-(2-butyl-octyloxy)-phenyl]-amino-phen-4-yl)-carbazole (350 mg, 0.339 mmol) in dry toluene (15 cm^3) via syringe and allowed to stir for 10 minutes. Then to this was added tertra ethyl ammonium hydroxide ($20^W/_W$) (6 cm^3) (de-oxygenated by bubbling argon through for 3-4 hours). The system was degassed and set to reflux for 72 hours. The solution was cooled and end capped first with bromo-m-xylene (0.1 cm^3) and allowed to reflux for 1 hour @ 120°C and then allowed to cool, followed by the addition of 3,5-dimethyl phenyl boronic acid (0.21 g) and allowed to reflux for 1 hour @ 120°C. The reaction was cooled to room temperature and the polymer solution was treated in the following manner; the solution was reduced on to approximately ~ 10 cm^3, this solution was precipitated into distilled methanol (500 cm^3) and allowed to stir overnight. The precipitate was filtered off using a micro pore filtration system under an argon atmosphere, and then dissolved in chloroform (200 cm^3). The insoluble materials in the chloroform solution were filtered off using the micro pore filtration system under an argon atmosphere, and then the filtrate was concentrated invacuo. The concentrated chloroform solution (~10 cm^3) was once again precipitated into distilled

methanol (500 cm^3) and allowed to stir overnight. The precipitate was filtered off using a micro pore filtration system and dried under vacuum.

The compound was then placed into a round bottom flask and treated with N,N-diethylphenylazothioformamide as follows: The polymer was dissolved in THF (~ 1 cm3 to each 20 mg of sample) under an argon atmosphere and N,N-diethylphenylazothioformamide was added (~ 10 time excess with respect to the amount of Pd catalyst used) and allowed to stir at reflux for 3 hours and after this the solution was cooled and allowed to stir at room temperature for a further 3 hours. The polymer solution was then concentrated to approximately ~ 10 cm^3 and the above precipitation and filtrations process was repeated giving the polymer mass 0.64 g, yielding 98%.

CHN – ($C_{60}H_{70}N_4O_2S$) Expected: C, 78.90; H, 7.95; N, 6.13; S, 3.51, Br, 0.00.% Achieved: C, 78.40; H, 7.83; N, 6.09; S, 3.99; Br 0.00.%; IR (KBr) 3046, 2931, 2847, 1603, 1501, 1458, 1277, 1229, 1099, 1024, 891, 801, 716.; ^1H NMR: ($CDCl_3$) δ_H: 8.80 (br m, 2H), 8.0 – 7.80 (br m, 4H), 7.50 (br m, 2H), 7.30 (br m, 2H), 7.20 – 7.00 (br m, 4H), 6.85 (br m, 4H), 3.75 (br m, 4H) 1.75 (br m, 2H), δ 1.55 – 1.15 (br m, 32H), δ 0.85 (br m, 12H).; ^{13}C NMR: ($CDCl_3$) δ_C: 155 (2C), 153 (2C), 152 (2C), 139 (2C), 125 (2C), 124 (8C), 121 (6C), 118 (4C), 113 (6C), 107 (4C), 71 (2C), 60 (2C); 38 (2C); 31 (2C); 29 (4C); 26 (2C); 24 (2C), 23 (2C), 21 (2C), 11 (4C).:

GPC: Mn 11,000 / Mw 15,000 / PDI 1.35

4.9.6 Poly-(9,9'-dioctyl-fluorene-2,7-diyls) [27] (40) Suzuki (a)

Into an oven dried flask was placed $Pd_2(dba)_3$ (5 mg, 0.0054 mmol), tri-*p*-phenyl phosphine (16 mg, 0.0054 mmol) and dry THF (10 cm^3). The reaction vessel was degassed and set under an argon atmosphere before being allowed to stir at 60°C for 30 minutes. The solution was cooled and a solution of 2,7-dibromo-9,9-dioctyl-*9H*-fluorene (343 mg, 0.626 mmol), 2,7-Bis(trimethylene boronate)-9,9-dioctyl-*9H*-fluorene (350 mg, 0.626 mmol) in dry THF (20 cm^3) via syringe and allowed to stir for 10 minutes. Then to this was added sodium hydrogen carbonate (1 g, 11.9 mmol) and water (10 cm^3) (de-oxygenated by bubbling argon through for 3-4 hours). The system was degassed and set to reflux for 24 hours. The solution was cooled and end

capped first with bromo-m-xylene (0.1 cm^3) and allowed to reflux for 1 hour @ 120°C and then allowed to cooled to room temperature, followed by the addition of 3,5-dimethyl phenyl boronic acid (0.12 g) and allowed to reflux for 1 hour @ 120°C. The reaction was cooled and the solution precipitated into methanol (500 cm^3) and allowed to stir overnight. The precipitate was filtered off using a micro pore filtration system, and then dissolved in chloroform (200 cm^3). The insoluble materials in the chloroform solution were filtered off using the micro pore filtration system, and then the filtrate was concentrated invacuo. The concentrated chloroform solution (~10 cm^3) was poured onto methanol (500 cm^3) and allowed to stir overnight. The precipitate was filtered off using a micro pore filtration system and dried under vacuum giving the polymer mass 0.61 g, yielding 91%.
CHN Br - ($C_{29}H_{40}$) Expected: C, 89.16; H, 10.84; Br, 0.00.% Achieved: C, 86.15; H, 9.86; Br 0.00.%;
GPC: Mn 14,000 / Mw 51,000 / PDI 3.65

4.9.7 Poly-(9,9'-dioctyl-fluorene-2,7-diyls) (41) Suzuki (b) P5.AK

Into a oven dried flask was placed 2,7-dibromo-9,9-dioctyl-*9H*-fluorene (495 mg, 0.895 mmol), 2,7-Bis(trimethylene boronate)-9,9-dioctyl-*9H*-fluorene (502 mg, 0.895 mmol) in dry THF (20 cm^3). Then to this was added $Pd_2(dba)_3$ (2.5 mg, 0.0027 mmol), tri-*o*-tolyl phosphine (5.7 mg, 0.0018 mmol) and dry THF (10 cm^3) was added via syringe and allowed to stir for 10 minutes. To this was added tertra ethyl ammonium hydroxide ($20^W/_W$) (3.2 cm^3) (de-oxygenated by bubbling argon through for 3-4 hours) and the system was degassed and set under argon to reflux for 24 hours. The solution was cooled and end capped first with bromo-m-xylene (0.1 cm^3) and allowed to reflux for 1.5 hour @ 120°C and then allowed to cool, followed by the addition of 3,5-dimethyl phenyl boronic acid (0.15 g) and allowed to reflux for 1.5 hour @ 120°C. The reaction was cooled and the polymer solution was treated in the following manner; the solution was reduced on to approximately ~ 10 cm^3, this solution was precipitated into distilled methanol (500 cm^3) and allowed to stir overnight. The precipitate was filtered off using a micro pore filtration system under an argon atmosphere, and then dissolved in chloroform (200 cm^3). The insoluble

materials in the chloroform solution were filtered off using the micro pore filtration system under an argon atmosphere, and then the filtrate was concentrated invacuo. The concentrated chloroform solution (~10 cm^3) was once again precipitated into distilled methanol (500 cm^3) and allowed to stir overnight. The precipitate was filtered off using a micro pore filtration system and dried under vacuum.

The compound was then placed into a round bottom flask and treated with N,N-diethylphenylazothioformamide as follows: The polymer was dissolved in THF (~ 1 cm3 for each 20 mg of sample) under an argon atmosphere and N,N-diethylphenylazothioformamide was added (~ 10 time excess with respect to the amount of Pd catalyst used) and was allowed to stir at reflux for 3 hours and after this the solution was cooled and allowed to stir at room temperature for a further 3 hours. The polymer solution was then concentrated to approximately ~ 10 cm^3 and the above precipitation and filtrations process was repeated giving the polymer mass 0.96 g, yielding 99%.

CHN Br - ($C_{29}H_{40}$) Expected: C, 89.16; H, 10.84; Br, 0.00.% Achieved: C, 88.46; H, 10.43; Br 0.00.%; IR (KBr) 3063, 2925, 2853, 1458, 1255, 819, 794, 717.; ^{1}H NMR: ($CDCl_3$) δ_H: 7.75 (br, 2H), 7.55 (br, 4H), 1.50 (br, 2H), δ 1.25 – 1.00 (br, 24H), δ 0.75 (br m, 6H).; ^{13}C NMR: ($CDCl_3$) δ_C: 151 (2C), 141 (2C), 140 (2C), 126 (2C), 122 (2C), 119 (2C), 55 (1C); 40 (2C); 31 (2C); 30 (2C); 29 (2C), 23 (2C), 22 (2C), 14 (2C).:

GPC: Mn 64,300 / Mw 174,000 / PDI 2.70

4.10 References

1. Yamamoto, T., Hidershima, C., Suehiro, K., Tashiro, M., Prakash, G.K.S., Olah, G.A.; *J. Org. Chem.*, **1991**, *56*, 6248.
2. Choy, N., Russell, K.C., Alvarez, J.C., Fider, A.; *Tetra. Lett.*, **2000**, *41*, 1515.
3. Smith, K., James, D.M., Mistry, A.G., Bye, M.R., Faulkner, D.J., *Tetrahedron*, **1992**, *48*, 7479.
4. Georg, C.D., Paul, C.J.K., Piet, W.N.M.; *Eur. J. Org. Chem.*, **1998**, 359.
5. a) Clive, D.L.J., Anghoh, A.G., Bennent, S.M.; *J. Org. Chem.*, **1987**, *52*, 1339. b) Jeffery, T., Ferber, B.; *Tetra. Lett.*, **2003**, *44*, 193.
6. Zimmerman, S.C., Wang, Y., Bharathi, P., Moore, J.S.; *J. Am. Chem. Soc.*, **1998**, *120*, 2172.
7. Goodbrand, H.B., Hu, N.X.; *J. Org. Chem.*, **1999**, *64*, 670.
8. Klapers, A., Antilla, J.C., Huang, X., Buchwald, S.L.; *J. Am. Chem. Soc.*, **2001**, *123*, 7727.
9. Klapers, A., Huang, X., Buchwald, S.L.; *J. Am. Chem. Soc.*, **2002**, *124*, 7421.
10. Beginin, C., Gravzulevicius, J.V., Strohriegl, P.; *Macromol. Chem. Phys.*, **1994**, *95*, 2353.
11. Forbus, T.R., Taylor, S.L. Jr., Martin, J.C.; *J. Org. Chem.*, **1987**, *52*, 4156.
12. Wazeer, M.I.M., Ali, A. S., Arab, M.; *Spec. Chimi. Acta.*, **1987**, *43A*, 843.
13. Han, S., Xiao, Z., Bastow, K.F., Lee, K.; *Bio. Med. Chem. Lett.*, **2004**, *14*, 2979.
14. Strazzolini, P., Verardo, G., Giumanni, A.G.; *J. Org. Chem.*, **1988**, *53*, 3321.
15. Kundig, E.P., Lomberget, T., Bragg, R., Poulard, C., Bernardinelli, G.; *Chem. Commun.*, **2004**, 1548.
16. Hagen, A.P., Miller, T.S., Bynum, R.L., Kapila, V.P.; *J. Org. Chem.*, **1982**, *47*, 1345.
17. Parker, K.A., Spero, D.M., Koziski, K.A.; *J. Org. Chem.*, **1987**, *52*, 183.
18. Tyagi, Y.T., Kummar, A., Raj, H.G., Vohra, P., Gupta, G., Kumari, R., Kumar, P., Gupta, R.K.; *Euro. J. Med. Chem.*, **2003**, *40*, 413.
19. Novak, Z., Timari, G., Kotschy,A.; *Tetrahedron*, **2003**, *59*, 7509.
20. Jian, H., Tour, J.M.; *J. Org. Chem.*, **2003**, *68*, 5091.

21. Yang, W., Hou, Q., Liu, C., Niu, Y., Huang, J., Yang, R., Yong, C.; *J. Mat. Chem.*, **2003**, *13*, 1351.
22. Jo, J., Chi, C., Hoger, S., Wegner, G., Yoon, D.Y.; *Eur. J. Chem.*, **2004**, *10*, 2681.
23. Nielsen, K.T., Bechgaard, K., Krebs, F.C.; *Macromolecules*, **2005**, *38*, 658.
24. Zhan, X., Liu, Y., Wu, X., Wang, S. Zhu, D.; *Macromolecules*, **2002**, *35*, 2529.
25. Pilgram, K., Zupan, M., Skiles, R.; *J. Het. Chem.*, **1970**, *7*, 629.
26. Yamamoto, T., Hayashi, Y., Yamamoto, A.; *Bull. Chem. Soc. Jpn.*, **1978**, *51*, 2091.
27. Suzuki, A.; *J. Organomet. Chem.*, **2002**, *653*, 83.
28. Pardo, A., Reyman, D., Poyato, J.M.L., Medina, F.; *J. Lumin.*, **1992**, *51*, 269.
29. Gritzner, G.; *P. Appl. Chem.*, **1990**, *62*, 1839.

5.0.0 Results and Discussion

5.1.0 Synthesis of 2,7-dibromo-*9H*-carbazole

The preparation of 2,7-dibromo-*9H*-carbazole is outlined in the scheme shown. The description of the various steps involved is provided below.

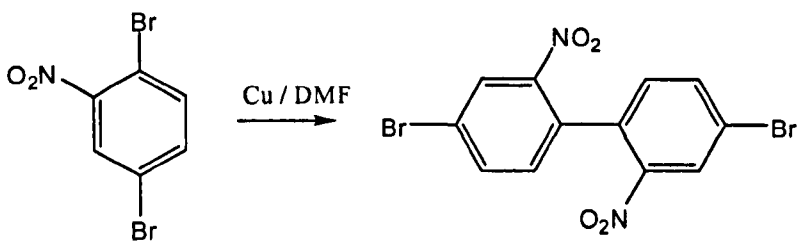

Scheme 1 74% **1**

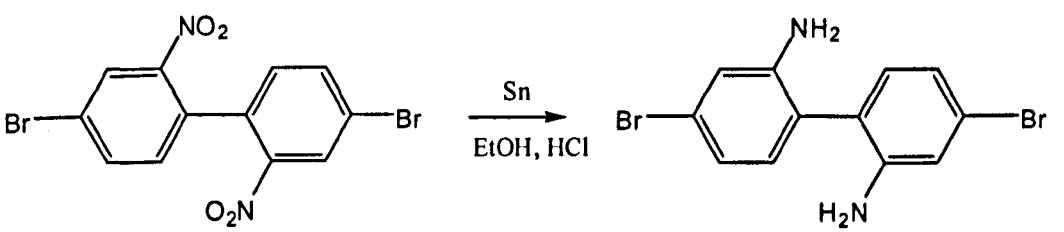

Scheme 2 **1** 88% **2**

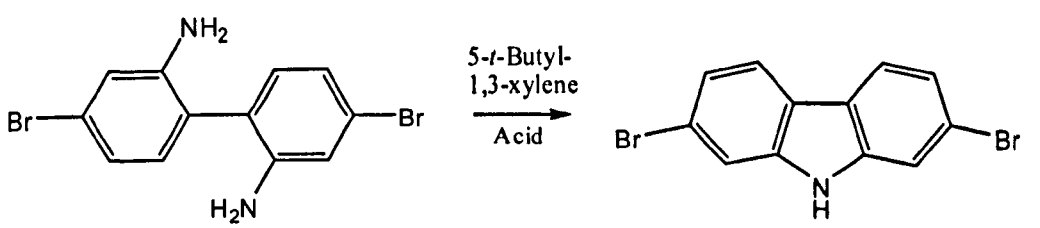

Scheme 3 **2** 87% **3**

5.1.1 4,4'-Dibromo-2,2'dinitrobiphenyl (1)

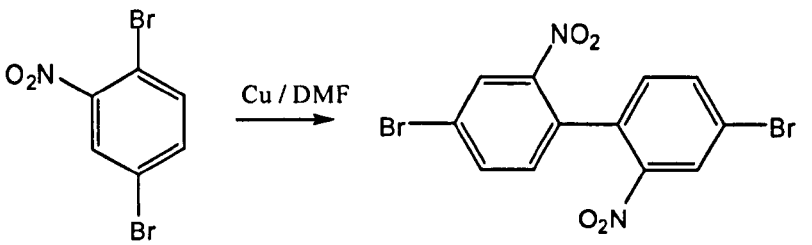

Scheme 1 74% **1**

4,4'-Dibromo-2,2'-dinitrobiphenyl **(1)** was obtained in a 74% yield, by a modified procedure of Yamamoto *et al.* [(1)] The product was prepared via a Ullmann coupling reaction of 2,5-dibromonitrobenzene using copper powder in a solution of dimethylformamide, as shown in scheme 1. The reaction was completed after heating the mixture for 2 hours at 120 °C, and following work-up to give the isolated product as a pale yellow powder.

The purity of the product was confirmed by TLC, GC mass spectra, melting point and elemental analysis. The structure of the product was identified by IR absorption, ^{1}H NMR and ^{13}C NMR.

The Ullmann coupling reaction proceeds via a two step process as shown in mechanism 1 on page 88. This first step is the nucleophilic attack by the copper into the C-Br bond ortho to the nitro group on the benzene ring. The attack is favoured due to the π-orbital stabilisation offered by the nitro group functionality. This activating effect of the nitro group ortho to the C – Br bond increases the electropositivity of the aromatic carbon atom at position 1 of the benzene ring, thus facilitating this first step. This is considered to be the rate determining step [(2)]. The mechanism of the second step, although not completely clear, proceeds by the copper bromide complex formed on the benzene ring generating a radical type system. A second molecule of 2,5-dibromonitrobenzene is attacks at this position on the carbon ring and the coupling takes place producing copper (II) bromide as a side product.

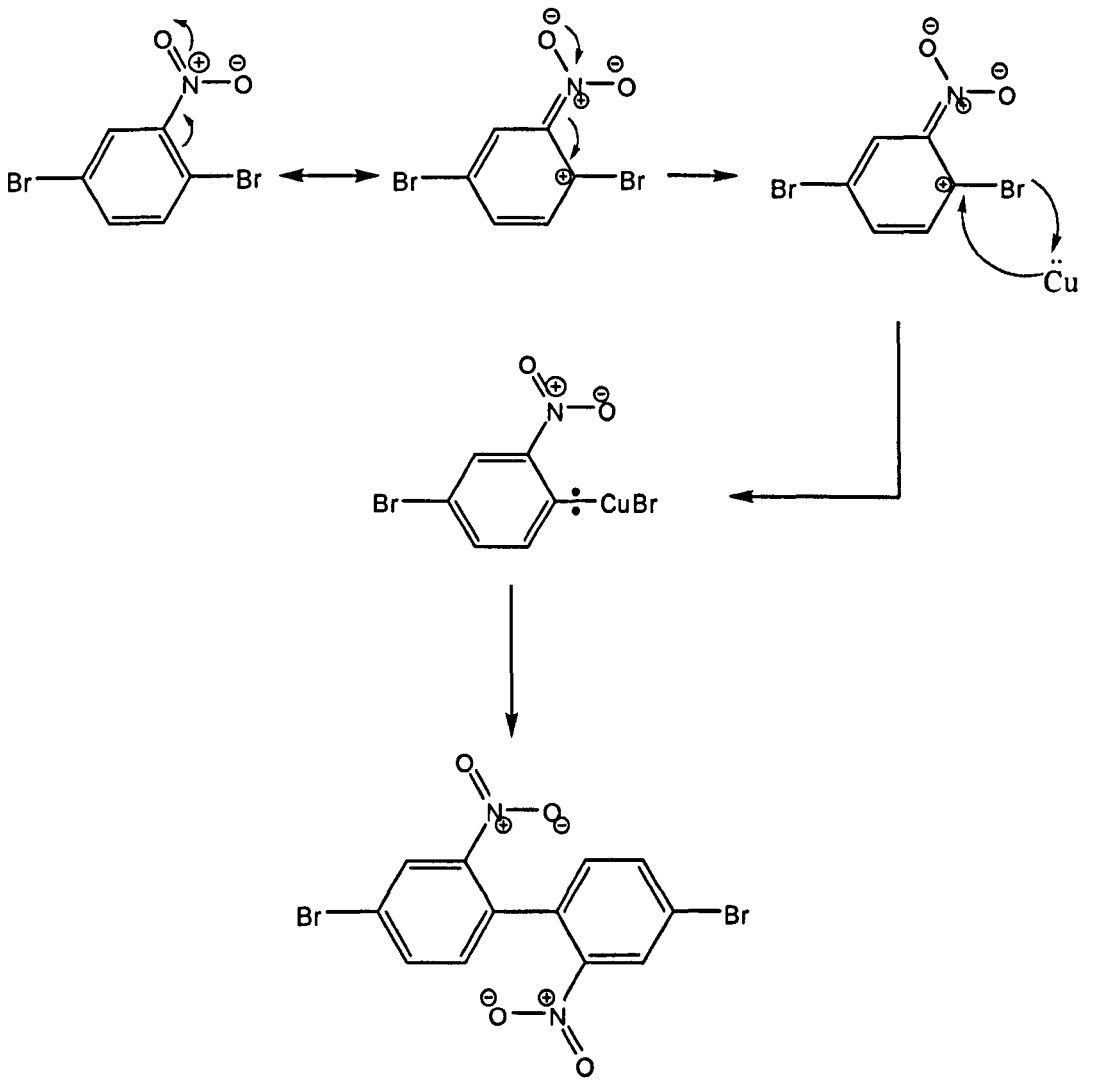

Mechanism 1, [3] Ullmann coupling reaction forming 4,4'-dibromo-2,2'-dinitrobiphenyl (1)

The purity of the product was confirmed by a single peak by GC with a retention time of 14.7 minutes. The mass spectra showed main integer masses for 4,4'-dibromo-2,2'-dinitrobiphenyl **(1)** at 400, 402, and 404 in a 1:2:1 ratio as expected due to ^{79}Br and ^{81}Br isotopes. The melting point of the product was 147-149 °C and was in agreement with reports from literature. The product was subjected to elemental analysis, for the compound $C_{12}H_6Br_2N_2O_4$ we calculated the expected percentage for the comprising elements to be: C, 35.85; H, 1.50; Br, 39.75; N, 6.97; O, 15.92.%; from analysis we obtained: C, 37.95; H, 1.47; Br, 40.70; N, 6.89.%; which fell into agreement to calculations.

The structure of the product was confirmed by IR spectrum giving peaks at 3071 cm^{-1} and 2850 cm^{-1} as the C-H stretch followed by 1925 cm^{-1}, 1860 cm^{-1}, 1786 cm^{-1} and 1780 cm^{-1} which can be designated to the combination or overtone vibrations of the out-of-plane deformation vibrations of the C-H bonds of the 1,2,4-trisubstituted benzene ring. Also the bands 1602 cm^{-1}, 1554 cm^{-1}, 1528 cm^{-1} and 1464 cm^{-1} can be denoted to C=C for the aromatic rings. The peaks arising at 1528 cm^{-1}, 1341 cm^{-1} are related to the stretching vibrations of the Ar-NO_2 groups, and a peak at 865 cm^{-1} stretching vibrations of the C-N bond. Finally the peak at 729 cm^{-1} can be linked to the stretching vibrations of the C-Br bonds.

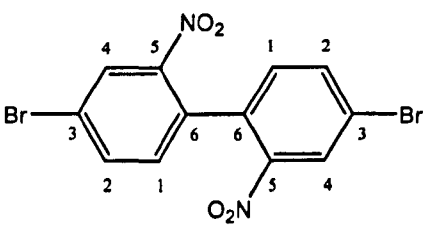

Figure 5.1, 4,4'-dibromo-2,2'-dinitrobiphenyl (1)

The ^{1}H-NMR spectrum identifies the product with 3 distinct signals equal in intensity. The signal at δ 8.37 ppm is linked to the protons assigned as position 4 on the ring system, which is a singlet due to no coupling with a near by proton. The protons at position 1 and 2 shown signals at δ 7.17 ppm and δ 7.83 ppm respectively as doublets due close proximity of coupling with one another.

The ^{13}C-NMR gave five peaks on the spectrum which have been estimated to the following positions of the compound δ 147 (2C) position 5, δ 138 (2C) position 2, δ 132 (4C) positions 1 and 6, δ 128 (2C) position 4 and δ 123 (2C) position 3. These peaks are in well agreement with the structure of 4,4'-dibromo-2,2'-dinitrobiphenyl **(1)**. These analytical results clearly verify that the product was 4,4'-dibromo-2,2'-dinitrobiphenyl **(1)**.

5.1.2 2,2'-Diamino-4,4'-dibromobiphenyl (2)

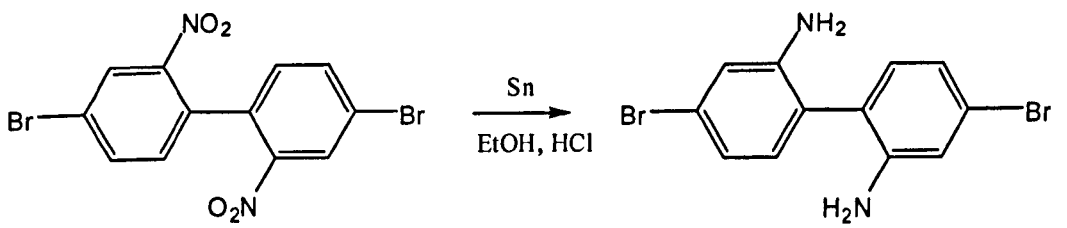

Scheme 2 **1** 88% **2**

2,2'-Diamino-4,4'-dibromobiphenyl **(2)** was obtained in a 88% yield, by a modified procedure of Yamamoto *et al.* [1] The product was obtained via a reduction reaction of 4,4'-dibromo-2,2'-dinitrobiphenyl **(1)** using tin powder in a solution mixture of ethanol (HPLC grade) and hydrochloric acid (conc.), as shown in scheme 2. The reaction was complete after heating the mixture for 2 hours at 90 °C to produce a homogeneous solution, and following work-up to give the isolated product as an ivory yellow crystalline solid.

The purity of the product was confirmed by TLC, GC mass spectra, melting point and elemental analysis. The structure of the product was identified by IR absorption, ^{1}H NMR and ^{13}C NMR.

This reaction is considered to be carried out in two parts, the first being the reduction of the reaction mixture followed by the basification of the mixture in the work-up. The reaction mixture was heterogeneous at first and as the reaction proceeded the tin powder was consumed and the mixture became clearer. This can be considered to occur due to the increased solubility of the product as an amine salt in acidic conditions. After 1 hour all the tin powder had been consumed, however the mixture was still heterogeneous probably because the reaction had not reached completion. After addition of a further portion of tin powder and refluxing for a further period of 1 hour the mixture became a homogeneous yellow solution along with a solid lump of excess tin powder. At this point the reaction was considered to have gone to completion and was cooled to room temperature and the tin powder was filtered off. The filtrate was then basified by pouring onto ice and aqueous sodium hydroxide

solution. This produced a fine white suspension probably due a complex formed with the tin. This was filtered off with the aid of Celite® filter gel and the filtrate was then extracted with diethyl ether. The product was obtained as a pale yellow powder.

The reduction of the nitro group to the amino group can be considered to take place mechanistically as follows. The reaction occurs under an acid solution to help formulate a protonated amine. The subsequent treatment with base generates the amine.

$$2ArNO_2 + 3Sn + 12H^+ \longrightarrow 2ArNH_2 + 4H_2O + 3Sn^{4+}$$

Mechanisms 2 [3], Reduction of 4,4'-dibromo-2,2'-dinitrobiphenyl **(1)** forming 2,2'-diamine-4,4'-dibromobiphenyl **(2)**

The purity of the product was confirmed by a single peak by GC with a retention time of 14.6 minutes. The mass spectra showed main integer masses for 2,2'-diamine-4,4'-dibromobiphenyl **(2)** at 340, 342, and 344 in a 1:2:1 ratio as expected due to ^{79}Br and ^{81}Br isotopes. The melting point of the product was 101-103 °C and was in agreement with reports from literature. The product was subjected to elemental analysis, for the compound $C_{12}H_{10}Br_2N_2$ we calculated the expected percentage for the comprising elements to be: C, 42.14; H, 2.95; Br, 46.72; N, 8.19.%; from analysis we obtained: C, 42.58; H, 2.35; Br, 47.80; N, 8.27.%; which fell into close agreement to calculations.

The structure of the product was confirmed by its IR spectrum giving peaks at 3396 cm^{-1}, 3289 cm^{-1}, 3186 cm^{-1} stretching vibrations of the $-NH_2$ groups. In reassurance we have lost peaks arising at 1528 cm^{-1}, 1341 cm^{-1} which were related to the stretching vibrations of the $Ar-NO_2$ groups. The peak at 3073 cm^{-1} as the C-H stretch followed by 1881 cm^{-1}, 1866 cm^{-1}, 1694 cm^{-1} and 1639 cm^{-1} which can be designated to the combination or overtone vibrations of the out-of-plane deformation vibrations of the C-H bonds of the 1,2,4-trisubstituted benzene ring. Also the bands 1579 cm^{-1}, 1558 cm^{-1}, 1491 cm^{-1} and 1474 cm^{-1} can be denoted to C=C for the aromatic rings. Peaks at 931 cm^{-1} to 554 cm^{-1} out-of-plane deformation vibrations of the $C-NH_2$

bonds, and finally the peak at 739 cm^{-1} can be linked to the stretching vibrations of the C-Br bonds.

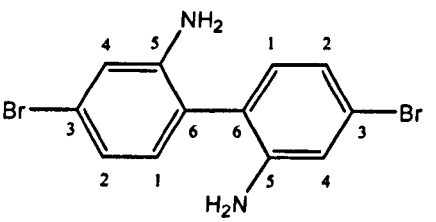

Figure 5.2, 2,2'-diamine-4,4'-dibromobiphenyl **(2)**

The ^{1}H-NMR spectrum identifies the product with 3 distinct signals in the spectra. The signal at δ 7.0 ppm is linked to the protons assigned at position 4 on the ring system, which is a singlet due to no coupling with the near proton; a change in chemical shift can be noted from the transformation of the nitro group to the amine. The protons at position 1 and 2 give rise to the signal at δ 6.97-6.82 ppm as a multiplet due close proximity of coupling with one another and the effect of the amine groups on the chemical shifts. This leaves a broad peak at δ 3.70 ppm which is assigned to the protons within the amine group.

The ^{13}C-NMR gave six peaks on the spectrum which have been estimated to the following positions of the compound δ 145 (2C) position 5, δ 132 (2C) position 1, δ 123 (2C) positions 2, δ 122 (2C) position 3, δ 119 (2C) position 6 and δ 118 (2C) position 4. These peaks are in well agreement with the structure of 2,2'-diamine-4,4'-dibromobiphenyl **(2)**. These analytical results clearly verify that the product was 2,2'-diamine-4,4'-dibromobiphenyl **(2).**

5.1.3 2,7-Dibromo-*9H*-carbazole (3)

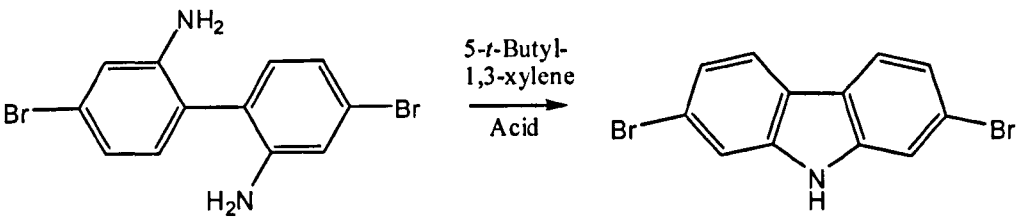

Scheme 3 **2** 87% **3**

2,7-Dibromo-*9H*-carbazole **(3)** was obtained in a 87% yield, by a modified procedure of Yamamoto *et al.* [(1)] The product was prepared via a cyclisation reaction. The reaction proceeded by ring closure of the amine groups of 2,2'-diamine-4,4'-dibromobiphenyl **(2)** using 4- dodecylbenzenesulfonic acid in the high boiling point solvent 5-*t*-butyl-*m*-xylene, as shown in scheme 3. The reaction was complete after heating the mixture for 24 hours at reflux temperature, following work-up was isolated the product as an orange crystalline solid. The purity of the product was confirmed by TLC, GC mass spectra, melting point [(4)] and elemental analysis. The structure of the product was identified by IR absorption, ^{1}H NMR and ^{13}C NMR.

The mechanism of this cyclisation reaction is not fully understood, attempts have been carried out to formulate a mechanism for this process, like that of the reaction of 2,2'-diamino-4,4'-dibromobiphenyl in the presence of aqueous hydrochloric acid carried out by Tauber [(36)] but in this reaction the reagents and conditions were contrasting and would clearly not work under the basis which was applied. The cyclisation reaction carried out occurs under homogeneous acid conditions using dodecylbenzenesulfonic acid which can withstand high reflux temperatures.

It can be assumed that the reaction mechanism is achieved through a two step process, the first of which would be the protonation of the amino group to $-NH_3^+$ which would develop a leaving group and the secondary amino group $-NH_2$ acts as a nucleophile. The second step would likely be a intermolecular cyclisation reaction to yield the product.

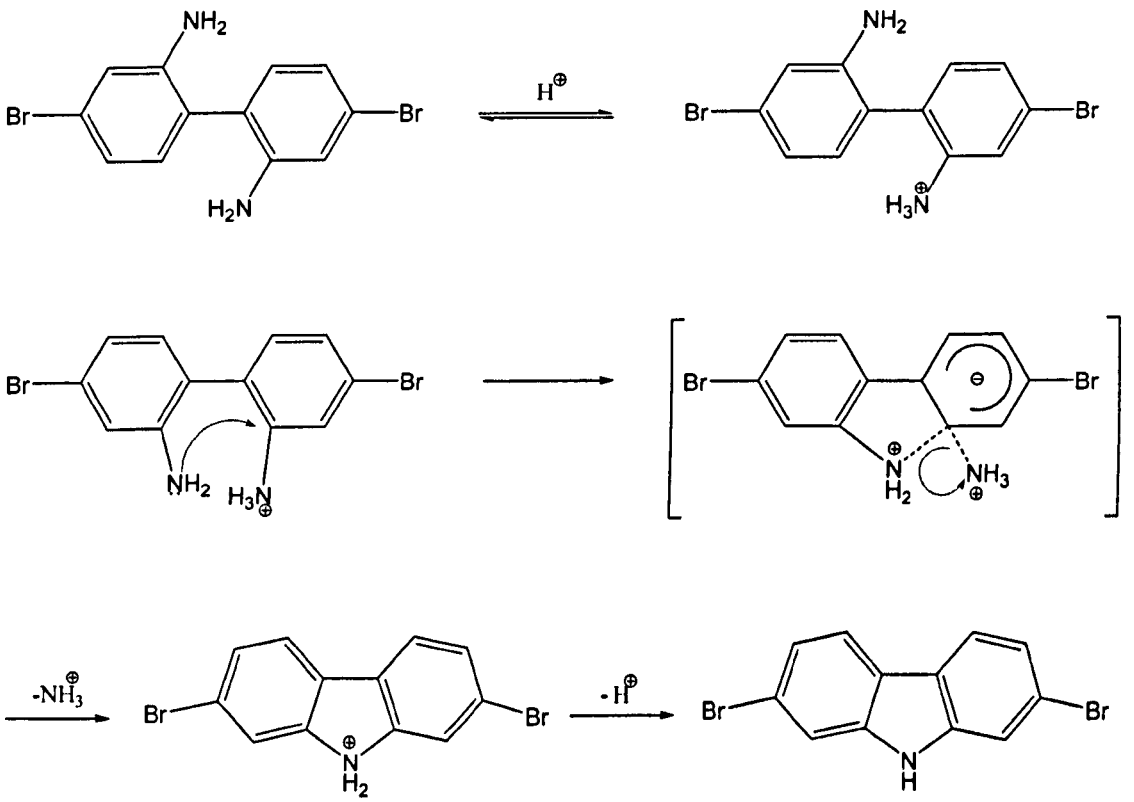

Mechanism 3, [5] formation of 2,7-dibromo-*9H*-carbazole **(3)**

The purity of the product was confirmed by a single peak by GC with a retention time of 15.0 minutes. The mass spectra showed main integer masses for 2,7-dibromo-*9H*-carbazole **(3)** at 323, 325, and 327 in a 1:2:1 ratio as expected due to ^{79}Br and ^{81}Br isotopes. The melting point of the product was 217-220 °C and was in agreement with reports from literature [4]. The product was subjected to elemental analysis, for the compound $C_{12}H_7Br_2N$ we calculated the expected percentage for the comprising elements to be: C, 44.35; H, 2.17; Br, 49.17; N, 4.31.%; from analysis we obtained: C, 44.95; H, 2.67; Br, 49.97; N, 4.21.%; which fell into close agreement to calculations.

The structure of the product was confirmed by IR spectrum giving peaks at 3400 cm^{-1} and 3100 cm^{-1} stretching vibrations of the tertiary –NH groups. The peak at 3074 cm^{-1} relates to the C-H stretch followed by 1889 cm^{-1} and 1705 cm^{-1}, 897 cm^{-1}, 861 cm^{-1}, 805 cm^{-1} which can be designated to the combination or overtone vibrations of the

out-of-plane deformation vibrations of the C-H bonds of the carbazole ring. The peaks arising at 1625 cm^{-1}, 1600 cm^{-1}, 1481 cm^{-1}, 1461 cm^{-1}, 1448 cm^{-1}, 1424 cm^{-1}, stretching vibrations due to C=C bonds of the carbazole ring, also the band at 1241 cm^{-1} can be denoted to C-N on the carbazole ring. Finally the peak at 732 cm^{-1} can be linked to the stretching vibrations of the C-Br bonds.

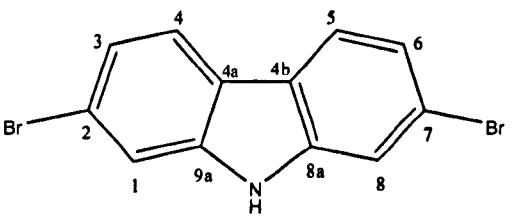

Figure 5.3, 2,7-dibromo-*9H*-carbazole **(3)**

The ^{1}H-NMR spectrum identifies the product with 4 signals in the spectra. The broad signal at δ 8.00 ppm is linked to the proton 9H on the carbazole ring system. It is the single proton from the attaching tertiary amine with an integral half that of the aromatic carbazole. The next signal is that arising at δ 7.85 ppm which is a doublet in relation to protons at positions 3 and 6. The next set is a singlet at δ 7.45 ppm due to no coupling with near protons; and relates to the protons positioned at 1 and 8. The protons at position 4 and 5 give rise to the signal at δ 7.25 ppm as a doublet.

The ^{13}C-NMR gave six peaks on the spectrum which have been estimated to the following positions of the compound δ 142 (2C) positions 9a and 9b, δ 124 (2C) positions 3 and 6, δ 123 (2C) positions 4a and 4b, δ 122 (2C) positions 5a and 5b, δ 120 (2C) positions 1 and 8 and δ 115 (2C) positions 2 and 7. These peaks are in well agreement with the structure of 2,7-dibromo-*9H*-carbazole **(3)**. These analytical results clearly verify that the product was 2,7-dibromo-*9H*-carbazole **(3).**

5.2.0 Synthesis of 2,7-dibromo-3,6-dimethyl-9H-carbazole

The preparation of 2,7-dibromo-3,6-dimethyl-*9H*-carbazole is outlined in the scheme shown. The description of the various steps involved is provided below.

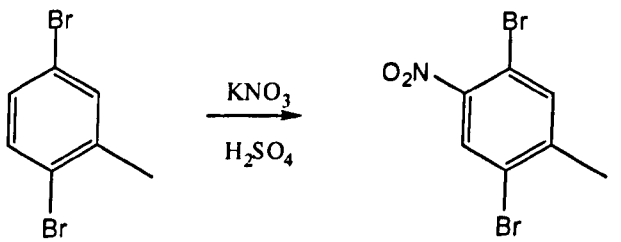

Scheme 4 89% **4**

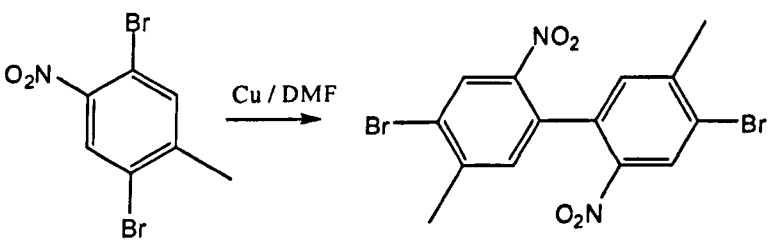

Scheme 5 86% **5**

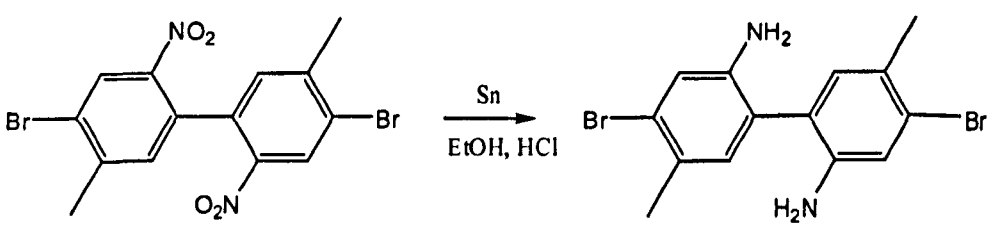

Scheme 6 **5** 89% **6**

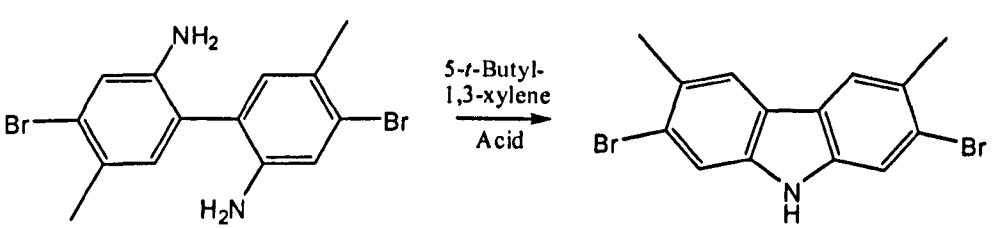

Scheme 7 **6** 82% **7**

5.2.1 2,5-Dibromo-4-nitro-toluene (4)

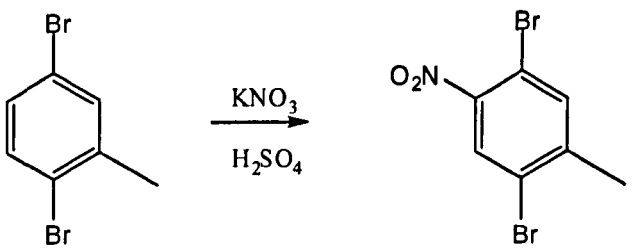

Scheme 4 89% **4**

2,5-Dibromo-4-nitro-toluene **(4)** was obtained in a 89% yield, by a modified procedure of Choye *et al.* [6] The product was prepared by the nitration of 2,5-dibromotoluene using potassium nitrate and sulphuric acid, as shown in scheme 4. The purity of the product was confirmed by TLC, GC mass spectra, melting point and elemental analysis. The structure of the product was identified by IR absorption, ^{1}H NMR and ^{13}C NMR

The reaction was carried out at 40°C, and after 1 hour it was observed that a pale yellow solid began to precipitate, after 3 hours the reaction was stopped and poured onto ice and water and then extracted into dichloromethane. The crude product was isolated as a yellow solid, and analysis showed it consisted of the desired product and un-reacted starting material. This was purified by re-crystallisation from ethanol to yield 2,5-dibromo-4-nitrotoluene **(4)** as yellow crystals. The recovered starting material was put back through another nitration reaction to yield more of the desired product.

The mechanism for the nitration of 2,5-dibromotoluene is electrophilic aromatic substitution. The reaction between potassium nitrate and sulphuric acid results in the generation of the nitronium ion (NO_2^+) electrophile. The mechanism then proceeds via electrophilic aromatic substitution mechanism.

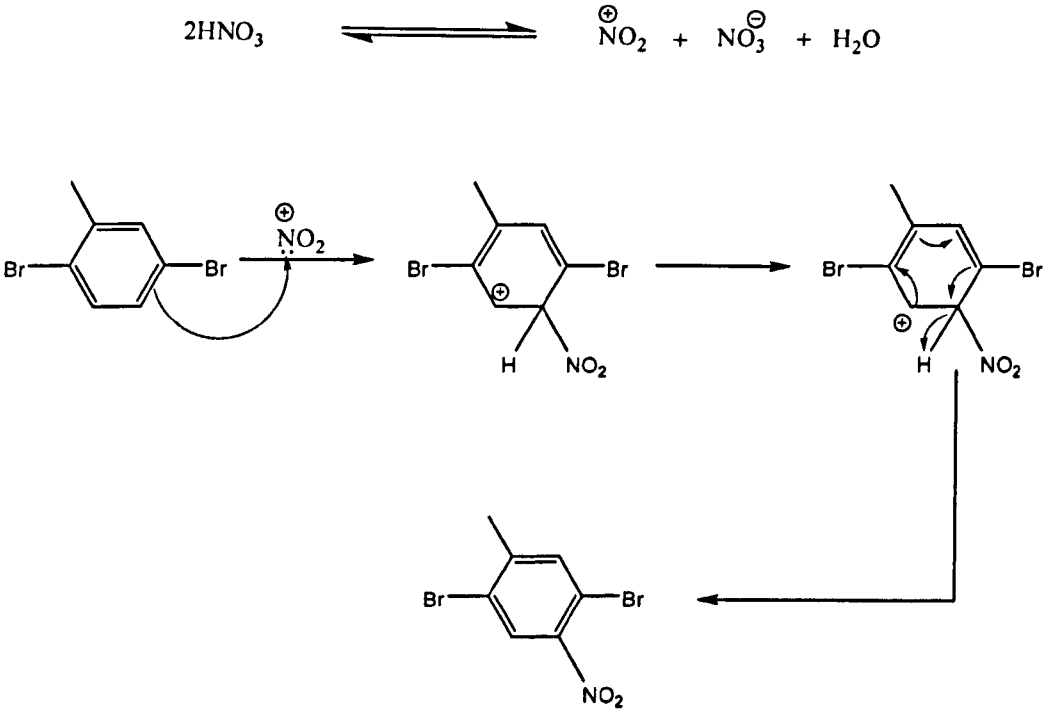

Mechanism 4, [7] formation of 2,5-dibromo-nitro-toluene **(4)**

The purity of the product was confirmed by a single peak by GC with a retention time of 14.39 minutes. The mass spectra showed main integer masses for 2,5-dibromo-nitro-toluene **(4)** at 293, 295, and 297 in a 1:2:1 ratio as expected due to ^{79}Br and ^{81}Br isotopes. The melting point of the product was 158-160 °C and was in agreement with reports from literature. The product was subjected to elemental analysis, for the compound $C_7H_5NO_2Br_2$ we calculated the expected percentage for the comprising elements to be: C, 28.47; H, 1.69; N, 4.75; Br, 54.24.%; from analysis we obtained: C, 28.52; H, 1.50; N, 4.60; Br, 54.30.%; which fell into close agreement to calculations.

The structure of the product was confirmed by IR spectrum giving peaks at 3090 cm^{-1} and 1769 cm^{-1},1258 cm^{-1}, 1135 cm^{-1}, 1028 cm^{-1}, 820 cm^{-1}, 749 cm^{-1}, 694 cm^{-1} as the C-H stretch followed by 2973 cm^{-1}, 2854 cm^{-1} and 1386 cm^{-1} the stretching vibration due methyl groups. Also the bands 1564 cm^{-1}, 1456 cm^{-1} can be denoted to C=C for the aromatic rings. The peaks arising at 1511 cm^{-1}, 1341 cm^{-1} are related to the stretching vibrations of the Ar-NO_2 groups, and a peak at 892 cm^{-1} stretching

vibrations of the C-N bond. Finally the peak at 749 cm^{-1} can be linked to the stretching vibrations of the C-Br bonds.

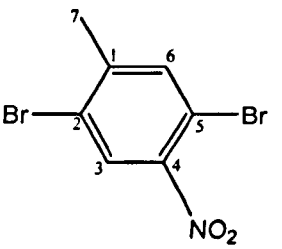

Figure 5.4, 2,5-dibromo-nitro-toluene **(4)**

The ^{1}H NMR shows two singlet in the aromatic region at δ 8.02 ppm and δ 7.55 ppm at position 3 and 6 respectively which are consistent with the structure of the product. And also the peak at δ 2.39 ppm linked to the methyl groups at position 7. The ^{13}C NMR spectra of the product was also in good agreement with the structure of 2,5-dibromo-4-nitrotoluene **(4)**.

The ^{13}C-NMR gave seven peaks on the spectrum which have been estimated to the following positions of the compound δ 147 (1C) position 4, δ 144 (1C) position 1, δ 136 (1C) position 6, δ 129 (1C) position 3, δ 123 (1C) positions 2, δ 113 (1C) position 5 and δ 22 (1C) position 7. These analytical results clearly verify that the product was 2,5-dibromo-4-nitro-toluene **(4)**.

5.2.2 4,4'-Dibromo-2,2'-dinitro-5,5'-dimethylbiphenyl (5)

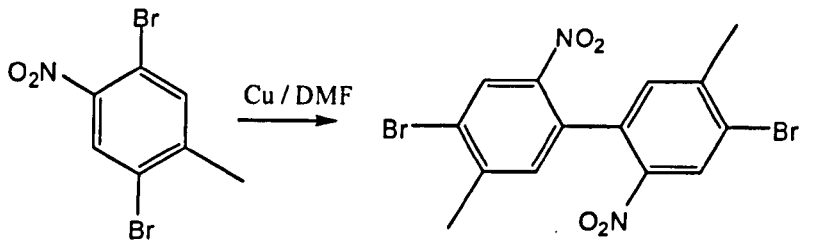

Scheme 5 86% **5**

4,4'-Dibromo-2,2'-dinitro-5,5'-dimethylbiphenyl (**5**) was obtained in a 86% yield, by a modified procedure of Yamamoto *et al.* [1] The product was prepared via a Ullmann coupling reaction of 2,5-dibromo-nitro-toluene using copper powder in a solution of dimethylformamide, as shown in scheme 5. The reaction was complete after heating the mixture for 2 hours at 120 °C, and following work-up to give the isolated product as a pale yellow powder. The purity of the product was confirmed by TLC, GC mass spectra, melting point and elemental analysis. The structure of the product was identified by IR absorption, ^{1}H NMR and ^{13}C NMR.

The reaction mechanism for the formation of 4,4'-dibromo-2,2'-dinitro-5,5'-dimethylbiphenyl (**5**) follows the same course as described and shown for the formation of 4,4'-dibromo-2,2'-dinitrobiphenyl (**1**) on pages 87 and 88.

The purity of the product was confirmed by a single peak by GC with a retention time of 11.4 minutes. The mass spectra showed main integer masses for 4,4'-dibromo-2,2'-dinitro-5,5'-dimethylbiphenyl (**5**) at 428, 430, and 432 in a 1:2:1 ratio as expected due to ^{79}Br and ^{81}Br isotopes. The melting point of the product was 241-243 °C and was in agreement with reports from literature. The product was subjected to elemental analysis, for the compound $C_{14}H_{10}N_2O_2Br_2$ we calculated the expected percentage for the comprising elements to be: C, 39.10; H, 2.34; N, 6.51; Br, 37.16.%; from analysis we obtained: C, 39.20; H, 2.79; N, 5.60; Br, 36.67.%; which fell into close agreement to calculations.

The structure of the product was confirmed by IR spectrum giving peaks at 3106 cm^{-1} and 1596 cm^{-1},1513 cm^{-1}, 1338 cm^{-1}, 1283 cm^{-1}, 810 cm^{-1}, 798 cm^{-1}, 699 cm^{-1} as the C-H stretch followed by 2961 cm^{-1} and 1382 cm^{-1} the stretching vibration due methyl groups. Also the bands 1562 cm^{-1}, 1434 cm^{-1} can be denoted to C=C for the aromatic rings. The peaks arising at 1511 cm^{-1}, 1341 cm^{-1} are related to the stretching vibrations of the Ar-NO_2 groups, and a peak at 894 cm^{-1} stretching vibrations of the C-N bond. Finally the peak at 738 cm^{-1} can be linked to the stretching vibrations of the C-Br bonds.

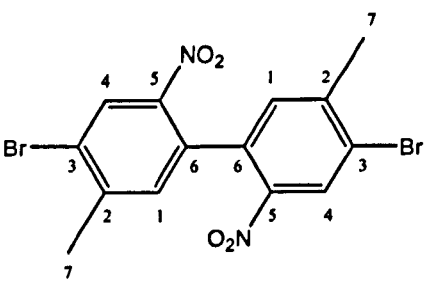

Figure 5.5, 4,4'-dibromo-2,2'-dinitro-5,5'-dimethylbiphenyl **(5)**

The ^{1}H-NMR spectrum identifies the product with 3 distinct signals equal in intensity. The signal at δ 8.36 ppm is linked to the protons assigned as position 4 on the ring system, which is a singlet due to no coupling with the near proton. The protons at position 1 shown signal at δ 7.06 ppm and the signal at δ 2.43 ppm is a singlet in proportions of 6 protons and relates to position 7.

The ^{13}C-NMR gave seven peaks on the spectrum which have been estimated to the following positions of the compound δ 146 (2C) position 5, δ 145 (2C) position 2, δ 133 (2C) positions 1, δ 132 (2) position 6, δ 128 (2C) position 4, δ 124 (2C) position 3 and δ 23 (2C) position 7. These peaks are in well agreement with the structure of 4,4'-dibromo-2,2'-dinitro-5,5'-dimethylbiphenyl **(5)**. These analytical results clearly verify that the product was 4,4'-dibromo-2,2'-dinitro-5,5'-dimethylbiphenyl **(5)**

5.2.3 4,4'-Diamino-2,2'-dibromo-5,5'-dimethylbiphenyl (6)

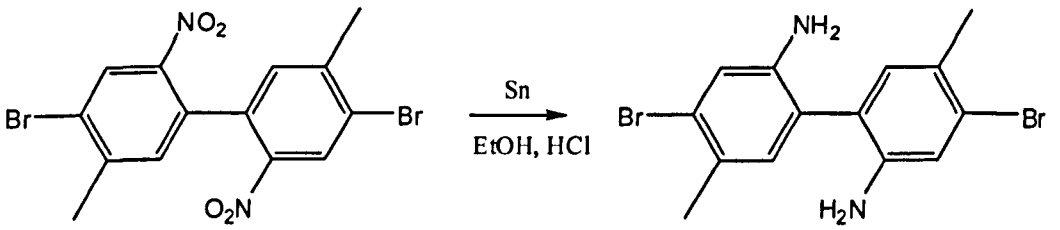

Scheme 6 **5** 89% **6**

4,4'-Diamino-2,2'-dibromo-5,5'-dimethylbiphenyl **(6)** was obtained in a 89% yield, by a modified procedure of Yamamoto *et al.* [(1)] The product was prepared via a reduction reaction of 4,4'-dibromo-2,2'-dinitro-5,5'-dimethylbiphenyl **(5)** using tin powder in a solution mixture of ethanol (HPLC grade) and hydrochloric acid (conc.), as shown in scheme 6. The reaction was complete after heating the mixture for 2 hours at 90 °C to produce a homogeneous solution, and following work-up to give the isolated product as an ivory yellow crystalline solid. The purity of the product was confirmed by TLC, GC mass spectra, melting point and elemental analysis. The structure of the product was identified by IR absorption, ^{1}H NMR and ^{13}C NMR.

The reaction mechanism for the formation of 4,4'-diamine-2,2'-dibromo-5,5'-dimethylbiphenyl **(6)** follows the same course as described and shown for the formation of 2,2'-diamine-4,4'-dibromobiphenyl **(2)** on pages 90 and 91.

The purity of the product was confirmed by a single peak by GC with a retention time of 12.8 minutes. The mass spectra showed main integer masses for 4,4'-diamine-2,2'-dibromo-5,5'-dimethylbiphenyl **(6)** at 368, 370, and 372 in a 1:2:1 ratio as expected due to ^{79}Br and ^{81}Br isotopes. The melting point of the product was 122-123 °C and was in agreement with reports from literature. The product was subjected to elemental analysis, for the compound $C_{14}H_{14}N_2Br_2$ we calculated the expected percentage for the comprising elements to be: C, 45.44; H, 3.81; N, 7.57; Br, 43.18.%; from analysis we obtained: C, 45.39; H, 3.84; N, 6.99; Br, 46.47.%; which fell into close agreement to calculations.

The structure of the product was confirmed by IR spectrum giving peaks at 3402 cm^{-1}, 3294 cm^{-1}, 3092 cm^{-1} stretching vibrations of the $-NH_2$ groups. In reassurance we have lost peaks arising at 1511 cm^{-1}, 1341 cm^{-1} which were related to the stretching vibrations of the Ar-NO_2 groups. The peak at 3015 cm^{-1}, 2960 cm^{-1} as the C-H stretch; Also the bands 1615 cm^{-1}, 1584 cm^{-1}, 1474 cm^{-1} and 1438 cm^{-1} can be denoted to C=C for the aromatic rings. Peaks at 925 cm^{-1} to 563 cm^{-1} out-of-plane deformation vibrations of the C-NH_2 bonds, and finally the peak at 718 cm^{-1} can be linked to the stretching vibrations of the C-Br bonds.

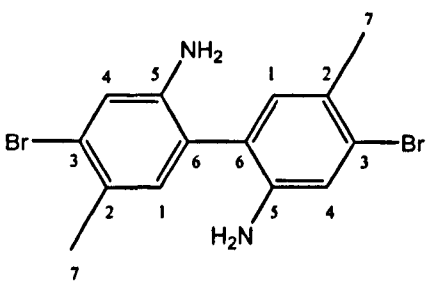

Figure 5.6, 4,4'-diamino-2,2'-dibromo-5,5'-dimethylbiphenyl **(6)**

The ^{1}H-NMR spectrum identifies the product with 3 distinct signals in the spectra. The signal at δ 6.98 ppm is linked to the protons assigned at position 4 on the ring system, which is a singlet due to no coupling with the near proton; a change in chemical shift can be noted from the transformation of the nitro group to the amine. The protons at position 2 give rise to the signal at δ 6.92 ppm as a multiplet due close proximity of with the coupling effect of the amine groups on the chemical shifts. This leaves a broad peak at δ 3.51 ppm which is assigned to the protons within the amine group and δ 2.29 ppm a singlet due to the protons of the methyl groups.

The ^{13}C-NMR gave seven peaks on the spectrum which have been estimated to the following positions of the compound δ 142 (2C) position 5, δ 132 (2C) position 1, δ 127 (2C) positions 2, δ 123 (2C) position 3, δ 119 (2C) position 6, δ 118 (2C) position 4 and δ 21 (2C) position 7. These peaks are in well agreement with the structure of 4,4'-Diamino-2,2'-dibromo-5,5'-dimethylbiphenyl **(6)**. These analytical results clearly verify that the product was 4,4'-diamino-2,2'-dibromo-5,5'-dimethylbiphenyl **(6)**

5.2.4 2,7-Dibromo-3,6-dimethyl-9H-carbazole (7)

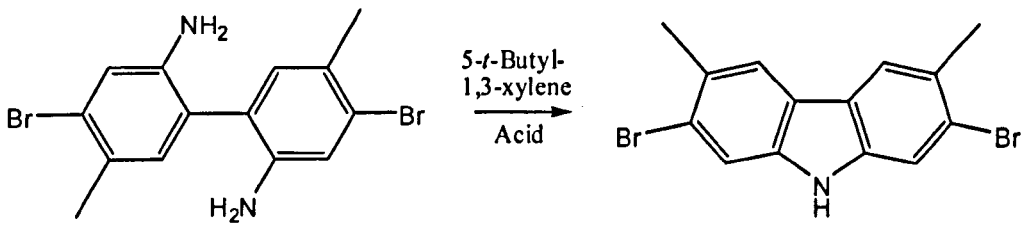

Scheme 7 **6** 82% **7**

2,7-Dibromo-3,6-dimethyl-9H-carbazole (**7**) was obtained in a 82% yield, by a modified procedure of Yamamoto *et al.* [1] The product was prepared via a cyclisation reaction. The reaction proceeded by ring closure of the amine groups of 4,4'-diamino-2,2'-dibromo-5,5'-dimethylbiphenyl (**6**) using 4- dodecylbenzenesulfonic acid in the high boiling point solvent 5-*t*-butyl-*m*-xylene, as shown in scheme 7. The reaction was complete after heating the mixture for 24 hours at reflux temperature, following work-up was isolated the product as an orange crystalline solid.

The purity of the product was confirmed by TLC, GC mass spectra, melting point and elemental analysis. The structure of the product was identified by IR absorption, ^{1}H NMR and ^{13}C NMR.

The reaction mechanism for the formation of 2,7-dibromo-3,6-dimethyl-9H-carbazole (**7**) follows the same course as described and shown for the formation of 2,7-dibromo-9H-carbazole (**3**) on pages 93 and 94.

The purity of the product was confirmed by a single peak by GC with a retention time of 11.4 minutes. The mass spectra showed main integer masses for 2,7-dibromo-3,6-dimethyl-*9H*-carbazole (**7**) at 351, 353, and 357 in a 1:2:1 ratio as expected due to ^{79}Br and ^{81}Br isotopes. The melting point of the product was 242-243 °C and was in agreement with reports from literature. [4] The product was subjected to elemental analysis, for the compound $C_{14}H_{11}NBr_2$ we calculated the expected percentage for the comprising elements to be: C, 47.63; H, 3.14; N, 3.97; Br, 45.26.%; from analysis we

obtained: C, 47.93; H, 3.30; N, 3.98; Br, 44.91.%; which fell into close agreement to calculations.

The structure of the product was confirmed by IR spectrum showed methyl stretching frequencies with peaks at 2921, 1479 and 1377 cm-1 and 3416 cm^{-1} stretching vibrations of the tertiary –NH groups. The peak at 2360 cm^{-1} relates to the C-H stretch followed by 1707 cm^{-1} and 1601 cm^{-1} 972 cm^{-1}, 874 cm^{-1}, 809 cm^{-1} which can be designated to the combination or overtone vibrations of the out-of-plane deformation vibrations of the C-H bonds of the carbazole ring. The peaks arising at 1450 cm^{-1}, 1324 cm^{-1}, 1303 cm^{-1} stretching vibrations due to C=C bonds of the carbazole ring, also the band at 1241 cm^{-1} can be denoted to C-N on the carbazole ring. Finally the peak at 724 cm^{-1} can be linked to the stretching vibrations of the C-Br bonds.

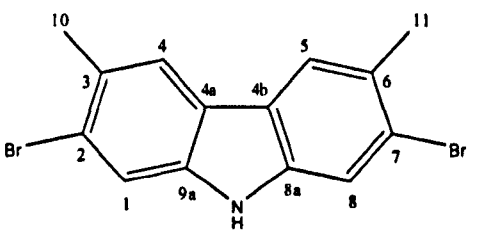

Figure 5.7, 2,7-dibromo-3,6-dimethyl-9H-carbazole **(7)**

The ^{1}H-NMR spectrum identifies the product with 3 signals in the spectra. The broad multiple signals at δ 7.86-7.80 ppm is linked to the proton 9H on the carbazole ring system and the protons arising at positions 1 and 8. The next set is a singlet at δ 7.60 ppm due to no coupling with near protons; and relates to the protons positioned at 4 and 5. The protons at position 10 and 11 give rise to the signal at δ 2.54 ppm as a singlet due to methyl groups.

The ^{13}C-NMR gave seven peaks on the spectrum which have been estimated to the following positions of the compound δ 140 (2C) positions 8a and 9a, δ 128 (2C) positions 3 and 6, δ 123 (2C) positions 4 and 5, δ 122 (2C) positions 4a and 4b, δ 120 (2C) positions 1 and 8, δ 115 (2C) positions 2 and 7 and finally δ 23 (2C) positions 10 and 11. These peaks are in well agreement with the structure of 2,7-dibromo-3,6-

dimethyl-*9H*-carbazole (**7**). These analytical results clearly verify that the product was 2,7-dibromo-3,6-dimethyl-*9H*-carbazole (**7**).

5.3.0 Synthesis of 3,6-dibromo-*9H*-carbazole

The preparation of 2,7-dibromo-*9H*-carbazole is outlined in the scheme shown. The description of the various steps involved is provided below.

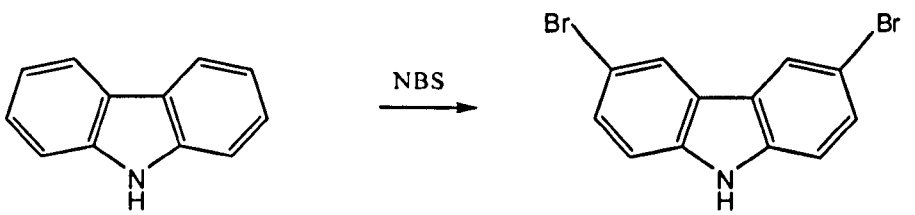

Scheme 8 74% **8**

5.3.1 3,6-Dibromo-*9H*-carbazole (8)

3,6-Dibromo-*9H*-carbazole (**8**) was obtained in a 74 % yield. The product was produce via a bromination reaction. [9] The reaction proceeded by the reaction of carbazole with N-bromosuccinimide and silica in DCM in the absence of light, as shown in scheme 8 above. The reaction was complete after work-up the reaction to give the isolated product as cream powder. The reaction is selective as to attacking the carbazole in the 3, 6 positions due to the directing effects of the nitrogen atom.

The purity of the product was confirmed by GC mass spectra and elemental analysis. The structure of the product was identified by ^{1}H NMR and ^{13}C NMR.

The purity of the product was confirmed by a single peak by GC with a retention time of 14.64 minutes. The mass spectra showed main integer masses for 3,6-dibromo-*9H*-carbazole (**8**) at 322, 324, and 326 in a 1:2:1 ratio as expected due to ^{79}Br and ^{81}Br isotopes. The product was subjected to elemental analysis, for the compound $C_{12}H_7NBr_2$ we calculated the expected percentage for the comprising elements to be:

C, 44.35; H, 2.17; N, 4.31; Br, 49.17.%; from analysis we obtained: C, 44.12; H, 2.19; N, 4.38; Br, 49.91.%; which fell into close agreement to calculations.

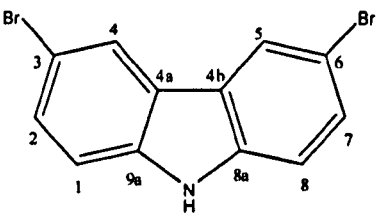

Figure 5.8, 3,6-dibromo-*9H*-carbazole **(8)**

The ^{1}H-NMR spectrum identifies the product with 3 signals in the spectra. The broad multiple signals at δ 8.10 ppm is linked to the proton 9H on the carbazole ring system and the protons arising δ 7.50 ppm at positions 4 and 5 as a doublet of doublets. The next set is a doublet at δ 7.30 ppm and relates to the protons positioned at 1, 2, 7, and 8.

The ^{13}C-NMR gave six peaks on the spectrum which have been estimated to the following positions of the compound δ 138 (2C) positions 8a and 9a, δ 129 (2C) positions 2 and 7, δ 124 (2C) positions 4 and 5, δ 123 (2C) positions 4a and 4b, δ 112 (2C) positions 3 and 6, δ 111 (2C) positions 1 and 8. These peaks are in well agreement with the structure of 3,6-dibromo-*9H*-carbazole **(8)**. These analytical results clearly verify that the product was 3,6-dibromo-*9H*-carbazole **(8)**.

5.4.0 Attempted synthesis of aryl substituted carbazole derivatives

5.4.1 1-Iodo-3,5-dimethoxybenzene (9) from 1-chloro-3,5-dimethoxybenzene

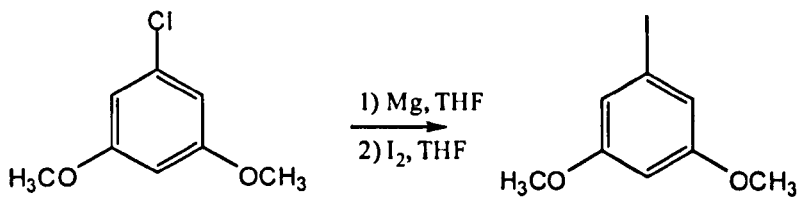

Scheme 9 36% 9

1-Iodo-3,5-dimethoxybenzene (9) was prepared from 1-chloro-3,5-dimethoxybenzene was obtained via the formation of a Grignard reaction, [10] yielding the product in a 36% yield as shown in scheme 9. The purity of the product was confirmed by TLC, GC mass spectra, melting point and elemental analysis. The structure of the product was identified by IR absorption, ^{1}H NMR and ^{13}C NMR.

The mechanism follows that of an aromatic Grignard reaction. The first step involves the formation of the Grignard followed by the substitution of the halide group.

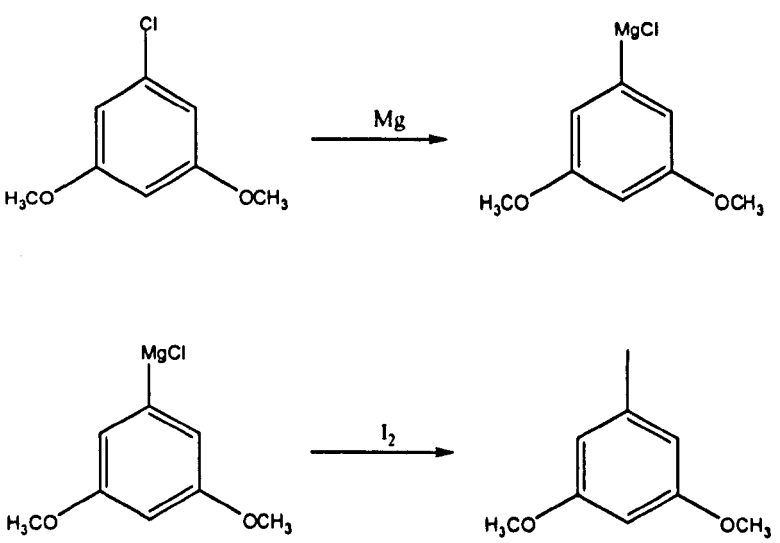

Mechanism 5, [10] formation of 1-iodo-3,5-dimethoxybenzene (9)

Reading into the literature [10] it was found that aromatic Grignard reactions are generally obtained in low yields. A disadvantage of this route is the troublesome and not always reproducible formation of the Grignard reagent. Activated magnesium was prepared in many ways, [11] but the use of these activated magnesium reagents resulted in the non-completion of this reaction. The reaction times were increased in a effort to drive the reaction to completion. It was found that similar results were achieved after 48 hours, beyond this reaction time there was no great effect into the formation of the product. Two main side product were formed, 1,3-dimethoxybenzene and 1,1',3,3'-tetramethoxybiphenyl. These bi-products were oils and hence prevented re-crystallisation of the compound. The bi-product could be removed via distillation or under high vacuum pressure.

After purification of the product via column chromatography it was found that the product was still slightly contaminated by the presence of the bi-products. Two methods for re-crystallisation were devised. The first was the use of the minimum amount of hot petroleum ether which upon cooling separated the bi-products from the products by precipitating out the solid crystals and leaving the bi-products as oil; this was not an optimised method for separation, as it often resulted in the bi-product having to be decanted from the solution. The second method was the use of hot methanol which solubilised the bi-product into solution leaving the product as a solid that could be filtered once cooled to leave white crystals. The analysis of the product is confirmed in the next section.

5.4.2 1-Iodo-3,5-dimethoxybenzene (10) from 3,5-dimethoxy-phenyl-amine [12]

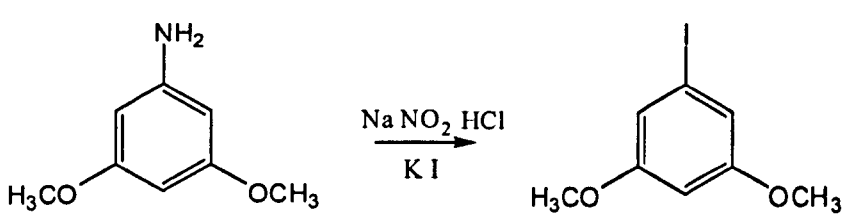

Scheme 10 76% 10

The purity of the product was confirmed by a single peak by GC with a retention time of 12.3 minutes. The mass spectra showed main integer masses for 1-iodo-3,5-dimethoxybenzene **(9 and 10)** at 151, 152 in a 1:3 ratio as expected due to ^{126}I and ^{129}I isotopes. The melting point of the product was 74-75 °C and was in agreement with reports from literature. The product was subjected to elemental analysis, for the compound $C_8H_9IO_2$ we calculated the expected percentage for the comprising elements to be: C, 36.39; H, 3.44; I, 48.06; O, 12.12.%; from analysis we obtained: C: 36.94, H: 3.33, I: 47.68.%; which fell into close agreement to calculations.

The IR spectra showed peaks as follows; 3069 cm^{-1}, 3005 cm^{-1}, 2963 cm^{-1}, 2931 cm^{-1}, 2833 cm^{-1} stretching due to C-H on a aromatic ring with a 1,3,5 tri substituted benzene ring; 1961 cm^{-1}, 1709 cm^{-1}, stretching due to overtone or combinational vibration of the out-of-plane deformation vibration of C-H bonds on 1,3,5 tri substituted benzene ring; 1571 cm^{-1}, 1468 cm^{-1}, 1450 cm^{-1}, 1438 cm^{-1}, 1422 cm^{-1}, stretching vibrations of the C-C bonds due to the 1,3,5 tri substituted benzene ring; 1028 cm^{-1}, stretching due to H_3C-O bonded to an aromatic ring; 984 cm^{-1}, stretching due to C-I bonded to an aromatic ring.

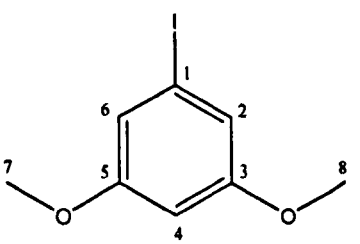

Figure 5.9, 1-iodo-3,5-dimethoxybenzene **(9, 10)**

The ^1H-NMR and ^{13}C-NMR were in well agreement with the structure of 1-iodo-3,5-dimethoxybenzene **(9 and 10)**. Looking at the ^1H-NMR, the main distinction between the product and the starting material is the change in chemical position between aromatic hydrogen in the 2,6 and 4 positions. These hydrogen subsequently show up as a doublet and triplet respectively due to the 1,3,5-tri-substituted benzene ring. The two hydrogens in position 2,6 have shifted further up field showing the effect of the change in halide group, which is in fact due to the electronic effects produced by the

more electron dense iodine group compared to that of the chlorine. This is a distinctive change in the aromatic structure which confirms the formation of the product.

The ^{13}C-NMR gave five peaks on the spectrum which have been estimated to the following positions of the compound, δ 160 (2C) positions 3 and 5, δ 115 (2C) positions 2 and 6, δ 100 (1C) positions 4, δ 94 (1C) positions 1 and δ 55 (2C) positions 7 and 8. These peaks are in well agreement with the structure of 1-iodo-3,5-dimethoxybenzene **(9 and 10)**. These analytical results clearly verify that the product was 1-iodo-3,5-dimethoxybenzene **(9 and 10)**.

5.4.3 5-Iodoresorcinol (11)

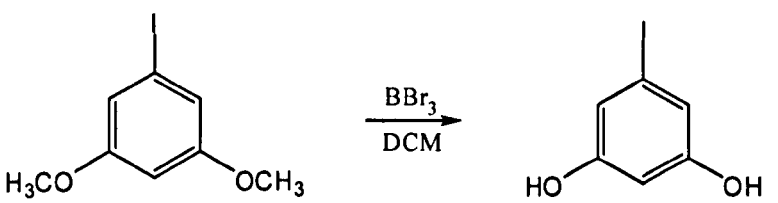

10 76% 11

Scheme 11

5-Iodoresorcinol [10] **(11)** was obtained in a 76% yield as a white crystalline solid as shown in scheme 11. The reaction was achieved via a de-methalation reaction with the use of boron tribromide which selectively removed the methyl groups as methyl bromide and leaving a secondary alcohol in place. The purity of the product was confirmed by TLC, GC mass spectra, melting point and elemental analysis. The structure of the product was identified by IR absorption, ^{1}H NMR and ^{13}C NMR.

Two methods were attempted in the synthesis of 5-iodoresorcinol **(11)**. The first was the preparation using hydroiodic acid; this resulted in the protonation of the oxygen and removal of the methyl group as shown below.

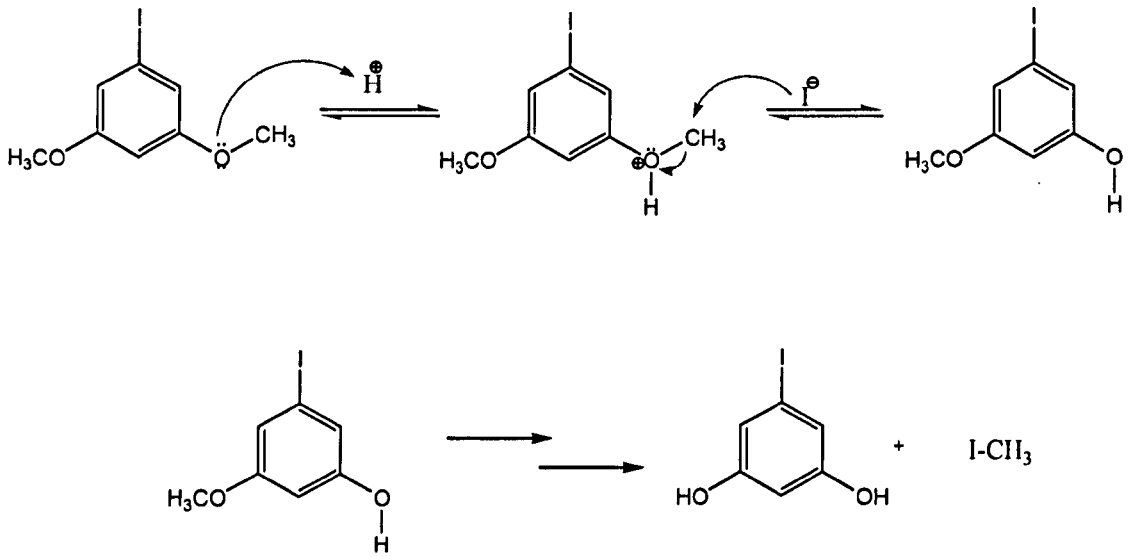

Mechanism 6, [7] formation of 1-iodoresorcinol **(11)** using hydroiodic acid

This method seemed to produce the product in the crude form, but was very difficult to purify. This was due to the large amounts of hydroiodic acid left in the product. Literature suggested the use of sodium thiosulphate as the agent to remove the excess iodine, after washing the organic layer with a 1M solution of sodium thiosulphate it was found that a vast amount of the product remained in the aqueous layer as a yellow in-soluble solid polymer. A number of solvents were used to separate the solid but there was no effect. Attempts were carried out to work up the reaction without the use of sodium thiosulphate, but the purification of the product was unmanageable due to the vast amount of iodine which quickly degraded the product when run through column chromatography.

The optimisation of the reaction came after great time was imparted in the set up and follow through of the reaction. The demethylation of 1,3-dimethoxybenzene derivatives is more difficult than other methoxy-benzene starting material[38] as stated in literature.

The use of boron tribromide was applied to the system. By reacting the starting material with the reagent at low temperatures allowing a complex to form which later

precipitated upon work up. This was extracted to yield the product. A suggestion to the mechanism can be shown below.

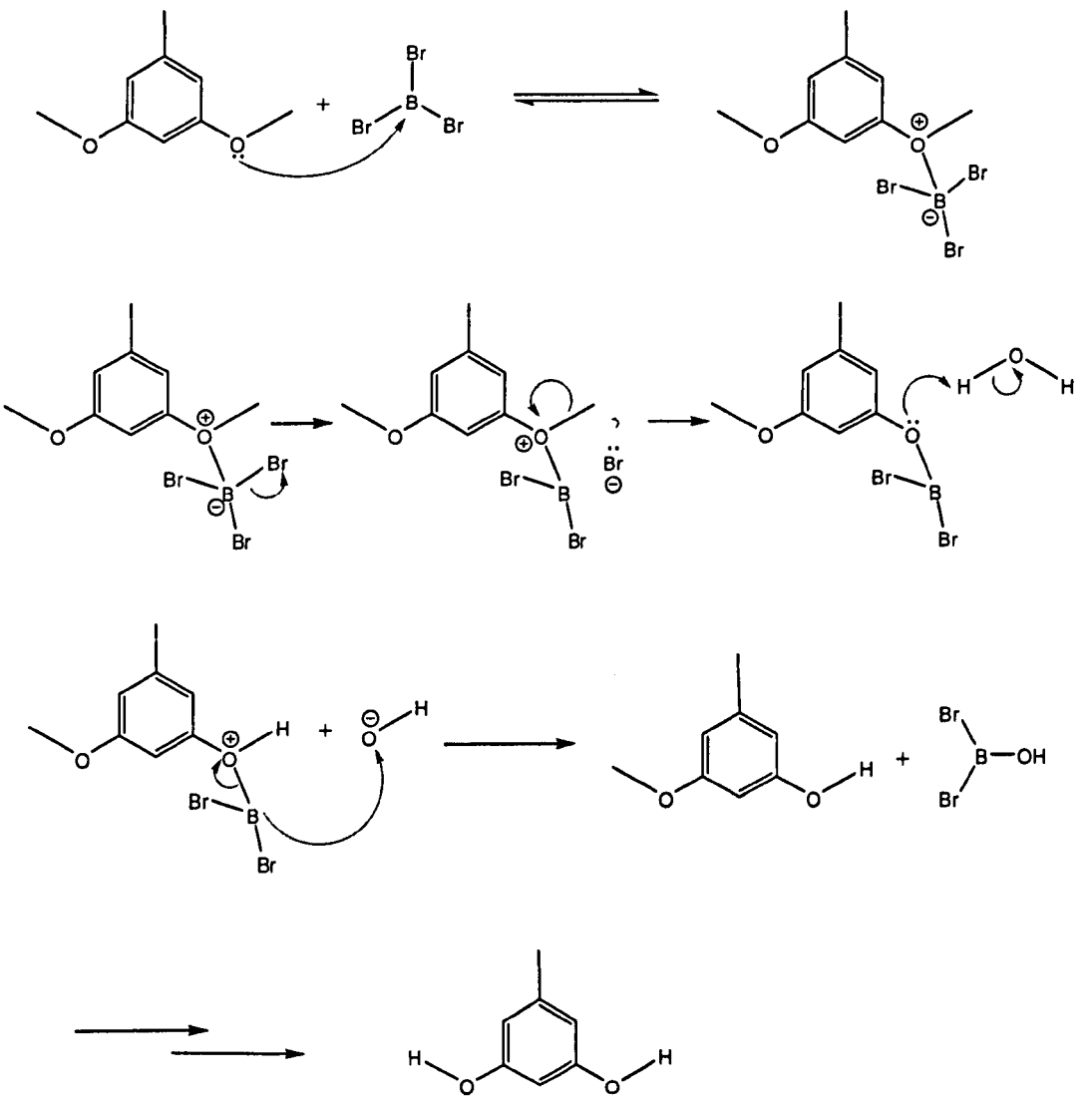

Mechanism 7, formation of 1-iodoresorcinol **(11)** using boron tribromide

The purity of the product was confirmed by a single peak by GC with a retention time of 16.6 minutes. The mass spectra showed main integer masses for 5-iodoresorcinol **(11)** at 236 and 238 in a 1:3 ratio as expected due to ^{126}I and ^{129}I isotopes. The melting point of the product was 85-86 °C and was in agreement with reports from literature. The product was subjected to elemental analysis, for the compound

$C_6H_5IO_2$ we calculated the expected percentage for the comprising elements to be: C, 30.53; H, 2.14; I, 53.77; O, 13.56.%; from analysis we obtained: C: 31.53, H: 2.20, I: 50.79.%; which fell into close agreement to calculations.

5-Iodoresorcinol was defined with IR spectra showing peaks as follows; 3591 cm^{-1}, 3236 cm^{-1} stretching due to O-H group; 3048 cm^{-1}, 2967 cm^{-1} stretching due to C-H on a aromatic ring with a 1,3,5-tri-substituted benzene ring; 1977 cm^{-1} stretching due to overtone or combinational vibration of the out-of-plane deformation vibration of C-H bonds on 1,3,5 tri substituted benzene ring; 1583 cm^{-1},1475 cm^{-1}, 1437 cm^{-1}, 1399 cm^{-1}, 1343 cm^{-1}, 1292 cm^{-1} stretching vibrations of the C-C bonds due to the 1,3,5 tri substituted benzene ring; 989 cm^{-1}, stretching due to C-I bonded to an aromatic ring; There was also no peak at 1028 cm^{-1}, stretching due to H_3C-O bonded to an aromatic ring which shows the loss of the dimethoxy group.

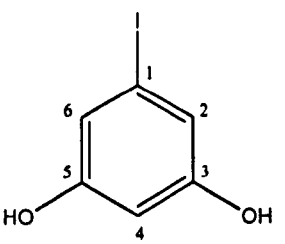

Figure 5.10, 1-iodoresorcinol **(11)**

From the ^{1}H-NMR we can notice the 1,3,5-tri-substituted benzene ring system functionalised with the iodine group is still intact, shown by the hydrogen's in the 2,6 and 4 position (doublet and triplet respectively) at the same chemical shift. There are distinctive peaks in the system that indicates the presence of alcohol groups at δ 8.65 ppm and δ 3.15 ppm. Also from the system we can notice the loss of the methyl groups that were positioned at the δ 3.75 ppm

The ^{13}C-NMR gave four peaks on the spectrum which have been estimated to the following positions of the compound, δ 160 (2C) positions 3 and 5, δ 117 (1C) position 4, δ 103 (2C) positions 2 and 6, δ 95 (1C) positions 1. These peaks are in good agreement with the structure of 5-iodoresorcinol **(11)**. These analytical results clearly verify that the product was 5-iodoresorcinol **(11)**.

5.4.4 1,3-Bis-(2-ethyl-hexyloxy)-5-iodobenzene (12)

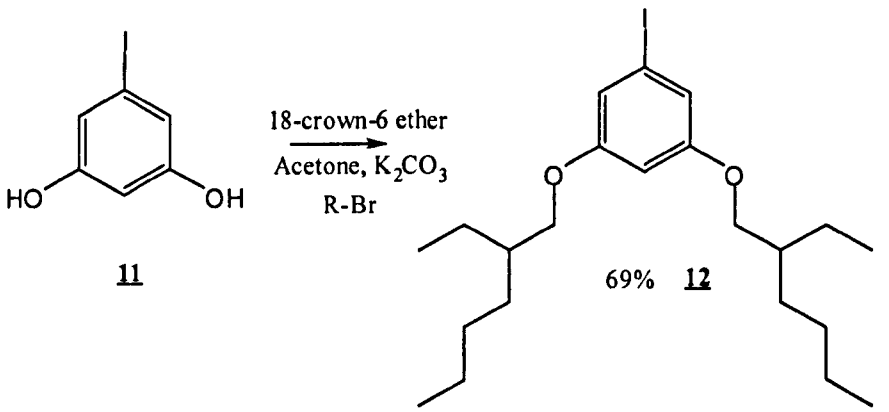

11 69% 12

Scheme 12

1,3-Bis-(2-ethyl-hexyloxy)-5-iodobenzene **(12)** was obtained in a 69% yield, by a modified procedure of Zimmerman *et al.* [14] The product was obtained via an alkylation as shown in scheme 12. The purity of the product was confirmed by TLC, mass spectra and elemental analysis. The structure of the product was identified by IR absorption, ^{1}H NMR and ^{13}C NMR.

The first method [15] for the formation of 1,3-bis-(2-ethyl-hexyloxy)-5-iodo-benzene **(12)** from 5-iodoresorcinol **(11)** used a procedure for the alkylation of hydroquinone mono-methyl ethers. This method was carried out in the presence of two different solvents (methanol and acetone) and potassium hydroxide. The reaction did not seem to not have taken place from analysis carried out, the NMR showed mainly the starting material and some possible formation of the half alkylated product; and very little of the expected product.

As thoughts into the reaction conditions matured, a rationalisation was made that the reaction mixture would have to be concentrated and conducted in anhydrous conditions, as water in the system would not allow the formation of the required oxygen anions to be alkylated. The use of acetone alone was undertaken as there seems to be the same amount of solubility of the products in this solvent. Potassium hydroxide flakes were to be used as they contained a lower percentage of water compared to the pellet form. [16] This reaction also did not achieve any major success.

Reading the literature we found a method that was used for the formation of complex dendrimers. [17] The complementary reaction was the attachment of sub-groups to 5-iodoresrocinol. This method used anhydrous potassium carbonate and 18-crown-6 ether to form and stabilise the oxygen anion which was then used to complex the molecule. This method was applied and found to be successful in an adequate yield.

The separation of the product through column chromatography was slow. This was first attempted using a mixture of ethyl acetate and pet, ether (5:95) as elutant, TLC showed good separation but due to the starting material not being noticeable under UV this did not allow a good separation of the product from the starting material and hence the product obtained was contaminated. The starting material was only noticeable through spray drying TLC plates with anisaldehyde developing solutions. The use of petroleum ether neat as the solvent gave the greatest separation between starting material and product as seen through the use of TLC but a down point was the extensive time needed to carry out the column since the product moved very slowly.

The mechanism follows the formation of a potassium complex which is stabilised through an 18-crown-6 ether which allows the removal of protons from the hydroxide groups and the stabilisation of the newly formed negative charge on the oxygen atoms. This in turn allows the attack to form the alkylated ether system

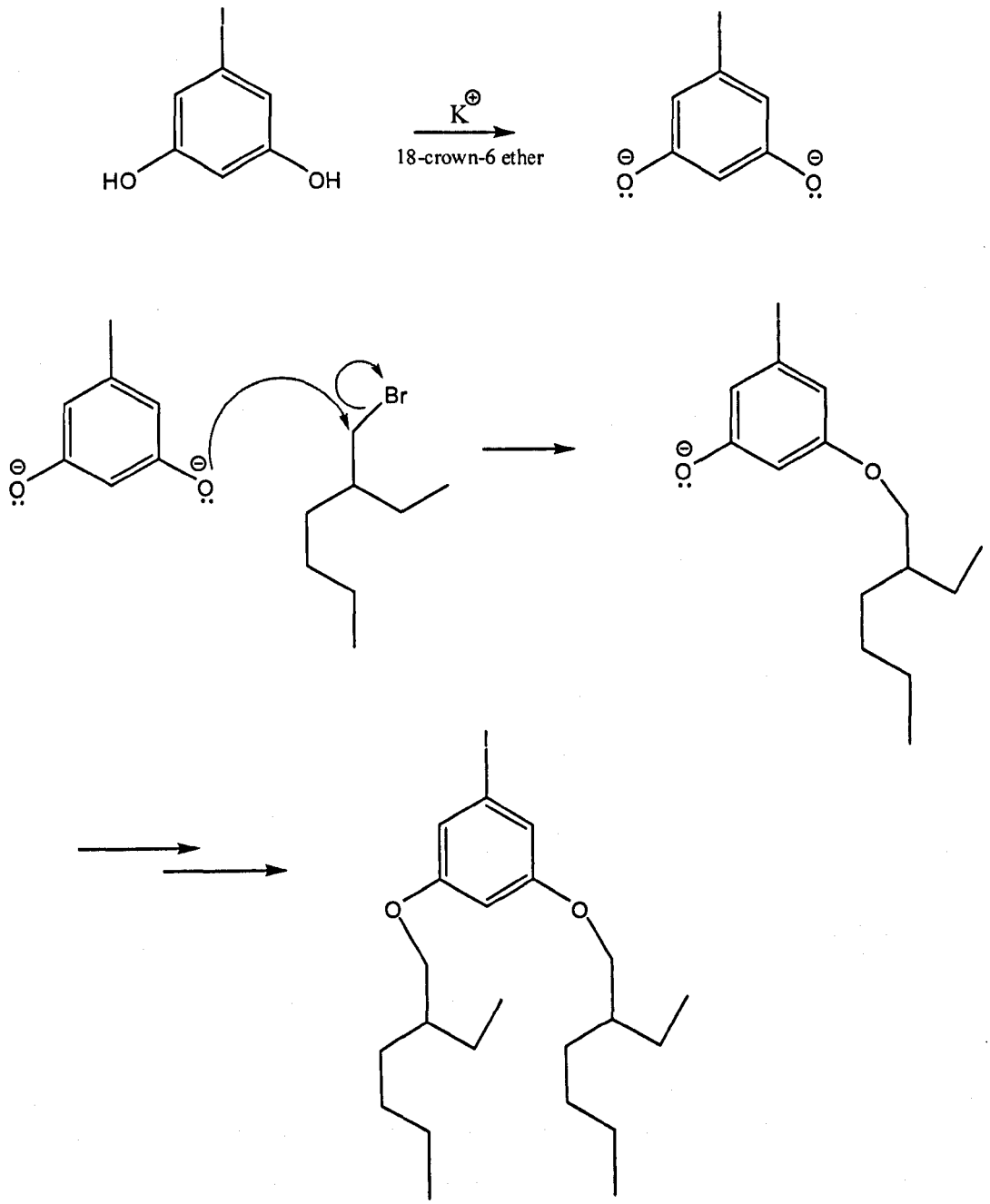

Mechanism 8, [5] Formation of 1,3-bis-(2-ethyl-hexyloxy)-5-iodobenzene **(12)**

The purity of the product was confirmed by the mass spectra showing main integer masses for 1,3-bis-(2-ethyl-hexyl-oxy)-5-iodo-benzene **(12)** at 460 and 462 in a 1:3 ratio as expected due to ^{126}I and ^{129}I isotopes. The product was subjected to elemental analysis, for the compound $C_{22}H_{37}IO_2$ we calculated the expected percentage for the

comprising elements to be: C, 57.39; H, 8.10; I, 27.56; O, 6.95.%; from analysis we obtained: C, 58.36; H, 8.00; I, 26.60.%; which fell into close agreement to calculations

The IR spectra showed peaks as follows; 3088 cm^{-1}, 2926 cm^{-1}, 2601 cm^{-1}stretching due to C-H on a aromatic ring; the peak at 1591 cm^{-1} relate stretching due to C-O bond; 1586 cm^{-1}, 1433 cm^{-1}, 1381 cm^{-1}, 1326 cm^{-1}, 1275 cm^{-1} stretching vibrations of the C-C bonds due benzene ring; 1170 cm^{-1} stretching due to C-O-Ar of an ether; 989 cm^{-1}, stretching due to C-I bonded to an aromatic ring; In respect we have lost two peaks at 3591 cm^{-1} and 3236 cm^{-1} which correspond to alcohol groups.

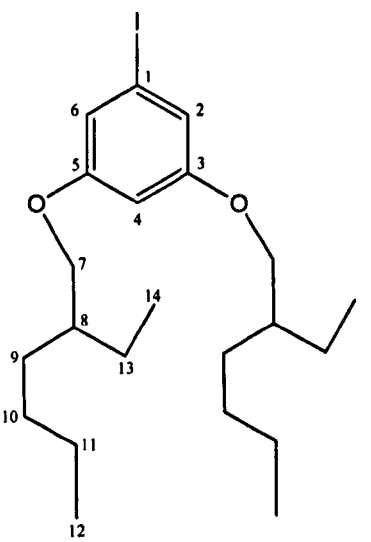

Figure 5.11, 1,3-bis-(2-ethyl-hexyloxy)-5-iodobenzene **(12)**

Looking at the ^{1}H-NMR we can notice the 1,3,5-tri-substituted benzene ring system functionalised with the iodine group is still intact, shown by the hydrogen in the 2,6 and 4 position (doublet and triplet respectively) at the same chemical shift. We have gained peaks in two areas; the first is the vast sets of multiple peaks that are associated to the alkyl chains that tend to be between δ 0.0 – 2.0 ppm. The second key peak is at δ 3.70 ppm, this resembles the attachment to the oxygen atom forming an ether. This peak is an important point to note. As the atom is further varied; for instance by the loss of iodine or only one of the two oxygen groups becoming

alkylated; this would cause a change in the chemical shift of this peak that can suggest any possible undesired compounds.

The ^{13}C-NMR gave twelve peaks on the spectrum which have been estimated to the following positions of the compound, δ 160 (2C) positions 3 and 5, δ 116 (1C) position 4, δ 101 (2C) positions 2 and 6, δ 94 (1C) positions 1, δ 76 (2C) position 7, δ 39 (2C) position 8, δ 29 (4C) positions 9 and 10, δ 22 (4C) positions 11 and 13, δ 14 (2C) position 12 and δ 11 (2C) position 14. These peaks are in good agreement with the structure of 1,3-bis-(2-ethyl-hexyl-oxy)-5-iodo-benzene **(12)**. These analytical results clearly verify that the product was 1,3-bis-(2-ethyl-hexyl-oxy)-5-iodo-benzene **(12)**.

5.4.5 Attempted synthesis of 2,7-dibromo-9-[3,5-bis(2-ethyl-hexyloxy)-phenyl]-*9H*-carbazole (13)

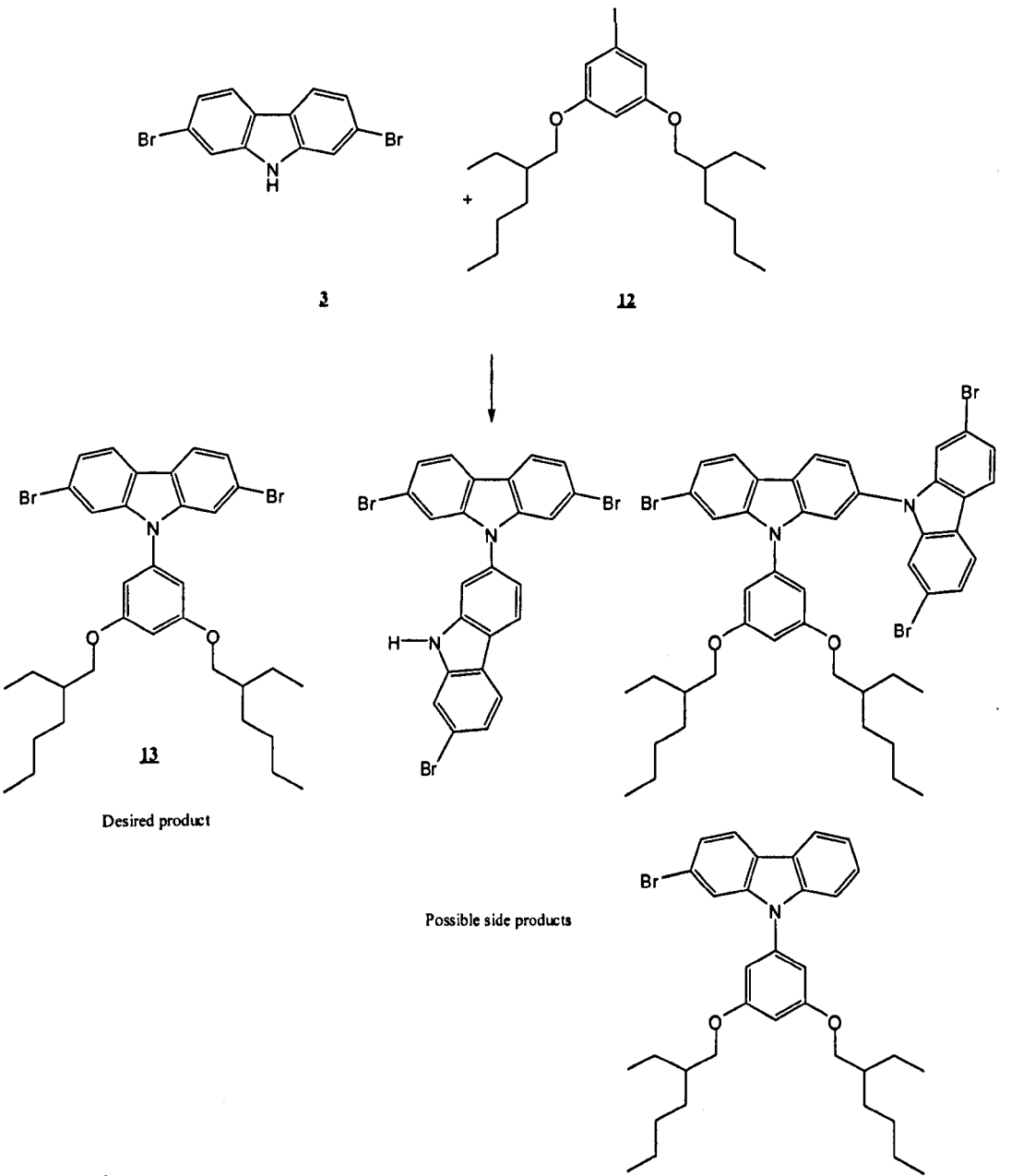

Scheme 13

The synthesis of 2,7-dibromo-9-[3,5-bis(2-ethyl-hexyloxy)-phenyl]-*9H*-carbazole **(13)** was attempted via a number of methods in an aid to produce an optimised system for the formation of the desired product, by the reaction of 2,7-dibromo-*9H*-

carbazole **(3)** and 1,3-bis-(2-ethyl-hexyloxy)-5-iodobenzene **(12)**. Unfortunately the compound was not isolated as a pure product which could be used in polymerisation reactions. A number of methods were attempted. These are discussed in the following section.

Method 1 [16] for the attempted synthesis of 2,7-dibromo-9-[3,5-bis(2-ethyl-hexyloxy)-phenyl]-*9H*-carbazole

This reaction involved the use of a Dean-Stark apparatus in the ideal situation to remove any amounts of water that may have been present from the use of potassium hydroxide (pellets); and also to increase the concentration of the reaction by removing toluene (solvent) from the system over the period of the reaction. As a catalytic reagent; tetrabutylammonium hydrogensulfate was added as a phase transfer catalyst to help the formation of the desired carbazole anion. From analysis of this reaction we found:

The TLC analysis showed the presence of the 2,7-dibromo-*9H*-carbazole, but none of the 1,3-bis-(2-ethyl-hexyloxy)-5-iodobenzene. This suggested one of two possible outcomes; the first was that 1,3-bis-(2-ethyl-hexyloxy)-5-iodobenzene was degraded under these conditions. The second was that the we had not formally formed the required anion of the carbazole which would suggest that 1,3-bis-(2-ethyl-hexyloxy)-5-iodobenzene had successfully formed the required complex with the copper but had no carbazole anion to react with.

The NMR obtained showed the presence of the 1,3-bis-(2-ethyl-hexyloxy)-5-iodobenzene and 2,7-dibromo-*9H*-carbazole as starting material, which has undergone no coupling. Also there were a number of other compounds present which can be suspected to be the reagents and complexes of copper formed.

It is an important point that the 2,7-dibromo-*9H*-carbazole anion is formed and to keep this salt in the organic phase of the reaction. For this the concentration of the reaction has to be kept high and a suitable catalyst needs to be employed.

Tetrabutylammonium hydrogensulfate acts as phase transfer catalyst and allows the carbazole anion formed to be stable in the organic phase of the reaction mixture.

Analysis of the ^{1}H-NMR show the presence of both starting materials which lead to the assumption that the starting 1,3-bis-(2-ethyl-hexyloxy)-5-iodobenzene is diluted extensively in the reaction so as not to allow the correct concentration to permit the formation of the product.

Method 2 [16] for the attempted synthesis of 2,7-dibromo-9-[3,5-bis(2-ethyl-hexyloxy)-phenyl]-*9H*-carbazole

This second method involved the use once again of a Dean-Stark apparatus but with the change of using potassium hydroxide (flakes) and 18-crown-6 ether to help form the carbazole anion. TLC analysis showed the presence of the 2,7-dibromo-*9H*-carbazole but no 1,3-bis-(2-ethyl-hexyloxy)-5-iodobenzene. As a promising point there were also spots that could indicate the formation of the product.

The NMR obtained showed the presence of the 2,7-dibromo-*9H*-carbazole as starting material. 1,3-Bis-(2-ethyl-hexyl-oxy)-5-iodo-benzene was also present in a very small amount, suggesting that it was that the reaction between the copper complex caused the removal of the iodo group in the reaction and becoming 1,3-bis-(2-ethyl-hexyloxy)-benzene. There were small amounts of a possible combination of the coupling reaction but this was hard to distinguish whether this was the product.

This reaction gave a indication that the starting carbazole materials was able to withstand these condition and more so that the reaction can allow coupling of the two monomers but the reaction is fairly low yielding.

The 18-crown-6 ether was used instead of tetrabutylammonium hydrogensulfate since it is well established that it could improve reactions involving nucleophilic substitutions involving potassium salts.

The Dean-Stark apparatus was used to concentrate the reaction mixture extensively which left the reaction mixture almost reacting without the aid of any solvent. The reaction is carried out on a small scale and hence the use of a Dean-Stark apparatus is not ideal as it is not an accurate method to insure the concentration of the reaction is in good control. The use of a Dean-Stark is primarily used to remove a calculated amount of water from a given system and then to increase the reaction concentration as the reaction time proceeds.

Method 3 [18,19] for the attempted synthesis of 2,7-dibromo-9-[3,5-bis(2-ethyl-hexyloxy)-phenyl]-*9H*-carbazole

The reaction was carried out to a modified procedure by Buchwald *et al.* [20] A method was needed to be employed in which the reaction concentration could be more accurately controlled. The option of ethylenediamine was used to chelate to the copper in assisting the coupling reaction. From the literature [19,21] many catalysts were used that had ligands with a diamine framework. These catalysts showed the amidation of aryl halides to nitrogen heterocycles in good yields. The choice of potassium carbonate or tri-potassium phosphate as the base was employed to reduce the presence of water in the reaction conditions. And finally the use of dioxane as a solvent as it favours solubility of complexes formed in solution.

The reaction showed the possible formation of a number of products including both starting materials. From the TLC there were a close alignment of spots where the top one was un-reacted 1,3-bis-(2-ethyl-hexyloxy)-5-iodobenzene. The second spot was the most highly fluorescent and was taken to be the product. There were a further two spots that are assumed to be complexities formed between the starting 2,7-dibromo-*9H*-carbazole and either the transfer catalyst ethylenediamine or substituted forms of 1,3-bis-(2-ethyl-hexyloxy)-5-iodobenzene reacting in the 2 or 7 position of 2,7-dibromo-*9H*-carbazole, or a branched form of 2,7-dibromo-*9H*-carbazole in the 2 or 7 positions.

The crude product was run through column chromatography (ethyl acetate: pet, ether 5:95) but the product was not obtained in a pure form. There were many contaminants which proved difficult to separate from the product.

The NMR obtained showed the possible presence of the coupled aryl carbazole as a product as well as a number of other products in close relation of the carbazole area which suggested that there were carbazole bi-products which fell into very similar areas on the TLC plate as to that of the reacted carbazole. We could have looked to using HPLC analysis techniques to try and separate the compounds but this would not have prove a good approach since these monomers are aimed for use in large scale synthesis and further polymerisations.

Method for the attempted synthesis of 2,7-dibromo-9-[3,5-bis(2-ethyl-hexyloxy)-phenyl]-*9H*-carbazole [18,19] (13)

This method was the closest we came to acquiring the required monomer. This method is stated in the experimental section. 2,7-dibromo-9-[3,5-bis(2-ethyl-hexyloxy)-phenyl]-*9H*-carbazole **(13)** was attempted via a modified procedure carried out by Buchwald *et al.* [20] The reaction is shown in scheme above. The compound was subjected to elemental and ^{1}H-NMR analysis.

The mechanism of this attachment is un-sure but it can be believed to follow the formation of the carbazole anion via a de-protonation with the aid of tri potassium phosphate. The copper and 1,10-phenanthroline complex is used to remove the iodine from the aromatic ring system. The copper attacks the carbon attached to the iodine and allows nucleophilic substitution to take place. This allows the attachment of the two monomers through formation of a new carbon-nitrogen bond.

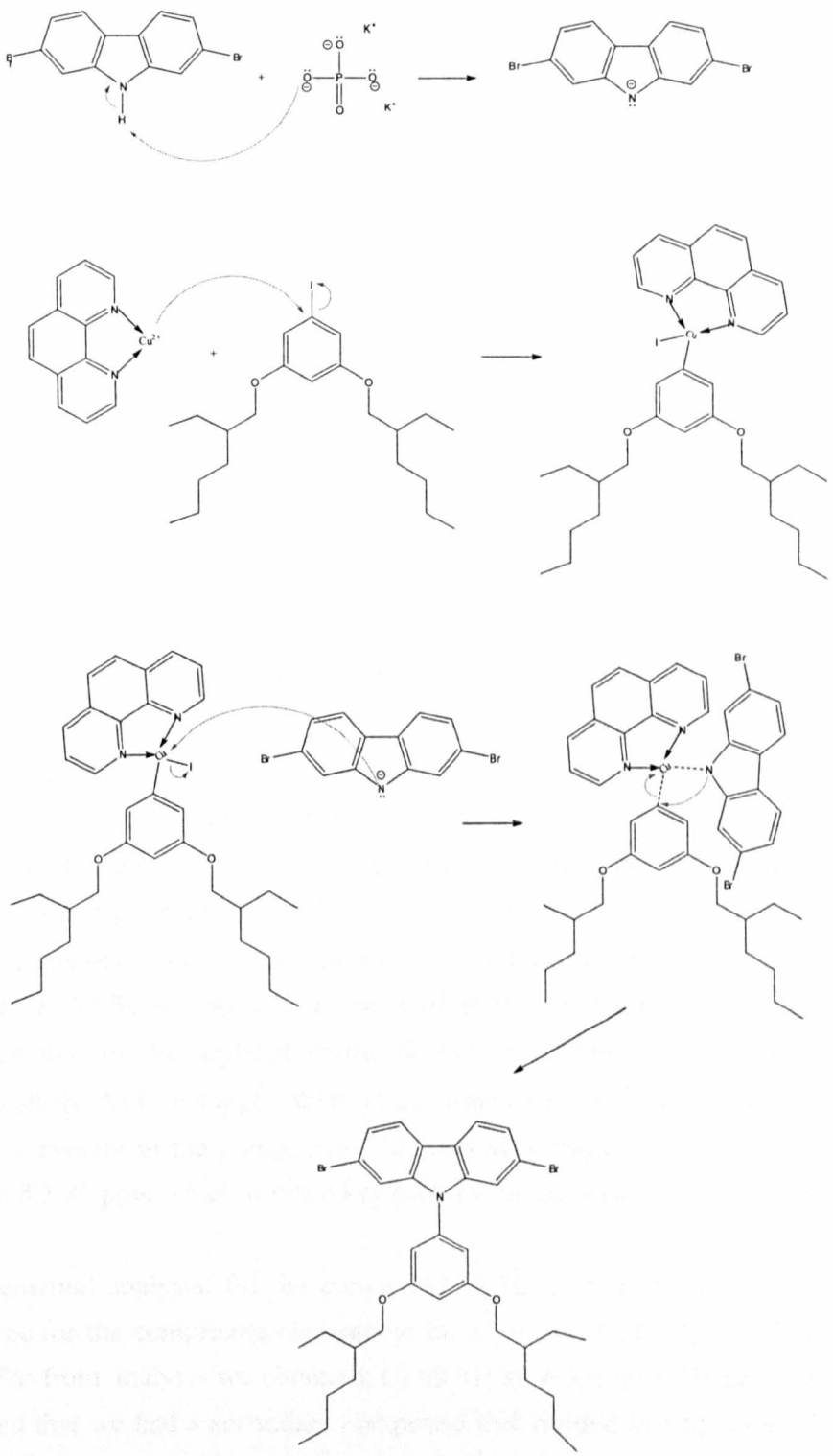

Mechanism 9, [7] Attempted synthesis of 2,7-dibromo-9-[3,5-bis(2-ethyl-hexyloxy)-phenyl]-*9H*-carbazole **(13)**

The product was purified through column chromatography which was a slow process since a non-polar solvent was used to create the greatest separation. There were very small and weak contaminants in the NMR which were due to the product and bi-products streaking between one another during the chromatographic separation. Purification was carried out to the best of abilities and it was found that there were two spots that sat directly above one another and could not be separated. The major spot being assumed to be that of the product and the second spot was a uncertain contaminants.

Looking at the ^{1}H-NMR we can notice that the 2,7-dibromo-9H-carbazole structure is in the same positions as expected, there is the loss of a peak at 10.67 ppm which coincided with the single hydrogen attached to the nitrogen atom. The 1,3,5 tri substituted benzene ring system has undertaken the loss of the iodine molecule to lose its distinguished pattern into a combination of the doublet and triplet at the 2,6 and 4 position respectively into a single chemical shift and now shown as a multiplet. We would expect this as to the close vicinity of the attached carbazole and its neighbouring hydrogen and also the replacement of the carbon iodine bond to a carbon nitrogen bond. Peaks corresponding to the alkyl chain are present; in two areas, the first is the vast sets of multiple peaks that are associated to an alkyl chain that tend to sit in the between δ 0.75 – 2.0 ppm. The second key peak has shifted to δ 3.75 ppm, this resembles the attachment to the oxygen atom forming an ether. Also from the ^{1}H-NMR we noticed a series of peaks in the carbazole region which resembled that of the arylated carbazole but they appeared to possess different chemical shifts. As if to suggest there was at least a second form of arylated carbazole compound present in the compound. This was also reinforced by a secondary peak arising at δ 3.80 ppm which was the key protons linked between ether groups.

From elemental analysis, for the compound $C_{34}H_{43}Br_2NO_2$ calculated the expected percentage for the comprising elements to be: C, 62.11; H, 6.59; Br, 24.30; N, 2.13; O, 4.87.%; from analysis we obtained: C, 63.81; H, 6.95; N, 2.23; Br, 20.84.%; This confirmed that we had a secondary compound that resided in very close vicinities to that of the desired compound; but was possible to separate via purification techniques. The low values of the bromine suggested that there was a loss of bromine

from the carbazole and this was a devastating blow since this compound could not be polymerised due to end terminating groups now present in the compound as contaminants.

5.4.6 Attempted synthesis of 2,7-dibromo-3,6-dimethyl-9-[3,5-bis(2-ethyl-hexyloxy)-phenyl]-*9H*-carbazole (14)

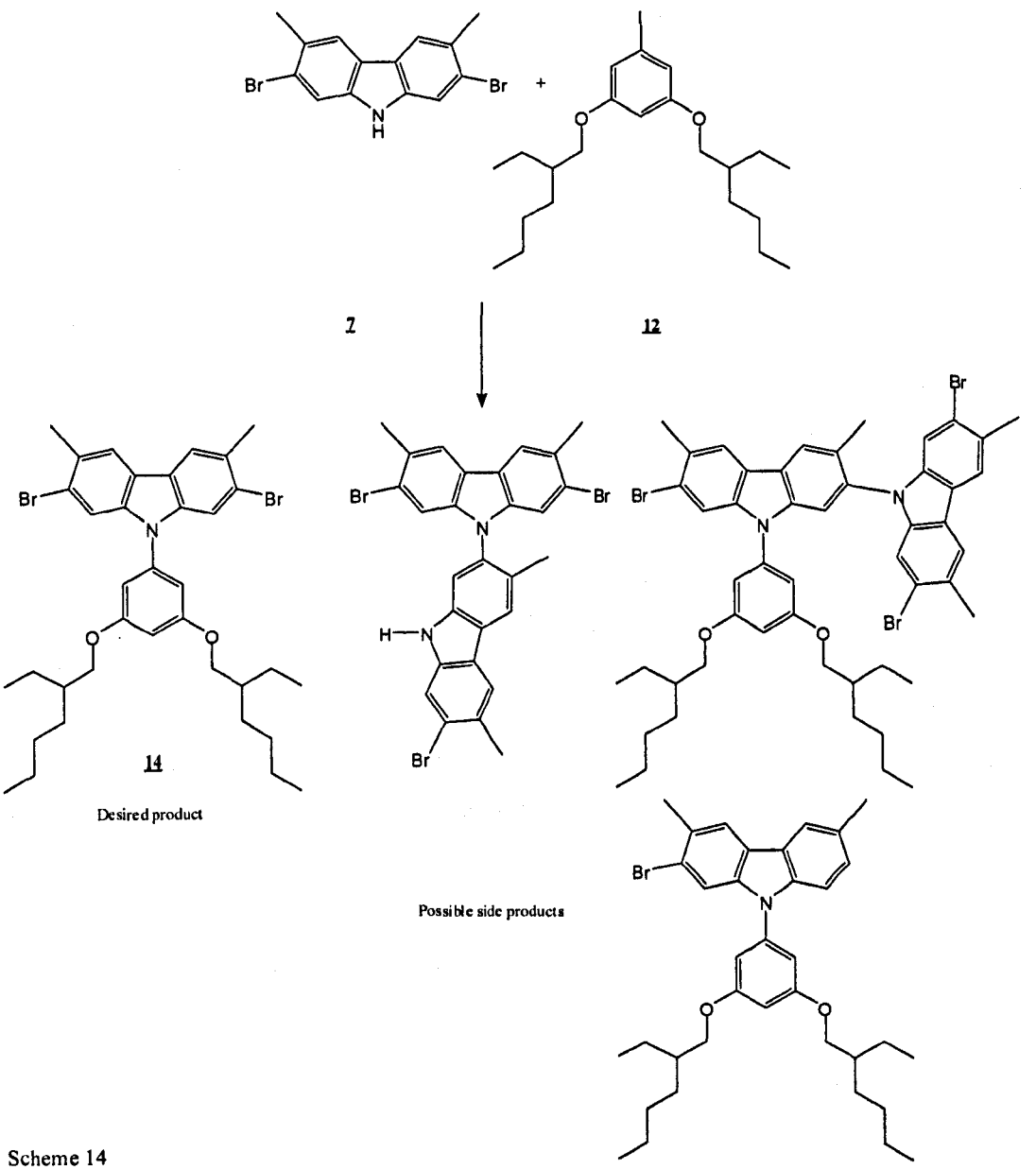

Scheme 14

After close inspection of the above reaction it was felt that by using carbazole that was protected in the 3, 6 positions may allow for complete conversion to a single desired product. We had seen that from the above reaction there was a distinctive loss of a bromine atom from the compound and it is believed that this occurs due to the complex copper catalyst formed not only attacks the iodine on the molecule but also moves its way to the bromine. So as to using the methylated carbazole would help block the approach of the complex and help prevent the loss of bromine.

Unfortunately this was not to be the case, from working up the reaction we found 2,7-dibromo-3,6-dimethyl-9-[3,5-bis(2-ethyl-hexyloxy)-phenyl]-*9H*-carbazole **(14)** was produced but there was the loss of bromine which had also taken place. The reaction is shown in scheme above. The compound was subjected to elemental and ^{1}H-NMR analysis. The mechanism of this reaction is assumed to follow that in the above discussion section.

The ^{1}H-NMR showed the major compound as the desired product but there were a series of peaks in the carbazole region that were distinctive to the effect of the loss of bromine from the compound. A number of purification techniques were applied to separate the compounds but were unsuccessful.

From elemental analysis, for the compound $C_{34}H_{43}Br_2NO_2$ we calculated the expected percentage for the comprising elements to be: C, 63.07; H, 6.91; Br, 23.31; N, 2.04; O, 4.67.%; from analysis we obtained: C, 65.12; H, 7.11; N, 2.18; Br, 19.43.%; This confirmed that we had a secondary compound that resided in very close vicinities to that of the desired compound; but was not possible to separate via purification techniques.

5.4.7 Attempted synthesis of 2,7-dibromo-3,6-dimethyl-9-[3,5-dimethoxy-phenyl]-*9H*-carbazole (15)

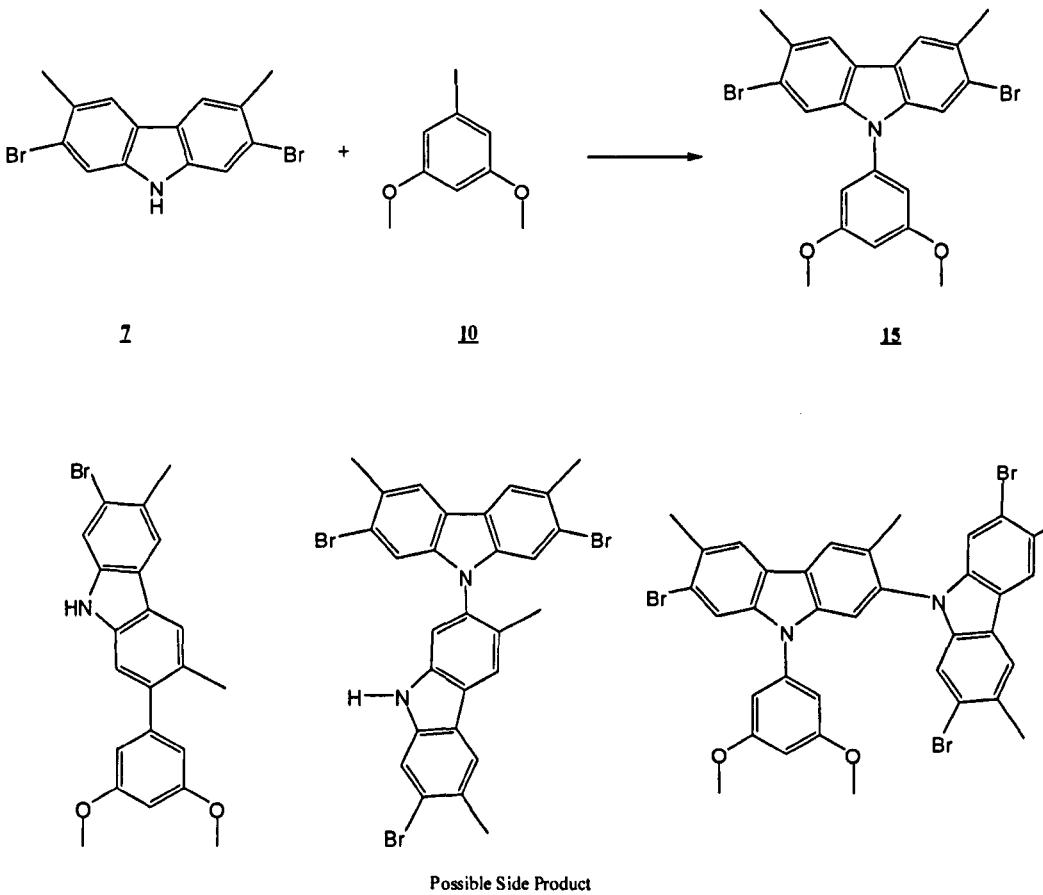

7 10 15

Possible Side Product

Scheme 15

The synthesis of the compound 2,7-dibromo-3,6-dimethyl-9-[3,5-dimethoxy-phenyl]-*9H*-carbazole **(15)** was attempted by a number of ways in order to obtain the intermediate compound. By reacting 2,7-dibromo-3,6-dimethyl-*9H*-carbazole (7) and 1-iodo-3,5-dimethoxybenzene **(10)** together with various catalysts and solvent conditions in a aim to prevent the loss of bromine occurring in the reaction.

The reaction was carried out with the use of the following solvents: dioxane, THF and toluene, also the following ligands were used to bind with the Cu(I)Cl: dimethyl ethylenediamine, ethylenediamine and 1,10-phenanthorline. The reactions were also

carried out in different ratios in order to help push the reaction in favour for the compound being produced.

The table below indicates the results obtained and the percentage conversion to the desired compound. The conversion was calculated by NMR analysis comparing the ratio the desired compound to that if the starting material.

Table 1, Coupling reaction attempted with the use of different ligands, coupling with Cu(I)Cl.

Exp.	Compound ratio (7)	(10)	Solvent	Ligand	Conversion %
1	1	1.1	Dioxane	dimethyl ethylenediamine	51
2	1	1.1	THF	dimethyl ethylenediamine	44
3	1	1.1	Toluene	dimethyl ethylenediamine	58
4	1	2	Dioxane	dimethyl ethylenediamine	59
5	1	2	THF	dimethyl ethylenediamine	56
6	1	2	Toluene	dimethyl ethylenediamine	67
7	1	1.1	Dioxane	ethylenediamine	55
8	1	1.1	THF	ethylenediamine	54
9	1	1.1	Toluene	ethylenediamine	67
10	1	2	Dioxane	ethylenediamine	59
11	1	2	THF	ethylenediamine	59
12	1	2	Toluene	ethylenediamine	70
13	1	1.1	Dioxane	1,10-phenanthroline	69
14	1	1.1	THF	1,10-phenanthroline	67
15	1	1.1	Toluene	1,10-phenanthroline	89
16	1	2	Dioxane	1,10-phenanthroline	78
17	1	2	THF	1,10-phenanthroline	75
18	1	2	Toluene	1,10-phenanthroline	91

From these results we first found that this reaction overall proves to take place better in toluene as the solvent, followed by THF and finally by dioxane. The final overall

solvent was taken to be toluene and this was also backed by literature which stated it (toluene) was a far superior solvent to that of dioxane. [20]

In the first set of reaction carried out the ratio of 2,7-dibromo-3,6-dimethyl-*9H*-carbazole (7) and 1-iodo-3,5-dimethoxybenzene **(10)** was at 1:1.1 and this left a lot of unreacted starting 2,7-dibromo-3,6-dimethyl-*9H*-carbazole (7) so by increasing the amount of 1-iodo-3,5-dimethoxybenzene **(10)** we would be able to increase the favourability of the reaction towards the formation of the product whilst keeping the amount of catalytic ligand to the same amount which would lower the chances of the Cu (I) complex attacking the bromines on the carbazole.

It was found in the literature that the chelating ligand which binds to the Cu (I) complex can contribute to the formation of bi-products formed during reactions as well as having the ability to help direct the Cu (II) to the desire product. [22] We first carried out these reactions with the use of dimethyl ethylenediamine, which showed to produce the greatest amount of bi-products and to add to this it also exhibited the lowest conversion of reactants to product. We then moved from this ligand to use ethylene diamine. This ligand produced much less bi-product which were distinguished from NMR but there was still a low conversion of reactants to products. Moving back to literature once again it was decided to that the use of 1,10-phenthroline [23] would provide better results in which would allow low bi-product formation and a good conversion rate since these ligands are known to inhibit copper assisted coupling reactions[22] the use of 1,10-phenathroline posed further advantages like, it prevents the aggregation of or improves the solubility of the copper complex, the decomposition of the copper complex is inhibited by 1,10-phenathroline and that 1,10-phenathroline prevents the multiple ligation to a single copper centre, which in turn might prevent the formation of side products from other complex copper reagents formed. This ligand coupled with toluene as a solvent produced the best results but this was still not useful due to there still being compounds that had lost bromine which could not be removed from the product due to the two compounds having the similar R_f values.

5.4.8 9-[3,5-(Dimethoxy)-phenyl]-*9H*-carbazole (16)

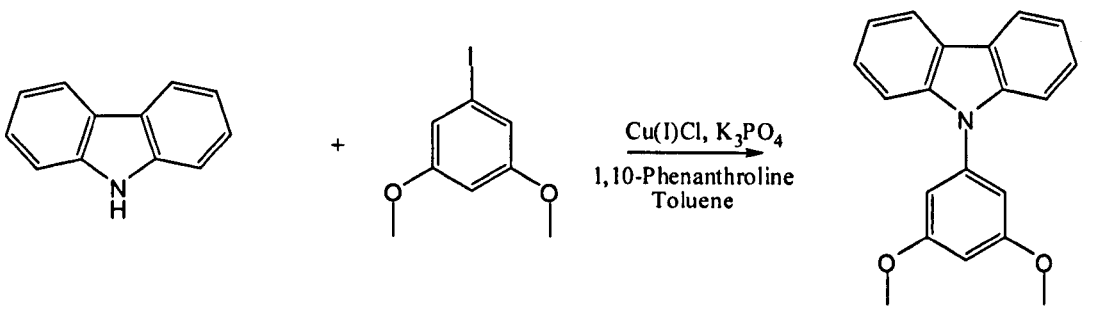

8 10 59% 16

Scheme 16

9-[3,5-(Dimethoxy)-phenyl]-9H-carbazole **(16)** was obtained in a 59% yield, by a modified copper catalysis reaction [16,18] as shown in scheme above. The reaction was complete after heating the mixture for 48 hours at reflux temperature, and following work-up to give the isolated product as a pale white solid. The purity of the product was confirmed by TLC, GC mass spectra and elemental analysis. The structure of the product was identified by ^{1}H NMR and ^{13}C NMR.

This reaction was undertaken due to the difficulties observed in the previous reaction above. Due to the loss of bromine from the carbazole molecule it was looked towards the formation of non brominated carbazole molecules.

The reaction is expected to be carried out by the formation of a copper complex between the ligand 1,10-phenanthroline, which then moves to react with 1,3-bis-(2-ethyl-hexyloxy)-5-iodobenzene **(12)**. Meanwhile de-protonation of the carbazole occurs and a substitution reaction takes place to yield the product.

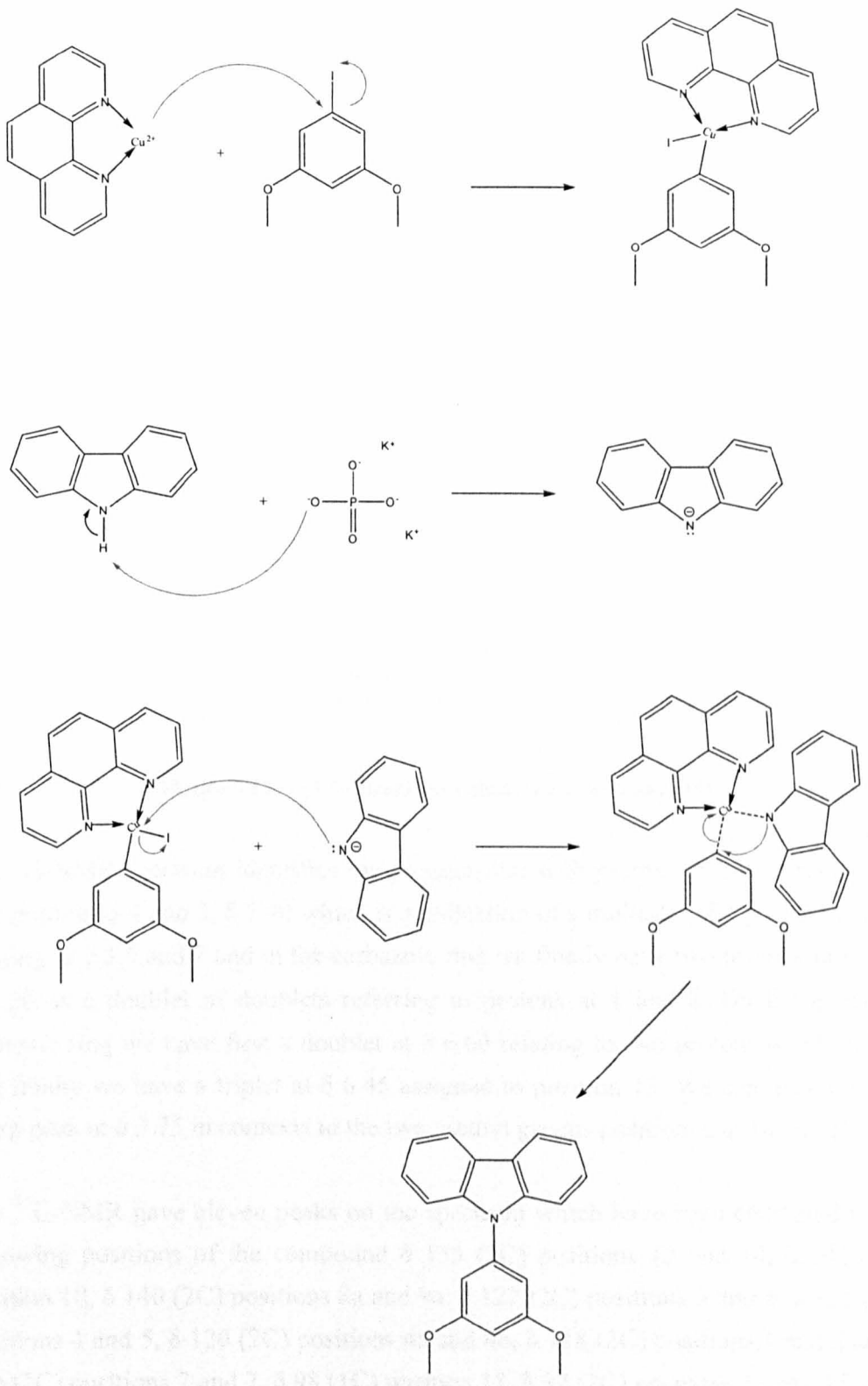

Mechanism 10, The formation 9-[3,5-(dimethoxy)-phenyl]-*9H*-carbazole **(16)**

The purity of the product was confirmed by a single peak by GC with a retention time of 13.47 minutes. The mass spectra showed main integer masses for 9-[3,5-(dimethoxy)-phenyl]-*9H*-carbazole **(16)** at 303 and 304. The product was subjected to elemental analysis, for the compound $C_{20}H_{17}NO_2$ calculated the expected percentage for the comprising elements to be: C, 79.19; H, 5.65; N, 4.62; O, 10.55.%; from analysis we obtained: C, 79.36; H, 5.30; N, 4.83.%; which fell into close agreement to calculations.

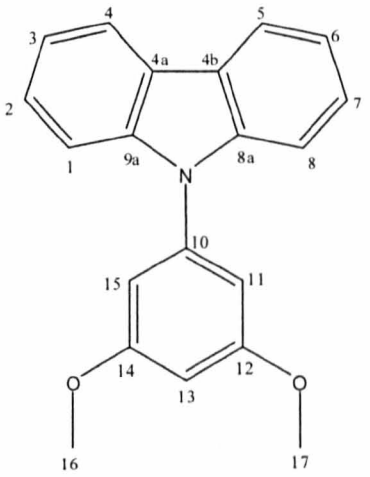

Figure 5.12, 9-[3,5-(dimethoxy)-phenyl]-*9H*-carbazole **(16)**

The ^{1}H-NMR spectrum identifies the product first with protons at δ 8.10 relating to two protons at 4 and 5, δ 7.40 which is a indication of a multiplet of 4 protons in total relating to 2,3,6 and 7 and in the carbazole ring we finally have two protons falling at δ 7.20 as a doublet of doublets referring to protons at 1 and 8. On the attaching aromatic ring we have first a doublet at δ 6.60 relating to two protons of 11 and 15 and finally we have a triplet at δ 6.45 assigned to position 13. We can also note the sharp peak at δ 3.75 in contexts to the two methyl groups positioned at 16 and 17.

The ^{13}C-NMR gave eleven peaks on the spectrum which have been estimated to the following positions of the compound δ 155 (2C) positions 12 and 14, δ 141 (1C) position 10, δ 140 (2C) positions 8a and 9a, δ 122 (2C) positions 3 and 6, δ 121 (2C) positions 4 and 5, δ 120 (2C) positions 4a and 4b, δ 118 (2C) positions 1 and 8 and δ 110 (2C) positions 2 and 7, δ 98 (1C) position 13, δ 92 (2C) positions 11 and 15, δ 55

(2C) position 16 and 17. These peaks are in well agreement with the structure of 9-[3,5-(dimethoxy)-phenyl]-*9H*-carbazole **(16)**. These analytical results clearly verify that the product was 9-[3,5(dimethoxy)-phenyl]-*9H*-carbazole **(16)**.

5.4.9 Attempted synthesis of 3,6-dibromo-9-[3,5-dimethoxy-phenyl]-*9H*-carbazole (17)

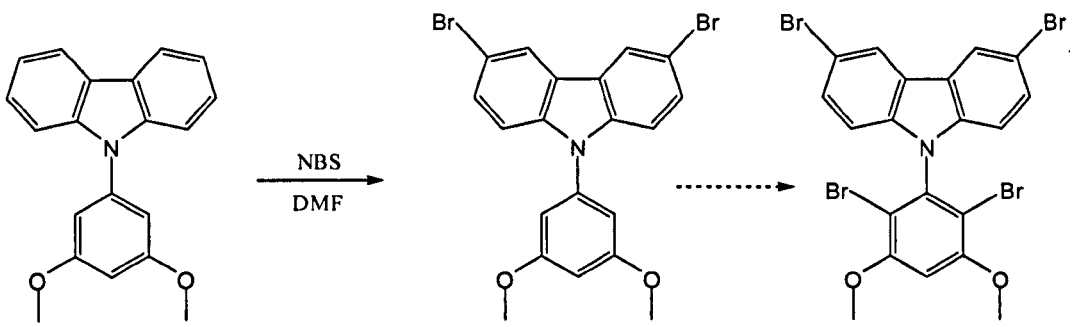

16 17 Un-desired product obtained

Scheme 17

From earlier reaction of carbazole with NBS it was seen that the 3,6-Dibromo-*9H*-carbazole (8) could be readlly formed due to the directing effects of the nitrogen group. Thus it was decided to brominate the 9-[3,5(dimethoxy)-phenyl]-*9H*-carbazole **(16)** as we could then move forward in the formation of our first target molecule. The reaction was carried out with the use of N-bromosuccinimide in the absence of light at – 20 °C.

From TLC analysis the reaction seemed to have taken place. Upon working up the compound and running analysis it was soon realised that the reaction was not selective. We had found that the reaction not only brominated the carbazole in the 3, 6 position due to the directing effects of the nitrogen, but there was also bromination in the 2 and 6 positions of the phenyl group attached to the nitrogen atom of the carbazole ring. This was suspected to have occurred due to the phenyl ring also being

electron rich as the result of its substitutions with the methoxy groups at the 3 and 5 positions.

5.4.10 Attempted synthesis of 3,6-diiodo-9-[3,5-dimethoxy-phenyl]-9H-carbazole (18)

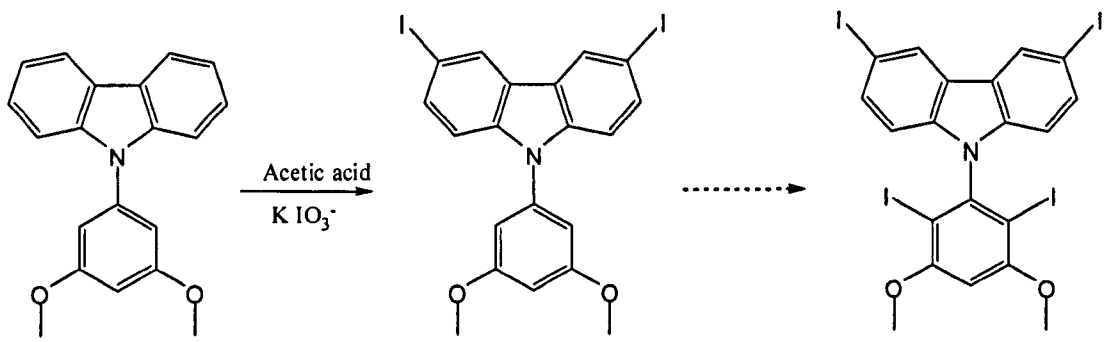

16 18 Un-desired product obtained

Scheme 18

After the above reaction an attempt was made to obtain the 3,6-iodocarbazole derivative. This was carried out since it was known that iodination of the carbazole ring was able to proceed cleanly in good yields. And also that the iodine molecule is larger in size to that of bromine and it was hoped that due to steric hindrance the attachment of iodine to the phenyl ring system would not occour.

Unfortunately this reaction produced the same effect as the reaction above. Upon work up the compound was soon realised to have been iodinated on the phenyl ring as well. We had found that the reaction not only iodinated the carbazole in the 3, 6 position due to the directing effects of the nitrogen, but there was also iodination in the 2 and 6 positions of the phenyl group attached to the 9-position of the carbazole ring. This was suspected to have occurred due to the phenyl ring also being electron rich as a result of its substitution with two methoxy groups.

5.4.11 9-(3,5-dihydroxy-phenyl)-*9H*-carbazole (19)

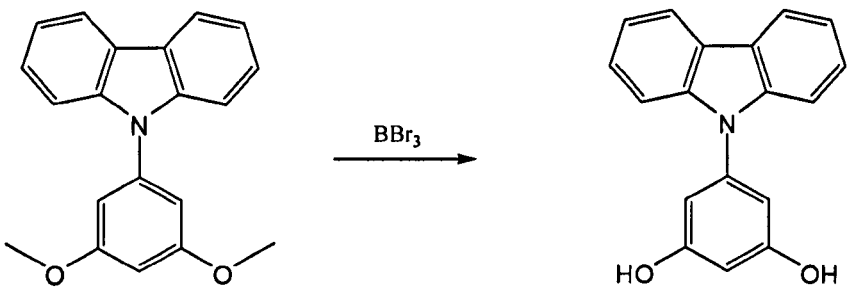

16 58% 19

Scheme 19

9-(3,5-Dihydroxy-phenyl)-*9H*-carbazole **(19)**[10] was obtained in a 58% yield. The reaction was achieved via a dimethalation reaction with the use of boron tribromide which selectively removed the methyl groups as methyl bromide and leaving a secondary alcohol in place as shown in scheme above.

The purity of the product was confirmed by TLC, GC mass spectra and elemental analysis. The structure of the product was identified by ^{1}H NMR and ^{13}C NMR

The compound is produced by the removal of the dimethoxy groups using boron tribromide. The reaction can be assumed to take place mechanistically as shown below.

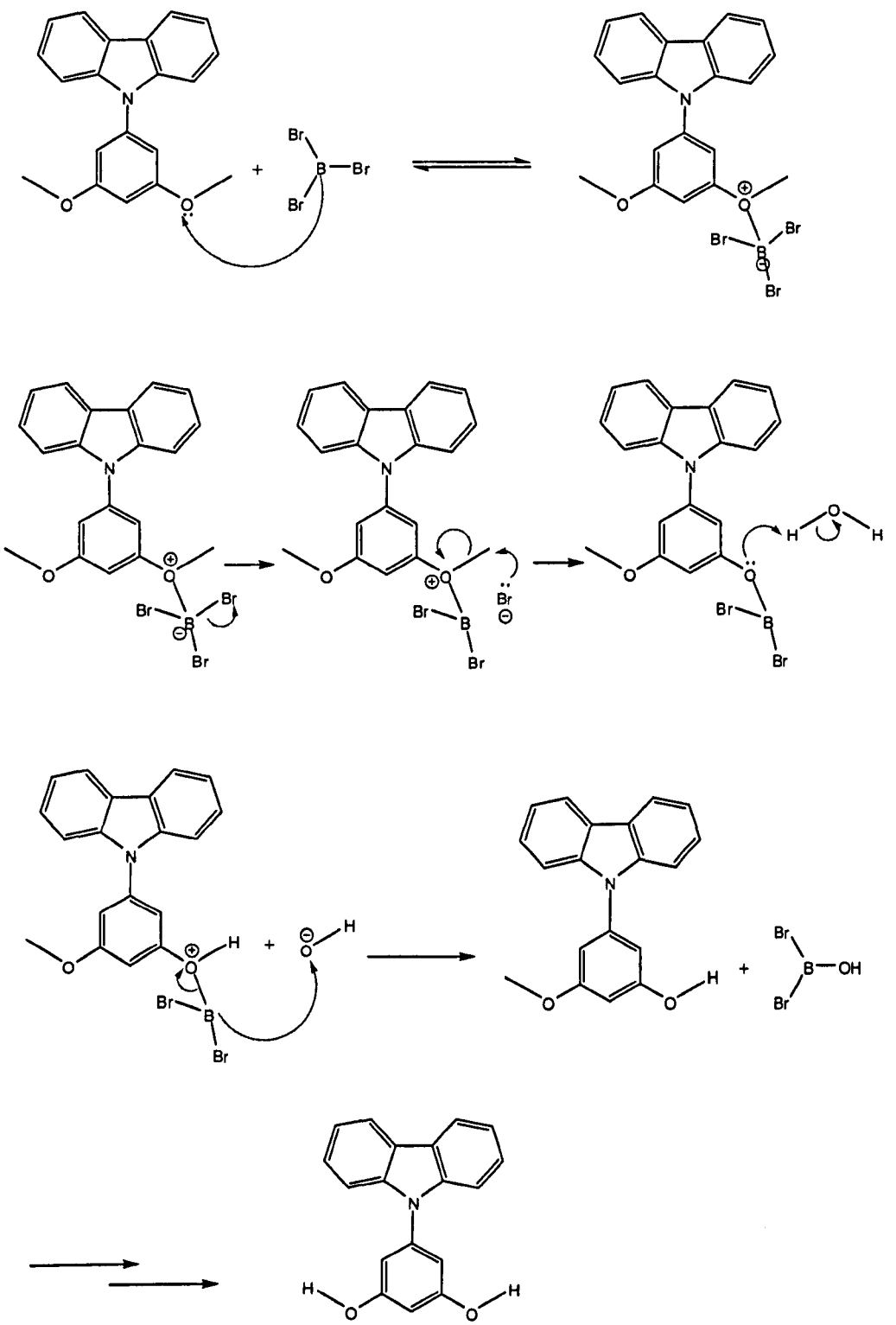

Mechanism 11, Formation of 9-(3,5-dihydroxy-phenyl)-*9H*-carbazole **(19)**

The purity of the product was confirmed by a single peak by GC with a retention time of 15.56 minutes. The mass spectra showed main integer masses for 9-(3,5-dihydroxy-phenyl)-*9H*-carbazole **(19)** at 275 and 276. The product was subjected to elemental analysis, for the compound $C_{18}H_{13}NO_2$ we calculated the expected percentage for the comprising elements to be: C, 78.53; H, 4.76; N, 5.09; O, 11.62.%; from analysis we obtained: C, 78.26; H, 4.98; N, 5.00.%; which fell into close agreement to calculations.

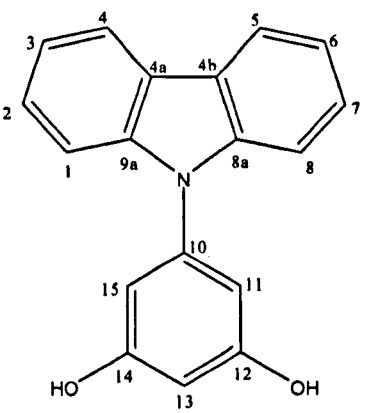

Figure 5.13, 9-(3,5-dihydroxy-phenyl)-*9H*-carbazole **(19)**

The ^{1}H-NMR spectrum identifies the product with protons at δ 8.10 relating to two protons at 4 and 5, δ 7.40 which is a indication of a multiplet of 4 protons in total relating to 2,3,6 and 7 and in the carbazole ring we finally have two protons falling at δ 7.20 as a doublet of doublets referring to protons at 1 and 8. On the attaching aromatic ring we have first a doublet at δ 6.60 relating to two protons of 11 and 15 and finally we have a triplet at δ 6.45 assigned to position 13. We can also notice the broad peak at δ 5.50 assigned to the two protons of the hydroxide groups.

The ^{13}C-NMR gave ten peaks on the spectrum which have been estimated to the following positions of the compound δ 158 (2C) positions 12 and 14, δ 141 (1C) position 10, δ 140 (2C) positions 8a and 9a, δ 122 (2C) positions 3 and 6, δ 121 (2C) positions 4 and 5, δ 120 (2C) positions 4a and 4b, δ 118 (2C) positions 1 and 8 and δ 111 (2C) positions 2 and 7, δ 100 (1C) position 13 and δ 95 (2C) positions 11 and 15. These peaks are in good agreement with the structure proposed for 9-(3,5-dihydroxy-

phenyl)-*9H*-carbazole **(19)**. These analytical results clearly verify that the product was 9-(3,5-dihydroxy-phenyl)-*9H*-carbazole **(19)**.

5.4.12 Attempted synthesis of 9-(3,5-bis(2,2,2-trifluoro-acetoxy)-phenyl)-*9H*-carbazole (20)

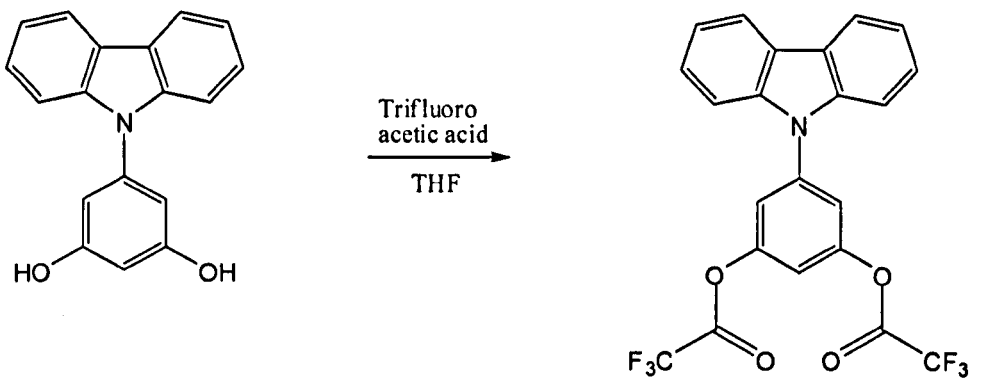

19 **20**

Scheme 20

The synthesis of 9-(3,5-bis(2,2,2-trifluoro-acetoxy)-phenyl)-*9H*-carbazole **(20)** was attempted via a number of methods in an aid to produce an optimised system for the formation of the desired product.

Due to difficulties found with the formation of the desired compound and the effect seen with the attachment of the arylated group to the carbazole moiety as seen in the attempted synthesis of 2,7-dibromo-9-[3,5-bis(2-ethyl-hexyloxy)-phenyl]-*9H*-carbazole **(13)**, and the recent problems encountered with the halogenations of the arylated carbazoles as seen in reactions like the attempted synthesis of 3,6-dibromo-9-[3,5-dimethoxy-phenyl]-*9H*-carbazole **(17)** a reasonable attempt in reducing the reactivity of the of the attached arylated group was undertaken.

It was hoped that by protecting the dihydroxy groups with tri fluoro acetate components would draw the electron reactivity of the aryl group away from the

contribution felt from the effects of the nitrogen lone pairs. In turn, allowing successive halogenations of the carbazole moiety.

The scheme above gives a representation of the desire reaction that was undertaken. The reaction was attempted a number of times, but the reaction reached only up to 50% conversion in the best of cases. There were a number of different bases that were used in an attempt to protect the hydrogen of the hydroxy group. (triethylamine, DMAP and di-isopropyl-amine) The bases used showed no differences in comparison between one another, in other words from proton NMR analysis an estimation of the desired compound could be made to be approximately 50% where the rest of the mixture was seen to manly be starting material. As well as to a change in the base material used, the concentration and reaction times of each reaction were increased in an attempt to push the equilibrium of the reaction to complete conversion, none of these changes had played an effect on the reaction.

A number of attempts were carried out into trying to extract the compound from the crude. Attempts were first carried out in washing the compound and re-crystallising the organic material. This did not affect the crude material. This then moved us to run column chromatography of the compound. Even though great care was taken to basify the column before exposure to the compound, the crude product degraded to the starting hydroxy aryl carbazole compound.

Due to new approaches in methods formulated for the attachment of arylated compounds to the carbazole moiety further work on this part of the project ceased.

5.5.0 Synthesis of Tri-aryl amino substituted carbazole derivatives

5.5.1 3,6-Dibromo-9-(4-nitro-phenyl)-*9H*-carbazole (21)

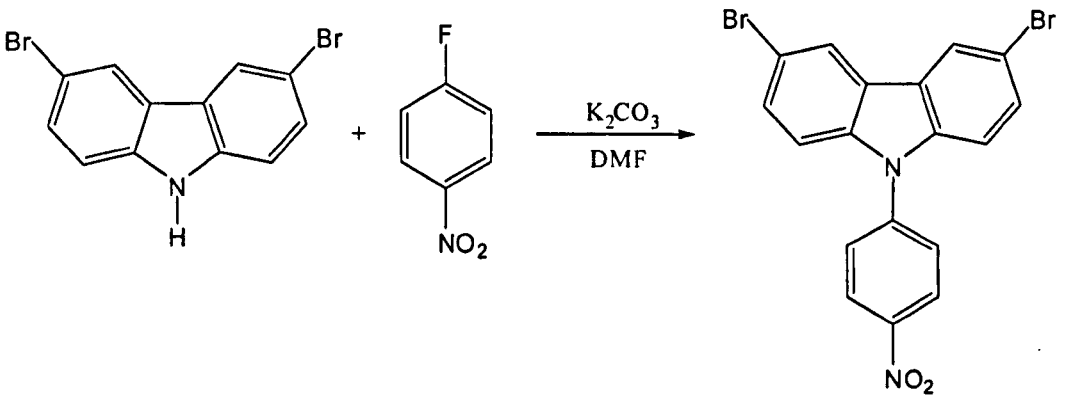

8 80% 21

Scheme 21

3,6-Dibromo-9-(4-nitro-phenyl)-*9H*-carbazole **(21)** was obtained in a 80% yield, by a modified procedure of Jian *et al.* [24] The product was obtained via a nucleophilic substitution reaction for the coupling of 3,6-dibromo-9H-carbazole with 4-fluoro-nitrobenzene using potassium carbonate in a solution of dimethylformamide, as shown in the scheme above. The reaction was complete after heating the mixture for 48 hours at 120 °C, and following work-up to give the isolated product as a pale yellow solid.

The purity of the product was confirmed by TLC, GC mass spectra, melting point and elemental analysis. The structure of the product was identified by IR absorption, ^{1}H NMR and ^{13}C NMR.

The nucleophilic substitution reaction proceeds via a two step process as shown in mechanism below. The first is the formation of the carbazole anion via the reaction with potassium carbonate. This anion can then react to substitute the fluorine on 4-fluoro-nitrobenzene yielding the product and potassium fluoride as a bi-product.

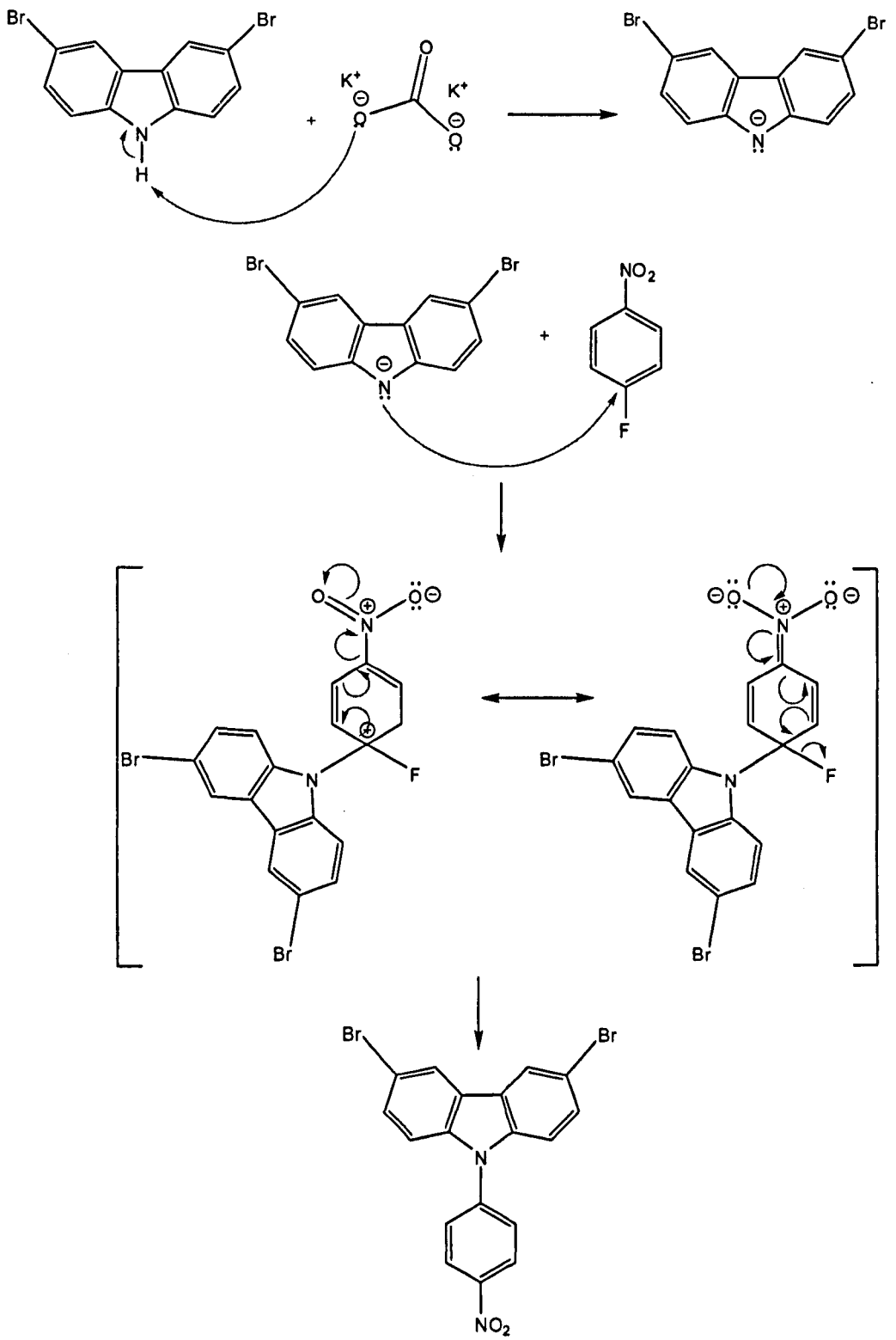

Mechanism 12, Nucleophilic substitution reaction forming 3,6-dibromo-9-(4-nitro-phenyl)-*9H*-carbazole **(21)**

The purity of the product was confirmed by a single peak by GC with a retention time of 23.38 minutes. The mass spectra showed main integer masses for 3,6-dibromo-9-(4-nitro-phenyl)-*9H*-carbazole **(21)** at 444, 446, and 448 in a 1:2:1 ratio as expected due to ^{79}Br and ^{81}Br isotopes. The melting point of the product was 125-126 °C. The product was subjected to elemental analysis. For the compound $C_{18}H_{10}N_2Br_2O_2$ we calculated the expected percentages for the comprising elements to be: C, 48.46; H, 2.26; N, 6.28; Br, 35.82; O, 7.17.%; from analysis we obtained: C: 48.51 H: 1.99 N: 6.30 Br: 35.89.%; which fell in close agreement to calculations.

The structure of the product was confirmed by IR spectrum giving peaks at 3034 cm^{-1} as the aromatic C-H stretch followed by 1893 cm^{-1}, 1893 cm^{-1}, 1752 cm^{-1} and 1695 cm^{-1} which can be designated to the combination or overtone vibrations of the out-of-plane deformation vibrations of the C-H bonds of the benzene ring. Also the bands 1604 cm^{-1} , 1505 cm^{-1}, 1470 cm^{-1} and 1449 cm^{-1} can be denoted to C=C for the aromatic rings. The peak arising at 1373 cm^{-1} are related to the stretching vibrations of the Ar-NO_2 groups, and a peak at 923 cm^{-1} stretching vibrations of the C-N bond. Finally the peak at 763 cm^{-1} can be linked to the stretching vibrations of the C-Br bonds.

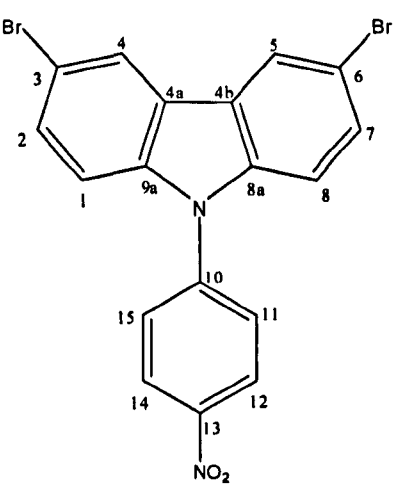

Figure 5.14, 3,6-dibromo-9-(4-nitro-phenyl)-*9H*-carbazole **(21)**

The ^{1}H-NMR spectrum identifies the product with 5 signals in the spectra. The doublet signal at δ 8.49 ppm is assigned to the protons 4 and 5 on the carbazole ring system. The next signal is that arising at δ 8.15 ppm which is a doublet in relation to protons at positions 12 and 14. The next set is a singlet at δ 7.69 ppm due to coupling with near protons; and relates to the protons positioned at 1 and 8. The protons at position 2 and 7 give rise to the signal at δ 7.49 ppm as doublet of doublets. And we finally have a doublet giving rise at δ 7.25 relating to protons 11 and 15.

The ^{13}C-NMR gave nine peaks on the spectrum which have been estimated to the following positions of the compound δ 147 (1C) position 10, δ 144 (1C) position 13, δ 140 (2C) positions 8a and 9a, δ 125 (2C) positions 12 and 14, δ 123 (2C) positions 11 and 15, δ 122 (2C) positions 4a and 4b, δ 121 (4C) positions 4, 5, 2 and 7, δ 117 (2C) positions 3 and 6 and δ 113 (2C) positions 1 and 8. These peaks are in good agreement with the structure proposed for 3,6-dibromo-9-(4-nitro-phenyl)-*9H*-carbazole **(22)**. These analytical results clearly verify that the product was 3,6-dibromo-9-(4-nitro-phenyl)-*9H*-carbazole **(22)**.

5.5.2 3,6-Dibromo-9-(4-amino-phenyl)-*9H*-carbazole (22)

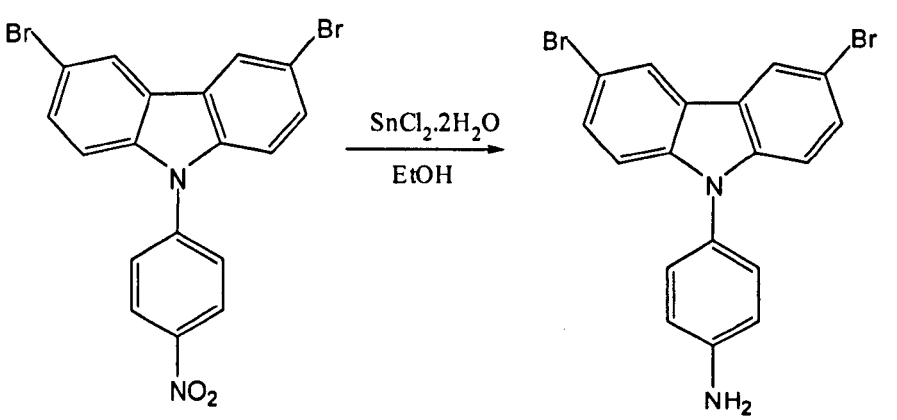

21 94% **22**

Scheme 22

3,6-Dibromo-9-(4-amino-phenyl)-*9H*-carbazole **(22)** was obtained in a 94% yield, by a modified procedure of Jian *et al.* [24] The product was obtained via a reduction

reaction from the nitro group to the amine using tin chloride dihydrate in a solution of ethanol, as shown in scheme above. The reaction was complete after heating the mixture for 48 hours at 85 °C, and following work-up to give the isolated product as white ivory crystals. The purity of the product was confirmed by TLC, GC mass spectra, melting point and elemental analysis. The structure of the product was identified by IR absorption, ^{1}H NMR and ^{13}C NMR.

The purity of the product was confirmed by a single peak by GC with a retention time of 13.72 minutes. The mass spectra showed main integer masses for 3,6-dibromo-9-(4-amino-phenyl)-*9H*-carbazole **(22)** at 414, 416, and 418 in a 1:2:1 ratio as expected due to ^{79}Br and ^{81}Br isotopes. The melting point of the product was 210-212 °C. The product was subjected to elemental analysis, for the compound $C_{18}H_{12}N_2Br_2$ calculated the expected percentage for the comprising elements to be: C, 51.96 H, 2.91 N, 6.73 Br, 38.41.%; from analysis we obtained: C, 51.86 H, 2.96 N, 6.56 Br, 38.57.%; which fell into close agreement to calculations.

The structure of the product was confirmed by IR spectrum giving peaks at 3420 cm^{-1}, 3329 cm^{-1} peaks due to the presence of Ar-NH_2 3034 cm^{-1} as the aromatic C-H stretch followed by 1893 cm^{-1}, 1893 cm^{-1}, 1752 cm^{-1} and 1695 cm^{-1} which can be designated to the combination or overtone vibrations of the out-of-plane deformation vibrations of the C-H bonds of the benzene ring. Also the bands 1604 cm^{-1}, 1505 cm^{-1}, 1470 cm^{-1} and 1449 cm^{-1} can be denoted to C=C for the aromatic rings. The peak at 923 cm^{-1} stretching vibrations of the C-N bond, finally the peak at 788 cm^{-1} can be linked to the stretching vibrations of the C-Br bonds.

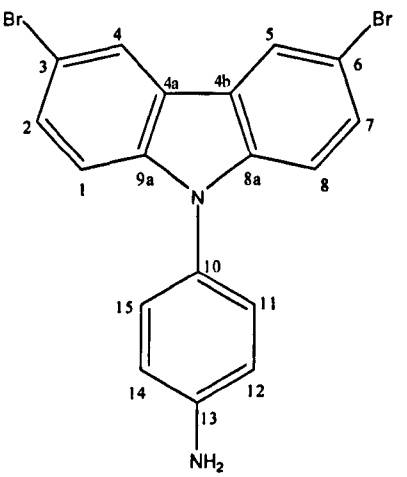

Figure 5.15, 3,6-dibromo-9-(4-amino-phenyl)-*9H*-carbazole **(22)**

The ^{1}H-NMR spectrum identifies the product with 5 signals in the spectra. The doublet signal at δ 8.15 ppm is linked to the protons 4 and 5 on the carbazole ring system. The next signal is that arising at δ 7.40 ppm which is a doublet of doublets in relation to protons at positions 12 and 14, δ 7.20 – 7.14 ppm as multiplet relating to protons 1,2,7 and 8, δ 6.85 relating to protons 11 and 15. And we finally have a singlet giving rise at δ 3.85 relating to protons from the amine group.

The ^{13}C-NMR gave eight peaks on the spectrum which have been estimated to the following positions of the compound δ 145 (1C) position 13, δ 139 (2C) positions 8a and 9a, δ 131 (1C) position 10, δ 122 (4C) positions 4a, 4b, 11 and 15, δ 124 (4C) positions 2, 4, 5 and 7, δ 117 (2C) positions 3 and 6, δ 116 (2C) positions 12 and 14, δ 113 (2C) positions 1 and 8. These peaks are in good agreement with the structure proposed for 3,6-dibromo-9-(4-amino-phenyl)-*9H*-carbazole **(22)**. These analytical results clearly verify that the product was 3,6-dibromo-9-(4-amino-phenyl)-*9H*-carbazole **(22)**.

5.5.3 4-(2-Butyl-octyloxy-)-1-iodobenzene (23)

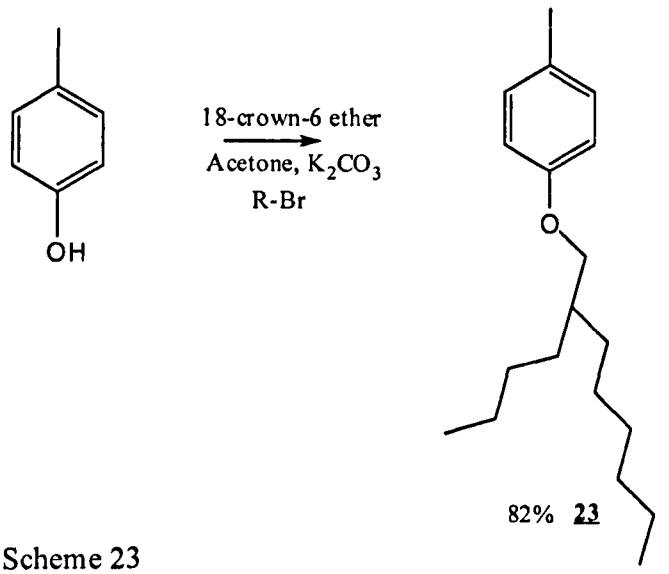

Scheme 23

4-(2-Butyl-octyloxy)-1-iodobenzene **(23)** was obtained in an 82 % yield, by a modified procedure of Zimmerman [14] *et al.* The product was obtained via an alkylation as shown in scheme above. The purity of the product was confirmed by TLC, mass spectra. The structure of the product was identified by ^{1}H NMR and ^{13}C NMR.

The reaction was very similar to the formation of 1,3-bis-(2-ethyl-hexyl-oxy)-5-iodo-benzene **(12)** and was carried out in a very similar manor. The mechanism follows the formation of a potassium complex which is stabilised through an 18-crown-6 ether which stabilisaties the K^+ ions and help keep it in solution. This in turn allows the attack, through a Sn2 reaction to form the alkylated ether system.

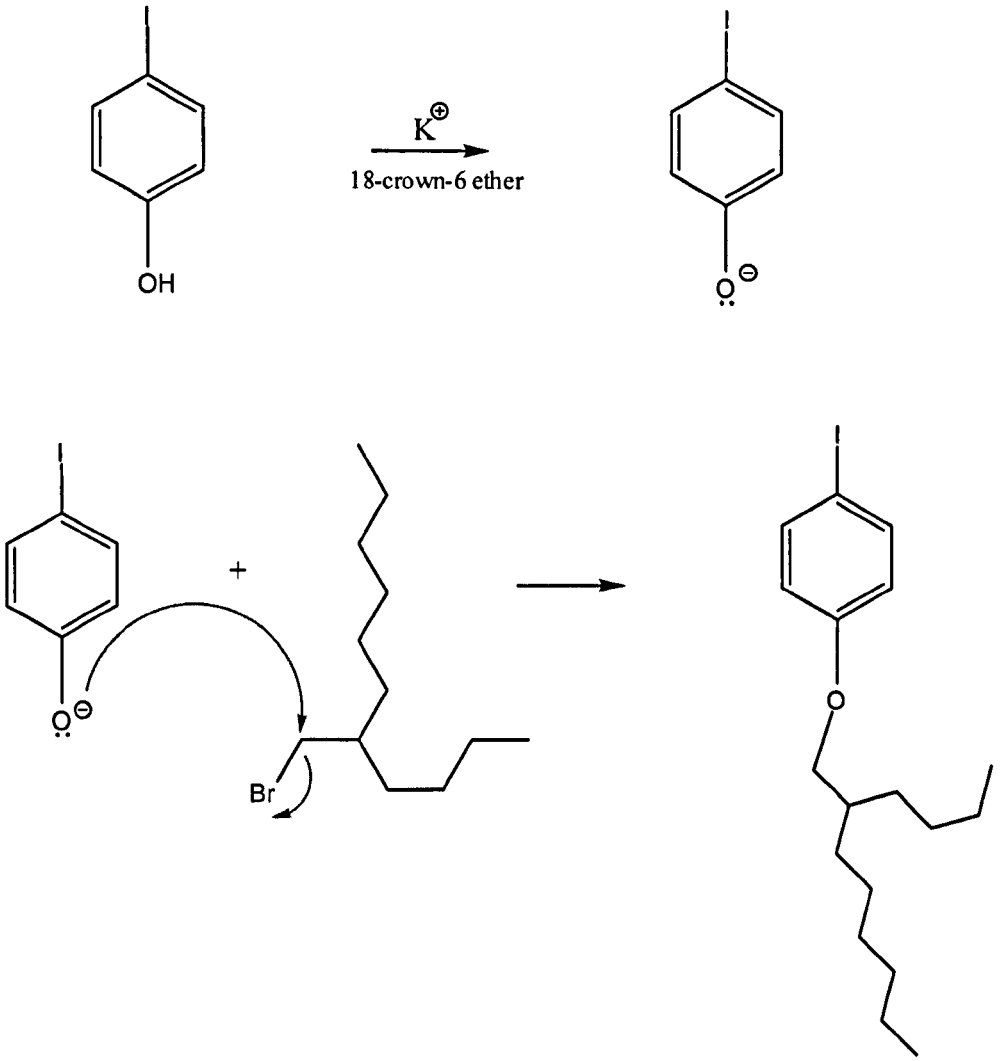

Mechanism 13, formation 4-(2-butyl-octyloxy)-1-iodobenzene **(23)**

The purity of the product was confirmed by a single spot on TLC analysis. The mass spectra showed main integer masses for 4-(2-butyl-octyloxy)-1-iodobenzene **(24)** at 388 and 390 in a 1:3 ratio as expected due to ^{126}I and ^{129}I isotopes.

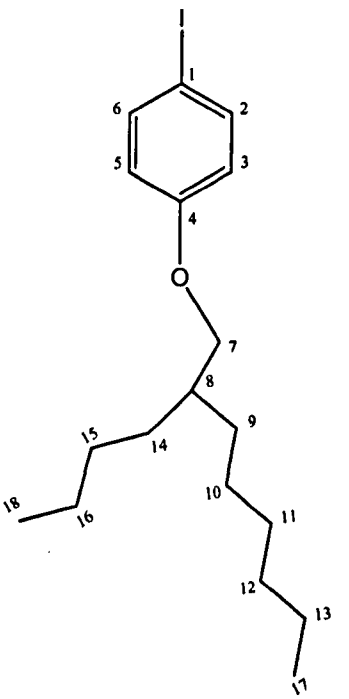

Figure 5.16, 4-(2-butyl-octyloxy)-1-iodobenzene **(23)**

Looking at the ^{1}H-NMR the protons at δ 7.53 and δ 6.54 ppm both of which are doublets with integrations matching that of two protons and are related to hydrogen at positions 2,6 and 3,5 respectively. The key peak is at δ 3.78 ppm, this resembles the two protons at 7 on the above diagram indicating attachment to the oxygen atom forming an ether in the alkyl chain. The next peak is also a signature peak, as it is the only single proton which is distinguished at δ 1.75 ppm with a quintet and assigned to position 8. Following this is a multiplet of $-CH_2$ protons running from positions 9-16. Finally we have the 6 protons at positions 17 and 18 coresponding to those of the methyl groups.

The ^{13}C-NMR gave eleven peaks on the spectrum which have been estimated to the following positions of the compound, δ 159 (1C) position 4, δ 138 (2C) positions 2 and 6, δ 116 (2C) positions 3 and 5, δ 82 (1C) positions 1, δ 76 (1C) position 7, δ 37 (1C) position 8, δ 36 (1C) positions 9 , δ 35 (1C) position 15, δ 31 (4C) positions 10,11,12,14, δ 27 (2C) positions 16 and 13 and finally δ 14 (2C) at positions 17 and 18. These peaks are in well agreement with the structure of 4-(2-butyl-octyloxy)-1-

iodobenzene (**23**). These analytical results clearly verify that the product was 4-(2-butyl-octyloxy)-1-iodobenzene (**23**).

5.5.4 3,6-Dibromo-9-(bis-[4-(2-butyl-octyloxy)-phenyl]-amino-phen-4-yl)-carbazole (24)

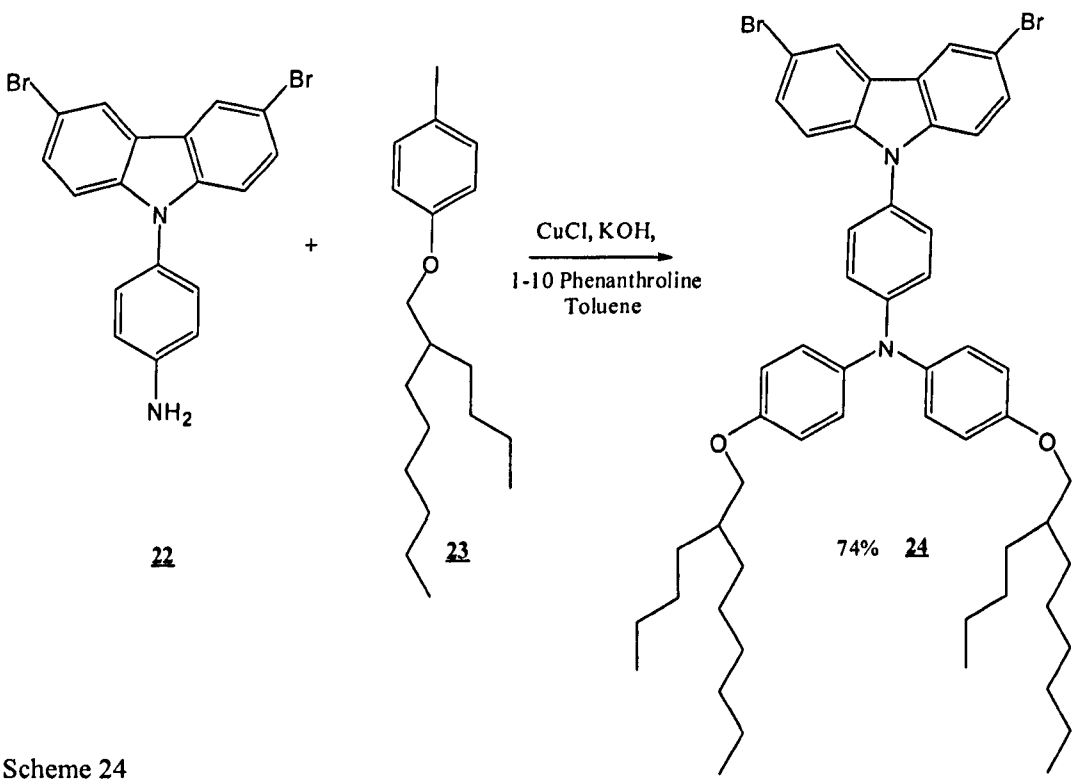

Scheme 24

3,6-Dibromo-9-(bis-[4-(2-butyl-octyloxy)-phenyl]-amino-phen-4-yl)-carbazole (**24**) was obtained in a 74% yield, by a modified copper catalysed procedure. The product was obtained via the reaction of 3,6-dibromo-9-(4-amino-phenyl)-*9H*-carbazole (**22**) with 4-(2-butyl-octyloxy-)-1-iodobenzene (**23**) with the aid of a complex between copper (I) chloride and 1,10-phenanthroline, as shown in the scheme above. The reaction was complete after heating the mixture for 48 hours at 110 °C, and following work-up to give the isolated product as brown oil/solid compound. The purity of the product was confirmed by elemental analysis. The structure of the product was identified by IR absorption, ^{1}H NMR and ^{13}C NMR.

The mechanism of the reaction is believed to occur by a first reaction of the phenyl amine group with potassium hydroxide which would remove a proton from the amine a leave a reacting anion. The copper and 1,10-phenanthroline would undergo an oxidative addition with the aryl iodide group which would react with the imide anion to yield the formation of a new carbon-nitrogen bond. This reaction is then repeated to yield the tri-aryl amine compound.

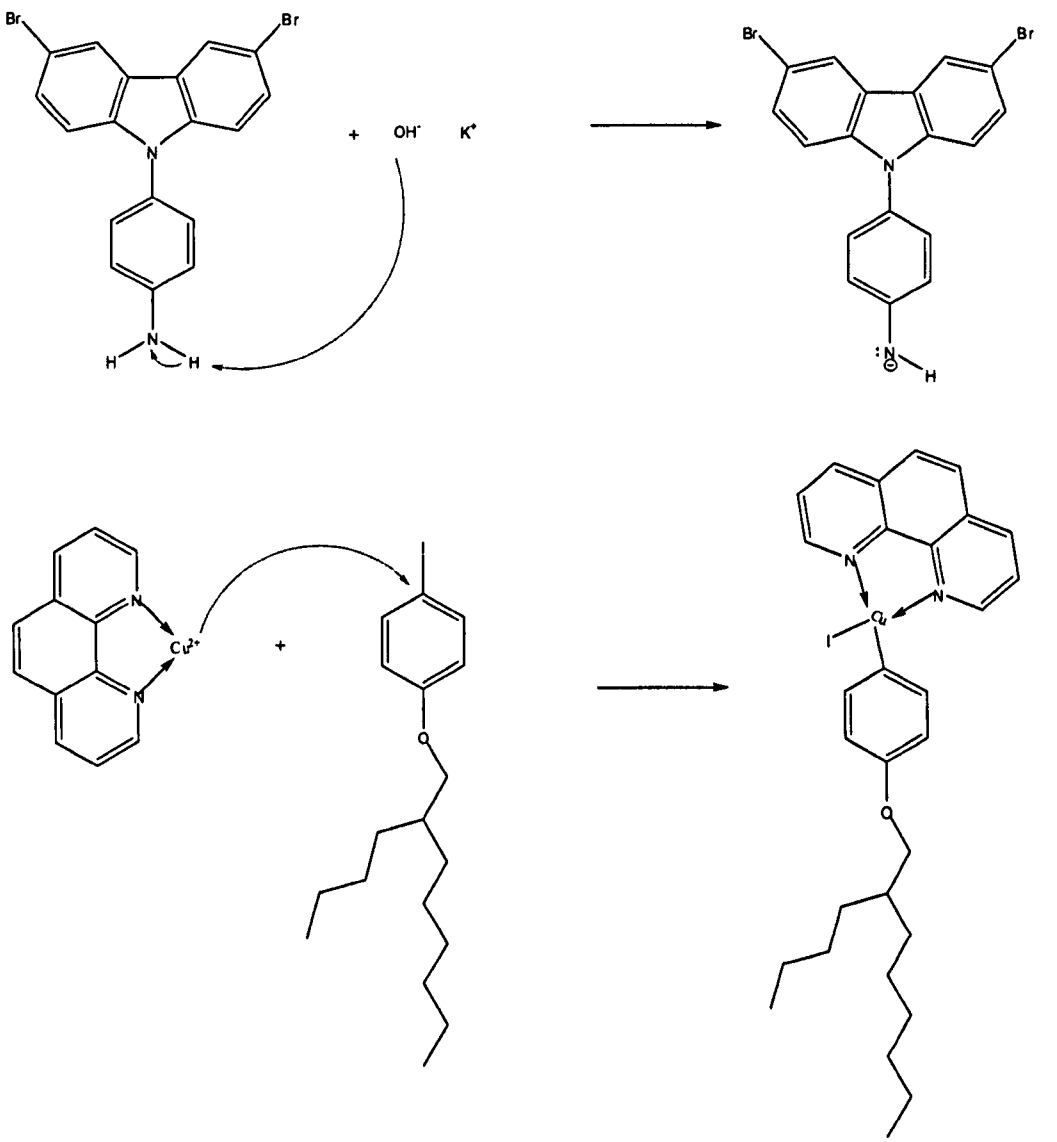

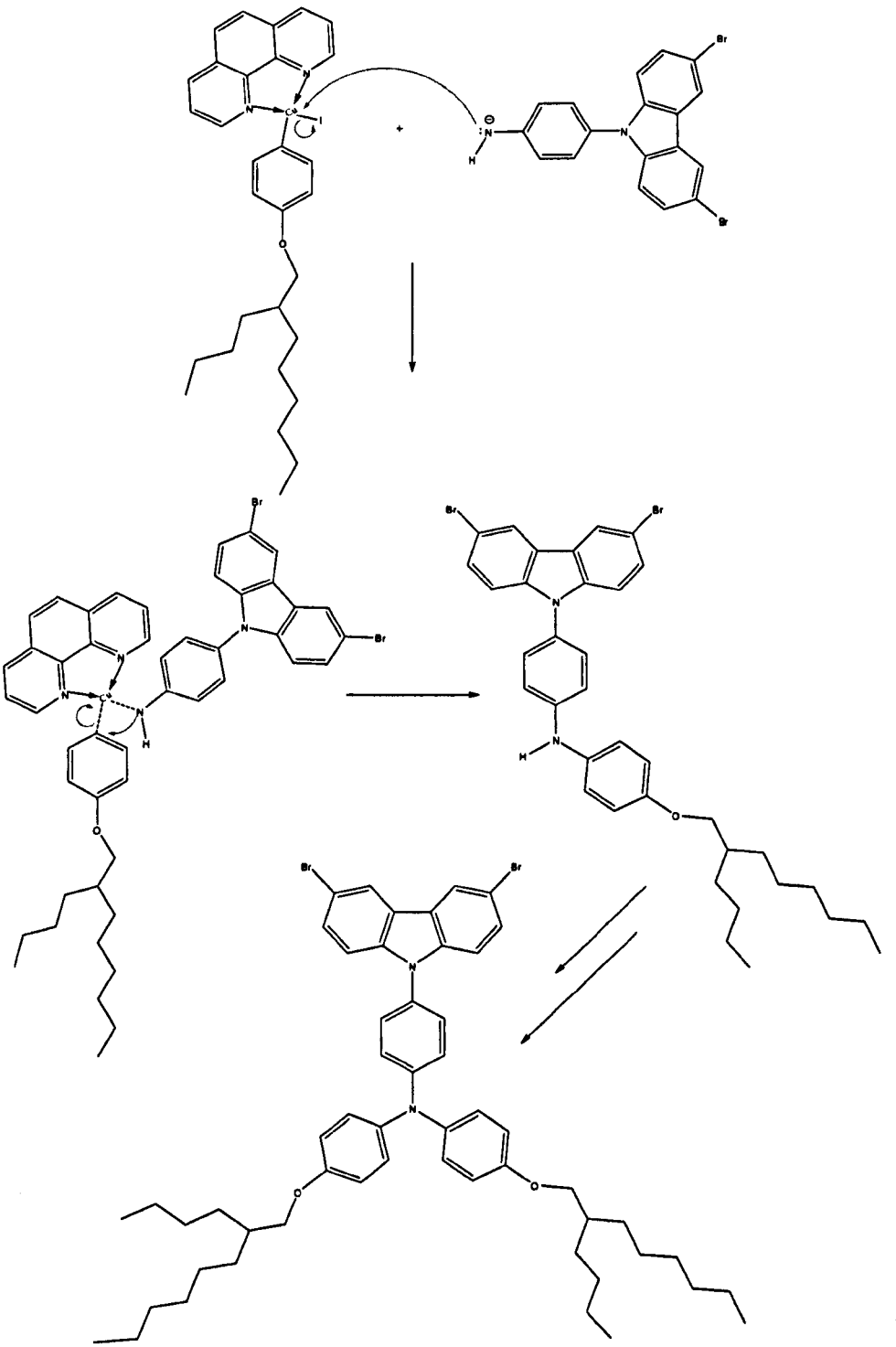

Mechanism 14, 3,6-Dibromo-9-(bis-[4-(2-butyl-octyloxy)-phenyl]-amino-phen-4-yl)-carbazole **(24)**

The purity of the product was confirmed by elemental analysis, for the compound $C_{54}H_{68}N_2Br_2O_2$ calculated the expected percentage for the comprising elements to be: C, 69.22 H, 7.32 N, 2.99 Br, 17.06 O, 3.42.%; from analysis we obtained: C, 68.47 H, 7.19 N, 2.96 Br, 17.38.%; which fell into close agreement to calculations.

The structure of the product was confirmed by IR spectrum giving peaks at 3054 cm^{-1}, 3032 cm^{-1}, 2987 cm^{-1}, 2685 cm^{-1} as the aromatic C-H stretch followed by 1893 cm^{-1}, 1752 cm^{-1} and 1695 cm^{-1}, 1604 cm^{-1} which can be designated to the combination or overtone vibrations of the out-of-plane deformation vibrations of the C-H bonds of the benzene ring. 1591 cm^{-1} stretching due to C-O bond; Also the bands 1505 cm^{-1}, 1470 cm^{-1}, 1449 cm^{-1}, 1373 cm^{-1}, 1334 cm^{-1} be denoted to C=C for the aromatic rings. 1170 cm^{-1} stretching due to C-O-Ar of an ether; the peak at 923 cm^{-1} stretching vibrations of the C-N bond. Finally the peak at 742 cm^{-1} can be linked to the stretching vibrations of the C-Br bonds.

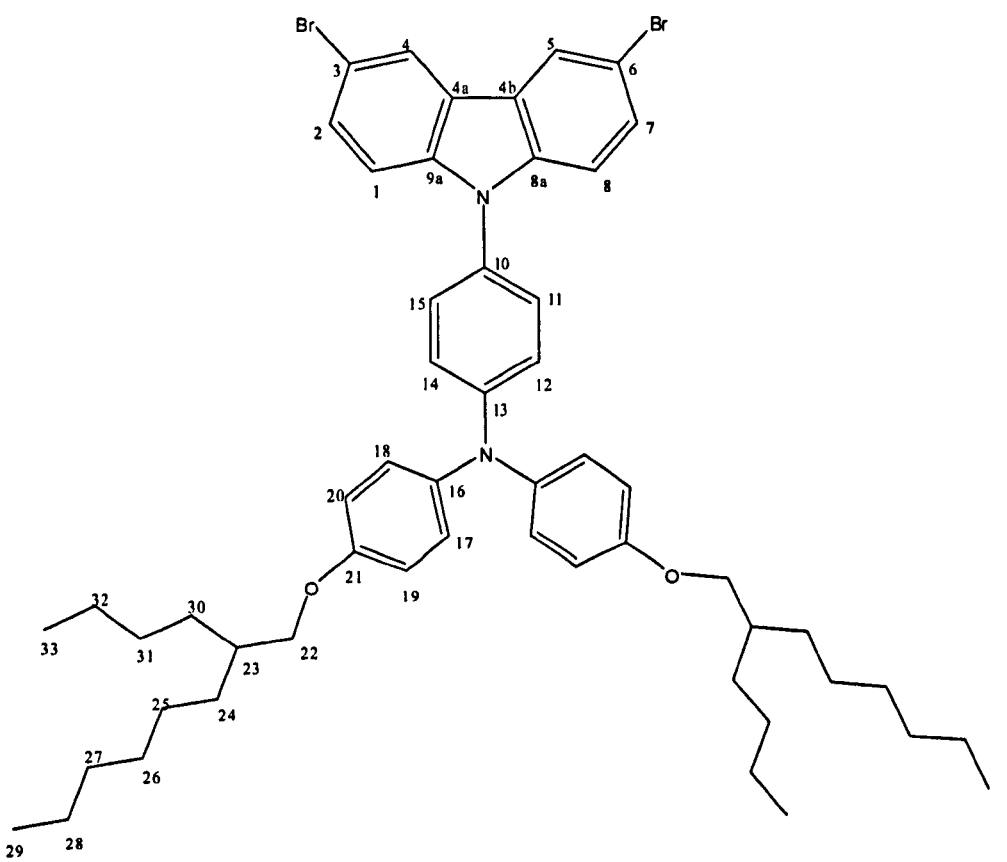

Figure 5.17, 3,6-Dibromo-9-(bis-[4-(2-butyl-octyloxy)-phenyl]-amino-phen-4-yl)-carbazole **(24)**

The ^{1}H-NMR spectrum identifies the product with eleven signals in the spectra. The doublet signal at δ 8.15 ppm is linked to the protons 4 and 5 on the carbazole ring system. The next signal is that arising at δ 7.45 ppm which is a doublet of doublets in relation to protons at positions 12 and 14, δ 7.25 ppm which is a doublet of doublets in relation to protons at positions 1 and 8, δ 7.20 ppm which is a doublet of doublets in relation to protons at positions 2 and 7, δ 7.10 ppm which is a doublet of doublets in relation to protons at positions 17 and 28, δ 7.05 ppm which is a doublet in relation to protons at positions 11 and 15, δ 6.85 ppm relating to protons 19 and 20. And we have a singlet giving rise at δ 3.75 ppm relating to protons from position 22, The next peak is also a signature peak, as it is the only single proton which is distinguished at δ 1.75 ppm with a quintet and linked to position 23; the peaks between 1.55-1.15 ppm are those related to positions 24-28 and 30-32 for the –CH2 groups; and finally we have peak at 0.85 ppm coinciding to methyl groups at positions 29 and 33

The ^{13}C-NMR gave nineteen peaks on the spectrum which have been estimated to the following positions of the compound δ 156 (2C) position 21, δ 140 (1C) position 13, δ 139 (4C) positions 17 and 18, δ 129 (2C) positions 8a, 9a, δ 128 (4C) positions 11, 12, 14 and 15, δ 127 (1C) positions 10, δ 126 (2C) positions 4a and 4b, δ 123 (4C) positions 2, 4, 5 and 7, δ 119 (2C) positions 3 and 6, δ 116 (4C) positions 19 and 20, 113 (2C) positions 1 and 8, δ 111 (2C) position 16, δ 71 (2C) position 22, δ 38 (2C) position 23, δ 31 (2C) positions 25 , δ 29 (4C) position 26 and 31, δ 27 (6C) positions 24, 27, and 30 δ 23 (4C) positions 28 and 32 and finally δ 14 (4C) at positions 29 and 33. These peaks are in well agreement with the structure of 3,6-dibromo-9-(bis-[4-(2-butyl-octyloxy)-phenyl]-amino-phen-4-yl)-carbazole **(24)**. These analytical results clearly verify that the product was 3,6-dibromo-9-(bis-[4-(2-butyl-octyloxy)-phenyl]-amino-phen-4-yl)-carbazole **(24)**.

5.5.5 3,6-Dibromo-9-(bis-[3,5-bis-(2-ethyl-hexyloxy)-phenyl]-amino-phen-4-yl)-carbazole (25)

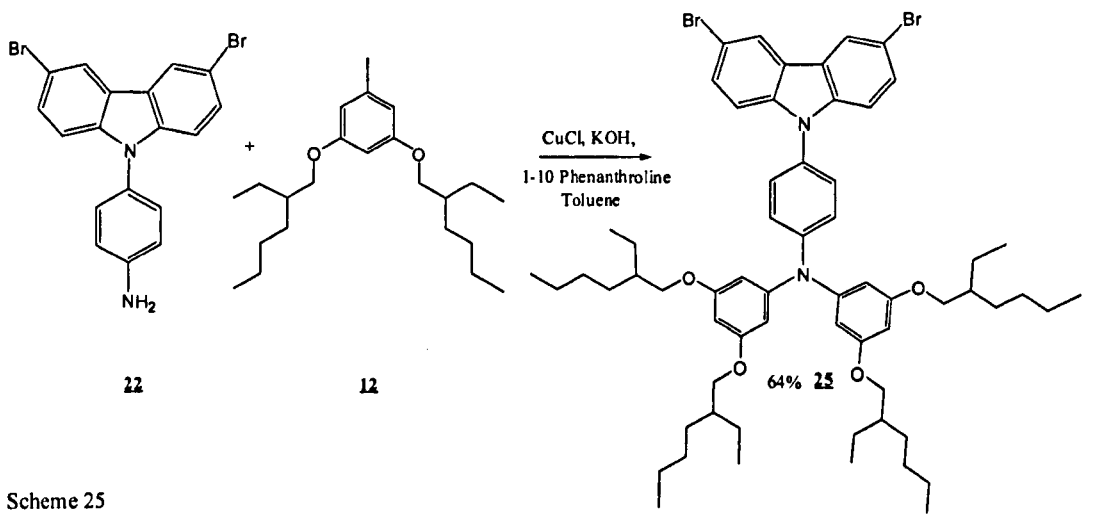

22 12

Scheme 25

3,6-Dibromo-9-(bis-[3,5-bis-(2-ethyl-hexyloxy)-phenyl]-amino-phen-4-yl)-carbazole **(25)** was obtained in a 74% yield, by a modified copper catalysed procedure. The product was produce via the reaction of 3,6-dibromo-9-(4-amino-phenyl)-*9H*-carbazole **(22)** with 1,3-bis-(2-ethyl-hexyloxy)-5-iodobenzene **(12)** with the aid of a complex between copper (I) chloride and 1,10-phenanthroline, as shown in above. The reaction was complete after heating the mixture for 48 hours at 110 °C, and following work-up to give the isolated product as brown oil/solid compound. The purity of the product was confirmed by elemental analysis. The structure of the product was identified by IR absorption, ^{1}H NMR and ^{13}C NMR. The mechanism of the reaction can be believed to occur as described in the above discussion of 3,6-dibromo-9-(bis-[4-(2-butyl-octyloxy)-phenyl]-amino-phen-4-yl)-carbazole **(24)**.

The purity of the product was confirmed by; elemental analysis, for the compound $C_{62}H_{84}N_2Br_2O_4$ calculated the expected percentage for the comprising elements to be: C, 68.88; H, 7.83; Br, 14.78; N, 2.59; O, 5.92.%; from analysis we obtained: C: 69.23 H: 7.18, N: 2.34, Br: 14.90.% which fell into close agreement to calculations.

The structure of the product was confirmed by IR spectrum giving peaks at 3185 cm^{-1} 3056 cm^{-1} 3017 cm^{-1} as the aromatic C-H stretch followed by 1831 cm^{-1}, 1794 cm^{-1} and 1651 cm^{-1},1594 cm^{-1}which can be designated to the combination or overtone vibrations of the out-of-plane deformation vibrations of the C-H bonds of the benzene ring. 1581 cm^{-1} stretching due to C-O bond; Also the bands 1515 cm^{-1}, 1470 cm^{-1} (m-s), 1469 cm^{-1}, 1373 cm^{-1}, 1334 cm^{-1} be denoted to C=C for the aromatic rings. 1170 cm^{-1} stretching due to C-O-Ar of an ether; the peak at 931 cm^{-1} stretching vibrations of the C-N bond. Finally the peak at 776 cm^{-1} can be linked to the stretching vibrations of the C-Br bonds.

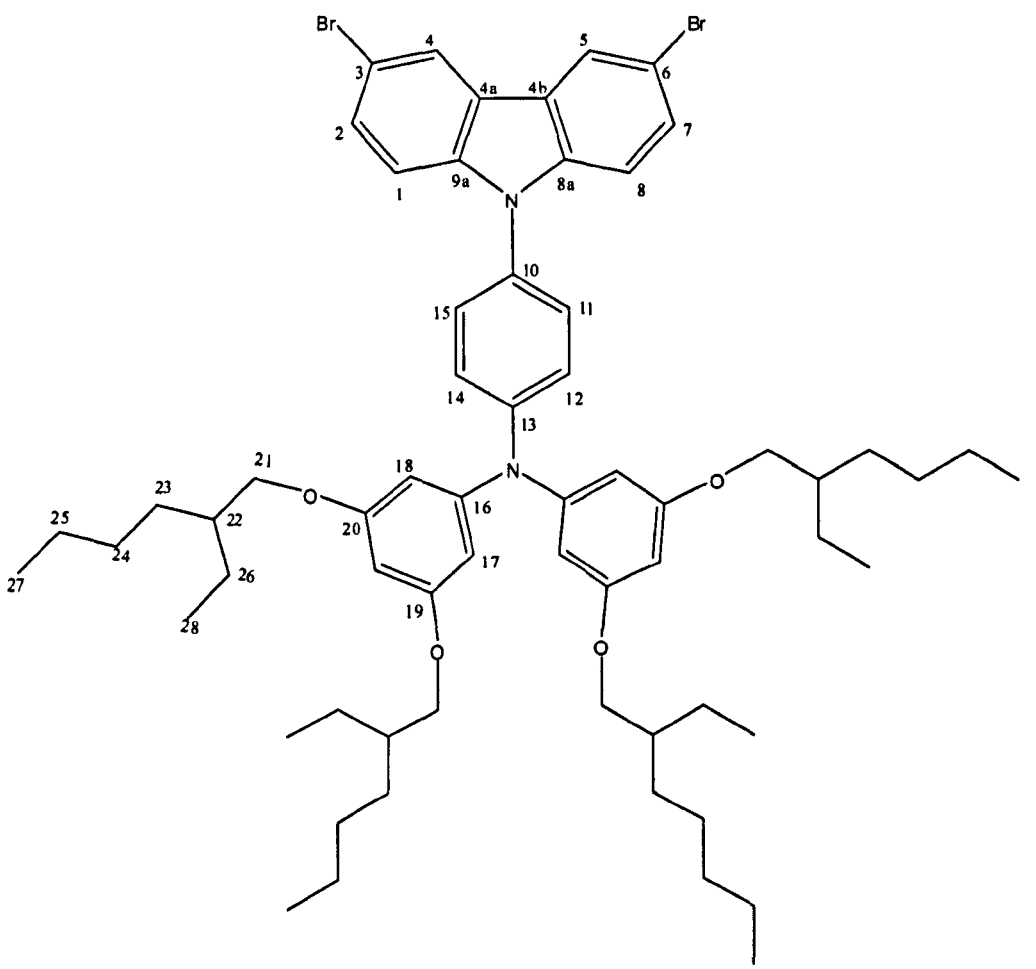

Figure 5.18, 3,6-dibromo-9-(bis-[3,5-bis-(2-ethyl-hexyloxy)-phenyl]-amino-phen-4-yl)-carbazole **(25)**

The ^{1}H-NMR spectrum identifies the product with eleven signals in the spectra. The doublet signal at δ 8.15 ppm is linked to the protons 4 and 5 on the carbazole ring system. The next signal is that arising at δ 7.45 ppm which is a doublet of doublets in relation to protons at positions 12 and 14, δ 7.30 – 7.05 ppm which is a multiplet in relation to protons at positions 1, 2, 7, 8, 11 and 15, δ 6.30 ppm which is in relation to protons at position 29, δ 6.10 ppm relating to protons 17 and 18. And we have a doublet giving rise at δ 3.75 ppm relating to protons from position 21, The next peak is also a signature peak, as it is the only single proton which is distinguished at δ 1.65 ppm with a quintet and linked to position 22; the peaks between 1.55-1.15 ppm are those related to positions 23-26 for the $-CH_2$ groups; and finally we have peak at 0.85 ppm coinciding to methyl groups at positions 27 and 28

The ^{13}C-NMR gave nineteen peaks on the spectrum which have been estimated to the following positions of the compound δ 159 (4C) positions 19 and 20, δ 143 (1C) position 13, δ 139 (2C) positions 8a and 9a, δ 131 (1C) positions 10, δ 122 (4C) positions 17 and 18, δ 121 (4C) positions 11, 12, 14 and 15, δ 117 (2C) positions 4a and 4b, δ 116 (6C) positions 1, 2, 4, 5, 7 and 8, δ 113 (2C) positions 3 and 6, δ 111 (4C) positions 16 and 29, δ 77 (4C) position 21, δ 76 (4C) position 22, δ 70 (4C) positions 26 , δ 39 (4C) position 23, δ 29 (4C) position 24, δ 22 (4C) positions 25 and finally δ 14 (8C) at positions 27 and 28. These peaks are in well agreement with the structure proposed for 3,6-dibromo-9-(bis-[3,5-bis-(2-ethyl-hexyloxy)-phenyl]-amino-phen-4-yl)-carbazole **(25)**. These analytical results clearly verify that the product was 3,6-dibromo-9-(bis-[3,5-bis-(2-ethyl-hexyloxy)-phenyl]-amino-phen-4-yl)-carbazole **(25)**.

5.5.6 Attempted synthesis of 3,6-bis-(4,4,5,5-tetramethyl-[1,3,2]dioxaborolan-2-yl)-9-(bis-[3,5-bis-(2-ethyl-hexyloxy)-phenyl]-amino-phen-4-yl)-carbazole (26)

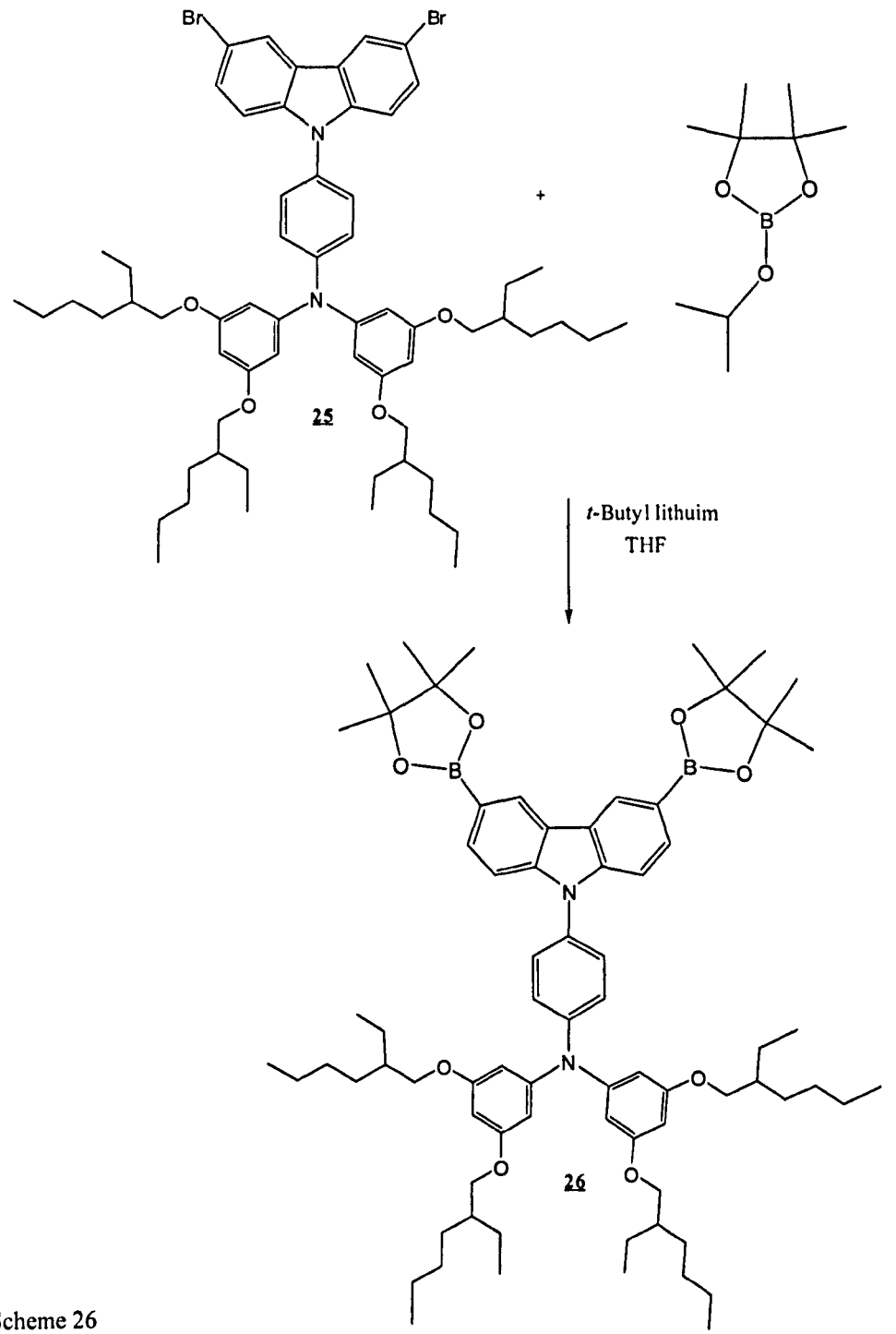

Scheme 26

The synthesis of 3,6-bis-(4,4,5,5-tetramethyl-[1,3,2]dioxaborolan-2-yl)-9-(bis-[3,5-bis-(2-ethyl-hexyloxy)-phenyl]-amino-phen-4-yl)-carbazole **(26)** was attempted via a modified procedure of Yang *et al.* [25] The reaction involved substituting the two bromide groups of 3,6-dibromo-9-(bis-[3,5-bis-(2-ethyl-hexyloxy)-phenyl]-amino-phen-4-yl)-carbazole **(25)** for boronic ester groups using *t*-butyllithium and 2-isopropoxy-4,4,5,5-tetramethyl- 1,3,2-dioxaborolane as shown in scheme 26 above. The reaction proceeds via a two step procedure. The first step involved in the reaction mechanism is lithium halogen exchange, which is carried out by reacting the 3,6-dibromo-9-(bis-[3,5-bis-(2-ethyl-hexyloxy)-phenyl]-amino-phen-4-yl)-carbazole **(25)** in tetrahydrofuran with *t*-butyllithium at -78°C. Step two in the reaction procedure is nucleophilic attack by the lithiated carbazole on 2-isopropoxy-4,4,5,5-tetramethyl-1,3,2-dioxaborolane, which is again carried out at -78°C. The mechanism proceeds via a four membered ring transition state as shown. After allowing the reaction mixture to rise to ambient temperature and stirring for 36 hours the reaction was stopped and worked-up.

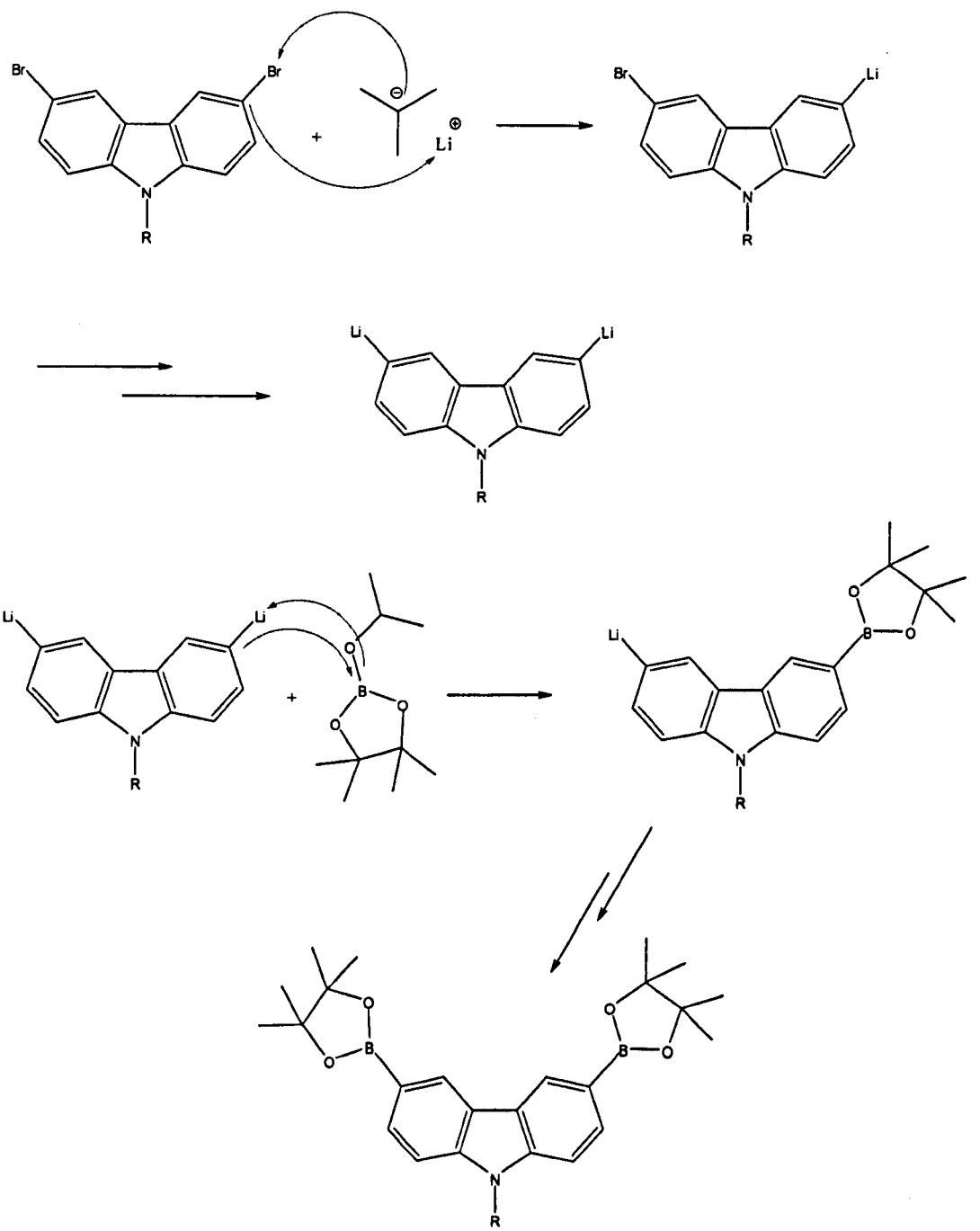

Mechanism 15, formation of 3,6-bis-(4,4,5,5-tetramethyl-[1,3,2]dioxaborolan-2-yl)-9-(bis-[3,5-bis-(2-ethyl-hexyloxy)-phenyl]-amino-phen-4-yl)-carbazole **(26)** using *t*-butyllithium and 2-isopropoxy-4,4,5,5-tetramethyl- 1,3,2-dioxaborolane

Unfortunately the product found from this reaction was found to be contaminated. TLC analysis was inconclusive due to large amounts of streaking between products

even with the use of substance like pyridine or triethylamine to help basify the silica on TLC plate. It was first possibly thought that boronic acid derivative could have formed by cleavage of the bis-boronic ester derivative. This was found not to be the case after treatment with pinacol in toluene in the presence of molecular sieves which did not reduce the number of side products. This method was rejected for an alternative method.

5.5.7 3,6-Bis-(4,4,5,5-tetramethyl-[1,3,2]dioxaborolan-2-yl)-9-(bis-[4-(2-butyl-octyloxy)-phenyl]-amino-phen-4-yl)-carbazole (27)

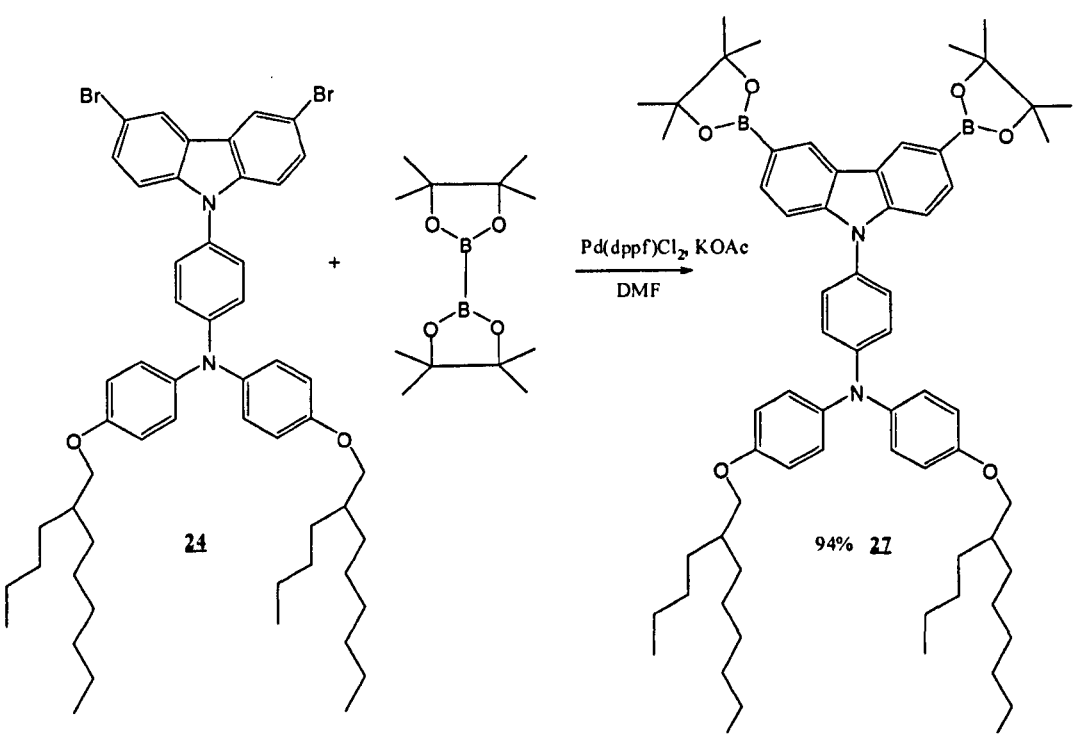

Scheme 27

3,6-Bis-(4,4,5,5-tetramethyl-[1,3,2]dioxaborolan-2-yl)-9-(bis-[4-(2-butyl-octyloxy)-phenyl]-amino-phen-4-yl)-carbazole **(27)** was obtained in a 94% yield by a modified procedure of Jo *et al,* [26] as shown in the Scheme above. The reaction was complete after heating the mixture for 12 hours at 60 °C, and work-up the isolated product as a light brown oil / solid.

The purity of the product was confirmed by TLC, GC mass spectra, melting point and elemental analysis. The structure of the product was identified by IR absorption, ^{1}H NMR and ^{13}C NMR.

This reaction was achieved with the use of bis(pinacolate)diboron in a palladium catalysed reaction. This allowed successive substitution of the two bromine atoms with a boronate ester group. The reaction was catalysed with the use of $Pd(dppf)Cl_2$ and potassium acetate as shown below.

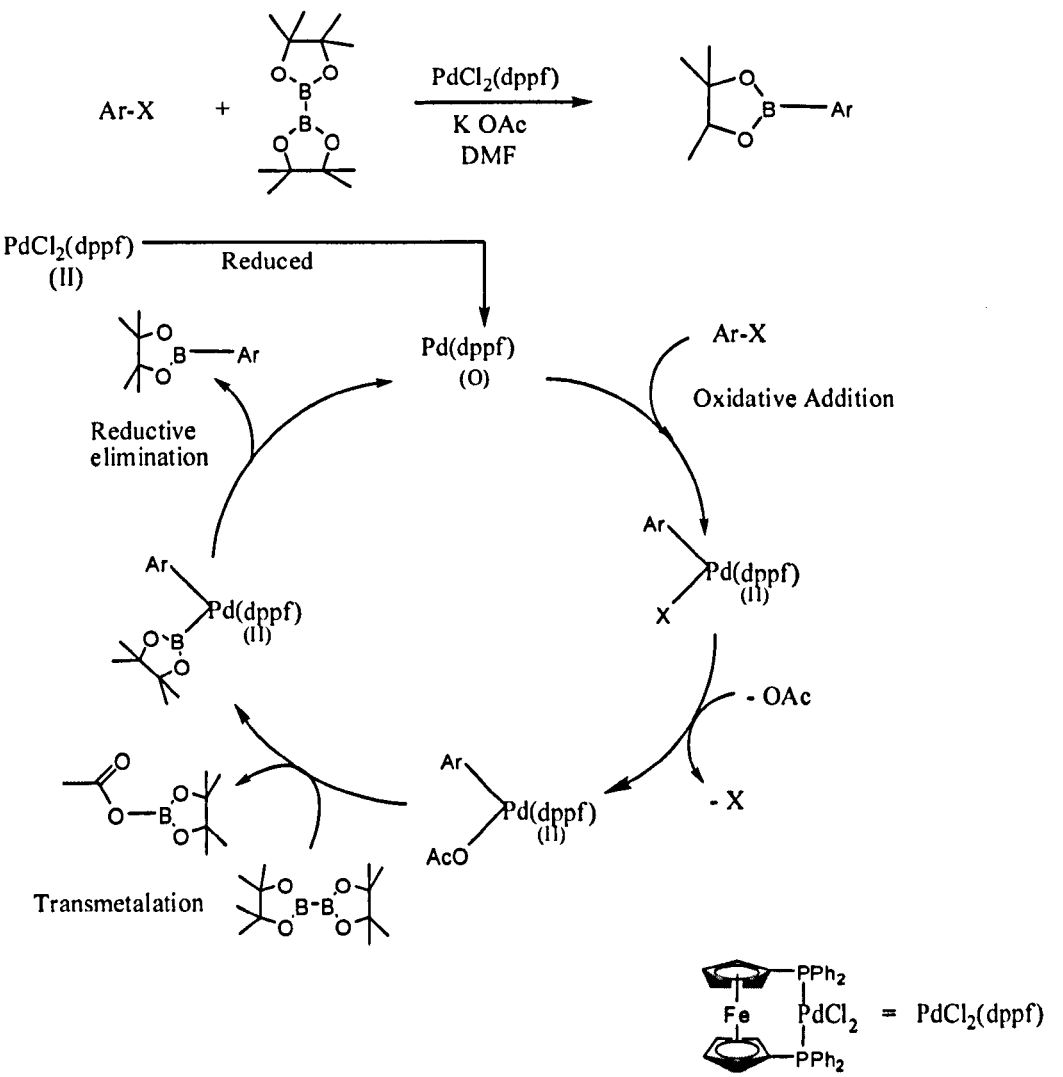

Mechanism 16, 3,6-Bis-(4,4,5,5-tetramethyl-[1,3,2]dioxaborolan-2-yl)-9-(bis-[4-(2-butyl-octyloxy)-phenyl]-amino-phen-4-yl)-carbazole **(27)**

The purity of the product was confirmed by; elemental analysis, for the compound $C_{66}H_{92}N_2Br_2O_2$ calculated the expected percentage for the comprising elements to be: C:76.88 H:8.99 N:2.72 Br:2.10 O:9.31.%; from analysis we obtained: C:77.01; H:9.03 N:2.37.%; which fell into close agreement to calculations.

The structure of the product was confirmed by IR spectrum giving peaks 2943, 2924, 2852, 1458 and 1370 cm-1 and peaks due to aromatic C – H bonds are found at 1246, 1145, 1010, 858, 792, 738 and 701 cm-1. C – C stretching vibrations of the aromatic rings can be seen at 1551 and 1437 cm-1 and the peak at 1285 cm-1 is due to the C – N bond. The peak at 1271 cm-1 corresponds to the C – B – C stretching frequency and the peak at 1326 cm-1 is due to the B – O stretch. Meanwhile the stretching vibration of the C – Br bonds of bis-[2-butyl-octyl-oxy)-phenyl]-4-[3,6-dibromo-carbazol-9-yl]-phenyl-amine **(30)** at 776 cm-1 disappeared, which further confirmed the reaction had gone to completion.

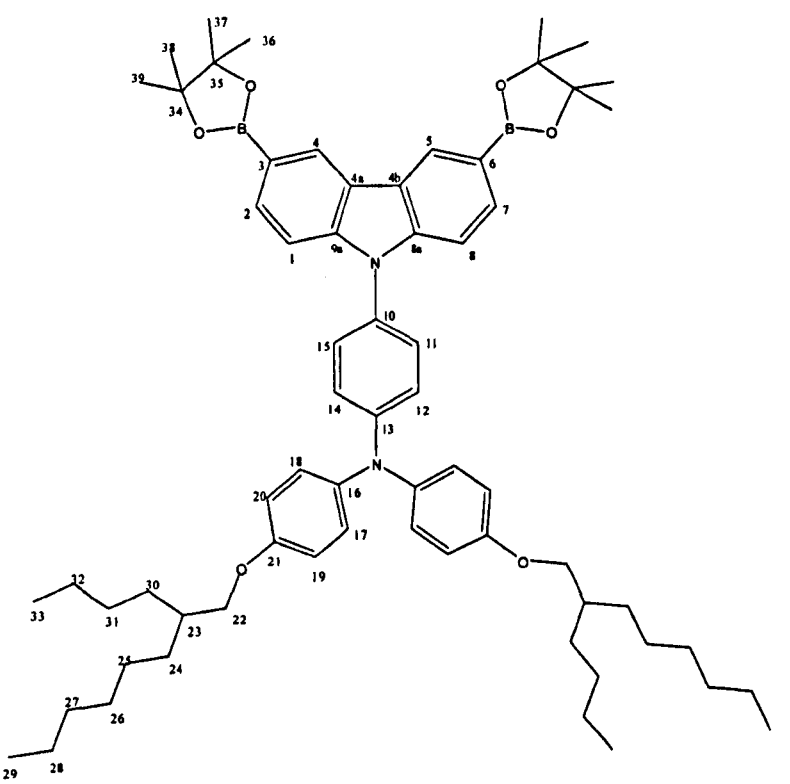

Figure 5.19, 3,6-bis-(4,4,5,5-tetramethyl-[1,3,2]dioxaborolan-2-yl)-9-(bis-[4-(2-butyl-octyloxy)-phenyl]-amino-phen-4-yl)-carbazole **(27)**

The ^{1}H-NMR spectrum identifies the product with eleven signals in the spectra. The doublet signal at δ 8.15 ppm is linked to the protons 4 and 5 on the carbazole ring system. The next signal is that arising at δ 7.45 ppm which is a doublet of doublets in relation to protons at positions 12 and 14, δ 7.25 ppm which is a doublet of doublets in relation to protons at positions 1 and 8, δ 7.20 ppm which is a doublet of doublets in relation to protons at positions 2 and 7, δ 7.10 ppm which is a doublet of doublets in relation to protons at positions 17 and 28, δ 7.05 ppm which is a doublet in relation to protons at positions 11 and 15, δ 6.85 ppm relating to protons 19 and 20. And we have a singlet giving rise at δ 3.75 ppm relating to protons from position 22, The next peak is also a signature peak, as it is the only single proton which is distinguished at δ 1.75 ppm with a quintet and linked to position 23; at δ 1.40 we have a distinctive singlet peak relating to protons at 36,37,38 and 39 as methyl groups attached to the boronic ester; the peaks between 1.55-1.15 ppm are those related to positions 24-28 and 30-32 for the $-CH_2$ groups; and finally we have peak at 0.85 ppm coinciding to methyl groups at positions 29 and 33.

The ^{13}C-NMR gave nineteen peaks on the spectrum which have been estimated to the following positions of the compound δ 156 (2C) position 21, δ 140 (1C) position 13, δ 140 (4C) positions 17 and 18, δ 132 (1C) positions 10, δ 129 (2C) positions 8a, 9a, δ 128 (2C) positions 11 and 12, δ 127 (2C) 14 and 15, δ 126 (2C) positions 4a and 4b, δ 123 (4C) positions 2, 4, 5 and 7, δ 119 (2C) positions 3 and 6, δ 116 (4C) positions 19 and 20, 113 (2C) positions 1 and 8, δ 111 (2C) position 16, δ 83 (4C) positions 34 and 35, δ 71 (2C) position 22, δ 38 (2C) position 23, δ 31 (2C) positions 25 , δ 29 (4C) position 26 and 31, δ 27 (8C) positions 36,37,38 and 39, δ 24 (12C) positions 22,24, 27,30 and 33, δ 23 (4C) positions 28 and 32 and finally δ 14 (2C) at position 29. These peaks are in good agreement with the structure proposed for 3,6-bis-(4,4,5,5-tetramethyl-[1,3,2]dioxaborolan-2-yl)-9-(bis-[4-(2-butyl-octyloxy)-phenyl]-amino-phen-4-yl)-carbazole **(27)**. These analytical results clearly verify that the product was 3,6-bis-(4,4,5,5-tetramethyl-[1,3,2]dioxaborolan-2-yl)-9-(bis-[4-(2-butyl-octyloxy)-phenyl]-amino-phen-4-yl)-carbazole **(27)**.

5.6.0 Other Compounds Used

5.6.1 Preparation of the palladium scavenger N,N-diethyl-phenyl-azo-thio-formamide (28)

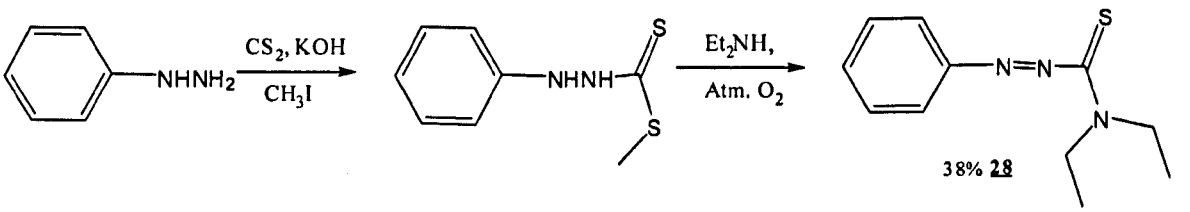

Scheme 28

N, N'-Diethyl-phenyl-azo-thio-formamide **(28)** was obtained in a 44 % yield, by a procedure of Krebs *et al.* [27] The product was made via a two step process in a one pot synthesis as shown in scheme above. The purity of the product was confirmed by TLC, melting point. The structure of the product was identified by ^{1}H NMR and ^{13}C NMR.

This compound was desired due to its ability to dissolve palladium nanoparticles formed during catalysis. [28] Since it has been observed from polymers made in the group only small amounts of contaminants are required to alter the physical properties of the desired polymer. The reaction was carried out in a one-pot synthesis and started by the reaction of phenyl hydrazine with carbon disulphide followed by methyl iodide to form methyl-2-phenylhydrazinecarbodithioate which was observed by the colour change from the orange precipitate to the light yellow solution. To this was then added diethylamine and the reaction refluxed for a period of time. The solution was cooled and oxidised by pumping atmospheric oxygen through the system to yield the desired compound.

Purification of the product was achieved first by column chromatography followed by re-crystallisation to yield N, N'-diethyl-phenyl-azo-thio-formamide **(28)** as a single spot product.

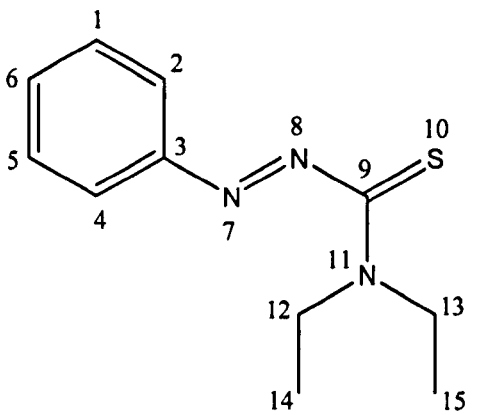

Figure 5.20, N, N'-diethyl-phenyl-azo-thio-formamide **(28)**

Looking at the ^{1}H-NMR we can notice protons at δ 7.95 - 7.81 which are designated to positions 2 and 4 as a multiplet followed by δ 7.62 – 7.44 which are connected to protons at 1,5 and 6 also sitting as a multiplet. We then have protons at δ 4.02 and δ 3.51 which resemble positions 12 and 13 as quintets. And finally we have methyl protons at 14 and 15 which fall at δ 1.41 and δ 1.18 as triplets.

The ^{13}C-NMR gave nine peaks on the spectrum which have been estimated to the following positions of the compound, δ 194 (1C) position 9, δ 151 (2C) positions 1 and 5, δ 132 (2C) positions 2 and 4, δ 129 (1C) positions 6, δ 123 (1C) position 6, δ 48 (1C) position 12, δ 45 (1C) positions 13, δ 13 (1C) position 15, δ 11 (1C) position 14. These peaks are in well agreement with the structure of N, N'-diethyl-phenyl-azo-thio-formamide **(28)**. These analytical results clearly verify that the product was N, N'-diethyl-phenyl-azo-thio-formamide **(28)**.

5.7 Preparation of the Polymers

5.7.1 Attempted synthesis of poly(9-(bis-[3,5-bis-(2-ethyl-hexyloxy)-phenyl]-amino-phen-4-yl)-carbazole-3,6-diyl) (34) kumada P1.AK

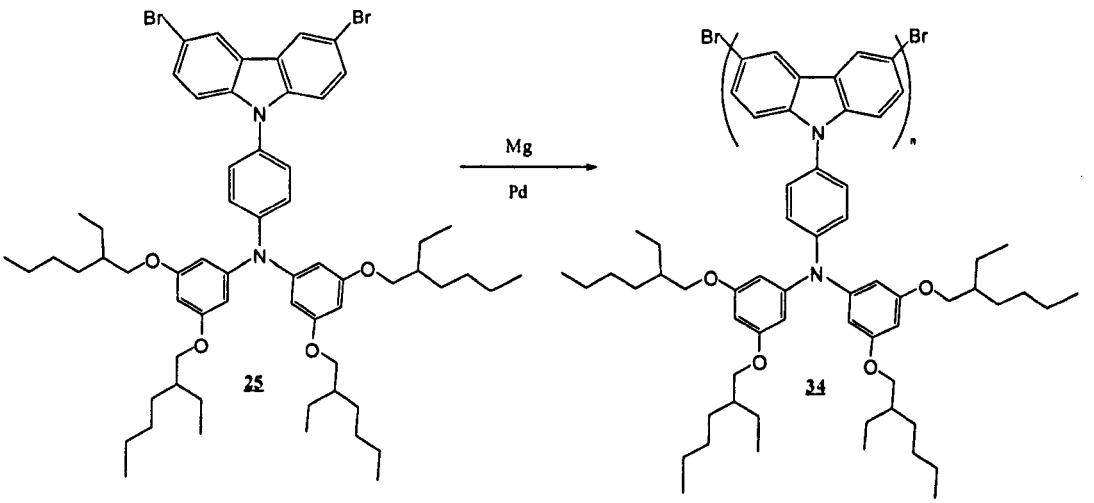

Scheme 29

Synthesis of poly(9-(bis-[3,5-bis-(2-ethyl-hexyloxy)-phenyl]-amino-phen-4-yl)-carbazole-3,6-diyl) **(34)** was attempted by a Pd(II) Grignard-type electrocatalysed dehalogenation polycondensation reaction via a method prescribed by Yamamoto *et al.* [29] The reaction was carried out in a sealed tube with 3,6-dibromo-9-(bis-[3,5-bis-(2-ethyl-hexyloxy)-phenyl]-amino-phen-4-yl)-carbazole **(25)** being reacted with activated magnesium in the presence of (2,2'-bi-pyridine) dichloropalladium (II) in THF. The reaction was monitored by the change in colour of the reaction mixture over the reflux period. The reaction mixture started in a pale yellow colour and as time went on the colour changed from orange to red followed by dark green to dark brown over the 72 hour period.

It is believe the mechanism for the formation of this Grignard-type dehalogenation polymerisation takes place as indicated below.

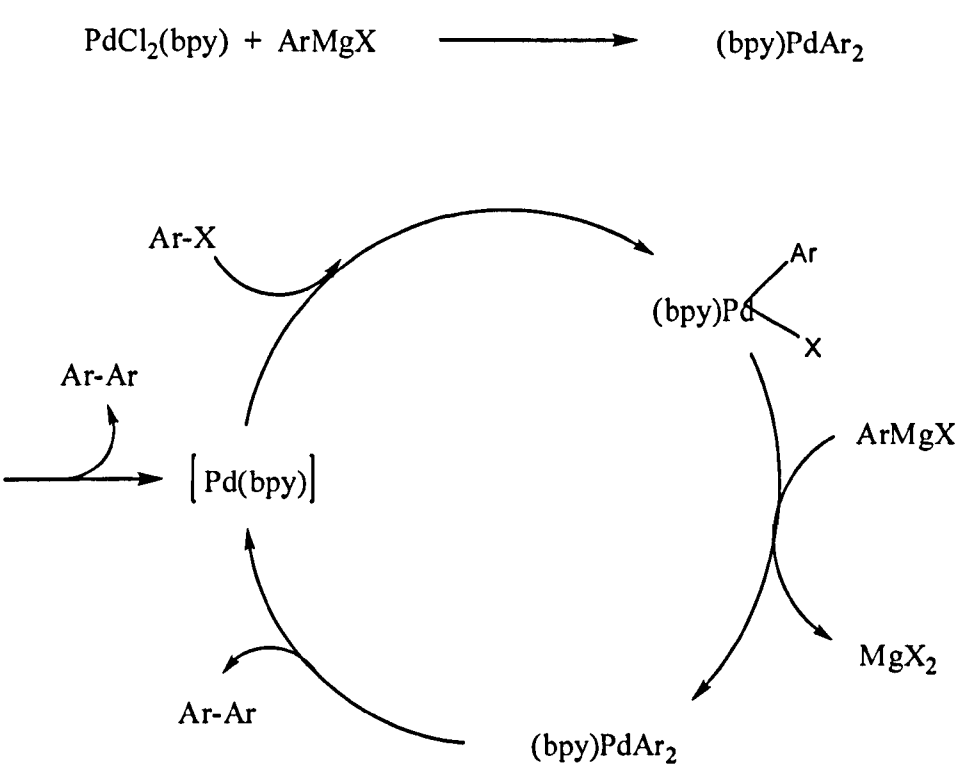

bpy - 2,2'-bipyridine
X - halogen atom
Ar - aryl group

Mechanism 17, formation of Poly(9-(bis-[3,5-bis-(2-ethyl-hexyloxy)-phenyl]-amino-phen-4-yl)-carbazole-3,6-diyl) **(34)**

From this indication it was expected the polymerisation to have taken place to yield a moderate polymer chain. The polymer was worked up in the prescribed method. In the filtration process it was noticed that the product was not precipitating out of solution but tended to remain as a clot on the micro-pore filter paper. This compound had the texture of a thick gel and dark brown in colour. This first assumption made at this point was that due to the four branched alkyl chains present the polymer may be extremely soluble and hence not precipitating out as expected.

Upon collecting the compound, analysis was carried out in the means of a ^{1}H NMR and GPC analysis. The proton NMR indicated very small amounts of broadness of the

peaks which lead to the assumption that the reaction did not reach polymerisation but rather an oligomer may have formed. The GPC result obtained confirmed this by the indication of the low moleculer weights achieved: Mn 2,900 / Mw 3,250 which showed a degree of polymerisation (DP) of approximately 3. This method was attempted below with the second synthesised monomer.

5.7.2 Attempted synthesis of poly(9-(bis-[4-(2-butyl-octyloxy)-phenyl]-amino-phen-4-yl)-carbazole-3,6-diyl) (35) kumada P2.AK

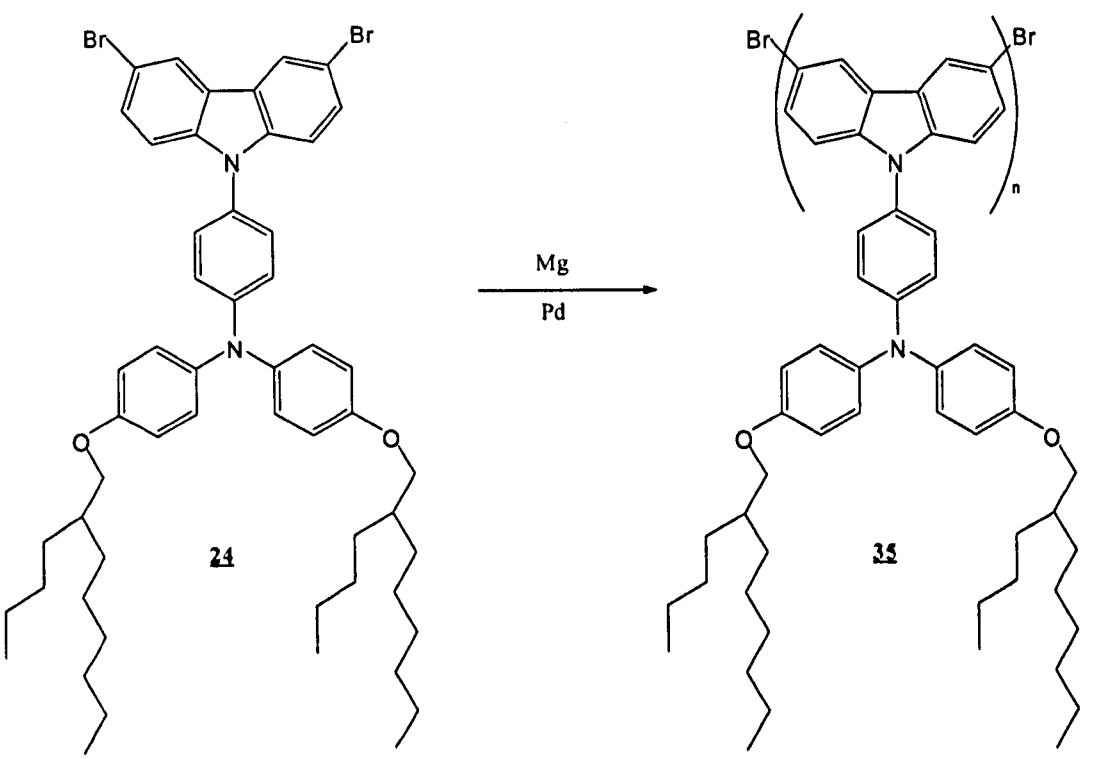

Scheme 30

Poly(9-(bis-[4-(2-butyl-octyloxy)-phenyl]-amino-phen-4-yl)-carbazole-3,6-diyl) **(35)** was attempted by a Pd(II) Grignard-type electrocatalysed dehalogenation polycondensation reaction via a method prescribed by Yamamoto *et al.* [29] The reaction was carried out in a sealed tube with 3,6-dibromo-9-(bis-[4-(2-butyl-

octyloxy)-phenyl]-amino-phen-4-yl)-carbazole **(24)** being reacted with activated magnesium in the presence of (2,2'-bi-pyridine) dichloropalladium (II) in THF.

As in the above reaction there was a suspect that this reaction did not achieve polymerisation, and upon collecting the ^{1}H NMR and GPC data from the compound we noticed that the proton NMR indicated no change in the peaks showing the starting material. The GPC result obtained confirmed this by the indication of the moleculer weights achieved were in proportion to that of the starting material: Mn 900 / Mw 1,250.

It was concluded that this method was not the most appropriate for the formation of poly-aryl carbazoles. This reaction may have been flawed due to the size alkyl aryl groups [30] present which most likely contributed to steric hindrance [31] in the reaction paths between the catalytic palladium complex and the reacting Grignard and halogen atoms.

5.7.3 Poly(9-(bis-[4-(2-butyl-octyloxy)-phenyl]-amino-phen-4-yl)-carbazole-3,6-diyl) (36) Suzuki (a) P3.AK

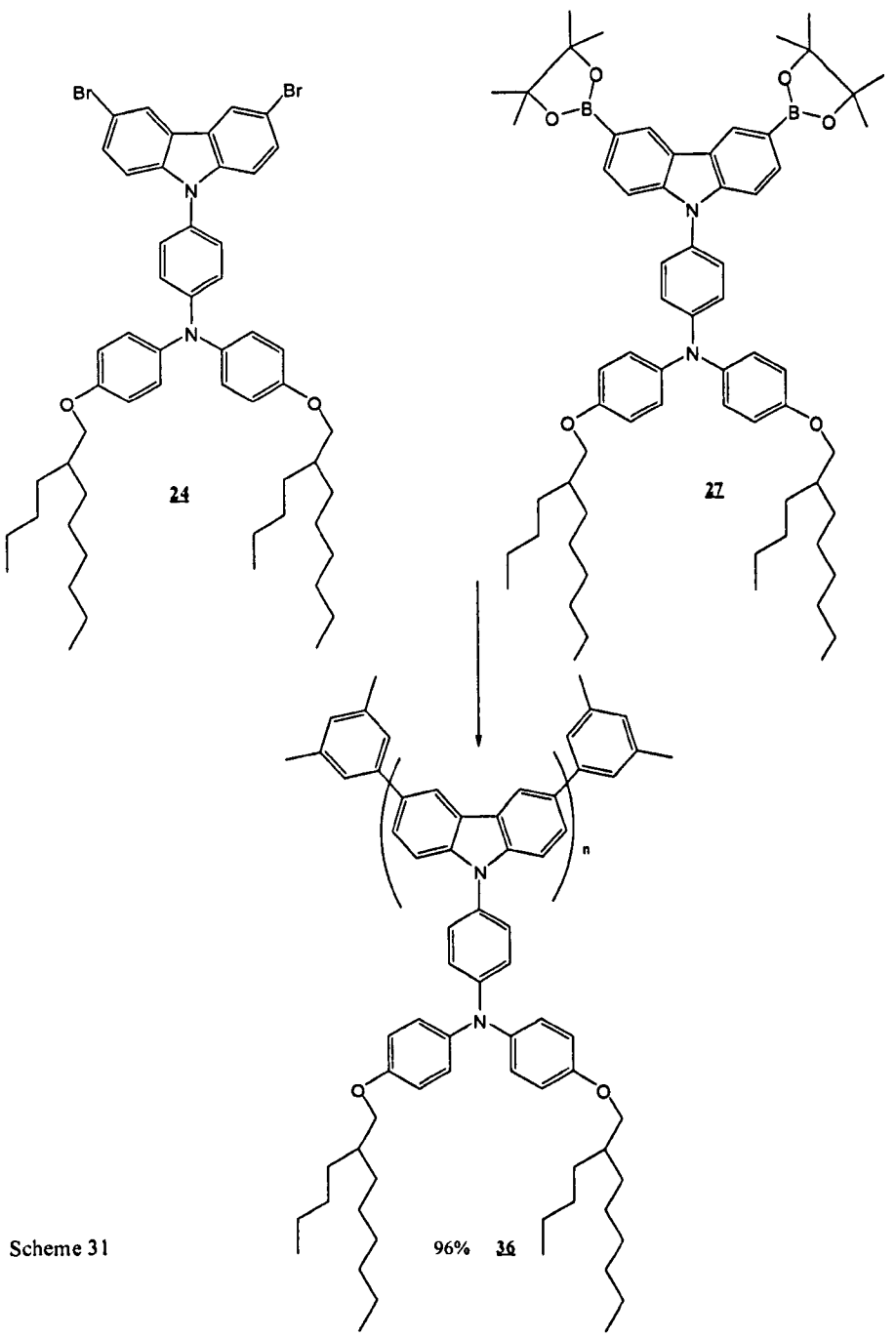

Scheme 31

Poly(9-(bis-[4-(2-butyl-octyloxy)-phenyl]-amino-phen-4-yl)-carbazole-3,6-diyl) **(36)** was obtained in 96% yield. The product was obtained via a Suzuki type cross-coupling reaction of 3,6-dibromo-9-(bis-[4-(2-butyl-octyloxy)-phenyl]-amino-phen-4-yl)-carbazole **(24)** and 3,6-bis-(4,4,5,5-tetramethyl-[1,3,2]dioxaborolan-2-yl)-9-(bis-[4-(2-butyl-octyloxy)-phenyl]-amino-phen-4-yl)-carbazole **(27)** via a palladium-catalysed route, as shown in the scheme above.

The reaction was carried out in a round bottom flask and the catalyst was formed in situ, by reacting $Pd_2(dba)_3$ and tri-*p*-tolyl phosphine in THF, followed by addition of the two monomers 3,6-dibromo-9-(bis-[4-(2-butyl-octyloxy)-phenyl]-amino-phen-4-yl)-carbazole **(24)** and 3,6-bis-(4,4,5,5-tetramethyl-[1,3,2]dioxaborolan-2-yl)-9-(bis-[4-(2-butyl-octyloxy)-phenyl]-amino-phen-4-yl)-carbazole **(27)** and the base. The reaction was complete after refluxing the mixture for 24 hours. The polymer was end-capped and a first precipitation was carried out. Following this the polymer was dried, and treated with N,N-diethyl-phenyl-azo-thio-formamide **(28)** in order to remove any palladium nanoparticles that may have been left behind from the reaction. This lead to the polymer being re-precipitated once again, to yield the desired polymer as a pale ivory powder.

The polymer poly(9-(bis-[4-(2-butyl-octyloxy)-phenyl]-amino-phen-4-yl)-carbazole-3,6-diyl) **(36)** was characterised by the following techniques: ^{1}H NMR and ^{13}C NMR, IR absorption, elemental analysis, GPC, UV-vis spectroscopy, photoluminescence spectroscopy, thermo-gravimetric analysis (TGA), differential scanning calorimetry (DSC), and cyclic voltammetry (CV).

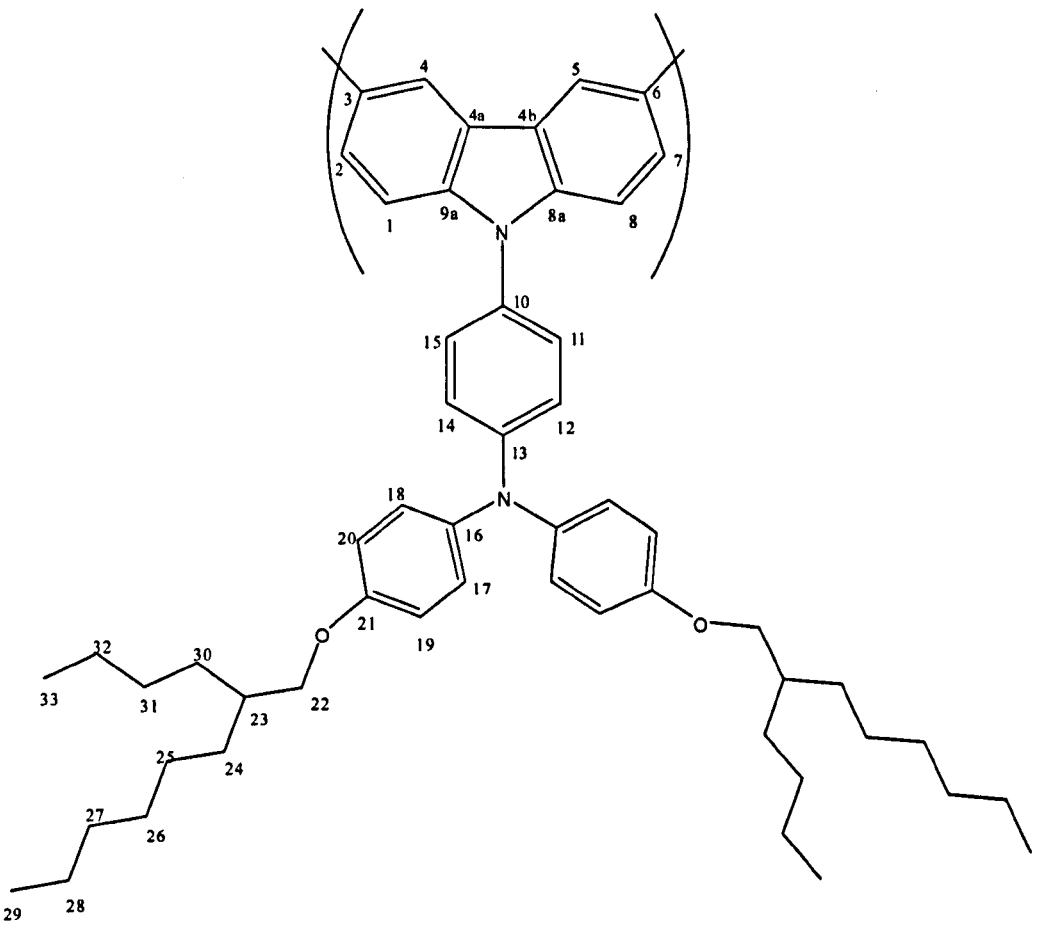

Figure 5.21, poly(9-(bis-[4-(2-butyl-octyloxy)-phenyl]-amino-phen-4-yl)-carbazole-3,6-diyl) **(36)**

Nuclear Magnetic Resonance Spectroscopy analysis

The ^{1}H-NMR spectrum identifies the product with ten broad signals in the spectra. The first broad peak at signal δ 8.50 ppm is linked to the protons 4 and 5 on the carbazole ring system. The next signal is that arising at δ 7.72 ppm can be assigned in relation to protons at positions 12 and 14, δ 7.45 ppm can be in relation to protons at positions 1, and 8, δ 7.35 ppm which is in relation to protons at positions 2 and 7, δ 7.20 – 7.00 ppm is a very broad shift relating to protons 11,15,17 and 18; δ 6.85 relates to the broad protons lying at 19 and 20. We have a clear broad peak at δ 3.75 ppm relating to protons from position 22, The next peak is also a signature peak, as it is the only single proton which is distinguished at δ 1.75 ppm linked to position 23;

the peaks between 1.55-1.15 ppm are those related to positions 24-28 and 30-32 for the $-CH_2$ groups; and finally we have peak at 0.85 ppm coinciding to methyl groups at positions 29 and 33. There are some smaller peaks in the spectra that will be related to the dimethyl phenyl end capping groups.

The ^{13}C-NMR gave nineteen peaks on the spectrum which have been estimated to the following positions of the compound δ 156 (2C) position 21, δ 141 (1C) position 13, δ 140 (2C) positions 8a and 9a, δ 128 (1C) positions 10, δ 127 (4C) positions 11, 12, 14 and 15, δ 125 (4C) positions 17 and 18, δ 123 (2C) positions 4a and 4b, δ 120 (4C) positions 2, 4, 5 and 7, δ 118 (2C) positions 3 and 6, δ 115 (6C) positions 16,19 and 20, 110 (2C) position 1 and 8, δ 71 (2C) position 22, δ 38 (2C) position 30, δ 31 (2C) positions 24 , δ 29 (4C) position 26 and 31, δ 26 (2C) positions 32, δ 24 (2C) position 25, δ 23 (2C) and 27, δ 21 (2C) positions 28 and finally δ 14 (4C) at positions 29 and 33.

Scheme 32, NMR for Poly(9-(bis-[4-(2-butyl-octyloxy)-phenyl]-amino-phen-4-yl)-carbazole-3,6-diyl) **(36)**

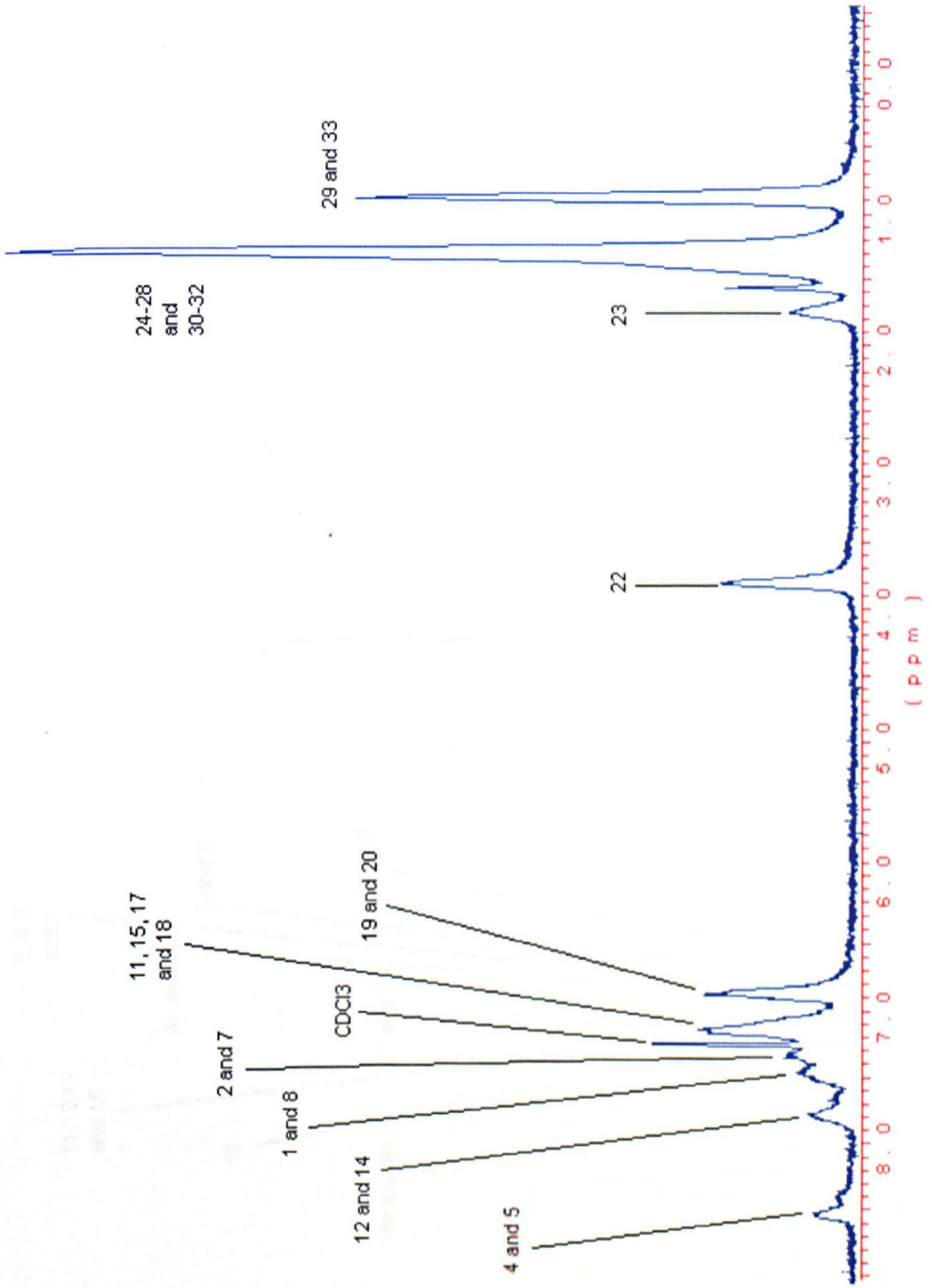

Scheme 33, NMR for Poly(9-(bis-[4-(2-butyl-octyloxy)-phenyl]-amino-phen-4-yl)-carbazole-3,6-diyl) **(36)**

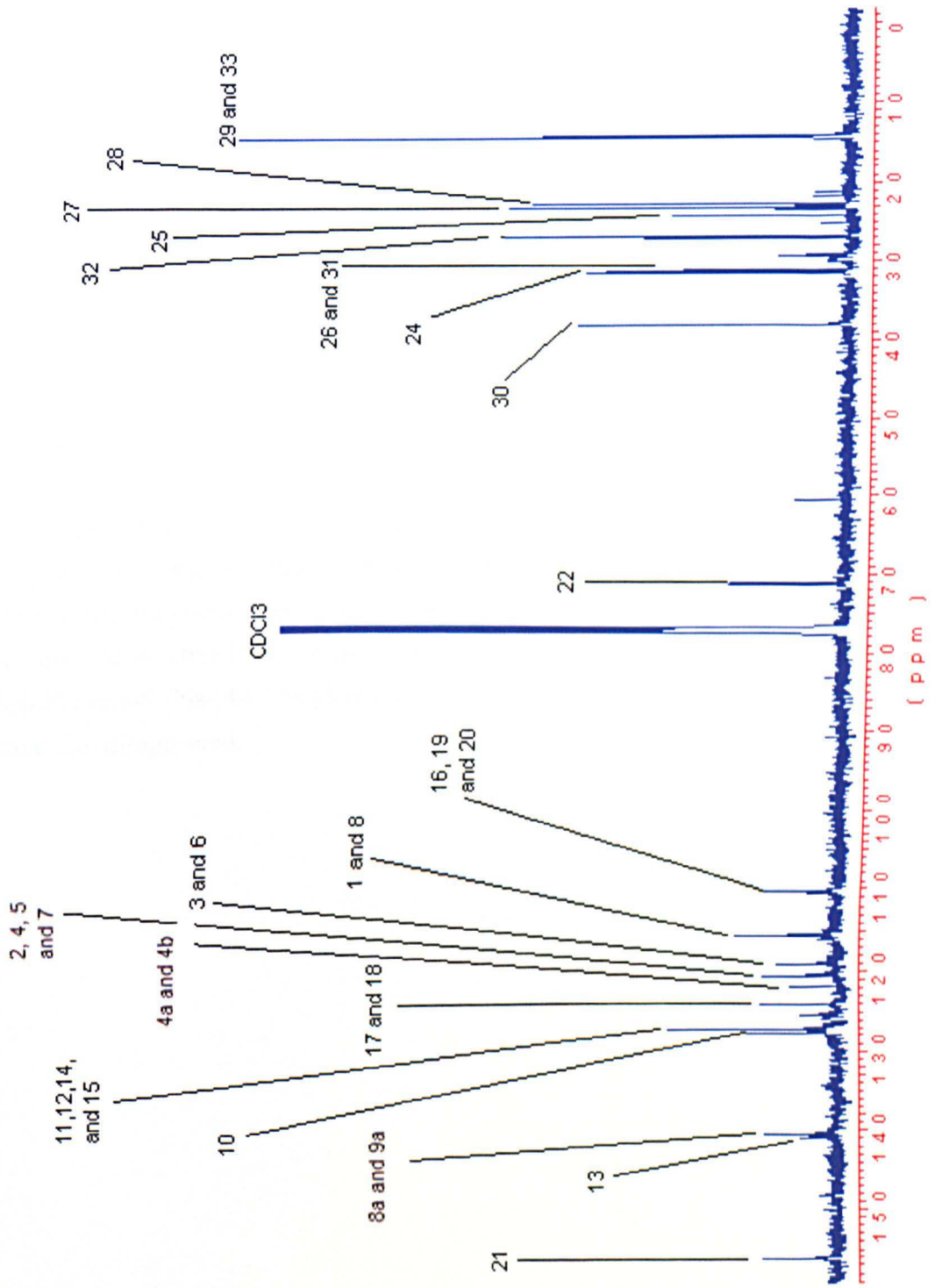

Infarred Spectroscopy analysis

The IR spectra of poly(9-(bis-[4-(2-butyl-octyloxy)-phenyl]-amino-phen-4-yl)-carbazole-3,6-diyl) **(36)** is shown below. The spectrum distinctively highlights the extensive components of the polymer.

It can be seen that characterising peak at 3046 cm^{-1} which falls in relation to aromatic benzene groups –CH stretch. Following this we have peaks at 2919 cm^{-1} and 2853 cm^{-1} which co-ordinate to the alkyl stretching frequencies of the methylene groups. At 1603 cm^{-1}, 1504 cm^{-1} and 1464 cm^{-1} we have a mixture of peaks related to the overtone and combination bands and also the deformations bands of the aromatic – CH groups and methylene $-CH_2-$ groups. We have a related peak at 1280 cm^{-1} and 794 cm^{-1} which falls into the tertiary amine sector $-NR_3$ bond. The peaks at 1235 cm^{-1} and 1106 cm^{-1} work to the C-O-C stretch due to alky / aryl ether. The peaks at 1291 cm^{-1} and 1326 cm^{-1} corresponding to the C – B – C and B – O stretching frequencies respectively of the monomers 3,6-bis-(4,4,5,5-tetramethyl-[1,3,2]dioxaborolan-2-yl)-9-(bis-[4-(2-butyl-octyloxy)-phenyl]-amino-phen-4-yl)-carbazole **(27)** disappeared. Meanwhile the stretching vibration of the C – Br bonds at 742 cm^{-1} from monomers 3,6-dibromo-9-(bis-[4-(2-butyl-octyloxy)-phenyl]-amino-phen-4-yl)-carbazole **(24)** have also disappeared.

Scheme 34, IR for Poly(9-(bis-[4-(2-butyl-octyloxy)-phenyl]-amino-phen-4-yl)-carbazole-3,6-diyl) **(36)**

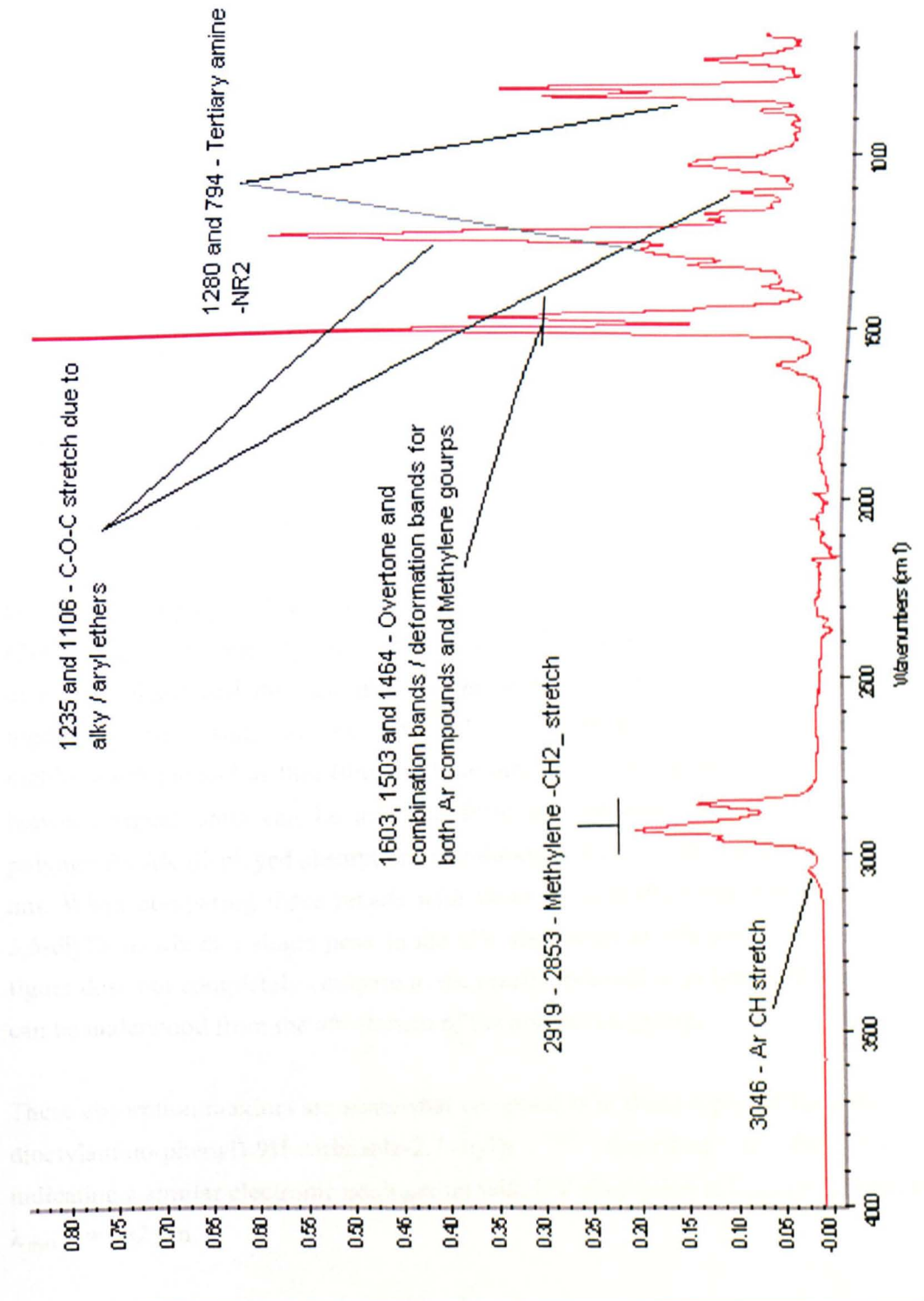

Elemental analysis and GPC analysis

The elemental analysis for polymer poly(9-(bis-[4-(2-butyl-octyloxy)-phenyl]-amino-phen-4-yl)-carbazole-3,6-diyl) **(36)** was calculated to have a CHN Br analysis of: C, 83.24; H, 9.06; N, 3.45; O, 4.11, Br, 0.00.%; for the compound $C_{54}H_{68}N_2O_2$. The following elemental analysis was achieved: C, 82.42; H, 8.91; N, 3.45; Br 0.00.%; This showed that the polymer has indeed the structure proposed.

The polymer poly(9-(bis-[4-(2-butyl-octyloxy)-phenyl]-amino-phen-4-yl)-carbazole-3,6-diyl) **(36)** also displayed the following results for GPC analysis. Mn 19,900 / Mw 31,500 / PDI 1.58 / DP 32. Comparing this with the poly-(9-(2-ethylhexyl)-carbazole-3,6-diyl)s from literature [31] it is seen that that polymerisation has worked extremely well as corresponding polymerisation were seen to have an average Mn 2700 and Mw 4000.

UV-visible absorption spectroscopy analysis

Scheme 35 on page 181 shows the UV-visible absorption spectra for poly(9-(bis-[4-(2-butyl-octyloxy)-phenyl]-amino-phen-4-yl)-carbazole-3,6-diyl) **(36)** in dichloromethane and the thin film for the same polymer. Table 2 shown on 182, highlights the results of the UV-visible absorption spectroscopy analysis in dichloromethane and as thin films of these polymers. The extent of π-orbital overlap between repeat units can be assessed from the electronic spectra obtained. The polymer P3.AK displayed absorptions in solution at $\lambda_{max\,1}$ = 261 nm and $\lambda_{max\,2}$ = 328 nm. When comparing these results with those of poly-(9-(2-ethylhexyl)-carbazole-3,6-diyl)s in which a single peak in the UV absorbtion at 308 nm [31] was seen, this figure dose not completely compare to the results received in polymer P3.AK and this can be understood from the attachment of the aryl amine group.

These absorption maxima are somewhat comparable to those reported for poly-(9-(4-dioctylamino-phenyl)-9H-carbazole-2,7-diyl)s [32] described in the literature indicating a similar electronic conjugation with UV absorption at $\lambda_{max\,1}$ = 273 nm and $\lambda_{max\,2}$ = 382 nm.

From literature it has been seen that the electronic conjugation has been limited to two carbazole repeat units due to the result of the 3,6-linkage along the polymer chain and this effect gives it a different perspective. We can assume the first peak seen at $\lambda_{max\ 1}$ in both poly(9-(bis-[4-(2-butyl-octyloxy)-phenyl]-amino-phen-4-yl)-carbazole-3,6-diyl) P3.AK and poly-(9-(4-dioctylamino-phenyl)-9H-carbazole-2,7-diyl) relates to the tri-aryl group present in the polymers, and it also gives rise to the difference in λ_{max2} between poly(9-(bis-[4-(2-butyl-octyloxy)-phenyl]-amino-phen-4-yl)-carbazole-3,6-diyl) and poly-(9-(4-dioctylamino-phenyl)-9H-carbazole-2,7-diyl) due to the polymer conjugation between the 3,6 and 2,7 polymers. These results are also seen to be followed in the thin films of these polymers.

The polymer showed absorption maxima at $\lambda_{max\ 1}$ 261 nm and $\lambda_{max\ 2}$ at 338 nm in the solid state. $\lambda_{max\ 2}$ is slightly higher in absorption spectra from films to that compaired with solution (338 nm Vs 328 nm) indicating a marginal increase of the electronic conjugation in the solid state.

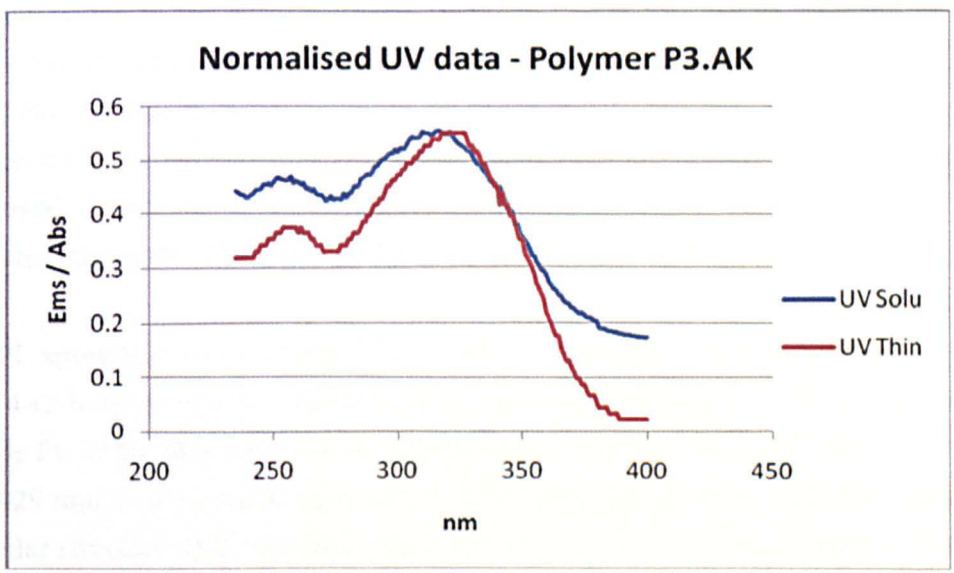

Scheme 35, UV for Poly(9-(bis-[4-(2-butyl-octyloxy)-phenyl]-amino-phen-4-yl)-carbazole-3,6-diyl) **(36)**

Polymer	λ max 1(nm)	λ max 2 (nm)
Solution	261	328
Thin Film	261	338

Table 2, UV for Poly(9-(bis-[4-(2-butyl-octyloxy)-phenyl]-amino-phen-4-yl)-carbazole-3,6-diyl) **(36)**

Photoluminescence spectroscopy (PL) analysis

PL spectroscopy analyse on both polymer solution and polymer film of poly(9-(bis-[4-(2-butyl-octyloxy)-phenyl]-amino-phen-4-yl)-carbazole-3,6-diyl) **(36)** were undertaken. Scheme 36 on page 183 shows the photoluminescence spectra on both polymer solutions and polymer films. The PL spectra of the solutions of poly(9-(bis-[4-(2-butyl-octyloxy)-phenyl]-amino-phen-4-yl)-carbazole-3,6-diyl) **(36)** appeared in the blue region of the electromagnetic spectrum. The λ^{em}_{max} value obtained was 435 nm with a slight shoulder peak falling at 460 nm. An excitation wavelength of 20 nm lower than the $\lambda_{max\ 2}$ of absorption of the polymer was employed. The features of the PL spectra of the polymer solutions were independent from the excitation wavelength employed. The polymer solutions exhibited Stokes shifts of about 100 nm, which indicated structural differences between the ground and excited states of the polymer.

The PL spectra of the thin films were similar to each other. The thin films of poly(9-(bis-[4-(2-butyl-octyloxy)-phenyl]-amino-phen-4-yl)-carbazole-3,6-diyl) **(36)** showed intense PL in the blue region of the spectra with a vibronic structure. The λ^{em}_{max} value was 429 nm, a value that is comparable to the emission spectra in solution indicating a similar structure of the excited state of the polymer both in solution and in the solid state.

Table 3 on page 183 highlights the results of the PL spectroscopy and UV-vis spectroscopy analysis in dichloromethane and as thin films for poly(9-(bis-[4-(2-butyl-octyloxy)-phenyl]-amino-phen-4-yl)-carbazole-3,6-diyl) **(36)**.

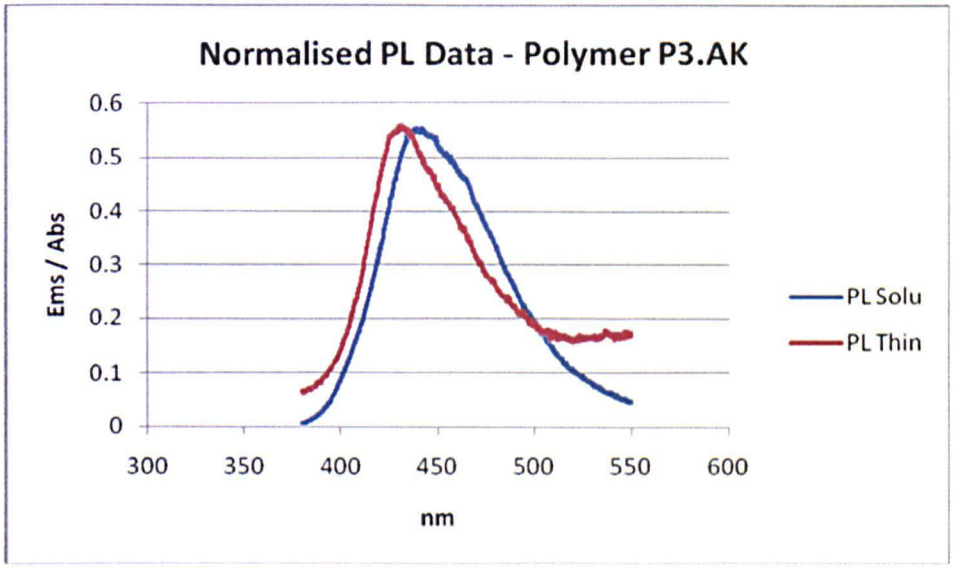

Scheme 36, PL for Poly(9-(bis-[4-(2-butyl-octyloxy)-phenyl]-amino-phen-4-yl)-carbazole-3,6-diyl) **(36)**

Polymer	Absorbance			
	λ max 1(nm)	λ max 2 (nm)	λ^{em}_{max}	Shift (nm)
Solution	261	328	435	107
Thin Film	261	338	429	91

Table 3, PL for Poly(9-(bis-[4-(2-butyl-octyloxy)-phenyl]-amino-phen-4-yl)-carbazole-3,6-diyl) **(36)**

Quantum Yields

Fluorescence quantum yield measurements were carried out for the poly(9-(bis-[4-(2-butyl-octyloxy)-phenyl]-amino-phen-4-yl)-carbazole-3,6-diyl) **(36)**. It was found that these polymers exhibited a yields of $\Phi_{fl} = 0.164 \pm 0.006$ in dichloromethane which were exceptionally high since yield measurements of $\Phi_{fl} = 0.065 \pm 0.006$ in dichloromethane were achieved for poly(9-alkyl-carbazole-3,6-diyl)s as reported in

litreature [31]. These high fluorescence quantum yields were due to the added aryl groups attached to the polymer which have positively affected the properties of the carbazole.

Cyclic Voltammetry (CV) analysis

CV analysis studies of thin films of poly(9-(bis-[4-(2-butyl-octyloxy)-phenyl]-amino-phen-4-yl)-carbazole-3,6-diyl) **(36)** were carried out in order to assess the electrochemical properties of the polymers. Scheme 37 and 38 on page 185 shows the CV curves of thin films of poly(9-(bis-[4-(2-butyl-octyloxy)-phenyl]-amino-phen-4-yl)-carbazole-3,6-diyl) **(36)**. Table 4 on page 186 below shows the results from these CV measurements.

The redox behavior of polymer P3.AK indicates a reversible redox wave with an oxidation wave at the potential E_{pa} 0.48 V and an associated reduction wave at a potential E_{pc} at 0.31 V. The oxidative reversibility of polymer P3.AK is maintained on repeated cycling between 0.0 and 0.85 V (vs Ag/Ag^{+}). However, this reversibility is lost if cycling goes beyond 0.9 V with an irreversible oxidation wave appearing at 0.91 V (vs Ag/Ag^{+}). This behavior indicates that there are two separate oxidation processes: the first one being attributed to the reversible oxidation of the triaryl amine substituent and the second one to that of the carbazole polymer backbone, which is seen by the oxidation wave at the potential E_{pa} 0.70 V and an associated reduction wave at a potential E_{pc} at 0.62 V. This second oxidation wave belongs to the carbazole polymer backbone which is reversible in the case of polymer P3.AK.

It is also worth noting that cyclic voltammetry studies in acetonitrile solutions of 2,7-dibromo-9-(4-dioctylamino-phenyl)-9*H*-carbazole [32] have shown that a reversible redox wave with an oxidation wave at E_{pa} 0.50 V and an associated reduction wave at E_{pc} 0.41 V are attributed to its 4-dioctylamino-phenyl groups.

The ionization potential (vs vacuum) of polymer P3.AK was estimated from the onset of its oxidation in cyclic voltammetry experiments as 5.0 eV. (on the basis that ferrocene/ ferrrocenium is 4.8 eV below the vacuum level) [33]

The ionization potentials of polymers P3.AK are similar to those of poly(9-alkyl-9*H*-carbazole-2,7-diyl)s [30] described in earlier studies. They are lower than those of poly(9,9-dioctyl-fluorene-2,7-diyl). [34] This could suggest an easier hole injection into films from ITO electrodes in electronic device applications.

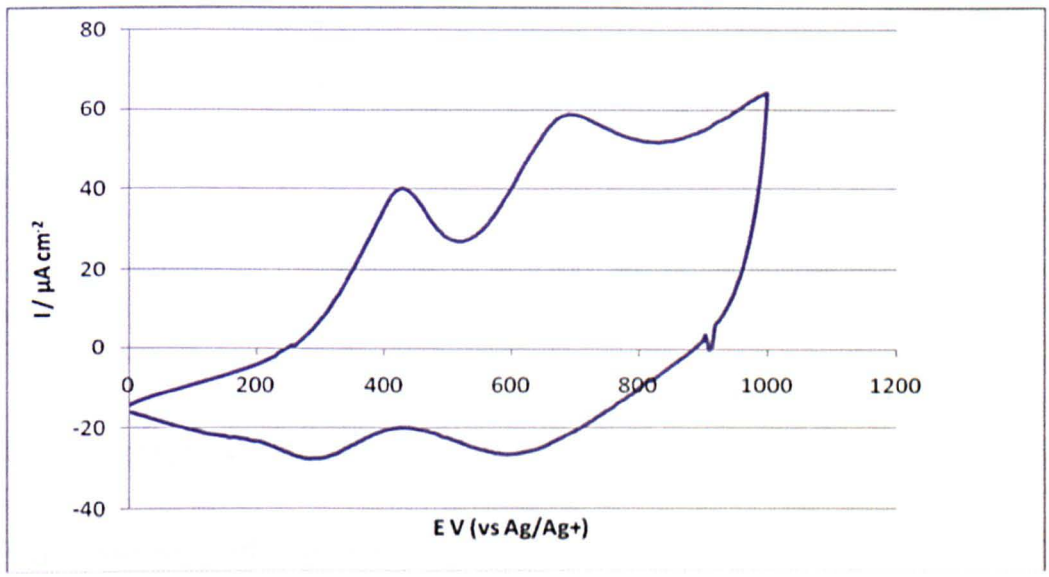

Scheme 37, CV curve for thin films of poly(9-(bis-[4-(2-butyl-octyloxy)-phenyl]-amino-phen-4-yl)-carbazole-3,6-diyl) **(36)** (single scan rate = 90 mV s^{-1})

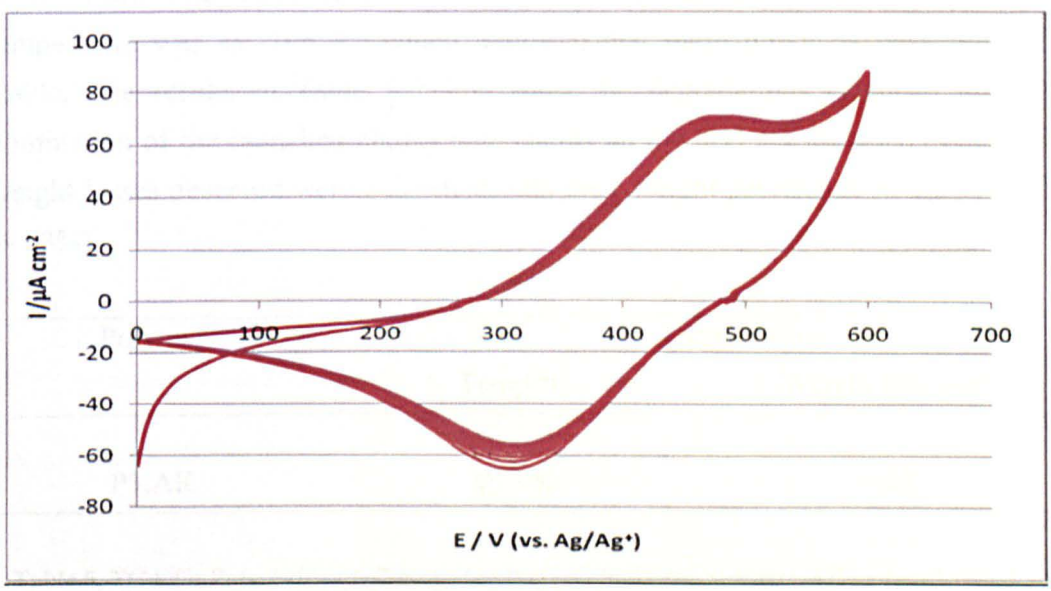

Scheme 38, CV curve for thin films of poly(9-(bis-[4-(2-butyl-octyloxy)-phenyl]-amino-phen-4-yl)-carbazole-3,6-diyl) **(36)** (multiple scan rate = 60 mV s^{-1})

Polymer	E_{pa} [a] / V	E_{pc} [a] / V	$E_{1/2}$ [a] / V	E_{pa} [b] / V	E_{pc} [b] / V	$E_{1/2}$ [b] / V	I_p [c] / V
	0.48	0.31	0.39	0.7	0.62	0.66	5.1

a) vs. Ag/Ag^+ 1st Oxidation wave

b) vs. Ag/Ag^+ 2nd Oxidation wave

c) vs. vacuum level

Table 4, CV curve for thin films of poly(9-(bis-[4-(2-butyl-octyloxy)-phenyl]-amino-phen-4-yl)-carbazole-3,6-diyl) **(36)** (single scan rate = 90 mV s^{-1})

Thermo-gravimetric Analysis (TGA)

TGA studies of poly(9-(bis-[4-(2-butyl-octyloxy)-phenyl]-amino-phen-4-yl)-carbazole-3,6-diyl) **(36)** were undertaken. Scheme 39 on page 187 shows the TGA curves of poly(9-(bis-[4-(2-butyl-octyloxy)-phenyl]-amino-phen-4-yl)-carbazole-3,6-diyl) **(36)**. The TGA of this polymer showed that the onset of degradation temperature was ca. 299 °C, which indicated that these polymers were thermally stable. The results in Table 5 below show the degradations originate from the elimination of the branched alkoxy side chains on the aryl substituents, because the weight losses observed were consistent with their weight percentage in the polymers (~ 53%).

Polymer	Degradation	
	Temp °C	Weight loss (wt%)
P3.AK	@ 500	53

Table 5, TGA for Poly(9-(bis-[4-(2-butyl-octyloxy)-phenyl]-amino-phen-4-yl)-carbazole-3,6-diyl) **(36)**

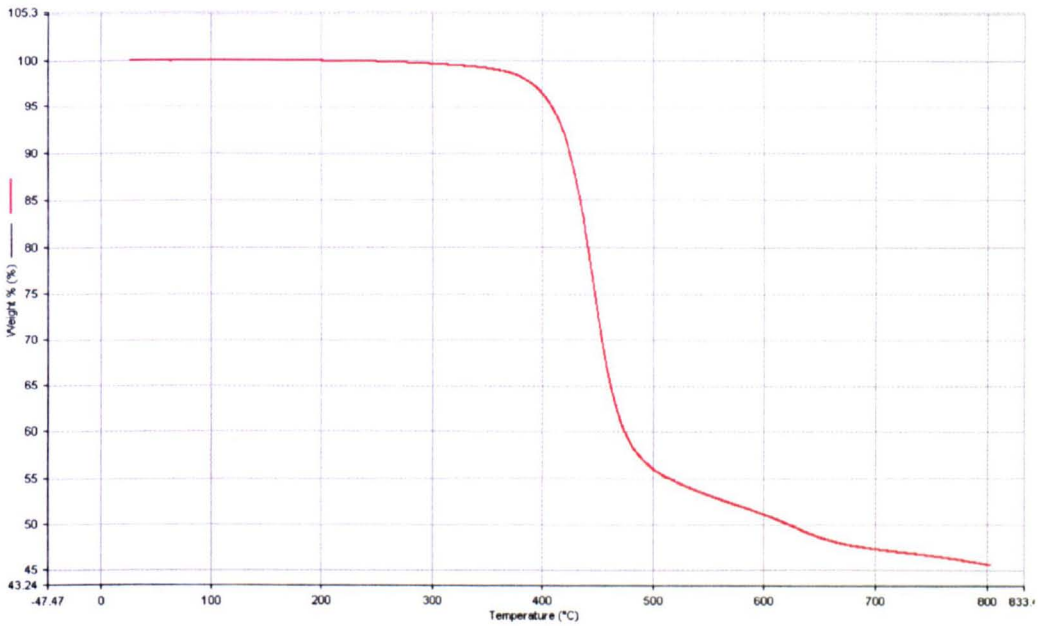

Scheme 39, TGA for Poly(9-(bis-[4-(2-butyl-octyloxy)-phenyl]-amino-phen-4-yl)-carbazole-3,6-diyl) **(36)**

Differential Scanning Calorimetry (DSC) analysis

DSC analysis studies on poly(9-(bis-[4-(2-butyl-octyloxy)-phenyl]-amino-phen-4-yl)-carbazole-3,6-diyl) **(36)** were carried out. The results are outlined in this section. Scheme 40 on page 188 shows the DSC curves of poly(9-(bis-[4-(2-butyl-octyloxy)-phenyl]-amino-phen-4-yl)-carbazole-3,6-diyl) **(36)**. Table 6 below shows the results of the DSC analysis of this polymer.

The DSC curve of poly(9-(bis-[4-(2-butyl-octyloxy)-phenyl]-amino-phen-4-yl)-carbazole-3,6-diyl) **(36)** showed a T_g peak at 136 °C on the first heating scan and a Tm peak at 146°C however, no counter peak was observed on the cooling scan and the Tg peak disappeared on the second heating scan, suggesting the polymer stayed in the crystalline state down to 0 °C on the cooling scan.

Polymer	Tg / °C	Tm / °C
P3.AK	136	146

Table 6, DSC or Poly(9-(bis-[4-(2-butyl-octyloxy)-phenyl]-amino-phen-4-yl)-carbazole-3,6-diyl) **(36)**

Scheme 40, DSC for Poly(9-(bis-[4-(2-butyl-octyloxy)-phenyl]-amino-phen-4-yl)-carbazole-3,6-diyl) **(36)**

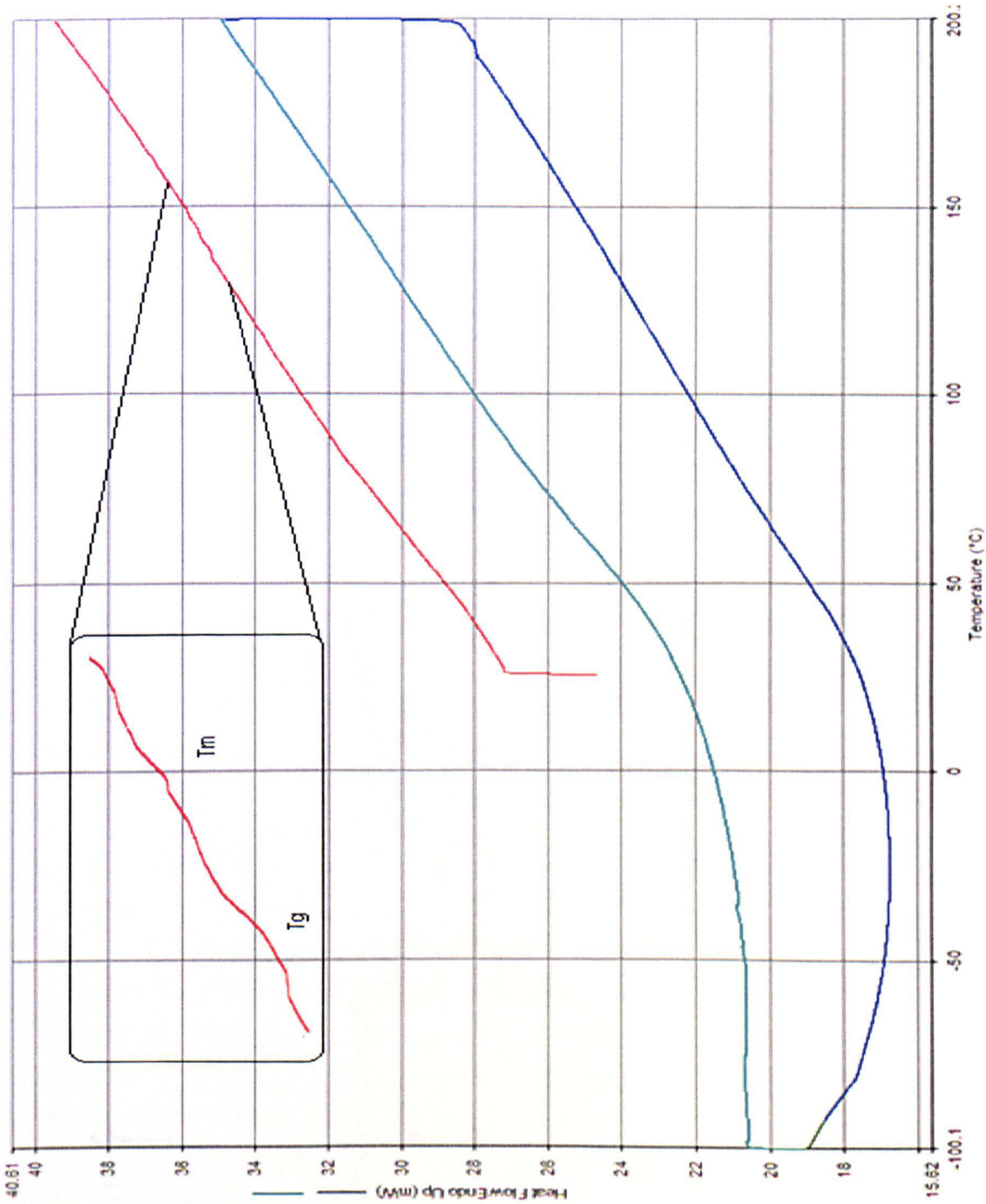

5.7.4 Poly{[9-(bis-[4-(2-butyl-octyloxy)-phenyl]-amino-phen-4-yl)-carbazole-3,6-diyl] -*alt*-[2,5-bis(*p*-phenylene)-1,3,4-oxadiazole]} (38) Suzuki (b) P4.AK

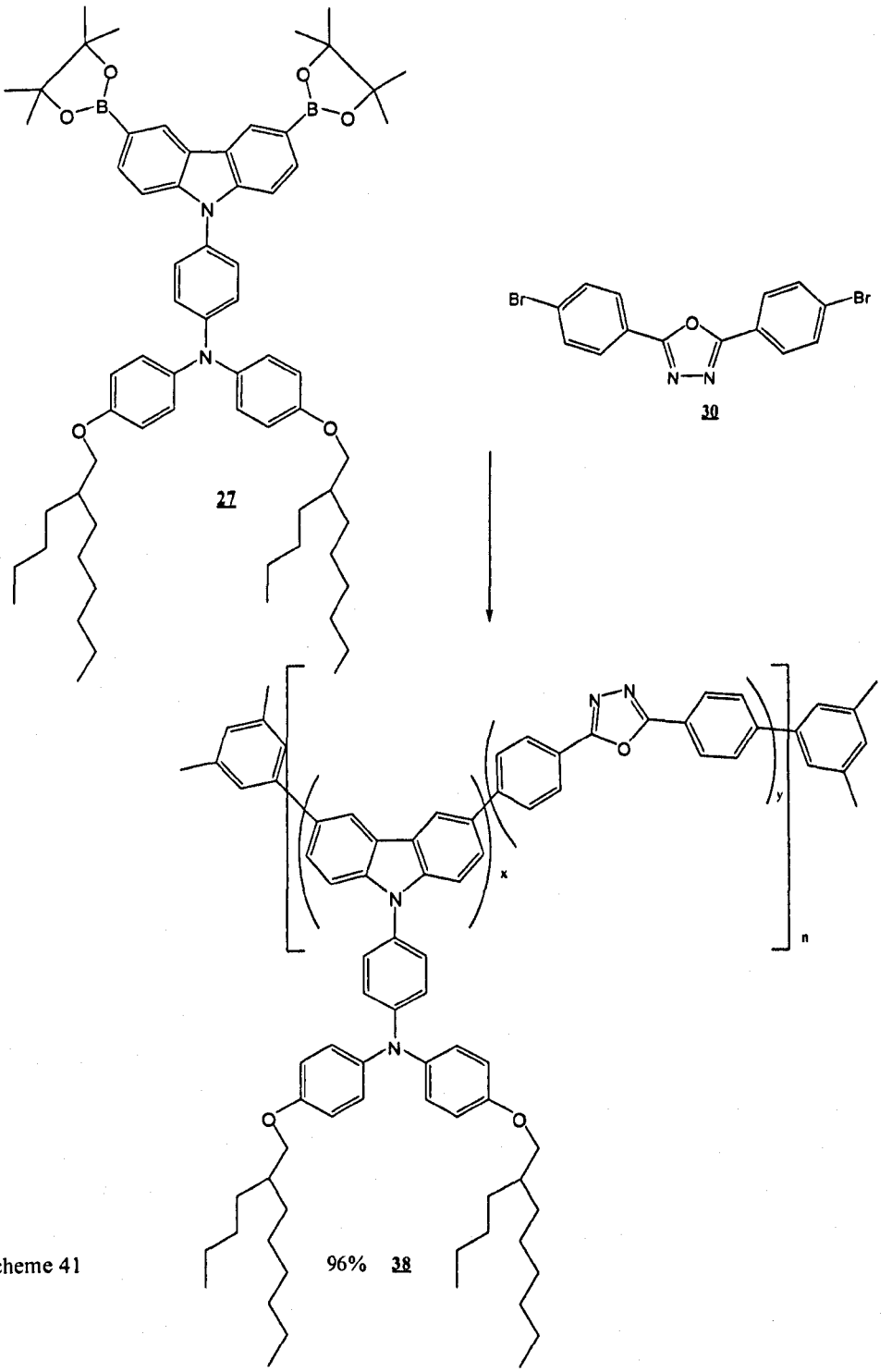

Scheme 41

Poly{[9-(bis-[4-(2-butyl-octyloxy)-phenyl]-amino-phen-4-yl)-carbazole-3,6-diyl] - *alt*-[2,5-bis(*p*-phenylene)-1,3,4-oxadiazole]} **(38)** was obtained in a 96% yield. The product was obtained via a Suzuki type cross-coupling reaction of 3,6-bis-(4,4,5,5-tetramethyl-[1,3,2]dioxaborolan-2-yl)-9-(bis-[4-(2-butyl-octyloxy)-phenyl]-amino-phen-4-yl)-carbazole **(28)** and 2,5-bis-(4-bromo-phenyl)-[1,3,4]-oxadiazole **(31)** via a palladium-catalysed route, as shown in the scheme above.

The reaction was first attempted in a round bottom flask and the catalyst was formed in situ, by reacting $Pd_2(dba)_3$ and tri-*p*-tolyl phosphine in THF. On reacting the catalyst together with the two monomers 3,6-bis-(4,4,5,5-tetramethyl-[1,3,2]dioxaborolan-2-yl)-9-(bis-[4-(2-butyl-octyloxy)-phenyl]-amino-phen-4-yl)-carbazole **(28)** and 2,5-bis-(4-bromo-phenyl)-[1,3,4]-oxadiazole **(31)** followed by the addition of the base (sodium hydrogen carbonate in water, the reaction was allowed to run for 24 hours. The polymer was end-capped and a first precipitation was undertaken. Following this the polymer was dried to yield a ivory powder. This was analysed and found to be the starting monomer end capped; this process had not worked in co-polymerising the two monomers. The reason was found to be that the monomer 2,5-bis-(4-bromo-phenyl)-[1,3,4]-oxadiazole **(31)** had limited solubility in the reaction conditions (THF and water), as the reflux temperature was reached the compound precipitated out of solution and was not able to take part in the polymerisation reaction.

The reaction was undertaken using a sealed tube system in which the catalyst palladium (II) acetate and tri-*p*-tolyl phosphine were reacted in toluene. The two monomers 3,6-bis-(4,4,5,5-tetramethyl-[1,3,2]dioxaborolan-2-yl)-9-(bis-[4-(2-butyl-octyloxy)-phenyl]-amino-phen-4-yl)-carbazole **(28)** and 2,5-bis-(4-bromo-phenyl)-[1,3,4]-oxadiazole **(31)** were dissolved in toluene and added, followed by the addition of tetraethyl ammonium hydroxide (20w/w) (de-oxygenated by bubbling argon through for 3-4 hours) as the base and the system was sealed and heated up to 120°C and allowed to reflux for 72 hours. The polymer was end-capped and a first precipitation was carried out. Following this the polymer was dried, and treated with N,N-diethyl-phenyl-azo-thio-formamide **(29)** in order to remove any palladium

nanoparticles that may have been left behind from the reaction. This lead to the polymer being re-precipitated once again, to yield the desired polymer as a pale forest green powder.

The polymer P4.AK was characterised by the following techniques: ^{1}H NMR and ^{13}C NMR, IR absorption, elemental analysis, GPC, UV-vis spectroscopy, photoluminescence spectroscopy, thermo-gravimetric analysis (TGA), differential scanning calorimetry (DSC), and cyclic voltammetry (CV).

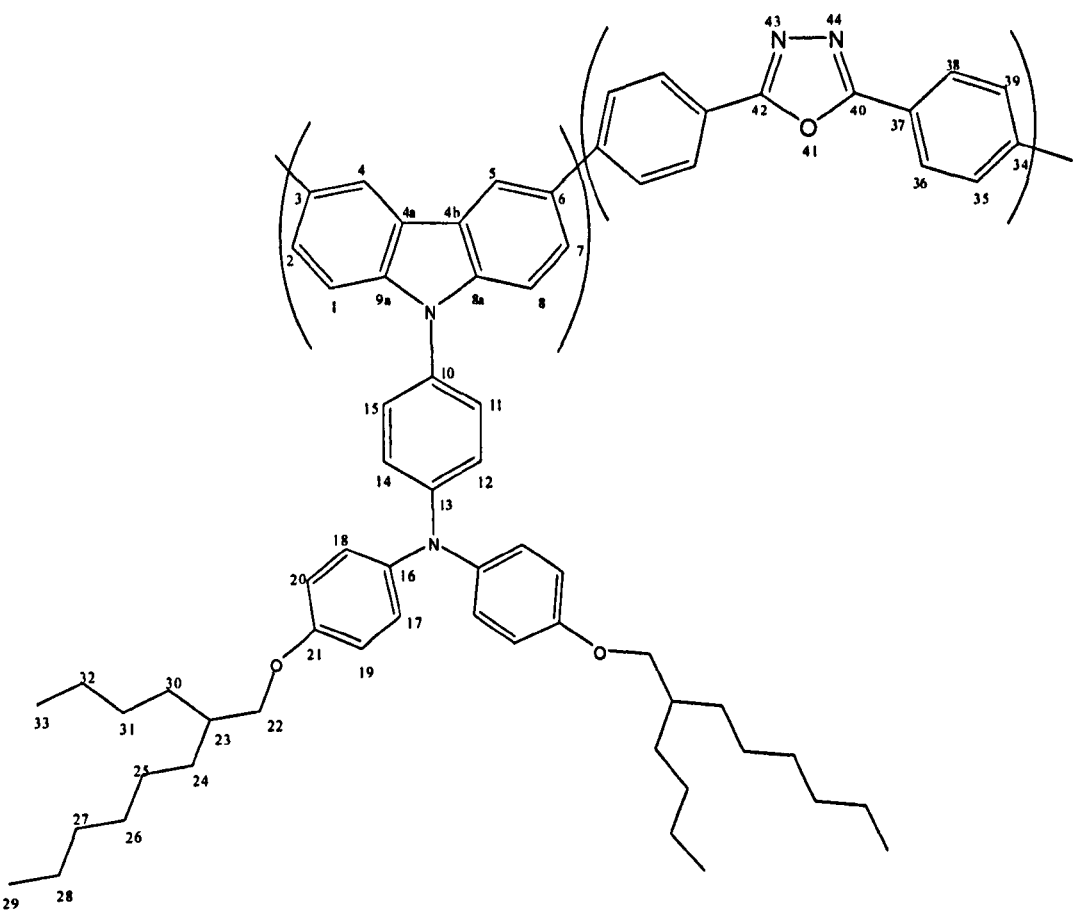

Figure 5.22, Poly{[9-(bis-[4-(2-butyl-octyloxy)-phenyl]-amino-phen-4-yl)-carbazole-3,6-diyl] -*alt*-[2,5-bis(*p*-phenylene)-1,3,4-oxadiazole]} **(38)**

Nuclear Magnetic Resonance Spectroscopy analysis

The ^{1}H-NMR spectrum of the polymer displayed ten broad signals. The first broad peak at signal δ 7.90 ppm is assigned to position 36 and 38, δ 7.72 ppm is assigned to the protons 4 and 5 on the carbazole ring system. δ 7.60 ppm is assigned to the 4 protons at 35 and 39. The next signal is that arising at δ 7.50 ppm can be assigned in relation to protons at positions 12 and 14, δ 7.45 ppm can be in relation to protons at positions 1, and 8, δ 7.35 – 6.90 ppm is a very broad shift relating to protons 2,7,11,15,17 and 18; δ 6.85 relates to the broad protons lying at 19 and 20. And we have a clear broad peak at δ 3.75 ppm relating to protons from position 22, The next peak is also a signature peak, as it is the only single proton which is distinguished at δ 1.75 ppm linked to position 23; the peaks between 1.55-1.15 ppm are those related to positions 24-28 and 30-32 for the –CH2 groups; and finally we have peak at 0.85 ppm coinciding to methyl groups at positions 29 and 33. There are some smaller peaks in the spectra that will be related to the dimethyl phenyl end capping groups.

The ^{13}C-NMR gave nineteen peaks on the spectrum which have been estimated to the following positions of the compound δ 159 (2C) position 40 and 42, δ 156 (2C) position 21, δ 149 (2C) position 37, δ 141 (1C) position 13, δ 140 (2C) positions 8a and 9a, δ 134 (2C) position 34, δ 128 (1C) positions 10, δ 127 (4+4C) positions 11, 12, 14 , 15, 35 and 39, δ 125 (2+4C) positions 17,18 and 36, δ 123 (2+2C) positions 4a and 4b and 38, δ 120 (4C) positions 2, 4, 5 and 7, δ 118 (2C) positions 3 and 6, δ 115 (6C) positions 16,19 and 20, 110 (2C) position 1 and 8, δ 71 (2C) position 22, δ 38 (2C) position 30, δ 31 (2C) positions 24 , δ 29 (4C) position 26 and 31, δ 26 (2C) positions 32, δ 24 (2C) position 25, δ 23 (2C) and 27, δ 21 (2C) positions 28 and finally δ 14 (4C) at positions 29 and 33.

Scheme 42, NMR of Poly{[9-(bis-[4-(2-butyl-octyloxy)-phenyl]-amino-phen-4-yl)-carbazole-3,6-diyl] -*alt*-[2,5-bis(*p*-phenylene)-1,3,4-oxadiazole]} **(38)**

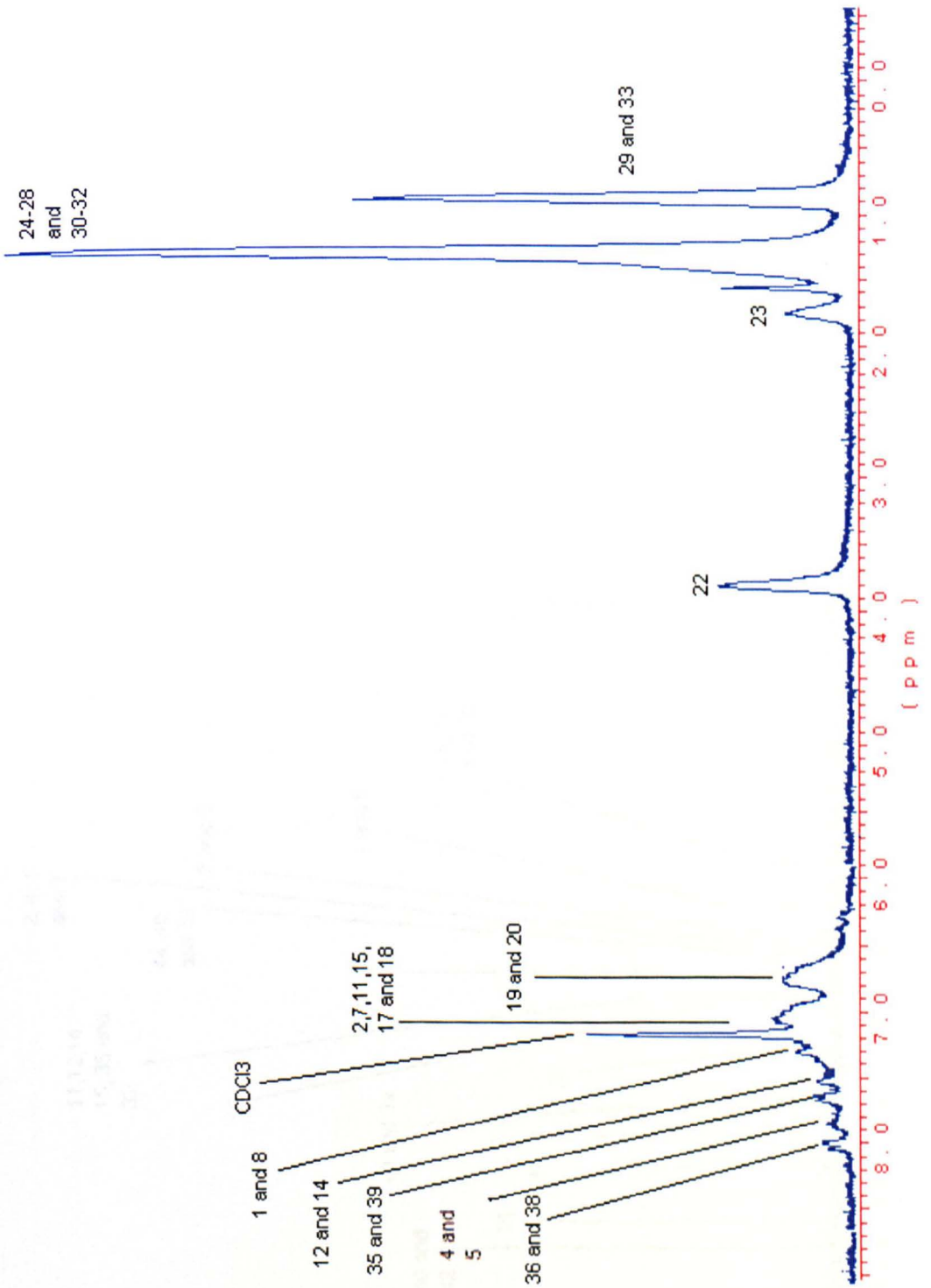

Scheme 43, NMR of Poly{[9-(bis-[4-(2-butyl-octyloxy)-phenyl]-amino-phen-4-yl)-carbazole-3,6-diyl] -*alt*-[2,5-bis(*p*-phenylene)-1,3,4-oxadiazole]} **(38)**

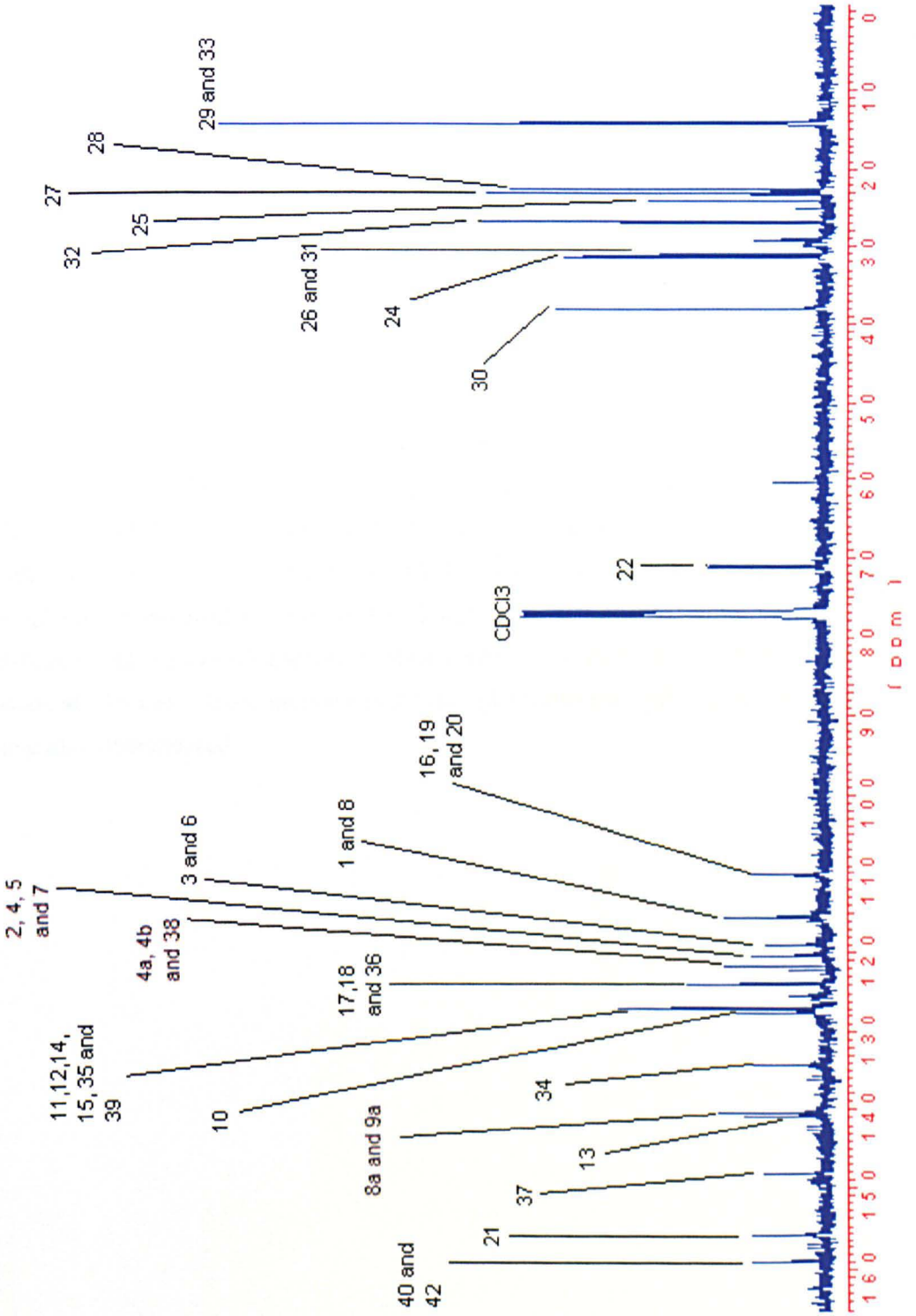

Infarred Spectroscopy analysis

The IR spectra of poly{[9-(bis-[4-(2-butyl-octyloxy)-phenyl]-amino-phen-4-yl)-carbazole-3,6-diyl] -*alt*-[2,5-bis(*p*-phenylene)-1,3,4-oxadiazole]} **(38)** is shown below. The spectrum distinctively highlights the extensive components of the polymer. We can see the characterising peak at 3046 cm^{-1} which falls in relation to aromatic benzene groups –CH stretch. Following this we have peaks at 2931 cm^{-1} and 2853 cm^{-1} which corespond to the alkyl stretching frequencies of the methylene groups. We have a well defined peak at 1640 cm^{-1}, which falls into the regions of imine / oxime –C=N. At 1603 cm^{-1} and 1501 cm^{-1} we have a mixture of peaks related to the overtone and combination bands and also the deformations bands of the aromatic –CH groups and methylene $-CH_2-$ groups. We have a related peak at 1271 cm^{-1} and 728 cm^{-1} which falls into the tertiary amine sector $-NR_3$ bond. The peaks at 1235 cm^{-1} and 1006 cm^{-1} corresponds to the C-O-C stretch due to alkyl / aryl ether. The peaks at 1313 cm^{-1} and 1291 cm^{-1} correspond to the C – B – C and B – O stretching frequencies respectively of the monomers 3,6-bis-(4,4,5,5-tetramethyl-[1,3,2]dioxaborolan-2-yl)-9-(bis-[4-(2-butyl-octyloxy)-phenyl]-amino-phen-4-yl)-carbazole **(27)** have disappeared. Meanwhile the stretching vibration of the C – Br bonds at 776 cm^{-1} from monomers 2,5-bis-(4-bromo-phenyl)-[1,3,4]-oxadiazole **(30)** have also disappeared.

Scheme 44, IR of Poly{[9-(bis-[4-(2-butyl-octyloxy)-phenyl]-amino-phen-4-yl)-carbazole-3,6-diyl] -*alt*-[2,5-bis(*p*-phenylene)-1,3,4-oxadiazole]} **(38)**

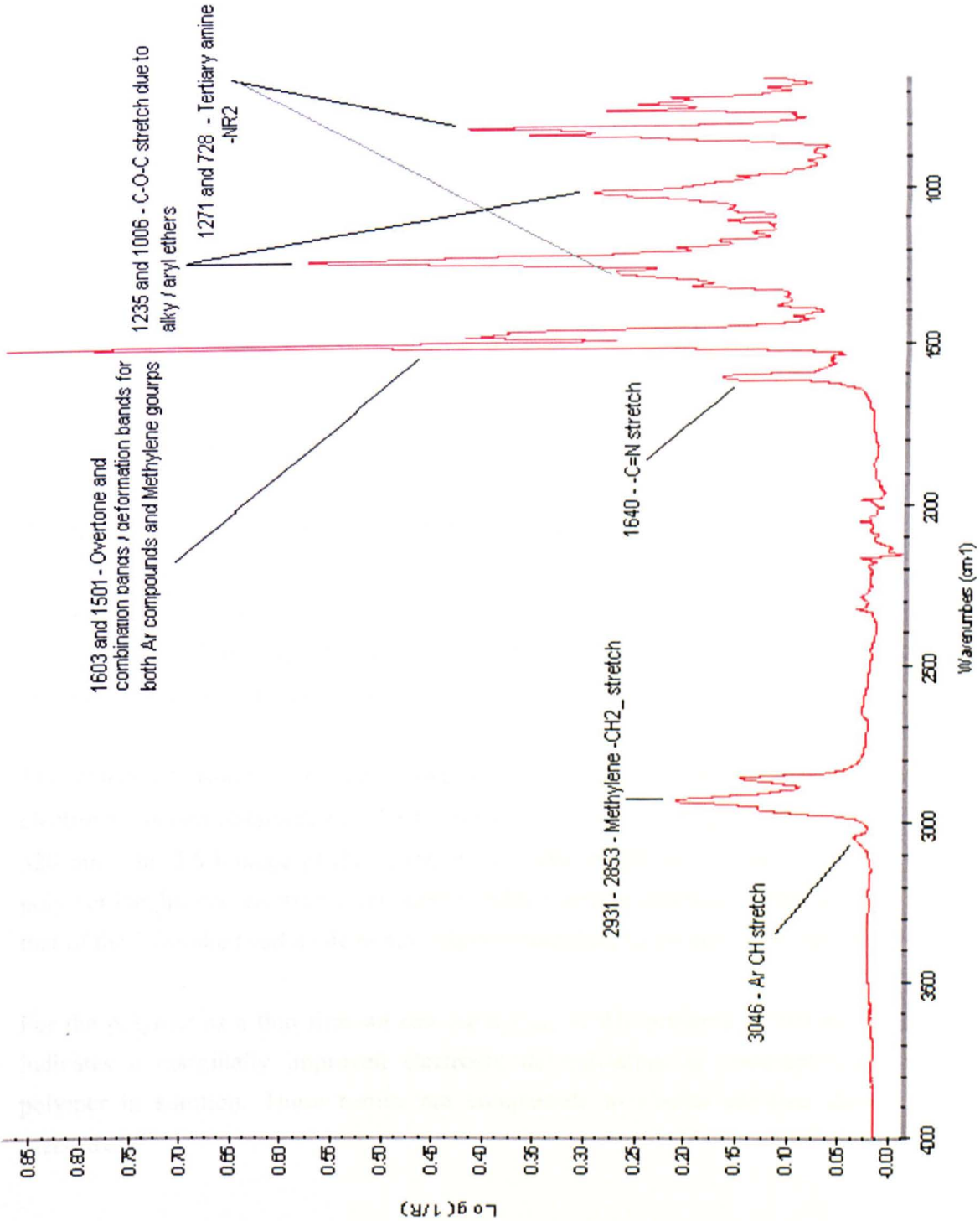

Elemental analysis and GPC analysis

The polymer poly{[9-(bis-[4-(2-butyl-octyloxy)-phenyl]-amino-phen-4-yl)-carbazole-3,6-diyl] -*alt*-[2,5-bis(*p*-phenylene)-1,3,4-oxadiazole]} **(38)** was calculated to have a CHN Br analysis of: C, 81.72; H, 7.87; N, 5.41; O, 4.80, Br, 0.00.%; for the compound $C_{68}H_{78}N_4O_3$. The following elemental analysis was achieved: C, 79.65; H, 7.58; N, 4.72; Br 0.00.%; This showed the polymer as having the structure proposed.

The polymer poly{[9-(bis-[4-(2-butyl-octyloxy)-phenyl]-amino-phen-4-yl)-carbazole-3,6-diyl] -*alt*-[2,5-bis(*p*-phenylene)-1,3,4-oxadiazole]} **(38)** also displayed the following results for GPC analysis. Mn 4,900 / Mw 7,900 / PDI 1.63 / DP 8.

UV-visible absorption spectroscopy analysis

Scheme 45 on page 198 shows the UV-visible absorption spectra of poly{[9-(bis-[4-(2-butyl-octyloxy)-phenyl]-amino-phen-4-yl)-carbazole-3,6-diyl]-*alt*-[2,5-bis(*p*-phenylene)-1,3,4-oxadiazole]} **(38)** in dichloromethane and the thin film for the same polymer. Table 7 on page 198 highlights the results of the UV-visible absorption spectroscopy analysis in dichloromethane and as thin films of the polymer.

The extent of π-orbital overlap between repeat units can be assessed from the electronic spectra obtained. For the polymer in solution the λ_{max} of this polymer is 320 nm. The 3,6-linkage of the carbazole alternate repeat unit ensures that the co-polymer has limited electronic conjugation with a similar electronic delocalisation to that of the 3,6-linked carbazole homo-polymer described in the previous section.

For the polymer as a thin film we can see a λ_{max} of this polymer at 330 nm which indicates a marginally improved electronic delocalisation in comparison of the polymer in solution. These results are comparable to similar reaction shown in literature. [35]

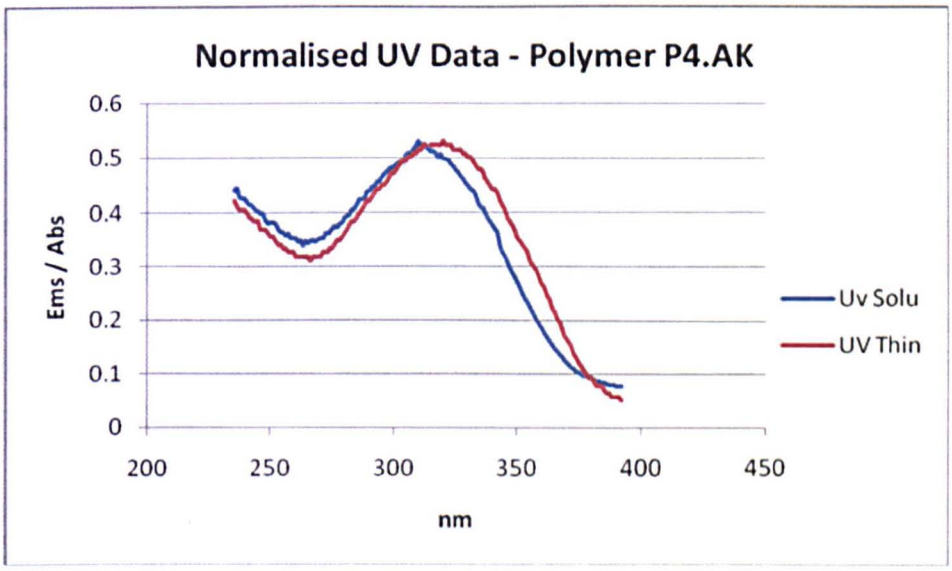

Scheme 45, UV of Poly{[9-(bis-[4-(2-butyl-octyloxy)-phenyl]-amino-phen-4-yl)-carbazole-3,6-diyl] -*alt*-[2,5-bis(*p*-phenylene)-1,3,4-oxadiazole]} **(38)**

Polymer	λ max 1(nm)
Solution	320
Thin Film	330

Table 7, UV of Poly{[9-(bis-[4-(2-butyl-octyloxy)-phenyl]-amino-phen-4-yl)-carbazole-3,6-diyl] -*alt*-[2,5-bis(*p*-phenylene)-1,3,4-oxadiazole]} **(38)**

Photoluminescence spectroscopy analysis

PL spectroscopy analyses on polymer solutions and polymer films of poly{[9-(bis-[4-(2-butyl-octyloxy)-phenyl]-amino-phen-4-yl)-carbazole-3,6-diyl]-*alt*-[2,5-bis(*p*-phenylene)-1,3,4-oxadiazole]} **(38)** were undertaken. Scheme 46 on page 199 shows PL spectroscopy analysis on both polymer solutions and polymer films The PL spectra of the solutions of poly{[9-(bis-[4-(2-butyl-octyloxy)-phenyl]-amino-phen-4-yl)-carbazole-3,6-diyl]-*alt*-[2,5-bis(*p*-phenylene)-1,3,4-oxadiazole]} **(38)** appeared in the blue region of the spectra with sharp emission bands. The λ^{em}_{max} value obtained

was 420 nm. An excitation wavelength of 20 nm lower than the λ_{max} of absorption of the polymer was employed. The feature of the PL spectra of the polymer solution was independent from the excitation wavelength employed. The polymer solutions exhibited Stokes shifts of approximate 100 nm, which indicated structural differences between the ground and excited states of the polymer. The PL spectra of the thin films were similar to those of the polymer in solution. The thin films of poly{[9-(bis-[4-(2-butyl-octyloxy)-phenyl]-amino-phen-4-yl)-carbazole-3,6-diyl]-*alt*-[2,5-bis(*p*-phenylene)-1,3,4-oxadiazole]} **(38)** showed intense PL in the blue region of the spectra with a vibronic structure. The λ^{em}_{max} value was 425 nm.

Table 8 on page 200 highlights the results of the PL spectroscopy and UV-vis spectroscopy analysis in dichloromethane and as thin films for poly{[9-(bis-[4-(2-butyl-octyloxy)-phenyl]-amino-phen-4-yl)-carbazole-3,6-diyl]-*alt*-[2,5-bis(*p*-phenylene)-1,3,4-oxadiazole]} **(38)**.

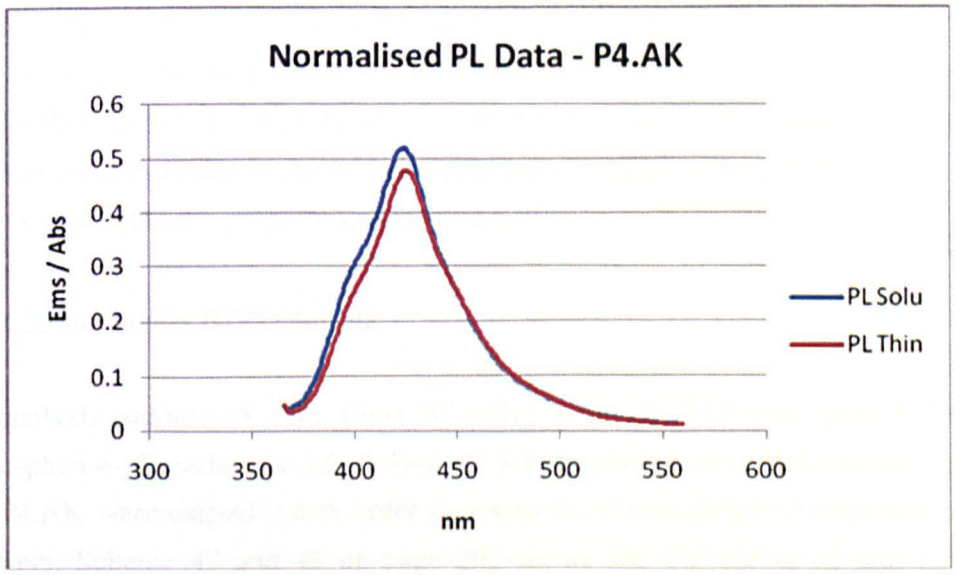

Scheme 46, PL of Poly{[9-(bis-[4-(2-butyl-octyloxy)-phenyl]-amino-phen-4-yl)-carbazole-3,6-diyl] -*alt*-[2,5-bis(*p*-phenylene)-1,3,4-oxadiazole]} **(38)**

Polymer	Absorbance λ max 1(nm)	PL emission λ^{em}_{max}	Stokes Shift (nm)
Solution	320	420	100
Thin Film	330	425	95

Table 8, PL of Poly{[9-(bis-[4-(2-butyl-octyloxy)-phenyl]-amino-phen-4-yl)-carbazole-3,6-diyl] -*alt*-[2,5-bis(*p*-phenylene)-1,3,4-oxadiazole]} **(38)**

Quantum Yields

Fluorescence quantum yield measurements were carried out for the poly{[9-(bis-[4-(2-butyl-octyloxy)-phenyl]-amino-phen-4-yl)-carbazole-3,6-diyl]-*alt*-[2,5-bis(*p*-phenylene)-1,3,4-oxadiazole]} **(38)** It was found that these polymers exhibited a yields of $\Phi_{fl} = 0.264 \pm 0.006$ in dichloromethane which were exceptionally high since yield measurements of $\Phi_{fl} = 0.065 \pm 0.006$ in dichloromethane were achieved for poly(9-alkyl-carbazole-3,6-diyl)s as reported in literature. [31] These high fluorescence quantum yield were due to the added aryl groups attached to the polymer which have positively effected the properties of the carbazole.

Cyclic Voltammetry (CV) analysis

CV analysis studies of thin films of poly{[9-(bis-[4-(2-butyl-octyloxy)-phenyl]-amino-phen-4-yl)-carbazole-3,6-diyl]-*alt*-[2,5-bis(*p*-phenylene)-1,3,4-oxadiazole]} **(38)** P4.AK were carried out in order to assess the electrochemical properties of the polymers. Scheme 47 and 48 on page 202 shows the CV curves of thin films of poly{[9-(bis-[4-(2-butyl-octyloxy)-phenyl]-amino-phen-4-yl)-carbazole-3,6-diyl]-*alt*-[2,5-bis(*p*-phenylene)-1,3,4-oxadiazole]} **(38)** P4.AK. Table 9 on page 203 below shows the results from these CV measurements.

The redox behavior of polymer P4.AK indicates a reversible redox wave with an oxidation wave at the potential E_{pa} 0.48 V and an associated reduction wave at a potential E_{pc} at 0.30 V. The oxidative reversibility of polymer P4.AK is maintained on repeated cycling between 0.0 and 0.85 V (vs Ag/Ag^{+}). However, this reversibility is lost if cycling goes beyond 0.9 V with an irreversible oxidation wave appearing at 0.91 V (vs Ag/Ag^{+}). This behavior indicates that there are two separate oxidation processes: the first one being attributed to the reversible oxidation of the tri aryl amine substituent and the second one to that of the carbazole polymer backbone, which is seen be the oxidation wave at the potential E_{pa} 0.88 V and an associated reduction wave at a potential E_{pc} at 0.75 V. This second oxidation wave belongs to the carbazole polymer backbone which is reversible in the case of polymer P4.AK.

It is also worth noting that cyclic voltammetry studies in acetonitrile solutions of 2,7-dibromo-9-(4-dioctylamino-phenyl)-9*H*-carbzole [32] have shown that a reversible redox wave with an oxidation wave at E_{pa} 0.50 V and an associated reduction wave at E_{pc} 0.41 V are attributed to its 4-dioctylamino-phenyl groups.

The ionisation potential (vs vacuum) of polymer P4.AK was estimated from the onset of its oxidation in cyclic voltammetry experiments as 5.0 eV (on the basis that ferrocene/ ferrrocenium is 4.8 eV below the vacuum level) [33].

The ionisation potentials of polymers P4.AK are similar to those of poly(9-alkyl-9*H*-carbazole-2,7-diyl)s [30] described in earlier studies. They are lower than those of poly(9,9-dioctyl-fluorene-2,7-diyl) [34]. This could suggest an easier hole injection into films from ITO electrodes in electronic device applications.

The 1.3,4-oxadiazole unit is an electron receptor. [37] Therefore the doping peaks of copolymers which contain alternating aromatic and 1,3,4-oxadiazole units are shifted to the positive side compared with the aromatic homopolymers. [38]

A study of the electrochemical properties of the polymer indicates that the polymer possesses promising electron-transporting / hole blocking properties and relatively high fluorescence owing to the introduction of oxadiazole. [36]

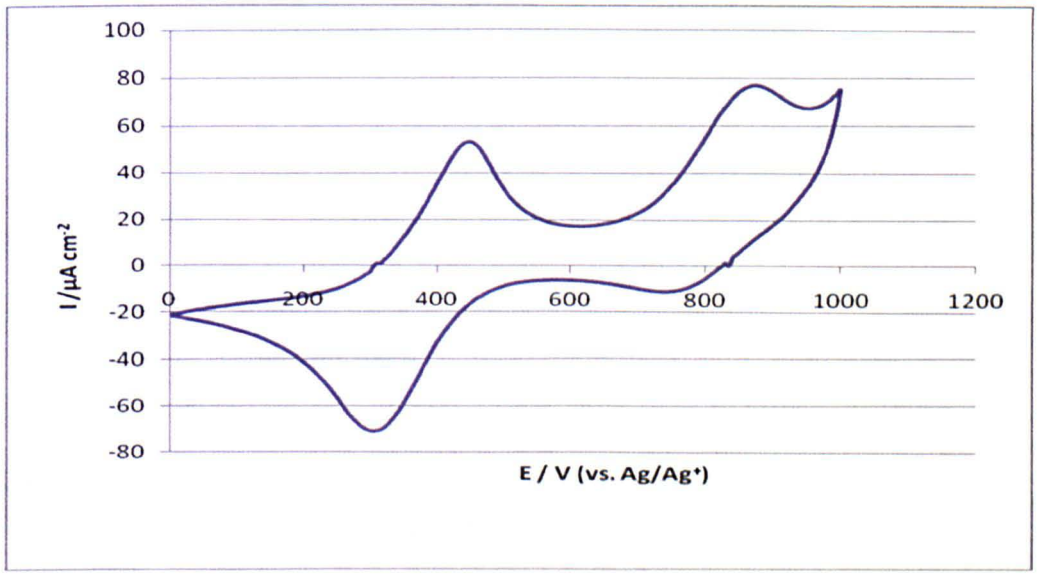

Scheme 47, CV curve for thin films of poly{[9-(bis-[4-(2-butyl-octyloxy)-phenyl]-amino-phen-4-yl)-carbazole-3,6-diyl]-*alt*-[2,5-bis(*p*-phenylene)-1,3,4-oxadiazole]} **(38)** (single scan rate = 90 mV s^{-1})

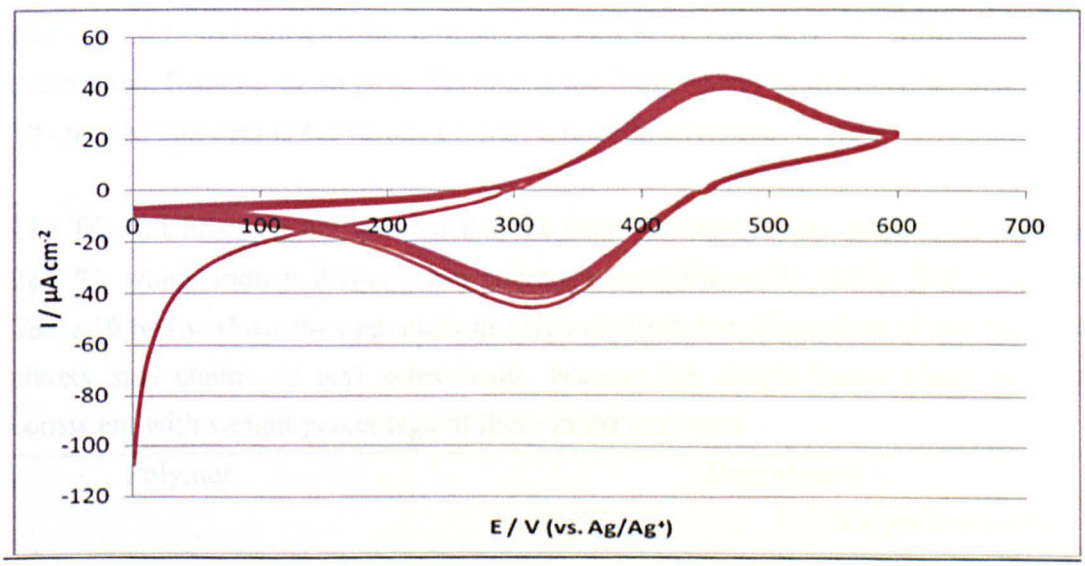

Scheme 48, CV curve for thin films of poly{[9-(bis-[4-(2-butyl-octyloxy)-phenyl]-amino-phen-4-yl)-carbazole-3,6-diyl]-*alt*-[2,5-bis(*p*-phenylene)-1,3,4-oxadiazole]} **(38)** (multiple scan rate = 60 mV s^{-1})

Polymer	E_{pa} [a] / V	E_{pc} [a] / V	$E_{1/2}$ [a] / V	E_{pa} [b] / V	E_{pc} [b] / V	$E_{1/2}$ [b] / V	I_p [c] / V
	0.48	0.3	0.39	0.88	0.75	0.81	5.1

a) vs. Ag/Ag^+ 1st Oxidation wave

b) vs. Ag/Ag^+ 2nd Oxidation wave

c) vs. vacuum level

Table 9, CV curve for thin films of poly{[9-(bis-[4-(2-butyl-octyloxy)-phenyl]-amino-phen-4-yl)-carbazole-3,6-diyl]-*alt*-[2,5-bis(*p*-phenylene)-1,3,4-oxadiazole]} **(38)** (single scan rate = 90 mV s^{-1})

Thermo-gravimetric Analysis (TGA)

TGA studies of poly{[9-(bis-[4-(2-butyl-octyloxy)-phenyl]-amino-phen-4-yl)-carbazole-3,6-diyl]-*alt*-[2,5-bis(*p*-phenylene)-1,3,4-oxadiazole]} **(38)** were undertaken. Scheme 49 on page 204 shows the TGA curves of the polymer and Table 10 on page 203 details the results of the TGA of this polymer.

The TGA of this polymer showed that the onset of degradation temperature was ca. 283 °C, which indicated that these polymers were thermally stable. The results in Table 10 below show the degradations originate from the elimination of the branched alkoxy side chains on aryl substituents, because the weight losses observed were consistent with weight percentage of these in the polymers.

Polymer	Degradation	
	Temp °C	Weight loss (wt%)
P4.AK	@500	58

Table 10, TGA of Poly{[9-(bis-[4-(2-butyl-octyloxy)-phenyl]-amino-phen-4-yl)-carbazole-3,6-diyl] - *alt*-[2,5-bis(*p*-phenylene)-1,3,4-oxadiazole]} **(38)**

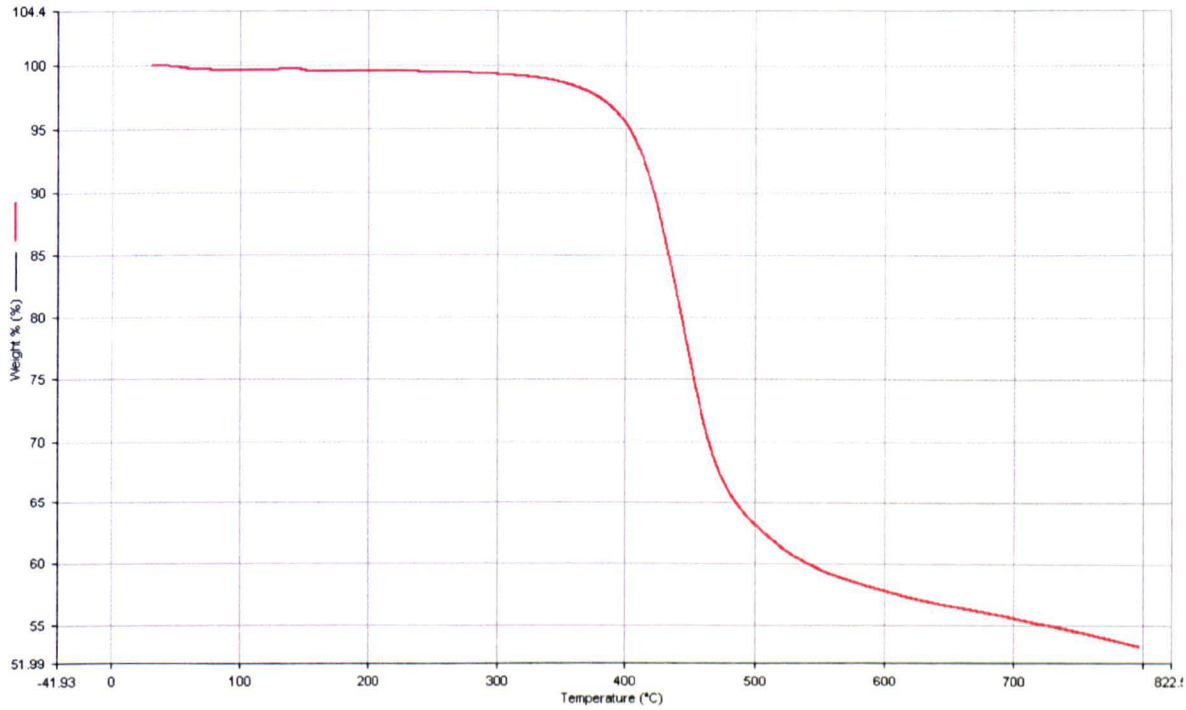

Scheme 49, TGA of Poly{[9-(bis-[4-(2-butyl-octyloxy)-phenyl]-amino-phen-4-yl)-carbazole-3,6-diyl] -*alt*-[2,5-bis(*p*-phenylene)-1,3,4-oxadiazole]} **(38)**

Differential Scanning Calorimetry (DSC) analysis

DSC analysis studies on poly{[9-(bis-[4-(2-butyl-octyloxy)-phenyl]-amino-phen-4-yl)-carbazole-3,6-diyl]-*alt*-[2,5-bis(*p*-phenylene)-1,3,4-oxadiazole]} **(38)** were carried out. The results are outlined in this section. Scheme 50 on page 206 shows the DSC curves for poly{[9-(bis-[4-(2-butyl-octyloxy)-phenyl]-amino-phen-4-yl)-carbazole-3,6-diyl]-*alt*-[2,5-bis(*p*-phenylene)-1,3,4-oxadiazole]} **(38)**. Table 11 below shows the results of the DSC analysis of this polymer.

The DSC curve of poly{[9-(bis-[4-(2-butyl-octyloxy)-phenyl]-amino-phen-4-yl)-carbazole-3,6-diyl]-*alt*-[2,5-bis(*p*-phenylene)-1,3,4-oxadiazole]} **(38)** showed a T_g peak at 80°C on the first heating scan and a Tm peak at 175°C however, a unidentifiable counter peak was observed on the cooling scan at 150°C and on the

unidentifiable counter peak was observed on the cooling scan at 150°C and on the second heating scan the Tg peak disappeared, suggesting the polymer stayed in the crystalline state down to 0 °C on the cooling scan.

Polymer	Tg / °C	Tm / °C
P4.AK	80	175

Table 11, DSC of Poly{[9-(bis-[4-(2-butyl-octyloxy)-phenyl]-amino-phen-4-yl)-carbazole-3,6-diyl] - *alt*-[2,5-bis(*p*-phenylene)-1,3,4-oxadiazole]} **(38)**

Scheme 50, DSC of Poly{[9-(bis-[4-(2-butyl-octyloxy)-phenyl]-amino-phen-4-yl)-carbazole-3,6-diyl] -*alt*-[2,5-bis(*p*-phenylene)-1,3,4-oxadiazole]} **(38)**

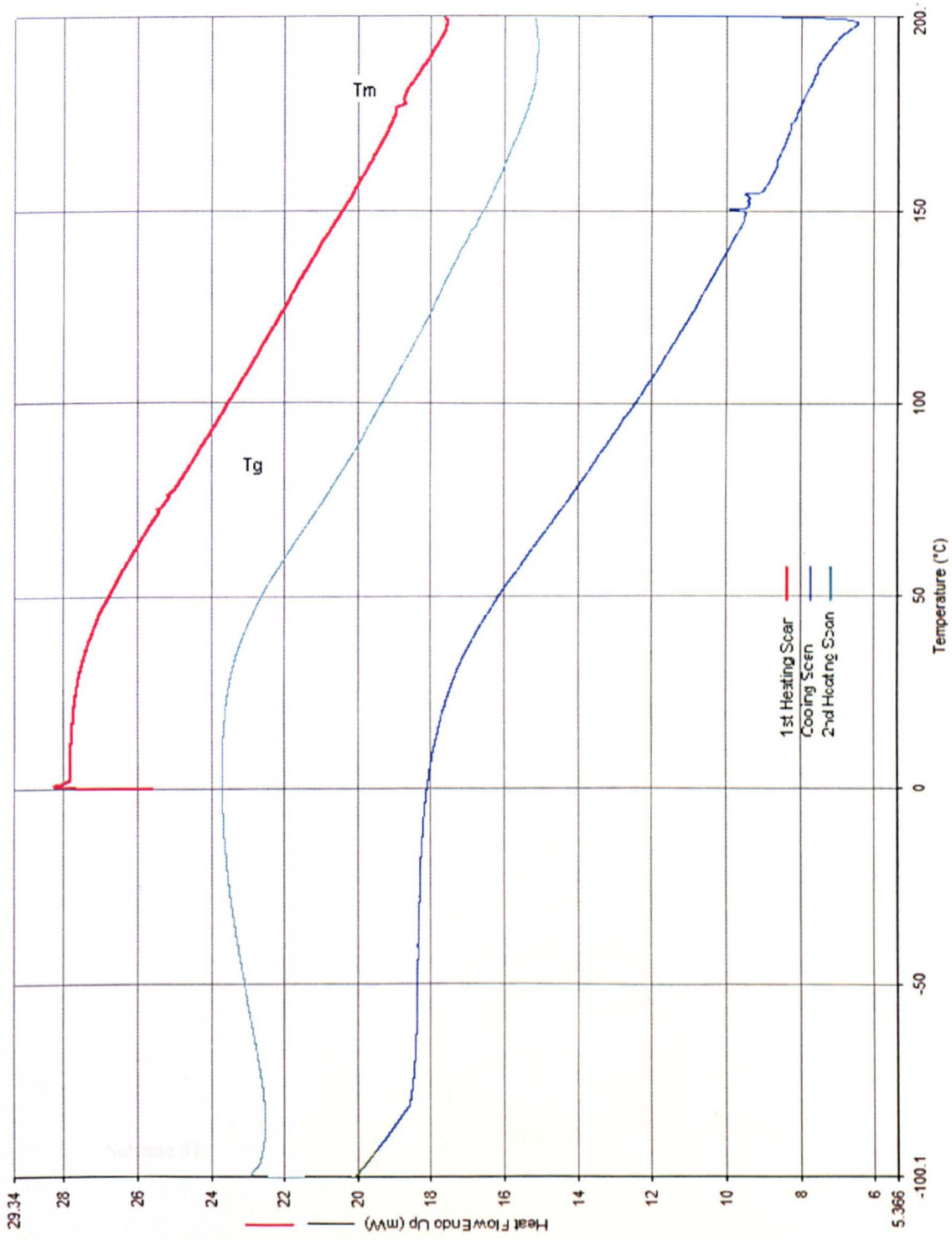

5.7.5 **Poly{[9-(bis-[4-(2-butyl-octyloxy)-phenyl]-amino-phen-4-yl)-carbazole-3,6-diyl] -*alt*-[benzo-2,1,3-thiadiazol-4,7-diyl]} (39) Suzuki (a)** P6.AK

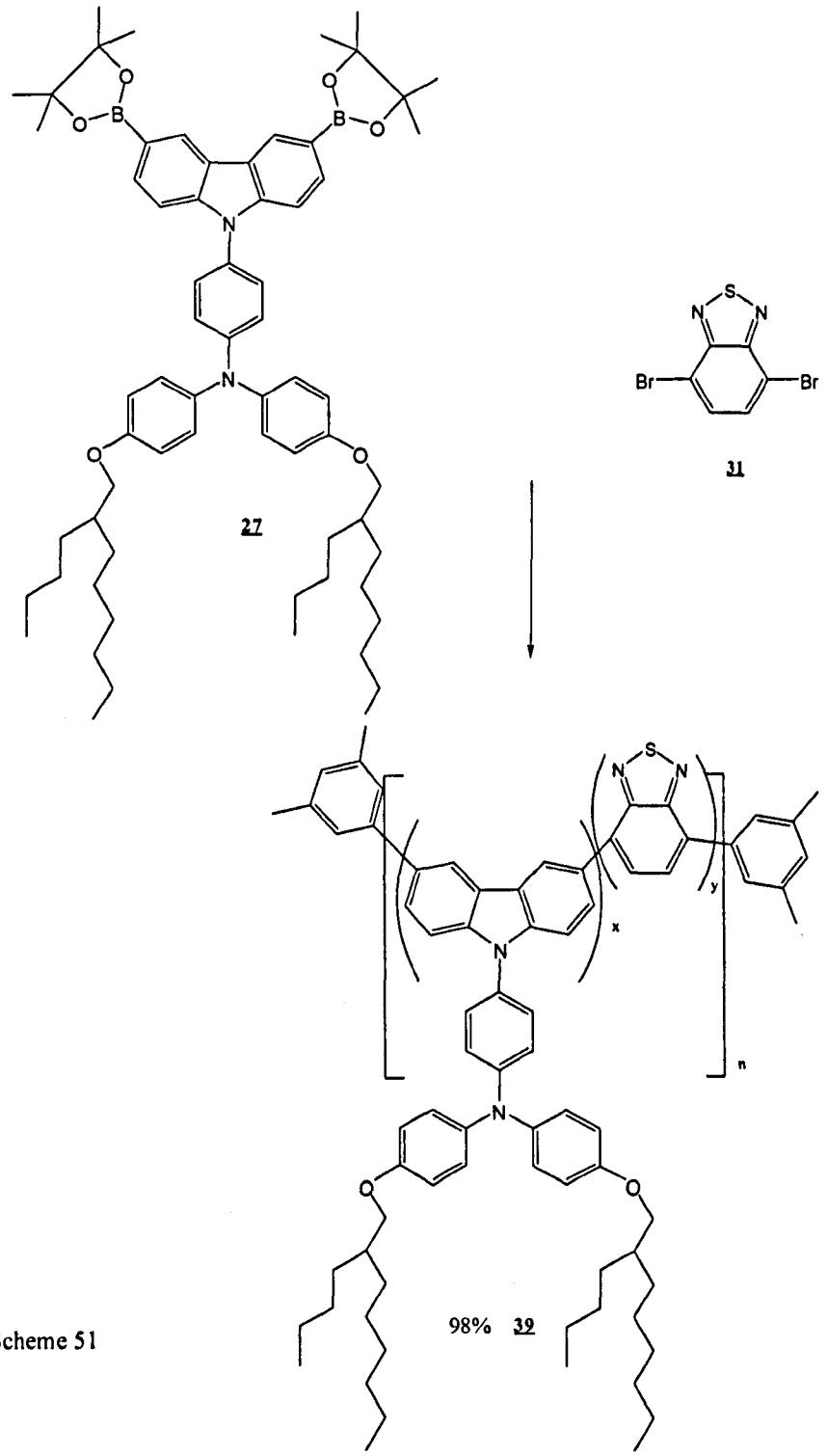

Scheme 51

Poly{[9-(bis-[4-(2-butyl-octyloxy)-phenyl]-amino-phen-4-yl)-carbazole-3,6-diyl] -*alt*-[benzo-2,1,3-thiadiazol-4,7-diyl]} **(39)** was obtained in a 98% yield. The product was produce via a Suzuki type cross-coupling reaction of 3,6-bis-(4,4,5,5-tetramethyl-[1,3,2]dioxaborolan-2-yl)-9-(bis-[4-(2-butyl-octyloxy)-phenyl]-amino-phen-4-yl)-carbazole **(27)** and 4,7-dibromobenzo[c][1,2,5]thiadiazole **(31)** via a palladium-catalysed route, as shown in scheme 51 on page 207.

The reaction was achieved using a sealed tube system in which the catalyst palladium (II) acetate and tri-p-tolyl phosphine were reacted in toluene. The two monomers 3,6-bis-(4,4,5,5-tetramethyl-[1,3,2]dioxaborolan-2-yl)-9-(bis-[4-(2-butyl-octyloxy)-phenyl]-amino-phen-4-yl)-carbazole **(27)** and 4,7-dibromobenzo[c][1,2,5]thiadiazole **(31)** which were dissolved in toluene were added, followed by the addition of tertra ethyl ammonium hydroxide (20w/w) (de-oxygenated by bubbling argon through for 3-4 hours) as the base and the system was sealed and heated up to 120°C for 72 hours. The polymer was end-capped and a first precipitation was undertaken. Following this the polymer was dried, and treated with N,N-diethyl-phenyl-azo-thio-formamide **(28)** in order to remove any palladium nanoparticals that may have been left behind from the reaction. This lead to the polymer being re-precipitated once again, to yield the desired polymer as a orange powder.

The polymer poly{[9-(bis-[4-(2-butyl-octyloxy)-phenyl]-amino-phen-4-yl)-carbazole-3,6-diyl] -*alt*-[benzo-2,1,3-thiadiazol-4,7-diyl]} **(39)** P6.AK was characterised by the following techniques: ^{1}H NMR and ^{13}C NMR, IR absorption, elemental analysis, GPC, UV-vis spectroscopy, photoluminescence spectroscopy, thermo-gravimetric analysis (TGA), differential scanning calorimetry (DSC), and cyclic voltammetry (CV).

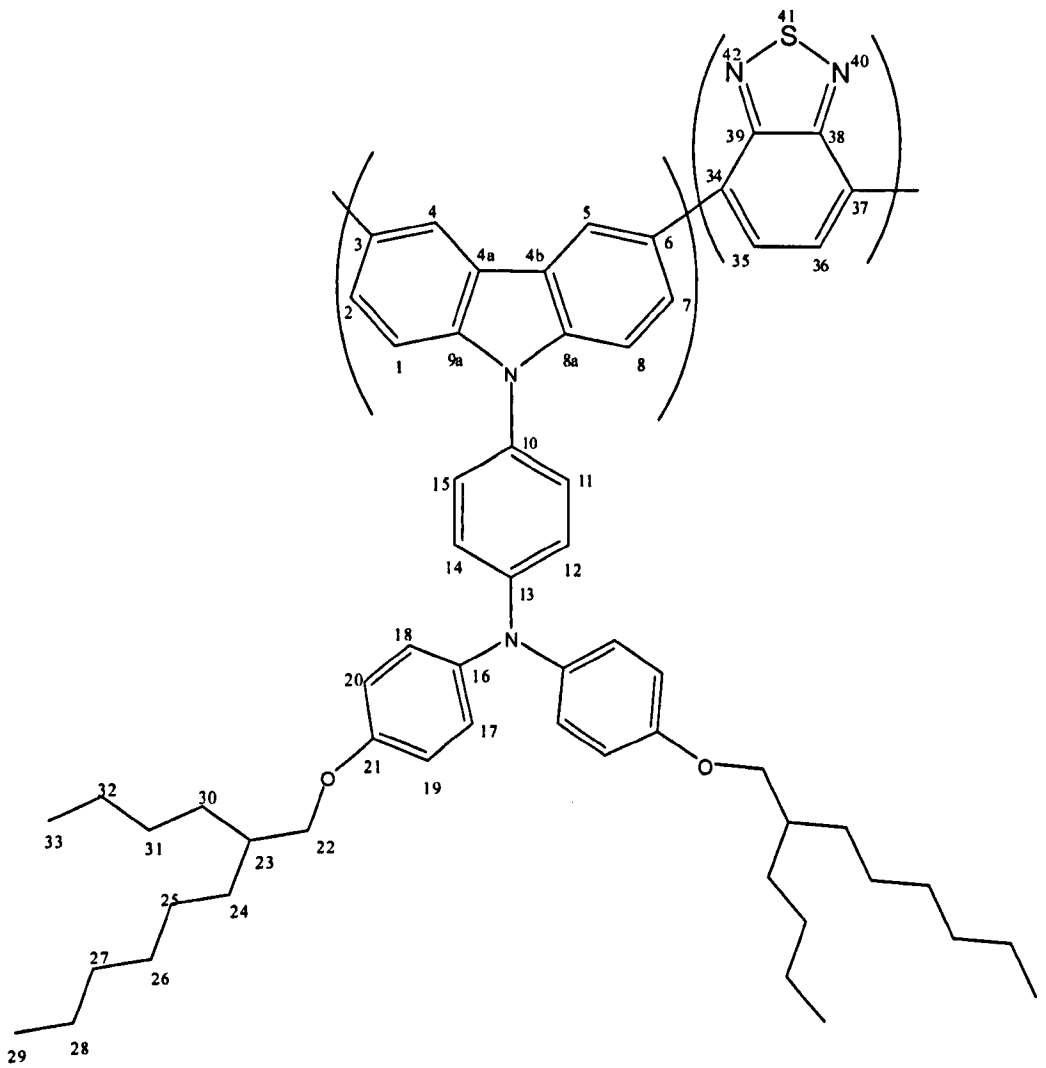

Figure 5.23, poly{[9-(bis-[4-(2-butyl-octyloxy)-phenyl]-amino-phen-4-yl)-carbazole-3,6-diyl] -*alt*-[benzo-2,1,3-thiadiazol-4,7-diyl]} **(39)**

Nuclear Magnetic Resonance Spectroscopy analysis

The ^{1}H-NMR spectrum identifies the product with ten broad signals in the spectrum. The first broad peak at δ 8.80 related to protons on the benzothiodiazol at positions 35 and 36, δ 8.00 – 7.80 ppm is linked to the protons 4, 5, 12 and 14 in the system. δ 7.50 ppm can be in relation to protons at positions 1, and 8, δ 7.30 ppm which is in relation to protons at positions 2 and 7, δ 7.20 – 7.00 ppm is a very broad shift relating to protons 11,15,17 and 18; δ 6.85 relates to the broad protons lying at 19 and

20. And we have a clear broad peak at δ 3.75 ppm relating to protons from position 22, The next peak is also a signature peak, as it is the only single proton which is distinguished at δ 1.75 ppm linked to position 23; the peaks between 1.55-1.15 ppm are those related to positions 24-28 and 30-32 for the $-CH_2$ groups; and finally we have peak at 0.85 ppm coinciding to methyl groups at positions 29 and 33. There are some smaller peaks in the spectra that will be related to the dimethyl phenyl end capping groups.

The ^{13}C-NMR gave nineteen peaks on the spectrum which have been estimated to the following positions of the compound δ 155 (2C) positions 38 and 39, δ 153 (2C) position 21, δ 152 (2C) position 13 and 10, δ 139 (2C) position 8a and 9a, δ 125 (2C) position 34 and 37, δ 124 (8C) positions 11, 12, 14, 15, 17 and 18, δ 121 (6C) position 2, 4, 5, 4a, 4b and 7, δ 118 (4C) position 3, 6, 35 and 36, δ 113 (6C) positions 16, 19 and 20, 107 (4C) position 1 and 8, δ 71 (2C) position 22, δ 38 (2C) position 30, δ 31 (2C) positions 24 , δ 29 (4C) position 26 and 31, δ 26 (2C) positions 32, δ 24 (2C) position 25, δ 23 (2C) and 27, δ 21 (2C) positions 28 and finally δ 11 (4C) at positions 29 and 33.

Scheme 52, NMR of Poly{[9-(bis-[4-(2-butyl-octyloxy)-phenyl]-amino-phen-4-yl)-carbazole-3,6-diyl] -*alt*-[benzo-2,1,3-thiadiazol-4,7-diyl]} **(39)**

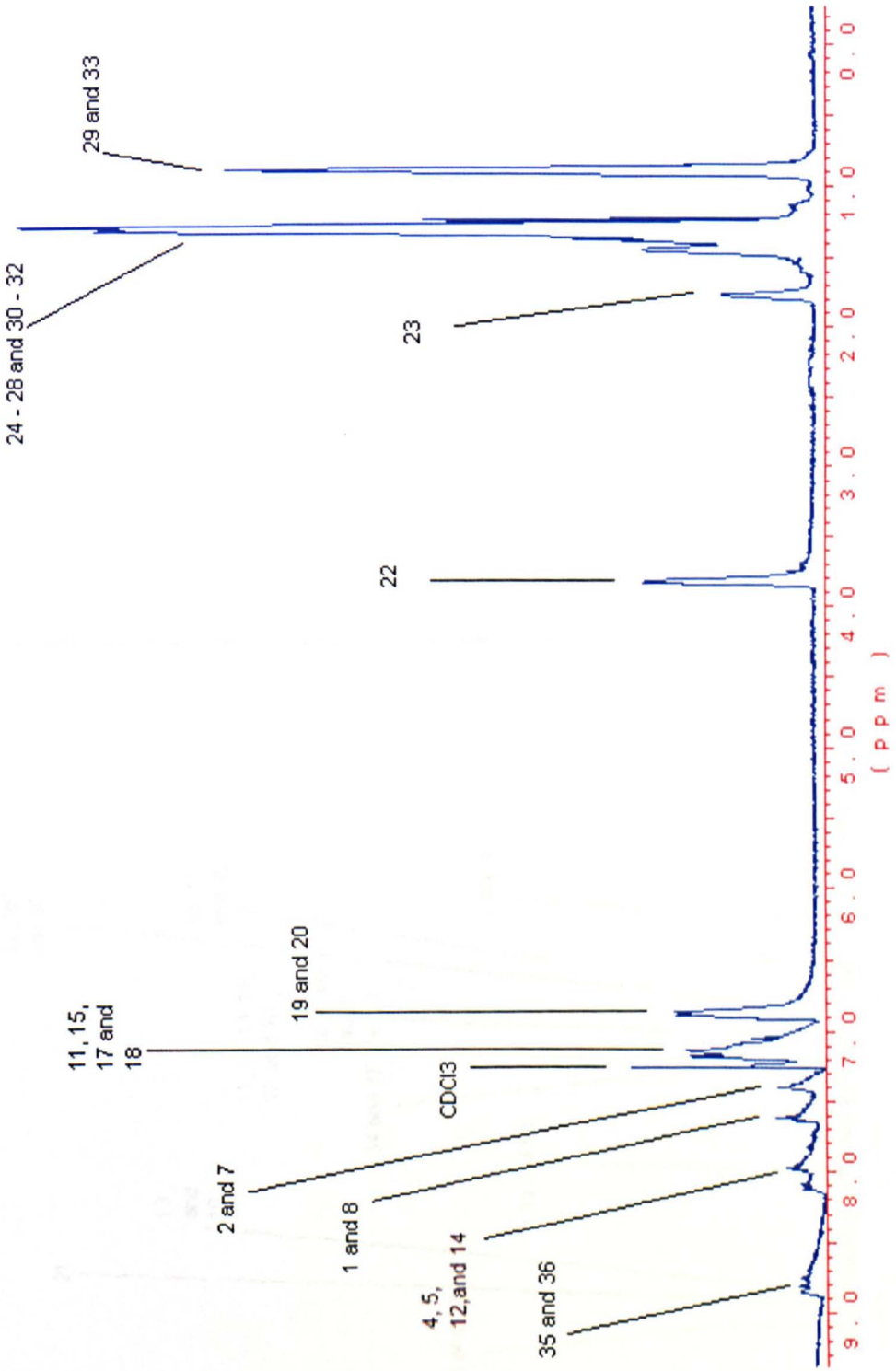

Scheme 53, NMR of Poly{[9-(bis-[4-(2-butyl-octyloxy)-phenyl]-amino-phen-4-yl)-carbazole-3,6-diyl] -*alt*-[benzo-2,1,3-thiadiazol-4,7-diyl]} **(39)**

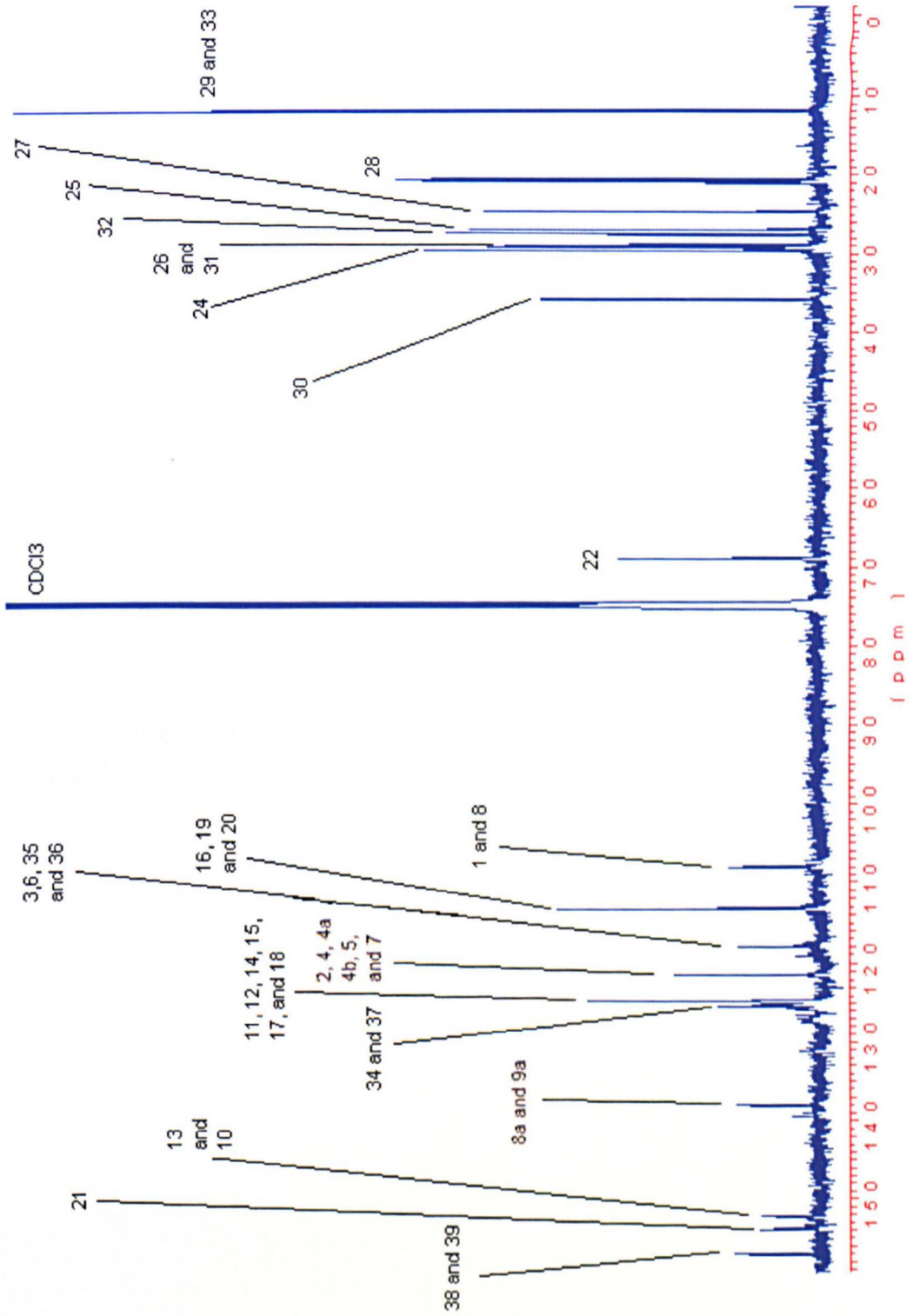

Infared Spectroscopy analysis

The IR spectra of poly{[9-(bis-[4-(2-butyl-octyloxy)-phenyl]-amino-phen-4-yl)-carbazole-3,6-diyl] -*alt*-[benzo-2,1,3-thiadiazol-4,7-diyl]} **(39)** is shown below. The spectrum distinctively highlights the extensive components of the polymer.

It can be seen that characterising peak at 3046 cm^{-1} which falls in relation to aromatic benzene groups –CH stretch. Following this we have peaks at 2931 cm^{-1} and 2847 cm^{-1} which co-ordinate to the alkyl stretching frequencies of the methylene groups. We have a well defined peak at 1640 cm^{-1}, which falls into calibration of and imine / oxime –C=N. At 1603 cm^{-1}, 1501 cm^{-1} and 1458 cm^{-1} we have a mixture of peaks related to the overtone and combination bands and also the deformations bands of the aromatic –CH groups and methylene $-CH_2-$ groups. We have a related peak at 1277 cm^{-1} and 716 cm^{-1} which falls into the tertiary amine sector –NR3 bond. The peaks at 1235 cm^{-1} and 1099 cm^{-1} work to the C-O-C stretch due to alky / aryl ether. The peaks at 1313 cm^{-1} and 1294 cm^{-1} corresponding to the C – B – C and B – O stretching frequencies respectively of the monomers 3,6-Bis-(4,4,5,5-tetramethyl-[1,3,2]dioxaborolan-2-yl)-9-(bis-[4-(2-butyl-octyloxy)-phenyl]-amino-phen-4-yl)-carbazole **(27)** disappeared. Meanwhile the stretching vibration of the C – Br bonds at 776 cm^{-1} from monomers 4,7-dibromobenzo[c][1,2,5]thiadiazole **(31)** have also disappeared.

Scheme 54, IR of Poly{[9-(bis-[4-(2-butyl-octyloxy)-phenyl]-amino-phen-4-yl)-carbazole-3,6-diyl] -*alt*-[benzo-2,1,3-thiadiazol-4,7-diyl]} **(39)**

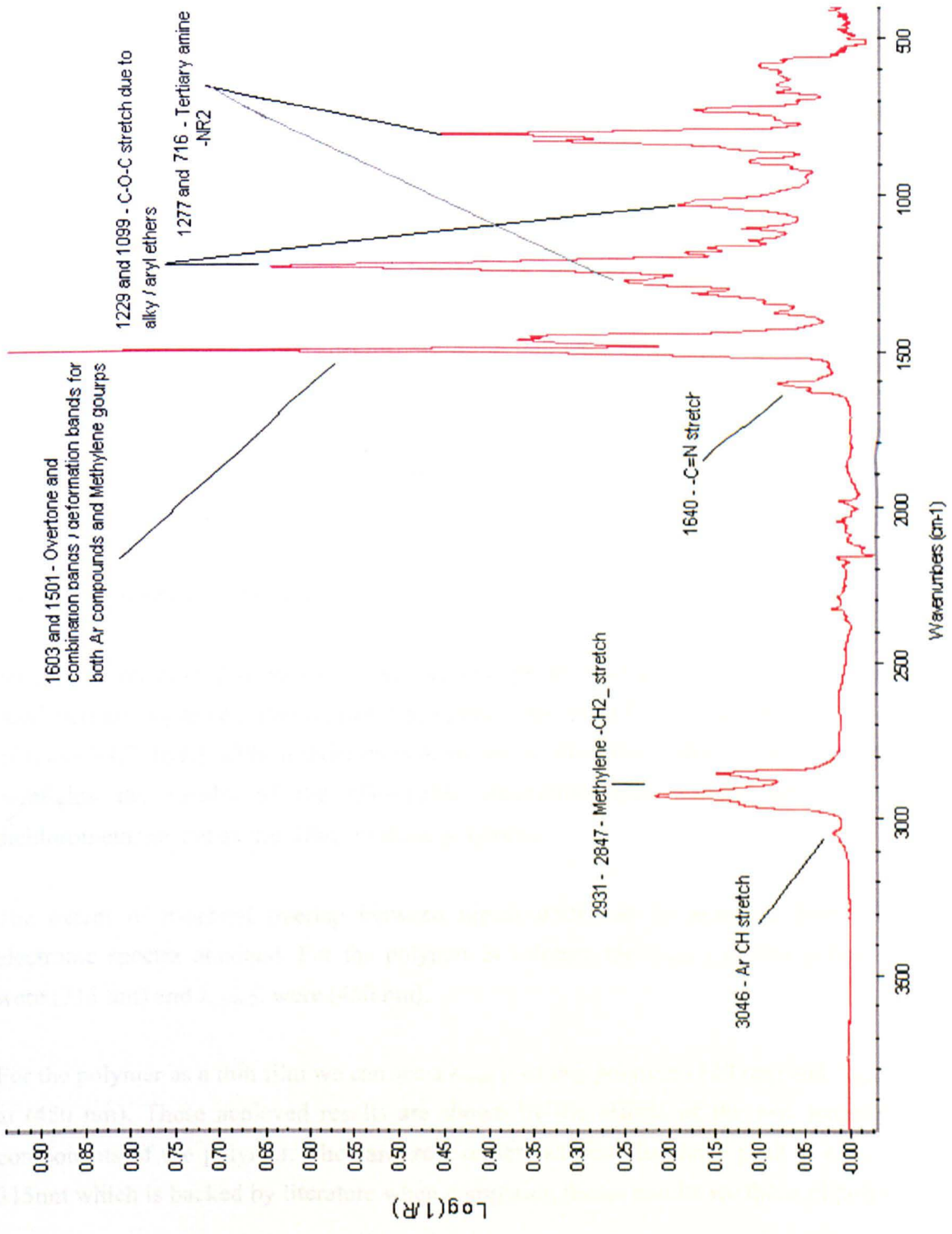

Elemental analysis and GPC analysis

The polymer poly{[9-(bis-[4-(2-butyl-octyloxy)-phenyl]-amino-phen-4-yl)-carbazole-3,6-diyl] -*alt*-[benzo-2,1,3-thiadiazol-4,7-diyl]} **(39)** P6.AK was calculated to have a CHN Br analysis of: C, 78.90; H, 7.95; N, 6.13; S, 3.51, Br, 0.00.%; for the compound $C_{60}H_{70}N_4O_2S$. The following elemental analysis was achieved: C, 78.40; H, 7.83; N, 6.09; S, 3.99; Br 0.00.%; This showed the polymer has the structure proposed.

The polymer poly-4-(2-butyloctyloxy)-N-(4-(2-butyloctyloxy)phenyl)-N-(4-(3-methyl-6-(7-methylbenzo[c][1,2,5]thiadiazol-4-yl)-9H-carbazol-9-yl)phenyl)benzenamine **(39)** also displayed the following results for GPC analysis. Mn 11,000 / Mw 15,000 / PDI 1.35 / DP 17. Comparing this with the poly-(9-(2-ethylhexyl)-carbazole-3,6-diyl)s from literature [31] it is seen that that polymerisation has worked extremely well as corresponding polymerisation were seen to have an average Mn 2700 and Mw 4000.

UV-visible absorption spectroscopy analysis

Scheme 55 on page 216 shows UV-visible absorption spectra of Poly{[9-(bis-[4-(2-butyl-octyloxy)-phenyl]-amino-phen-4-yl)-carbazole-3,6-diyl] -*alt*-[benzo-2,1,3-thiadiazol-4,7-diyl]} **(39)** in dichloromethane and as thin film. Table 12 on page 216 highlights the results of the UV-visible absorption spectroscopy analysis in dichloromethane and as thin films of these polymers.

The extent of π-orbital overlap between repeat units can be assessed from the electronic spectra obtained. For the polymer in solution the $\lambda_{max\ 1}$ of this polymer were (315 nm) and $\lambda_{max\ 2}$ were (450 nm).

For the polymer as a thin film we can see a $\lambda_{max\ 1}$ of this polymer (320 nm) and λ_{max2} at (480 nm). These achieved results are shown by the effects of the two separate components of the polymer. The carbazole moiety exhibits its shape peak at $\lambda_{max\ 1}$ 315nm which is backed by literature when comparing theses results we those of poly-

(9-(2-ethylhexyl)-carbzole-3,6-diyl)s in which we were able to see a single peak in the UV absorbtion at 308 nm .[31] The second peak seen to arise at $\lambda_{max\ 2}$ 450 nm is related to the benzo-thia-diazole moiety present in the polymer.

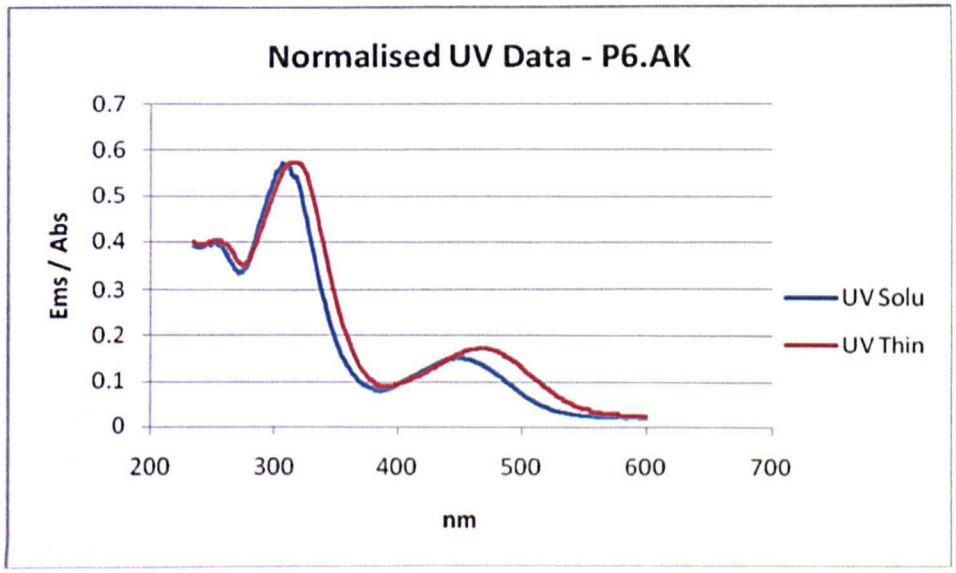

Scheme 55, UV of Poly{[9-(bis-[4-(2-butyl-octyloxy)-phenyl]-amino-phen-4-yl)-carbazole-3,6-diyl] -*alt*-[benzo-2,1,3-thiadiazol-4,7-diyl]} **(39)**

Polymer	λ max 1(nm)	λ max 2 (nm)
Solution	315	450
Thin Film	320	480

Table 12, UV of Poly{[9-(bis-[4-(2-butyl-octyloxy)-phenyl]-amino-phen-4-yl)-carbazole-3,6-diyl] -*alt*-[benzo-2,1,3-thiadiazol-4,7-diyl]} **(39)**

Photoluminescence spectroscopy analysis

PL spectroscopy analysis on both polymer solution and polymer film of poly{[9-(bis-[4-(2-butyl-octyloxy)-phenyl]-amino-phen-4-yl)-carbazole-3,6-diyl] -*alt*-[benzo-2,1,3-thiadiazol-4,7-diyl]} **(39)** were undertaken.

Scheme 56 on page 217 shows PL spectroscopy analysis on both polymer solutions and polymer films The PL spectra of the solutions of poly{[9-(bis-[4-(2-butyl-octyloxy)-phenyl]-amino-phen-4-yl)-carbazole-3,6-diyl] -*alt*-[benzo-2,1,3-thiadiazol-4,7-diyl]} **(39)** appeared in the red region of the spectra with sharp structure. The λ^{em}_{max} value obtained was 610 nm. An excitation wavelength of 20 nm lower than the $\lambda_{max\ 2}$ of absorption of the polymer was employed. The feature of the PL spectra of the polymer solution was independent from the excitation wavelength employed. The polymer solutions exhibited medium Stokes shifts, which indicated structural differences between the ground and excited states of these polymers.

The PL spectra of the thin films were similar to each other. The thin films of poly{[9-(bis-[4-(2-butyl-octyloxy)-phenyl]-amino-phen-4-yl)-carbazole-3,6-diyl] -*alt*-[benzo-2,1,3-thiadiazol-4,7-diyl]} **(39)** showed intense PL in the red region of the spectra with a vibronic structure. The λ^{em}_{max} value was 605 nm.

Table 13 on page 218 highlights the results of the PL spectroscopy and UV-vis spectroscopy analysis in dichloromethane and as thin films for poly{[9-(bis-[4-(2-butyl-octyloxy)-phenyl]-amino-phen-4-yl)-carbazole-3,6-diyl] -*alt*-[benzo-2,1,3-thiadiazol-4,7-diyl]} **(39)**.

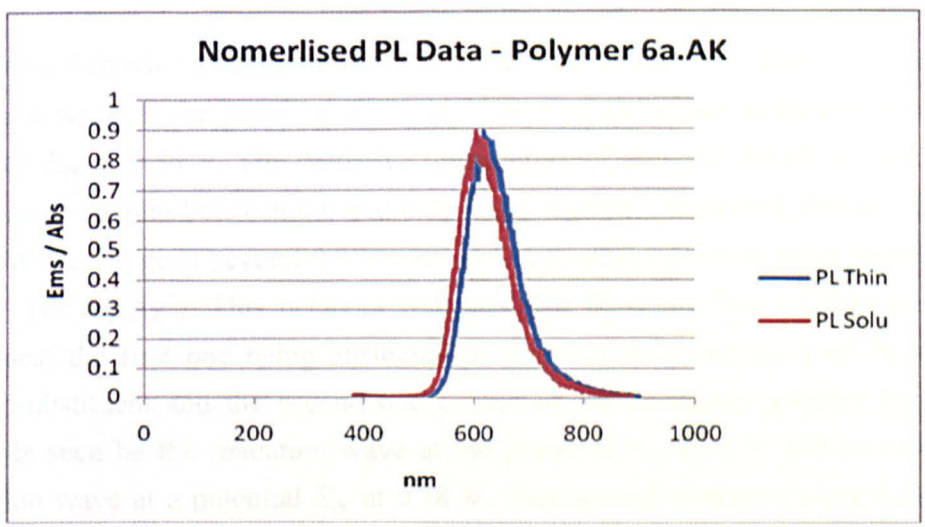

Scheme 56, PL of Poly{[9-(bis-[4-(2-butyl-octyloxy)-phenyl]-amino-phen-4-yl)-carbazole-3,6-diyl] -*alt*-[benzo-2,1,3-thiadiazol-4,7-diyl]} **(39)**

Polymer	Absorbance		PL mission	Stokes
	λ max 1(nm)	λ max 2 (nm)	$\lambda^{em}{}_{max}$	Shift (nm)
Solution	315	450	610	85
Thin Film	320	480	605	46

Table 13, PL of Poly{[9-(bis-[4-(2-butyl-octyloxy)-phenyl]-amino-phen-4-yl)-carbazole-3,6-diyl] -*alt*-[benzo-2,1,3-thiadiazol-4,7-diyl]} **(39)**

Cyclic Voltammetry (CV) analysis

CV analysis studies of thin films of poly{[9-(bis-[4-(2-butyl-octyloxy)-phenyl]-amino-phen-4-yl)-carbazole-3,6-diyl] -*alt*-[benzo-2,1,3-thiadiazol-4,7-diyl]} **(39)** P6.AK were carried out in order to assess the electrochemical properties of the polymers. Scheme 57 and 58 on page 219 and 220 shows the CV curves of thin films of poly{[9-(bis-[4-(2-butyl-octyloxy)-phenyl]-amino-phen-4-yl)-carbazole-3,6-diyl] -*alt*-[benzo-2,1,3-thiadiazol-4,7-diyl]} **(39)** P6.AK. Table 14 on page 220 below shows the results from these CV measurements.

The redox behavior of polymer P6.AK indicates a reversible redox wave with an oxidation wave at the potential E_{pa} 0.44 V and an associated reduction wave at a potential E_{pc} at 0.36 V. The oxidative reversibility of polymer P6.AK is maintained on repeated cycling between 0.0 and 0.85 V (vs Ag/Ag^{+}). However, this reversibility is lost if cycling goes beyond 0.9 V with an irreversible oxidation wave appearing at 0.91 V (vs Ag/Ag^{+}). This behavior indicates that there are two separate oxidation processes: the first one being attributed to the reversible oxidation of the tri aryl amine substituent and the second one to that of the carbazole polymer backbone, which is seen be the oxidation wave at the potential E_{pa} 0.82 V and an associated reduction wave at a potential E_{pc} at 0.78 V. This second oxidation wave belongs to the carbazole polymer backbone which is reversible in the case of polymer P6.AK.

It is also worth noting that cyclic voltammetry studies in acetonitrile solutions of 2,7-dibromo-9-(4-dioctylamino-phenyl)-9*H*-carbzole [32] have shown that a reversible redox wave with an oxidation wave at E_{pa} 0.50 V and an associated reduction wave at E_{pc} 0.41 V are attributed to its 4-dioctylamino-phenyl groups.

The ionisation potential (vs vacuum) of polymer P6.AK was estimated from the onset of its oxidation in cyclic voltammetry experiments as 5.0 eV. (on the basis that ferrocene/ ferrrocenium is 4.8 eV below the vacuum level) [33]

The ionisation potentials of polymers P6.AK are similar to those of poly(9-alkyl-9*H*-carbazole-2,7-diyl)s [30] described in earlier studies. They are lower than those of poly(9,9-dioctyl-fluorene-2,7-diyl). [34] This could suggest an easier hole injection into films from ITO electrodes in electronic device applications

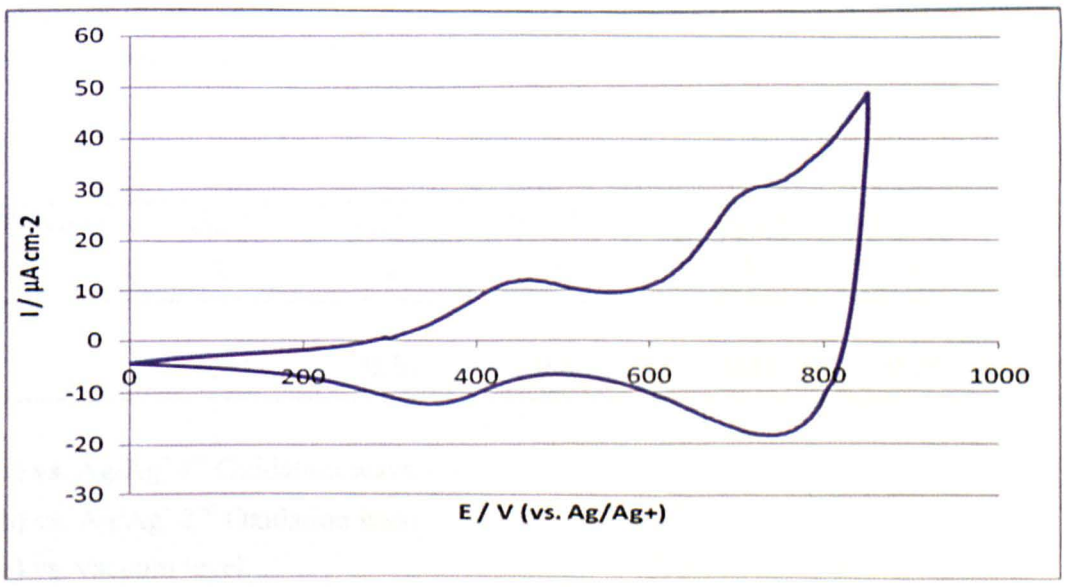

Scheme 57, CV curve for thin films of poly{[9-(bis-[4-(2-butyl-octyloxy)-phenyl]-amino-phen-4-yl)-carbazole-3,6-diyl] -*alt*-[benzo-2,1,3-thiadiazol-4,7-diyl]} **(39)** (single scan rate = 90 mV s^{-1})

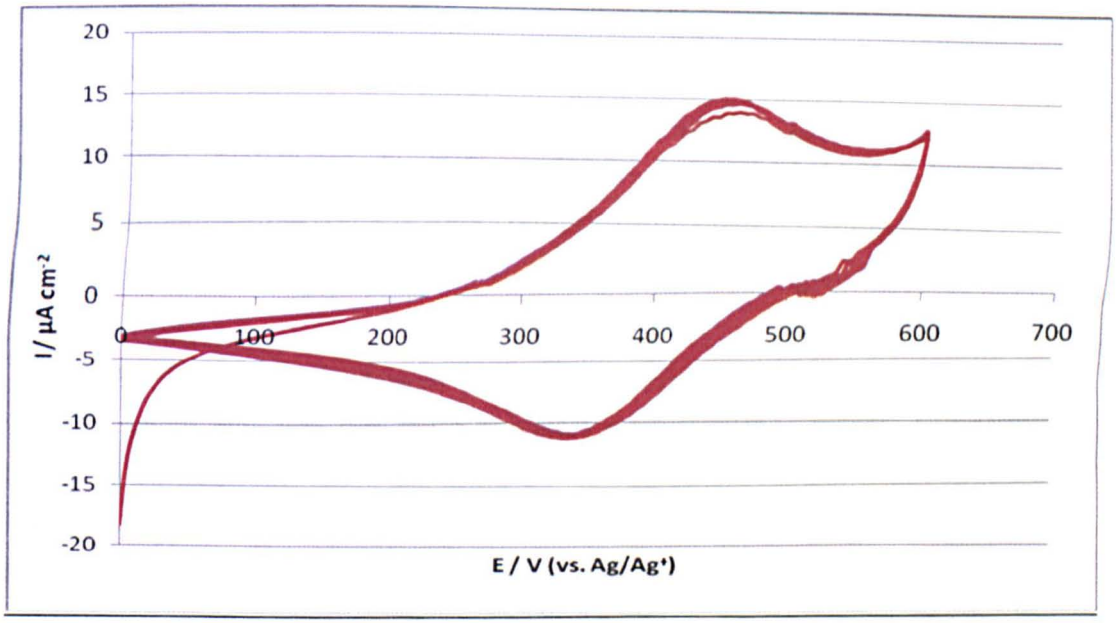

Scheme 58, CV curve for thin films of poly{[9-(bis-[4-(2-butyl-octyloxy)-phenyl]-amino-phen-4-yl)-carbazole-3,6-diyl] -*alt*-[benzo-2,1,3-thiadiazol-4,7-diyl]} **(39)** (multiple scan rate = 60 mV s^{-1})

Polymer	E_{pa} a) / V	E_{pc} a) / V	$E_{1/2}$ a) / V	E_{pa} b) / V	E_{pc} b) / V	$E_{1/2}$ b) / V	I_p c) / V
	0.44	0.36	0.4	0.82	0.78	0.8	5.1

a) vs. Ag/Ag^+ 1st Oxidation wave

b) vs. Ag/Ag^+ 2nd Oxidation wave

c) vs. vacuum level

Table 14, CV curve for thin films of poly{[9-(bis-[4-(2-butyl-octyloxy)-phenyl]-amino-phen-4-yl)-carbazole-3,6-diyl] -*alt*-[benzo-2,1,3-thiadiazol-4,7-diyl]} **(39)** (single scan rate = 90 mV s^{-1})

Thermo-gravimetric Analysis (TGA)

TGA studies of poly{[9-(bis-[4-(2-butyl-octyloxy)-phenyl]-amino-phen-4-yl)-carbazole-3,6-diyl] -*alt*-[benzo-2,1,3-thiadiazol-4,7-diyl]} **(39)** were undertaken. Scheme 59 below shows the TGA curves of poly{[9-(bis-[4-(2-butyl-octyloxy)-phenyl]-amino-phen-4-yl)-carbazole-3,6-diyl] -*alt*-[benzo-2,1,3-thiadiazol-4,7-diyl]} **(39)**.

The TGA of this polymer showed that the onset of degradation temperature was ca. 310 °C, which indicated that these polymers were thermally stable. The results in Table 15 on page 222 show the degradations originate from the elimination of the branched alkyoxy side chains and aryl substituent, because the weight losses observed were consistent with the weight percentage of these polymers.

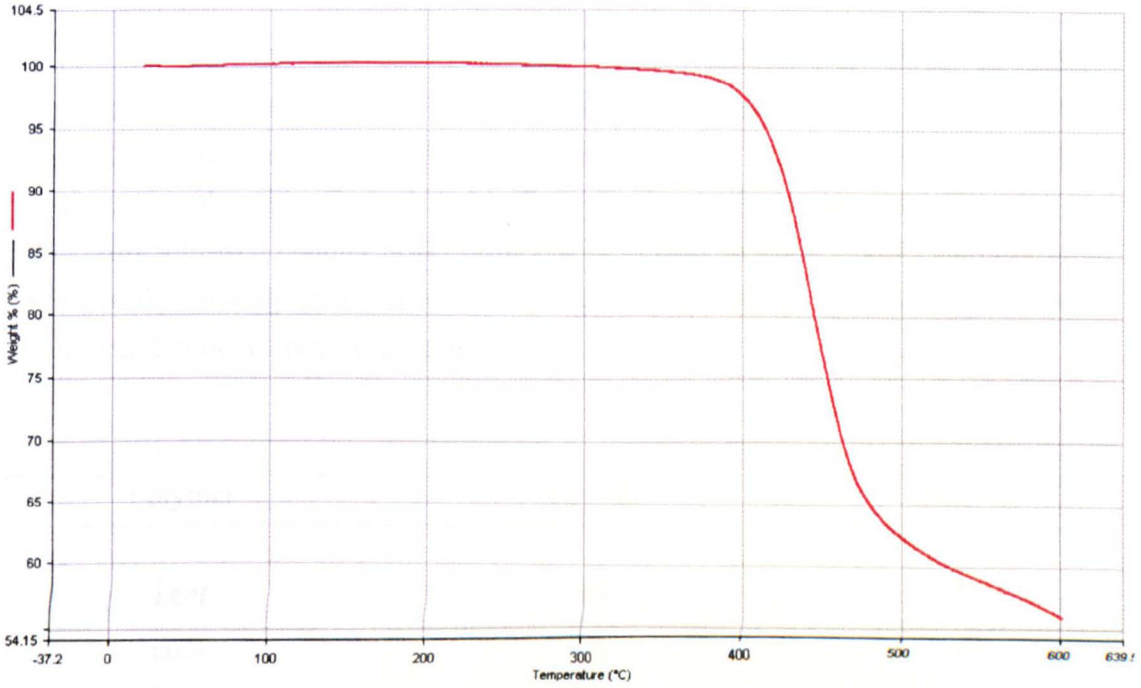

Scheme 59, TGA of Poly{[9-(bis-[4-(2-butyl-octyloxy)-phenyl]-amino-phen-4-yl)-carbazole-3,6-diyl] -*alt*-[benzo-2,1,3-thiadiazol-4,7-diyl]} **(39)**

Polymer	Degradation	
	Temp °C	Weight loss (wt%)
P6.AK	@ 500	57

Table 15, TGA of Poly{[9-(bis-[4-(2-butyl-octyloxy)-phenyl]-amino-phen-4-yl)-carbazole-3,6-diyl] -*alt*-[benzo-2,1,3-thiadiazol-4,7-diyl]} **(39)**

Differential Scanning Calorimetry (DSC) analysis

DSC analysis studies on poly{[9-(bis-[4-(2-butyl-octyloxy)-phenyl]-amino-phen-4-yl)-carbazole-3,6-diyl] -*alt*-[benzo-2,1,3-thiadiazol-4,7-diyl]} **(39)** were carried out. The results are outlined in this section.

Scheme 60 on page 223 shows the DSC curves for poly{[9-(bis-[4-(2-butyl-octyloxy)-phenyl]-amino-phen-4-yl)-carbazole-3,6-diyl] -*alt*-[benzo-2,1,3-thiadiazol-4,7-diyl]} **(39)**. Table 16 below shows the results of the DSC analysis of this polymer. This showed a T_g peak at 56 °C on the first heating scan and a Tm peak at 77°C. This followed counter peaks observed at T_g peak at - 26 °C and Tm peak at - 18 °C on the cooling scan and on the second heating scan at T_g peak at 59 °C was observered but no T_m peak was seen.

Polymer	Tg / °C	Tm / °C
heat	56	77
cool	-26	-18
heat	59	---

Table 16, DSC of Poly{[9-(bis-[4-(2-butyl-octyloxy)-phenyl]-amino-phen-4-yl)-carbazole-3,6-diyl] -*alt*-[benzo-2,1,3-thiadiazol-4,7-diyl]} **(39)**

Scheme 60, DSC of Poly{[9-(bis-[4-(2-butyl-octyloxy)-phenyl]-amino-phen-4-yl)-carbazole-3,6-diyl] -*alt*-[benzo-2,1,3-thiadiazol-4,7-diyl]} **(39)**

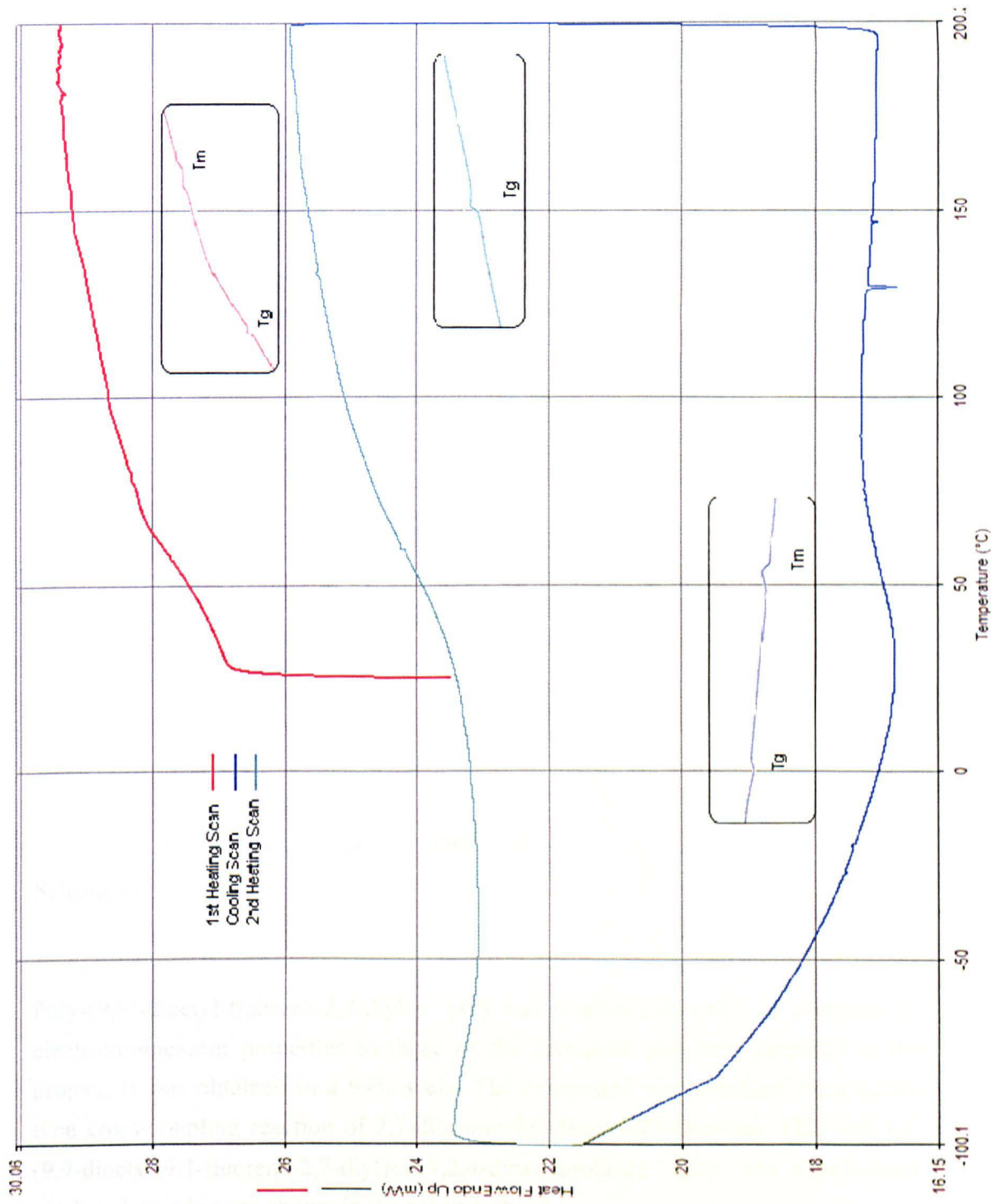

5.7.6 Poly-(9,9'-dioctyl-fluorene-2,7-diyls) (41) Suzuki

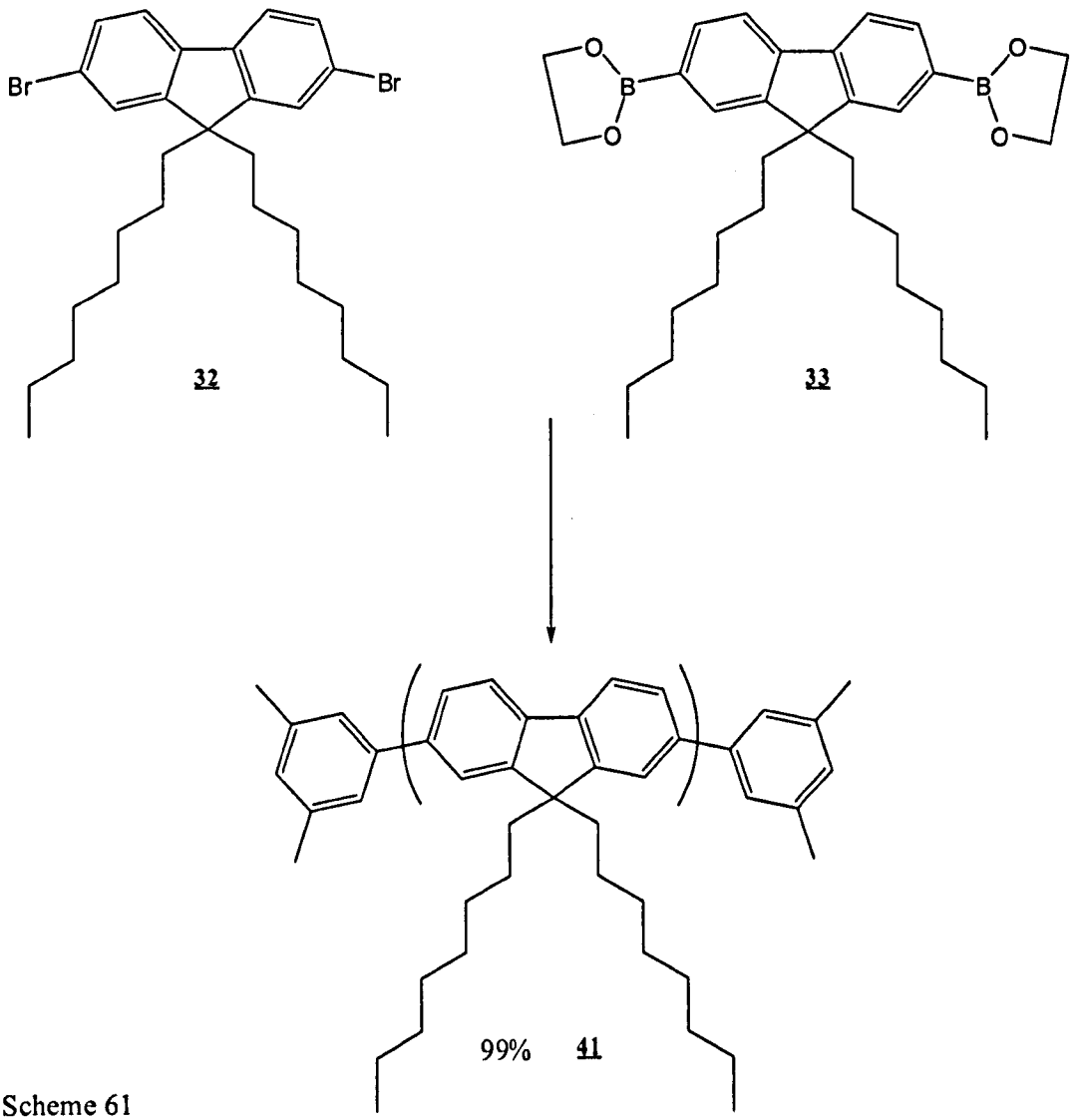

Scheme 61

Poly-(9,9'-dioctyl-fluorene-2,7-diyls) **(40)** was produced in order to compose it's electroluminescent properties to those of the carbazole polymers prepared in this project. It was obtained in a 99% yield. The compound was obtained via a Suzuki type cross-coupling reaction of 2,7-dibromo-9,9-dioctyl-9H-fluorene **(32)** and 4,4'-(9,9-dioctyl-9H-fluorene-2,7-diyl)bis(1,2,4-dioxaborolane) **(33)** via a palladium-catalysed reaction, as shown in the scheme above.

The first method for the reaction was carried out in a round bottom flask and the catalyst was formed in situ, by reacting $Pd_2(dba)_3$ and tri-*p*-tolyl phosphine in THF. On reacting the catalyst together the two monomers 2,7-dibromo-9,9-dioctyl-9H-fluorene **(32)** and 4,4'-(9,9-dioctyl-9H-fluorene-2,7-diyl)bis(1,2,4-dioxaborolane) **(33),** the base (sodium hydrogen carbonate in water) and refluxing the mixture for 24 hours. The polymer was end-capped and a first precipitation was undertaken. Following this the polymer was dried, and treated with N,N-diethyl-phenyl-azo-thio-formamide **(28)** in an order to remove any palladium nanoparticales that may have been left behind from the reaction. The polymer was re-precipitated once again, to yield the desired polymer as a pale yellow powder.

This method produced the polymer poly-(9,9'-dioctyl-fluorene-2,7-diyls) **(40)** (P.5a.AK) and was calculated to have a CHN Br analysis of: C, 89.16; H, 10.84; Br, 0.00.%; for the compound $C_{29}H_{40}$. The following elemental analysis was achieved: C, 86.15; H, 9.86; Br 0.00.%; This showed the polymer had the proposed structure.

The polymer **(40)** also displayed the following results for GPC analysis. Mn 14,000 / Mw 51,000 / PDI 3.65 / DP 131

These results were believed not be optimum since we achieved a low molecular weight to what had been expected. The second method for the reaction was carried out in a round bottom flask and the catalyst was formed instu, by reacting $Pd_2(dba)_3$ and tri-*o*-tolyl phosphine in THF. The polymer was obtained on reacting the catalyst together with the two monomers 2,7-dibromo-9,9-dioctyl-9H-fluorene **(32)** and 4,4'-(9,9-dioctyl-9H-fluorene-2,7-diyl)bis(1,2,4-dioxaborolane) **(33)**, the base (tertracthyl ammonium hydroxide (20w/w) and refluxing the mixture for 24 hours. The polymer was end-capped and a first precipitation was undertaken. Following this the polymer was dried, and treated with N,N-diethyl-phenyl-azo-thio-formamide **(28)** in an aid to remove any palladium nanoparticales that may have been left behind from the reaction. The polymer was re-precipitated once again, to yield the desired polymer as lime yellow strands.

The polymer (42) was characterised by the following techniques: ^{1}H NMR and ^{13}C NMR, IR absorption, elemental analysis, GPC, UV-vis spectroscopy, photoluminescence spectroscopy, thermo-gravimetric analysis (TGA), differential scanning calorimetry (DSC), and cyclic voltammetry (CV).

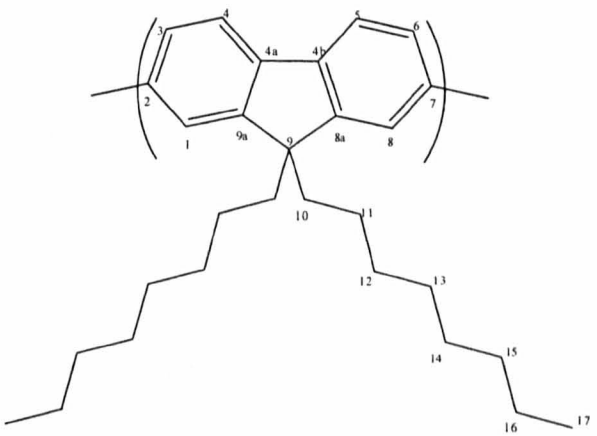

Figure 24, poly-(9,9'-dioctyl-fluorene-2,7-diyls) **(41)**

Nuclear Magnetic Resonance Spectroscopy analysis

The ^{1}H-NMR spectrum identifies the product with five signals in the spectra. The first broad peak at signal δ 7.75 related to protons in positions 1 and 8, δ 7.55 ppm is linked to the protons 3, 4, 5 and 6 in the system. δ 1.50 ppm can be in relation to protons at position 10, δ 1.25 – 1.00 ppm which is in relation to protons at positions 11 to 17 and finally δ 0.75 ppm is a broad shift relating to proton 21. There are some smaller peaks in the spectra that will be related to the dimethyl phenyl end capping groups.

The ^{13}C-NMR gave fourteen peaks on the spectrum which have been estimated to the following positions of the compound δ 151 (2C) positions 8a and 9a, δ 141 (2C) positions 4a and 4b, δ 140 (2C) position 2 and 7, δ 126 (2C) position 1 and 8, δ 122 (2C) positions 4 and 5, δ 119 (2C) positions 3 and 6, δ 55 (1C) position 9, δ 40 (2C) positions 10, δ 31 (2C) positions 15 , δ 30 (4C) position 14, δ 29 (2C) positions 12 and 13, δ 23 (2C) position 11, δ 22 (2C) position 16 and finally δ 14 (2C) at positions 17.

Scheme 62, NMR of Poly-(9,9'-dioctyl-fluorene-2,7-diyls) **(41)**

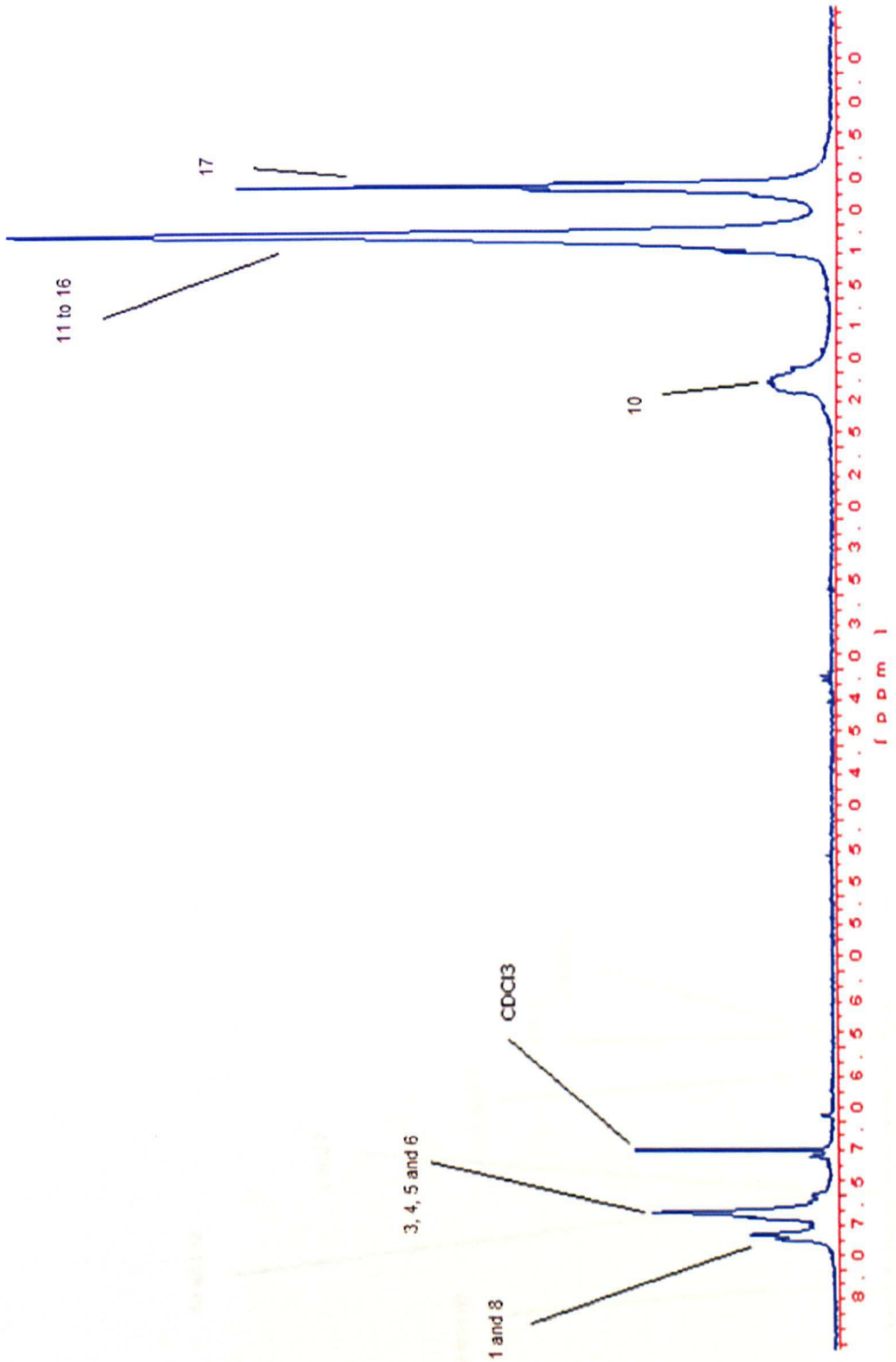

Scheme 63, NMR of Poly-(9,9'-dioctyl-fluorene-2,7-diyls) **(41)**

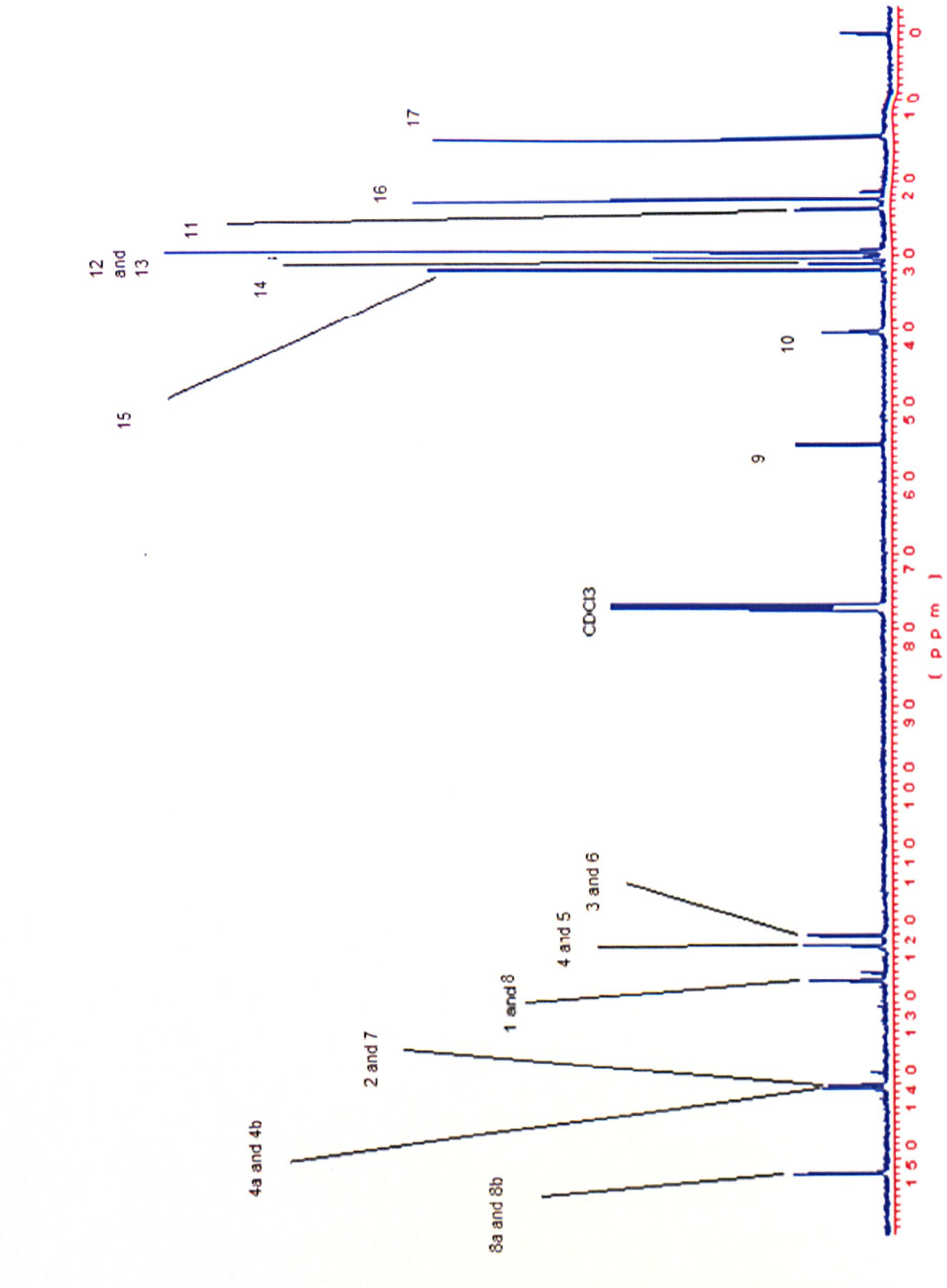

Infared Spectroscopy analysis

The IR spectra of poly-(9,9'-dioctyl-fluorene-2,7-diyls) **(41)** is shown below. The spectrum distinctively highlights the extensive components of the polymer. It can be seen that a small, not very defined peak at 3063 cm^{-1} which falls in relation to aromatic benzene groups –CH stretch. Following this we have peaks at 2925 cm^{-1} and 2853 cm^{-1} which co-ordinate to the alkyl stretching frequencies of the methylene groups. At 1458 cm^{-1} we have a peak related to the overtone and combination bands and also the deformations bands of the aromatic –CH groups and methylene $-CH_2-$ groups. The peaks at 1313 cm^{-1} and 1294 cm^{-1} corresponding to the C – B – C and B – O stretching frequencies respectively of the monomers 4,4'-(9,9-dioctyl-9H-fluorene-2,7-diyl)bis(1,2,4-dioxaborolane) **(33)** disappeared. Meanwhile the stretching vibration of the C – Br bonds at 792 cm^{-1} from monomers 2,7-dibromo-9,9-dioctyl-9H-fluorene **(32)** have also disappeared.

Scheme 64, IR of Poly-(9,9'-dioctyl-fluorene-2,7-diyls) **(41)**

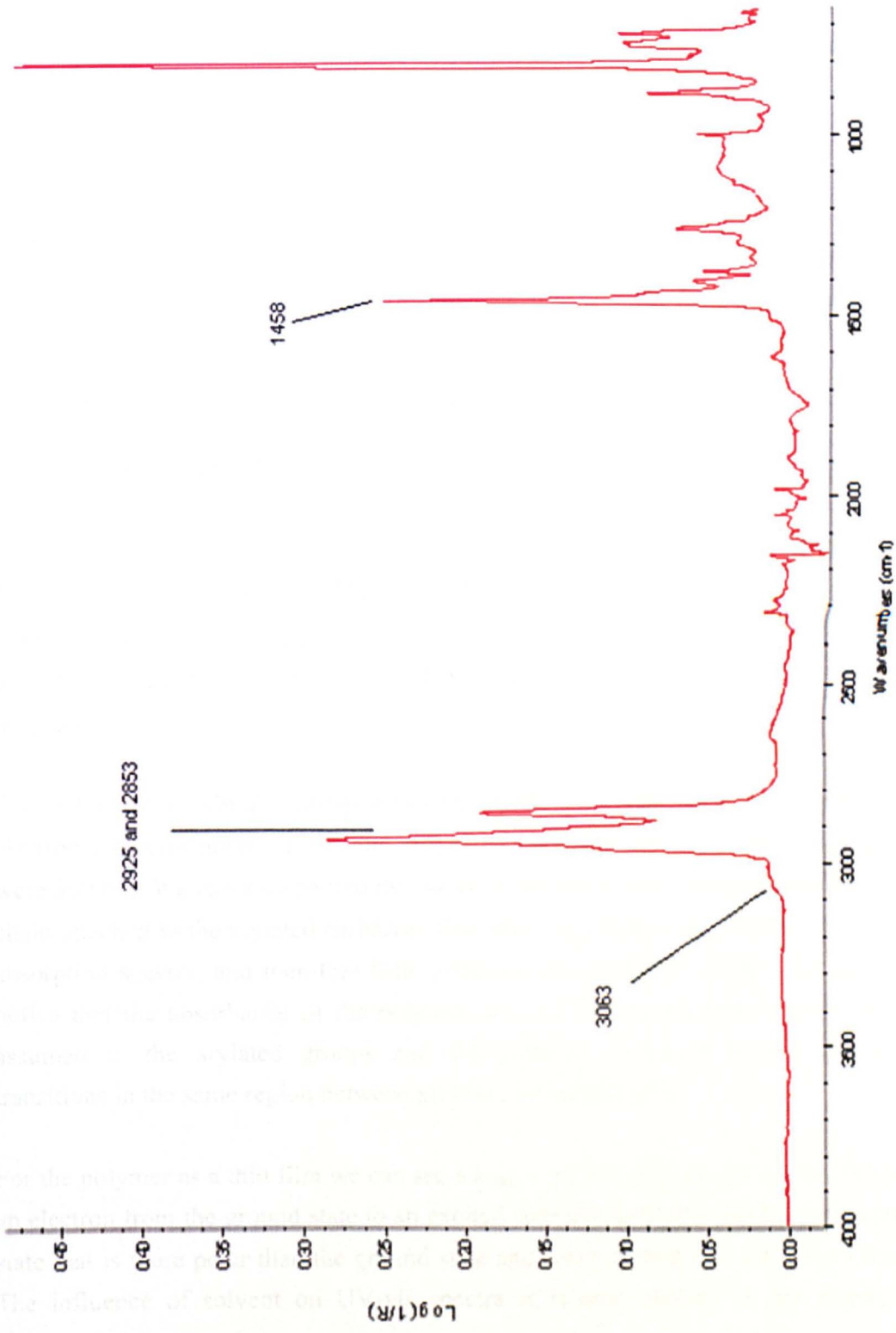

Elemental analysis and GPC analysis

The elemental analysis of poly-(9,9'-dioctyl-fluorene-2,7-diyls) **(41)** was calculated to have a CHN Br analysis of: C, 89.16; H, 10.84; Br, 0.00. for the formula $C_{29}H_{40}$. The following elemental analysis was achieved: C, 88.46; H, 10.43; Br 0.00. This showed the polymer had the structure proposed.

The polymer Poly-(9,9'-dioctyl-fluorene-2,7-diyls) **(41)** also displayed better average molecular weights than the previous reaction with the following results for GPC analysis. Mn 64,300 / Mw 174,000 / PDI 2.70 / DP 448

UV-visible absorption spectroscopy analysis

Scheme 65 on page 232 shows UV-visible absorption spectra for poly-(9,9'-dioctyl-fluorene-2,7-diyls) **(41)** in dichloromethane and the thin film for the same polymer. Table 17 on page 232 shown below, highlights the results of the UV-visible absorption spectroscopy analysis in dichloromethane and as thin films of these polymers.

The extent of π-orbital overlap between repeat units can be assessed from the electronic spectra obtained. For the polymer in solution the $\lambda_{max\ 1}$ of this polymer were 360 nm. We can assume that this result is not affected by the length of the alkyl chain attached to the arylated carbazole ring which has little effect on the UV-visible absorption spectra, and therefore little effect on the π-orbital overlap. We can also notice that the absorbance of the polymer at $\lambda_{max\ 2}$ is more intense which can be assumed to the arylated groups and the polymer backbone having electronic transitions in the same region between ground and excited state.

For the polymer as a thin film we can see a $\lambda_{max\ 1}$ of this polymer (370 nm). Moving an electron from the ground state to an excited state configuration leads to an excited state that is more polar than the ground state and more sensitive to salvation effects. The influence of solvent on UV-vis spectra is related directly to the degree of

interaction between the solute and the solvent, which as can be expected becomes greater as the polarity of the solvent increase, so the thin film UV-vis spectra for the polymer gives a more accurate indication to the polymers absorbance.

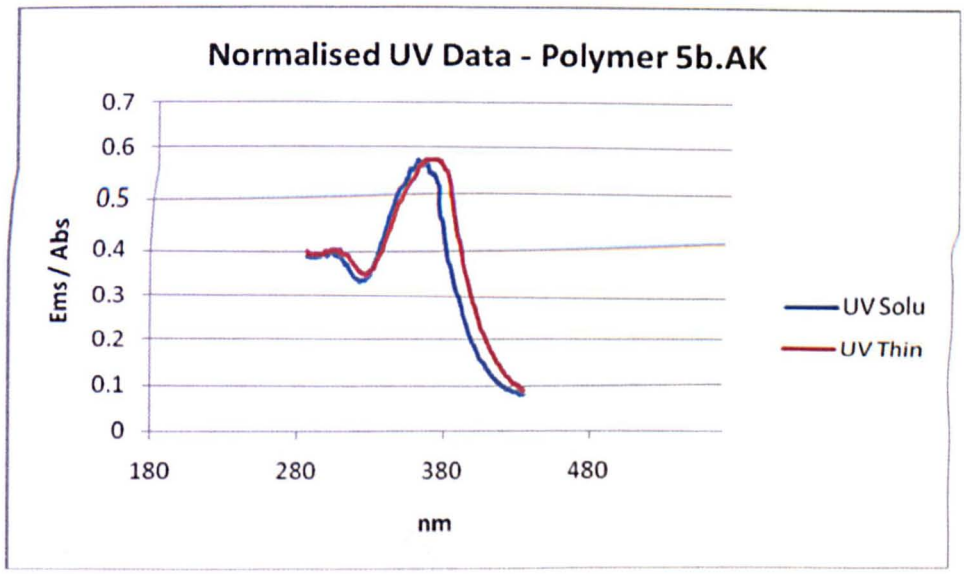

Scheme 65, UV of Poly-(9,9'-dioctyl-fluorene-2,7-diyls) **(41)**

Table 17, UV of Poly-(9,9'-dioctyl-fluorene-2,7-diyls) **(41)**

Polymer	λ max 1(nm)
Solution	360
Thin Film	370

Photoluminescence spectroscopy analysis

PL spectroscopy analysis on both polymer solution and polymer film of poly-(9,9'-dioctyl-fluorene-2,7-diyls) **(41)** were undertaken.

Scheme 66 on page 233 shows PL spectroscopy analysis on both polymer solutions and polymer films The PL spectra of the solutions of poly-(9,9'-dioctyl-fluorene-2,7-diyls) **(41)** appeared in the blue region of the spectra with sharp structure. The λ^{em}_{max} value obtained was 420 nm. An excitation wavelength of 20 nm lower than the $\lambda_{max\ 2}$

of absorption of the polymer was employed. The feature of the PL spectra of the polymer solution was independent from the excitation wavelength employed. The polymer solutions exhibited medium Stokes shifts, which indicated structural differences between the ground and excited states of these polymers.

The PL spectra of the thin films were similar to each other. The thin films of poly-(9,9'-dioctyl-fluorene-2,7-diyls) **(41)** showed intense PL in the blue region of the *spectra with a vibronic structure. The* λ^{em}_{max} value was 430 nm.

Table 18 below highlights the results of the PL spectroscopy and UV-vis spectroscopy analysis in dichloromethane and as thin films for poly-(9,9'-dioctyl-fluorene-2,7-diyls) **(41)**.

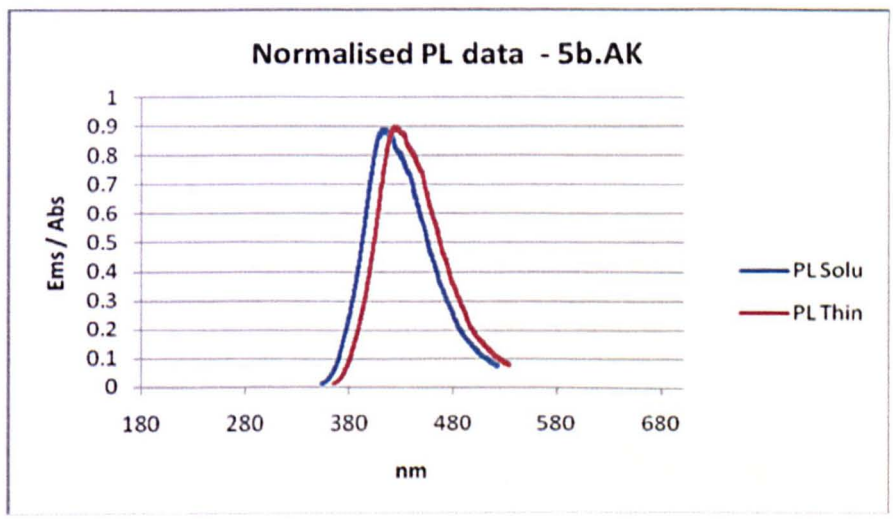

Scheme 66, PL of Poly-(9,9'-dioctyl-fluorene-2,7-diyls) **(41)**

Table 18, PL of Poly-(9,9'-dioctyl-fluorene-2,7-diyls) **(41)**

Polymer	Absorbance λ max 1(nm)	PL emission λ^{em}_{max}	Stokes Shift (nm)
Solution	360	420	60
Thin Film	370	430	60

Thermo-gravimetric Analysis (TGA)

TGA studies of poly-(9,9'-dioctyl-fluorene-2,7-diyls) **(41)** were undertaken. Scheme 67 below shows the TGA curves of poly-(9,9'-dioctyl-fluorene-2,7-diyls) **(41)**.

The TGA of this polymer showed that the onset of degradation temperature was ca. 340 °C, which indicated that these polymers were thermally stable. The results in Table 19 below show the degradations originate from the elimination of the aryl branched alkyl side chains, because the weight losses observed were consistent with weight percent of the aryl alkyl chains in the polymers.

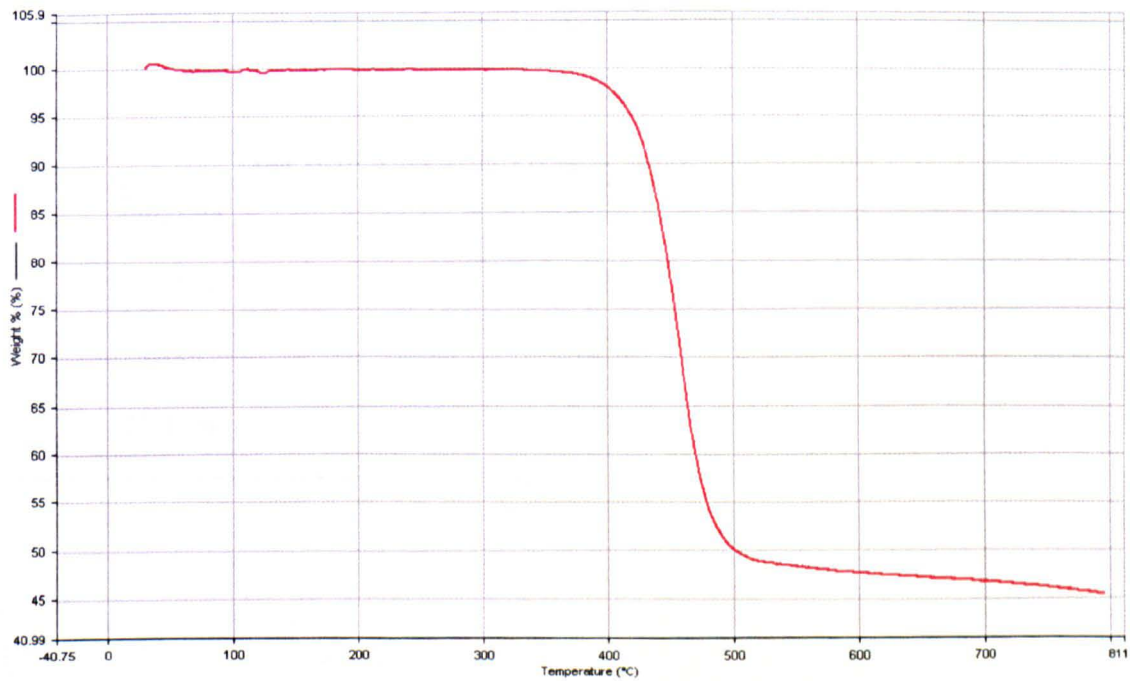

Scheme 67, TGA of Poly-(9,9'-dioctyl-fluorene-2,7-diyls) **(41)**

Table 19, TGA of Poly-(9,9'-dioctyl-fluorene-2,7-diyls) **(41)**

Polymer	Degradation	
	Temp °C	Weight loss (wt%)
P.6a.AK	340	50

Differential Scanning Calorimetry (DSC) analysis

DSC analysis studies of poly-(9,9'-dioctyl-fluorene-2,7-diyls) **(41)** were carried out. The results are outlined in this section.

Scheme 68 on page 236 shows the DSC curves for poly-(9,9'-dioctyl-fluorene-2,7-diyls) **(42)**. Table 20 below shows the results of the DSC analysis of this polymer.

The DSC curve of poly-(9,9'-dioctyl-fluorene-2,7-diyls) **(41)** showed a T_g peak at 108 °C on the first heating scan and a Tm peak at 167°C. This followed counter peaks observed at T_g peak at 137 °C on the cooling scan and on the second heating scan at T_g peak at 167 °C was observed but no T_m peak was seen.

Table 20,DCS of Poly-(9,9'-dioctyl-fluorene-2,7-diyls) **(41)**

Polymer	Tg / °C	Tm / °C
1st Heat	108	167
Cool	137	---
2nd Heat	167	---

Scheme 68, DSC of Poly-(9,9'-dioctyl-fluorene-2,7-diyls) **(41)**

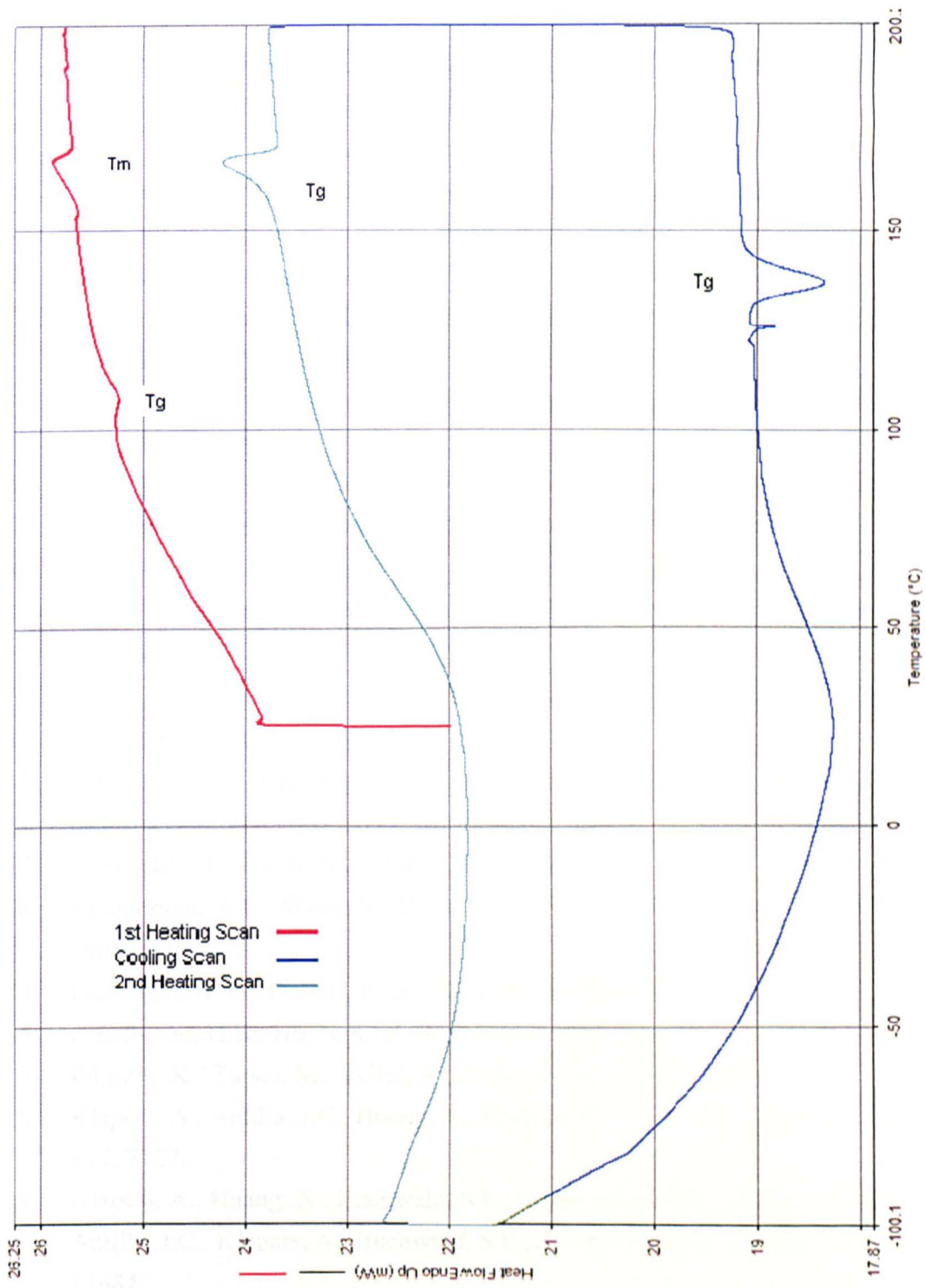

5.8 References

1. Yamamoto, T., Hidershima, C., Suehiro, K., Tashiro, M., Prakash, G.K.S., Olah, G.A.; *J. Org. Chem.*, **1991**, *56*, 6248.
2. Fanta, P.; *Chem. Rev.*, **1946**, *38*, 139.
3. Morrison, R.T., Boyd, R.N.; *Organic Chemistry*, 6th ed., Prentice-Hall International (UK) Ltd., London, **1992**.
4. Patrick, D.A., Boykin, D.W., Wilson, W.D., Tanious, F.A., Spychala, J., Bender, B.C., Hall, J.E., Dykstra, C.C., Ohemeng, K.A., Tidwell, R.R.; *Eur. J. Med. Chem.*, **1997**, *32*, 781.
5. Clayden, J., Greeves, N., Warren, S., Wothers, P.; *Organic Chemistry*, OUP, Oxford, UK, **2001**.
6. Choy, N., Russell, K.C., Alvarez, J.C., Fider, A.; *Tet. Lett.*, **2000**, *41*, 1515.
7. McMurry, J.; *Organic Chemistry*, 5th Ed., Brooks/Cole, USA, **2000**.
8. Tauber, E. *Ber,*. **1981**, *24*, 197.
9. Smith, K., James, D.M., Mistry, A.G., Bye, M.R., Faulkner, D.J., *Tetrahedron*, **1992**, *48*, 7479.
10. Georg, C.D., Paul, C.J.K., Piet, W.N.M.; *Eur. J. Org. Chem.*, **1998**, 359.
11. Lai, Y.H.; *Synth.*, **1981**, 585.
12. a) Clive, D.L.J., Anghoh, A.G., Bennent, S.M.; *J. Org. Chem.*, **1987**, *52*, 1339. b) Jeffery, T., Ferber, B.; *Tet. Lett.*, **2003**, *44*, 193.
13. Bhat, M.V., Kulkarni, S.U.; *Synth.*, **1983**, 249.
14. Zimmerman, S.C., Wang, Y., Bharathi, P., Moore, J.S.; *J. Am. Chem. Soc.*, **1998**, *120*, 2172.
15. Freedman, H. H., Dubois, R. A.; *Tet. Lett.*, **1975**, *38*, 3251.
16. Goodbrand, H.B., Hu, N.X.; *J. Org. Chem.*, **1999**, *64*, 670.
17. Pilgram, K., Zupan, M., Skiles, R.; *J. Het. Chem.*, **1970**, *7*, 629.
18. Klapers, A., Antilla, J.C., Huang, X., Buchwald, S.L.; *J. Am. Chem. Soc.*, **2001**, *123*, 7727.
19. Klapers, A., Huang, X., Buchwald, S.L.; *J. Am. Chem. Soc.*, **2002**, *124*, 7421.
20. Antilla, J.C., Klapars, A., Buchwald, S.L.; *J. Am. Chem. Soc.*, **2002**, *124*, 11684.
21. Maruyama, S., Zhang, Y., Wada, T., Sasabe, H.; *J. Chem. Soc., Perklin Trans. 1*, **1999**, 41.
22. Kiyomori, A., Marcoux, J., Buchwald, S.L.; *Tet. Lett.*, 1999, **40**, 2657.

23. Li, X., Mintz, A.E., Bu, X.R., Zehnder, O., Bosshard, C., Gunter, P.; *Tetrahedron*, **2000**, *56*, 5785.
24. Jian, H., Tour, J.M. ; *J. Org. Chem.*, **2003**, *68*, 5091.
25. Yang, W., Hou, Q., Liu, C., Niu, Y., Huang, J., Yang, R., Yong, C.; *J. Mat. Chem.*, **2003**, *13*, 1351.
26. Jo, J., Chi, C., Hoger, S., Wegner, G., Yoon, D.Y.; *Eur. J. Chem.*, **2004**, *10*, 2681.
27. Nielsen, K.T., Bechgaard, K., Krebs, F.C.; *Macromolecules*, **2005**, *38*, 658.
28. Jensen, K.A., Bechgaard, K., Pederson, C.T.; *Acta Chem. Scand.*, **1972**, *26*, 2913.
29. Yamamoto, T., Hayashi, Y., Yamamoto, A.; *Bull. Chem. Soc. Jpn.*, **1978**, *51*, 2091.
30. Iraqi, A., Wataru, I.; *Chem. Mater.*, **2004**, *16*, 442.
31. Iraqi, A., Wataru, I.; *Synth. Met.*, **2001**, *119*, 159.
32. Iraqi, A., Simmance, T.G., Yi, H., Stevenson, M., Lidzey, D.G.; *Chem. Mater.*, **2006**, *18*, 5789.
33. Pommerehne, J., Vestweber, H., Guss, W., Mahrt, R.F., Bassler, H., Porsch, M., Daub, J.; *Adn. Mater.*, **1995**, *7*, 551.
34. Janietz, S., Bradley, D.D.C., Grell, M., Giebeler, C., Inbasekaran, M., Woo, E.P.; *Appl. Phys. Lett.* **1998**, *73*, 2453.
35. Thomas, K.R.J., Jiann T. Lin, J.T., Tao, Y-T., Chuen, C-H.; *Chem. Mater.*, **2004**, *16*, 5437.
36. Meng, H., Chen, Z-K., Yu, W-L., Pei, J., Liu, X-L., Lai, Y-H., Huang, W.; *Synth. Met.*, **1999**, *100*, 297.
37. Hofman, D., Leibnitz, E., Schmolke, R., Schulz B.; *Angew. Mackromol. Chem.*, **1992**, *204*, 111.
38. Schulz, B., Knochenhauer, G., Brehmer, L., Janietz, S.; *Synth. Met.*, **1995**, *69*, 603.
39. Gaupp, C.L., Reynolds, J.R.; *Macromolecules*, **2003**, *36*, 6305.
40. Sotzing, G.A., Reddinger, J.L., Katritzky, A.R., Soloducho, J., Musgrave, R., Reynolds, J.R.; *Chem. Mater.*, **1997**, *9*, 1578.

6.0 Conclusion

The development of a new applied method to the formation of conjugated polymers incorporating arylated substituents at the 9 position of the carbazole ring has been realized. There have been three novel polymers that have been produced based around the poly-9-(aryl-carbazole-3,6-diyl)s and its co-polymers.

The monomer 3,6-dibromo-9-(4-nitro-phenyl)-*9H*-carbazole (**21**), was prepared successfully by a nueclophillic aromatic substitution reaction and was achieved in good yield. This gave direction to acquire the monomers 3,6-dibromo-9-(bis-[4-(2-butyl-octyloxy)-phenyl]-amino-phen-4-yl)-carbazole (**24**) and 3,6-dibromo-9-(bis-[3,5-bis-(2-ethyl-hexyloxy)-phenyl]-amino-phen-4-yl)-carbazole (**25**) in good overall yields.

The novel development of 3,6-bis-(4,4,5,5-tetramethyl-[1,3,2]dioxaborolan-2-yl)-9-(bis-[4-(2-butyl-octyloxy)-phenyl]-amino-phen-4-yl)-carbazole (**27**) was synthesised by a multistep reaction in a good overall yield.

The polymers (**36** P3.AK, **38** P4.AK and **39** P6.AK) were prepared by palladium catalysed Suzuki coupling type polymerisations of the monomers. The final step in the preparation of these polymers was endcapping, to replace the bromide or boronic ester groups with a dimethyl phenylene rings. In order to further purify the polymers N,N-diethyl-phenyl-azo-thio-formamide (**28**) was used to remove any palladium nanoparticles that may have been present.

Proton and carbon NMR spectroscopy, IR spectroscopy and elemental analysis were utilised to confirm the structures of polymers (**36** P3.AK, **38** P4.AK and **39** P6.AK).

Differential scanning calorimetry (DSC) analysis of polymers (**36** P3.AK, **38** P4.AK and **39** P6.AK) provided their glass transition temperatures (T_g), which ranged from 54 – 148 °C.

Thermalgravimetic analysis (TGA) of the polymers (**36** P3.AK, **38** P4.AK and **39** P6.AK) showed that these class of 3,6-linked aryl polymers were thermally stable with degradations in and around 280-360 °C.

UV-visible absorption spectroscopy analysis of solutions of polymers (36 P3.AK and 38 P4.AK) indicated from the absorption maxima were blue shifted due to 3,6- linked carbazole moiety, and were found to exhibit λ_{max} values in the range 325 – 345 nm. The UV-visible absorption spectroscopy analysis of solution of polymer (39 P6.AK) indicated from the absorption maxima were red shifted due to the effects of the thiodiazole co-monomer, and were found to exhibit λ_{max2} values in the range 420 – 445 nm.

Photoluminescence (PL) spectroscopy analysis of solutions of (36 P3.AK and 38 P4.AK) exhibited blue PL emission, with $\lambda^{em}{}_{max}$ between 410 – 440 nm. The shapes of the PL spectra of (36 P3.AK and 38 P4.AK) were, as for the UV-visible spectra, found to be dependent upon the degree of polymerization. The polymers exhibited varied Stokes shifts between 50 – 110 nm. The smaller Stokes shifts, indicating small structural differences between ground and excited states, whilst the larger values, indicating bigger structural differences between ground and excited states. The Photoluminescence (PL) spectroscopy analysis of solution of (39 P6.AK) exhibited red PL emission, with $\lambda^{em}{}_{max}$ between 590 – 610 nm. The shapes of the PL spectra were, as for the UV-visible spectra, found to be dependent upon the degree of polymerization. The polymers exhibited Stokes shifts between 50 – 60 nm.

Photoluminescence (PL) spectroscopy analysis of thin films of (36 P3.AK and 38 P4.AK) exhibited blue PL emission, with $\lambda^{em}{}_{max}$ between 420 – 450 nm. The polymers exhibited varied Stokes shifts between 50 – 100 nm. The Photoluminescence (PL) spectroscopy analysis of thin films of (39 P6.AK) exhibited red PL emission, with $\lambda^{em}{}_{max}$ between 595 – 610 nm. The polymer exhibited Stokes shifts between 50 – 60 nm.

Fluorescence quantum yield measurements were carried out for the polymers (36 P3.AK, 38 P4.AK). It was found that these polymers exhibited yields of $\Phi_{fl} = 0.164 \pm 0.006$ and $\Phi_{fl} = 0.294 \pm 0.006$ respectively in dichloromethane which were exceptionally high since yield measurements of $\Phi_{fl} = 0.065 \pm 0.006$ in dichloromethane were achieved for poly(9-alkyl-carbazole-3,6-diyl)s. These high fluorescence quantum yields were due to the added aryl groups attached to the polymer which have positively effected the properties of the carbazole.

Cyclic voltammetry (CV) analysis of thin films of (**36** P3.AK, **38** P4.AK and **39** P6.AK) was used to estimate the ionisation potentials (I_p) of these polymers. Polymers (**36** P3.AK, **38** P4.AK and **39** P6.AK) were found to have ionisation potentials between 5.00 – 5.10 eV. This is due to the nitrogen of the triphenylene amine group having the ability to donate its lone pair of electrons into the polymer backbone generating a more electron rich chain, which will have a lower ionisation potential. It should be noted that all of these polymers have lower ionisation potentials than poly(9,9-dioctyl-fluorene-2,7-diyl) (I_p = 5.8 eV), which would indicate easier hole injection into films from ITO electrodes in EL devices. All the polymers (**36** P3.AK, **38** P4.AK and **39** P6.AK) showed a two step reversible oxidation process. The first oxidation was due to the incorporation of the tri phenyl amine aryl group and the second was due to the 3,6-linked carbazole moiety. All of these polymers did not exhibit and reduction process.

The increased electrolytic stability of these new classes of materials with arylated-substituents at their 9- positions should enable their effective use as stable blue light emitting materials in display devices.

7.0 Future Work

This new approach to producing aryl carbazoles has brought forth a new category of compounds that can be synthesised. It would be first plausible to produce these same polymers with the use of 2,7-dibromo-*9H*-carbazole and, 2,7-dibromo-3,6-dimethyl-*9H*-carbazole in the place of 3,6-dibromo-9*H*-carbazole and evaluate there chemical and physical properties. It would be believed that these materials would prosess better conjugation due to the polymerisation taking place in the 2,7 positions of the carbazole and hence developing a better conjugated polymers that would be particularly suitable for wide band gap hosts for fluorescent and phosphorescent dopants.

The next stage in this project would be to commercialise the ability to attach aryl groups to the carbazole 9H position. By using this approach it would be a good direction to yield a compound similar to the first target monomer in which there would be one aryl group attached to the carbazole and to this have an alkoxy group attached in the para position of the aryl group. This should be carried out for all three class of carbazole moieties that have been used ,the 2,7-dibromo-*9H*-carbazole, 2,7-dibromo-3,6-dimethyl-*9H*-carbazole and 3,6-dibromo-9*H*-carbazole and an evaluation into their chemical and physical properties can be undertaken.

Once this has been explored it would be interesting to see the effect that take place on the chemical and physical properties of these aryl carbazoles the alkoxy groups and triaryl amino phenyl groups selectively attached in the orthaand meta positions of the first arly group attached to the carbazole moiety. It can be believed that these polymers would have different assets in regards to the electrochemical properties and and hance and possibly make wide band gap hosts for fluorescent and phosphorescent dopants in LED devices.

The next stage in the project would be to move towards using multiple aromatice compounds like antheracne linked to the carbazole at the 9 position. This anthracene

compound would be hoped to further the electronic properties of the polymer in forming adoubly conjugated system for electron transfer.

This anthracene compound can then be functionalised in the ortha, meta and para positions with alkoxy groups and trialky amine groups and see the effects on chemical and physical properties that this may have on the carbazole moieties.

This new applied method for the formation of aryl carbazoles has opened a vast area where research can be carried to produce a great number of interesting polymers and co-polymers based around the carbazole moiety.

8.0 Appendix I – List of Schemes

Scheme 1	4,4'-Dibromo-2,2'dinitrobiphenyl **(1)**	87
Scheme 2	2,2'-Diamino-4,4'-dibromobiphenyl **(2)**	90
Scheme 3	2,7-Dibromo-*9H*-carbazole **(3)**	93
Scheme 4	2,5-Dibromo-4-nitro-toluene **(4)**	97
Scheme 5	4,4'-Dibromo-2,2'-dinitro-5,5'-dimethylbiphenyl **(5)**	100
Scheme 6	4,4'-Diamino-2,2'-dibromo-5,5'-dimethylbiphenyl **(6)**	102
Scheme 7	2,7-Dibromo-3,6-dimethyl-*9H*-carbazole **(7)**	104
Scheme 8	Synthesis of 3,6-dibromo-*9H*-carbazole **(8)**	106
Scheme 9	1-Iodo-3,5-dimethoxybenzene **(9)**	108
Scheme 10	1-Iodo-3,5-dimethoxybenzene from 3,5-dimethoxy-phenyl-amine **(10)**	109
Scheme 11	5-Iodoresorcinol **(11)**	114
Scheme 12	1,3-Bis-(2-ethyl-hexyloxy)-5-iodobenzene **(12)**	115
Scheme 13	Attempted synthesis of 2,7-dibromo-9-[3,5-bis(2-ethyl-hexyloxy)-phenyl]-*9H*-carbazole **(13)**	120
Scheme 14	Attempted synthesis of 2,7-dibromo-3,6-dimethyl-9-[3,5-bis(2-ethyl-hexyloxy)-phenyl]-*9H*-carbazole **(14)**	127
Scheme 15	Attempted synthesis of 2,7-dibromo-3,6-dimethyl-9-[3,5-dimethoxy-phenyl]-*9H*-carbazole **(15)**	129
Scheme 16	9-[3,5-(Dimethoxy)-phenyl]-*9H*-carbazole **(16)**	132
Scheme 17	Attempted synthesis of 3,6-dibromo-9-[3,5-dimethoxy-phenyl]-*9H*-carbazole **(17)**	135
Scheme 18	Attempted synthesis of 3,6-diiodo-9-[3,5-dimethoxy-phenyl]-*9H*-carbazole **(18)**	136
Scheme 19	9-(3,5-dihydroxy-phenyl)-*9H*-carbazole **(19)**	137
Scheme 20	Attempted synthesis of 9-(3,5-bis(2,2,2-trifluoro-acetoxy)-phenyl)-*9H*-carbazole **(20)**	140
Scheme 21	3,6-Dibromo-9-(4-nitro-phenyl)-*9H*-carbazole **(21)**	142
Scheme 22	3,6-Dibromo-9-(4-amino-phenyl)-*9H*-carbazole **(22)**	143
Scheme 23	4-(2-Butyl-octyloxy-)-1-iodobenzene **(23)**	*148*
Scheme 24	3,6-Dibromo-9-(bis-[4-(2-butyl-octyloxy)-phenyl]-amino-phen-4-yl)-carbazole **(24)**	151
Scheme 25	3,6-Dibromo-9-(bis-[3,5-bis-(2-ethyl-hexyloxy)-phenyl]-amino-phen-4-yl)-carbazole **(25)**	156
Scheme 26	Attempted synthesis of 3,6-Bis-(4,4,5,5-tetramethyl-[1,3,2]dioxaborolan-2-yl)-9-(bis-[3,5-bis-(2-ethyl-hexyloxy)-phenyl]-amino-phen-4-yl)-carbazole **(26)**	158
Scheme 27	3,6-Bis-(4,4,5,5-tetramethyl-[1,3,2]dioxaborolan-2-yl)-9-(bis-[4-(2-butyl-octyloxy)-phenyl]-amino-phen-4-yl)-carbazole **(27)**	162
Scheme 28	Preparation of the palladium scavenger N,N-diethyl-phenyl-azo-thio-formamide **(28)**	166
Scheme 29	Attempted synthesis of poly(9-(bis-[3,5-bis-(2-ethyl-hexyloxy)-phenyl]-amino-phen-4-yl)-carbazole-3,6-diyl) **(34) kumada**	168
Scheme 30	Attempted synthesis of poly(9-(bis-[4-(2-butyl-octyloxy)-phenyl]-amino-phen-4-yl)-carbazole-3,6-diyl) **(35) kumada**	170
Scheme 31	Poly(9-(bis-[4-(2-butyl-octyloxy)-phenyl]-amino-phen-4-yl)-carbazole-3,6-diyl) **(36) Suzuki (a)**	172
Scheme 32	**Proton NMR** for Poly(9-(bis-[4-(2-butyl-octyloxy)-phenyl]-amino-phen-4-yl)-	

carbazole-3,6-diyl) **(36)** 176
Scheme 33 **Carbon NMR** for Poly(9-(bis-[4-(2-butyl-octyloxy)-phenyl]-amino-phen-4-yl)-carbazole-3,6-diyl) **(36)** 177
Scheme 34 **IR** for Poly(9-(bis-[4-(2-butyl-octyloxy)-phenyl]-amino-phen-4-yl)-carbazole-3,6-diyl) **(36)** 179
Scheme 35 **UV** for Poly(9-(bis-[4-(2-butyl-octyloxy)-phenyl]-amino-phen-4-yl)-carbazole-3,6-diyl) **(36)** 181
Scheme 36 **PL** for Poly(9-(bis-[4-(2-butyl-octyloxy)-phenyl]-amino-phen-4-yl)-carbazole-3,6-diyl) **(36)** 183
Scheme 37 **CV** curve for thin films of poly(9-(bis-[4-(2-butyl-octyloxy)-phenyl]-amino-phen-4-yl)-carbazole-3,6-diyl) **(36)** (single scan rate = 90 mV s^{-1}) 185
Scheme 38 **CV** curve for thin films of poly(9-(bis-[4-(2-butyl-octyloxy)-phenyl]-amino-phen-4-yl)-carbazole-3,6-diyl) **(36)** (multiple scan rate = 60 mV s^{-1}) 185
Scheme 39 **TGA** for Poly(9-(bis-[4-(2-butyl-octyloxy)-phenyl]-amino-phen-4-yl)-carbazole-3,6-diyl) **(36)** 187
Scheme 40 **DSC** for Poly(9-(bis-[4-(2-butyl-octyloxy)-phenyl]-amino-phen-4-yl)-carbazole-3,6-diyl) **(36)** 188
Scheme 41 Poly{[9-(bis-[4-(2-butyl-octyloxy)-phenyl]-amino-phen-4-yl)-carbazole-3,6-diyl] -*alt*-[2,5-bis(*p*-phenylene)-1,3,4-oxadiazole]} **(38) Suzuki (b)** 189
Scheme 42 **Proton NMR** for Poly{[9-(bis-[4-(2-butyl-octyloxy)-phenyl]-amino-phen-4-yl)-carbazole-3,6-diyl] -*alt*-[2,5-bis(*p*-phenylene)-1,3,4-oxadiazole]} **(38) Suzuki (b)** 193
Scheme 43 **Carbon NMR** for Poly{[9-(bis-[4-(2-butyl-octyloxy)-phenyl]-amino-phen-4-yl)-carbazole-3,6-diyl] -*alt*-[2,5-bis(*p*-phenylene)-1,3,4-oxadiazole]} **(38) Suzuki (b)** 194
Scheme 44 **IR** for Poly{[9-(bis-[4-(2-butyl-octyloxy)-phenyl]-amino-phen-4-yl)-carbazole-3,6-diyl] -*alt*-[2,5-bis(*p*-phenylene)-1,3,4-oxadiazole]} **(38) Suzuki (b)** 196
Scheme 45 **UV** for Poly{[9-(bis-[4-(2-butyl-octyloxy)-phenyl]-amino-phen-4-yl)-carbazole-3,6-diyl] -*alt*-[2,5-bis(*p*-phenylene)-1,3,4-oxadiazole]} **(38) Suzuki (b)** 199
Scheme 46 **PL** for Poly{[9-(bis-[4-(2-butyl-octyloxy)-phenyl]-amino-phen-4-yl)-carbazole-3,6-diyl] -*alt*-[2,5-bis(*p*-phenylene)-1,3,4-oxadiazole]} **(38) Suzuki (b)** 199
Scheme 47 **CV** curve for thin films of Poly{[9-(bis-[4-(2-butyl-octyloxy)-phenyl]-amino-phen-4-yl)-carbazole-3,6-diyl] -*alt*-[2,5-bis(*p*-phenylene)-1,3,4-oxadiazole]} **(38) Suzuki (b)** (single scan rate = 90 mV s^{-1}) 202
Scheme 48 **CV** curve for thin films of Poly{[9-(bis-[4-(2-butyl-octyloxy)-phenyl]-amino-phen-4-yl)-carbazole-3,6-diyl] -*alt*-[2,5-bis(*p*-phenylene)-1,3,4-oxadiazole]} **(38) Suzuki (b)** (multiple scan rate = 60 mV s^{-1}) 202
Scheme 49 **TGA** for Poly{[9-(bis-[4-(2-butyl-octyloxy)-phenyl]-amino-phen-4-yl)-carbazole-3,6-diyl] -*alt*-[2,5-bis(*p*-phenylene)-1,3,4-oxadiazole]} **(38) Suzuki (b)** 204
Scheme 50 **DSC** for Poly{[9-(bis-[4-(2-butyl-octyloxy)-phenyl]-amino-phen-4-yl)-carbazole-3,6-diyl] -*alt*-[2,5-bis(*p*-phenylene)-1,3,4-oxadiazole]} **(38) Suzuki (b)** 206
Scheme 51 Poly{[9-(bis-[4-(2-butyl-octyloxy)-phenyl]-amino-phen-4-yl)-carbazole-3,6-diyl] -*alt*-[benzo-2,1,3-thiadiazol-4,7-diyl]} **(39) Suzuki (a)** 207
Scheme 52 **Proton NMR** for Poly{[9-(bis-[4-(2-butyl-octyloxy)-phenyl]-amino-phen-4-yl)-carbazole-3,6-diyl] -*alt*-[benzo-2,1,3-thiadiazol-4,7-diyl]} **(39) Suzuki (a)** 211
Scheme 53 **Carbon NMR** for Poly{[9-(bis-[4-(2-butyl-octyloxy)-phenyl]-amino-phen-4-yl)-carbazole-3,6-diyl] -*alt*-[benzo-2,1,3-thiadiazol-4,7-diyl]} **(39) Suzuki (a)** 212
Scheme 54 **IR** for Poly{[9-(bis-[4-(2-butyl-octyloxy)-phenyl]-amino-phen-4-yl)-carbazole-3,6-diyl] -*alt*-[benzo-2,1,3-thiadiazol-4,7-diyl]} **(39) Suzuki (a)** 214
Scheme 55 **UV** for Poly{[9-(bis-[4-(2-butyl-octyloxy)-phenyl]-amino-phen-4-yl)-carbazole-3,6-diyl] -*alt*-[benzo-2,1,3-thiadiazol-4,7-diyl]} **(39) Suzuki (a)** 216

Scheme 56	**PL** for Poly{[9-(bis-[4-(2-butyl-octyloxy)-phenyl]-amino-phen-4-yl)-carbazole-3,6-diyl] -*alt*-[benzo-2,1,3-thiadiazol-4,7-diyl]} **(39) Suzuki (a)**	217
Scheme 57	**CV** curve for thin films of Poly{[9-(bis-[4-(2-butyl-octyloxy)-phenyl]-amino-phen-4-yl)-carbazole-3,6-diyl] -*alt*-[benzo-2,1,3-thiadiazol-4,7-diyl]} **(39) Suzuki (a)** (single scan rate = 90 mV s^{-1})	219
Scheme 58	**CV** curve for thin films of Poly{[9-(bis-[4-(2-butyl-octyloxy)-phenyl]-amino-phen-4-yl)-carbazole-3,6-diyl] -*alt*-[benzo-2,1,3-thiadiazol-4,7-diyl]} **(39) Suzuki (a)** (multiple scan rate = 60 mV s^{-1})	220
Scheme 59	**TGA** for Poly{[9-(bis-[4-(2-butyl-octyloxy)-phenyl]-amino-phen-4-yl)-carbazole-3,6-diyl] -*alt*-[benzo-2,1,3-thiadiazol-4,7-diyl]} **(39) Suzuki (a)**	221
Scheme 60	**DSC** for Poly{[9-(bis-[4-(2-butyl-octyloxy)-phenyl]-amino-phen-4-yl)-carbazole-3,6-diyl] -*alt*-[benzo-2,1,3-thiadiazol-4,7-diyl]} **(39) Suzuki (a)**	223
Scheme 61	Poly-(9,9'-dioctyl-fluorene-2,7-diyls) **(41) Suzuki (b)**	224
Scheme 62	**Proton NMR** for Poly-(9,9'-dioctyl-fluorene-2,7-diyls) **(41) Suzuki (b)**	227
Scheme 63	**Carbon NMR** for Poly-(9,9'-dioctyl-fluorene-2,7-diyls) **(41) Suzuki (b)**	228
Scheme 64	**IR** for Poly-(9,9'-dioctyl-fluorene-2,7-diyls) **(41) Suzuki (b)**	230
Scheme 65	**UV** for Poly-(9,9'-dioctyl-fluorene-2,7-diyls) **(41) Suzuki (b)**	232
Scheme 66	**PL** for Poly-(9,9'-dioctyl-fluorene-2,7-diyls) **(41) Suzuki (b)**	233
Scheme 67	**TGA** for Poly-(9,9'-dioctyl-fluorene-2,7-diyls) **(41) Suzuki (b)**.....	234
Scheme 68	**DSC** for Poly-(9,9'-dioctyl-fluorene-2,7-diyls) **(41) Suzuki (b)**	236

9.0.0 Appendix II – List of Figures

1.1	Diagram showing conjugation of π orbital's	1
1.2	Energy level diagram	2
1.3	Electron transfer in a polymer	4
1.4	Example of a degenerate polymer	6
1.5	Example of non-degenerate polymer	7
1.6	Diagrammatic representation of Metal Oxide Semiconductor	11
1.7	Diagrammatic representation of TFT LCD display	12
1.8	The solar irradiance averaged over three years from 1991 to 1993	14
1.9	Device structure of a hetero-junction PV cell	15
1.10	Diagram of a typical electrochemical cell	17
1.11	Mechanism for Kumada cross-coupling reaction	18
1.12	Mechanism for Stille cross-coupling reaction	20
1.13	Structure of boronic counter parts for Suzuki cross-coupling reaction	21
1.14	Mechanism for Suzuki cross-coupling reaction	22
1.15	A simple monochrome EL device.	25
1.16	The mechanism of EL for a conjugated polymer	27
1.17	Effect of bond length alternation	28
1.18	Energy level diagram	29
1.19	Example of emission of colours achieved by polymers	30
1.20	Electrochemical oxidation of N-alkylcarbazole	35
1.21	Formation of poly(3,6-carbazole)s	36
1.22	OLED / PLED device layout	38
1.23	Electrochemical instability of poly(9-alkyl-*9H*-carbazole-2,7-diyl)s	39
5.1	4,4'-Dibromo-2,2'dinitrobiphenyl **(1)**	89
5.2	2,2'-Diamino-4,4'-dibromobiphenyl **(2)**	92
5.3	2,7-Dibromo-9H-carbazole **(3)**	95
5.4	2,5-Dibromo-4-nitro-toluene **(4)**	99
5.5	4,4'-Dibromo-2,2'-dinitro-5,5'-dimethylbiphenyl **(5)**	101
5.6	4,4'-Diamino-2,2'-dibromo-5,5'-dimethylbiphenyl **(6)**	103
5.7	2,7-Dibromo-3,6-dimethyl-9H-carbazole **(7)**	105
5.8	3,6-Dibromo-9H-carbazole **(8)**	107
5.9	1-Iodo-3,5-dimethoxybenzene **(9)**	110
5.10	5-Iodoresorcinol **(11)**	114
5.11	1,3-Bis-(2-ethyl-hexyloxy)-5-iodobenzene **(12)**	118
5.12	9-[3,5-(Dimethoxy)-phenyl]-*9H*-carbazole **(16)**	134
5.13	9-(3,5-Dihydroxy-phenyl)-*9H*-carbazole **(19)**	139
5.14	3,6-Dibromo-9-(4-nitro-phenyl)-*9H*-carbazole **(21)**	144
5.15	3,6-Dibromo-9-(4-amino-phenyl)-*9H*-carbazole **(22)**	147
5.16	4-(2-Butyl-octyloxy-)-1-iodobenzene **(23)**	150
5.17	3,6-Dibromo-9-(bis-[4-(2-butyl-octyloxy)-phenyl]-amino-phen-4-yl)-carbazole **(24)**	154
5.18	3,6-Dibromo-9-(bis-[3,5-bis-(2-ethyl-hexyloxy)-phenyl]-amino-phen-4-yl)-carbazole **(25)**	157
5.19	3,6-Bis-(4,4,5,5-tetramethyl-[1,3,2]dioxaborolan-2-yl)-9-(bis-[4-(2-butyl-octyloxy)-phenyl]-amino-phen-4-yl)-carbazole **(27)**	164
5.20	*Preparation of the palladium* scavenger N,N-diethyl-phenyl-azo-thio-formamide **(28)**	167
5.21	Poly(9-(bis-[4-(2-butyl-octyloxy)-phenyl]-amino-phen-*4-yl)-carbazole-3,6-diyl*) **(36)**	

	Suzuki (a)	174
5.22	Poly{[9-(bis-[4-(2-butyl-octyloxy)-phenyl]-amino-phen-4-yl)-carbazole-3,6-diyl] -*alt*-[2,5-bis(*p*-phenylene)-1,3,4-oxadiazole]} **(38) Suzuki (b)**	191
5.23	Poly{[9-(bis-[4-(2-butyl-octyloxy)-phenyl]-amino-phen-4-yl)-carbazole-3,6-diyl] -*alt*-[benzo-2,1,3-thiadiazol-4,7-diyl]} **(39) Suzuki (a)**	209
5.24	Poly-(9,9'-dioctyl-fluorene-2,7-diyls) **(41) Suzuki (b)**	226

10.0.0 Appendix III – List of Mechanisms

1	4,4'-Dibromo-2,2'dinitrobiphenyl **(1)**	88
2	2,2'-Diamino-4,4'-dibromobiphenyl **(2)**	91
3	2,7-Dibromo-9H-carbazole **(3)**	94
4	2,5-Dibromo-4-nitro-toluene **(4)**	98
5	1-Iodo-3,5-dimethoxybenzene **(9)**	108
6	1-iodoresorcinol **(11)** using hydroiodic acid	112
7	5-Iodoresorcinol **(11)**	113
8	1,3-Bis-(2-ethyl-hexyloxy)-5-iodobenzene **(12)**	117
9	Attempted synthesis of 2,7-dibromo-9-[3,5-bis(2-ethyl-hexyloxy)-phenyl]-*9H*-carbazole **(13)**	125
10	9-[3,5-(Dimethoxy)-phenyl]-*9H*-carbazole **(16)**	133
11	9-(3,5-Dihydroxy-phenyl)-*9H*-carbazole **(19)**	138
12	3,6-Dibromo-9-(4-nitro-phenyl)-*9H*-carbazole **(21)**	143
13	4-(2-Butyl-octyloxy-)-1-iodobenzene **(23)**	149
14	3,6-Dibromo-9-(bis-[4-(2-butyl-octyloxy)-phenyl]-amino-phen-4-yl)-carbazole **(24)**	152
15	3,6-Bis-(4,4,5,5-tetramethyl-[1,3,2]dioxaborolan-2-yl)-9-(bis-[4-(2-ethyl-hexyloxy)-phenyl]-amino-phen-4-yl)-carbazole **(26)**	161
16	3,6-Bis-(4,4,5,5-tetramethyl-[1,3,2]dioxaborolan-2-yl)-9-(bis-[4-(2-butyl-octyloxy)-phenyl]-amino-phen-4-yl)-carbazole **(27)**	163
17	poly(9-(bis-[3,5-bis-(2-ethyl-hexyloxy)-phenyl]-amino-phen-4-yl)-carbazole-3,6-diyl) **(34)** **kumada**	169

11.0.0 Appendix IV – List of Tables

1	Coupling reaction attempted with the use of different ligands	130
2	**UV** for Poly(9-(bis-[4-(2-butyl-octyloxy)-phenyl]-amino-phen-4-yl)-carbazole-3,6-diyl) **(36)**	182
3	**PL** for Poly(9-(bis-[4-(2-butyl-octyloxy)-phenyl]-amino-phen-4-yl)-carbazole-3,6-diyl) **(36)**	183
4	**CV** curve for thin films of poly(9-(bis-[4-(2-butyl-octyloxy)-phenyl]-amino-phen-4-yl)-carbazole-3,6-diyl) **(36)** (single scan rate = 90 mV s^{-1})	186
5	**TGA** for Poly(9-(bis-[4-(2-butyl-octyloxy)-phenyl]-amino-phen-4-yl)-carbazole-3,6-diyl) **(36)**	188
6	**DSC** or Poly(9-(bis-[4-(2-butyl-octyloxy)-phenyl]-amino-phen-4-yl)-carbazole-3,6-diyl) **(36)**	187
7	**UV** of Poly{[9-(bis-[4-(2-butyl-octyloxy)-phenyl]-amino-phen-4-yl)-carbazole-3,6-diyl] -*alt*-[2,5-bis(*p*-phenylene)-1,3,4-oxadiazole]} **(38)**	198
8	**PL** of Poly{[9-(bis-[4-(2-butyl-octyloxy)-phenyl]-amino-phen-4-yl)-carbazole-3,6-diyl] -*alt*-[2,5-bis(*p*-phenylene)-1,3,4-oxadiazole]} **(38)**	200
9	**CV** curve for thin films of poly{[9-(bis-[4-(2-butyl-octyloxy)-phenyl]-amino-phen-4-yl)-carbazole-3,6-diyl]-*alt*-[2,5-bis(*p*-phenylene)-1,3,4-oxadiazole]} **(38)** (single scan rate = 90 mV s^{-1})	203
10	**TGA** of Poly{[9-(bis-[4-(2-butyl-octyloxy)-phenyl]-amino-phen-4-yl)-carbazole-3,6-diyl] -*alt*-[2,5-bis(*p*-phenylene)-1,3,4-oxadiazole]} **(38)**	203
11	**DSC** of Poly{[9-(bis-[4-(2-butyl-octyloxy)-phenyl]-amino-phen-4-yl)-carbazole-3,6-diyl] -*alt*-[2,5-bis(*p*-phenylene)-1,3,4-oxadiazole]} **(38)**	205
12	**UV** of Poly{[9-(bis-[4-(2-butyl-octyloxy)-phenyl]-amino-phen-4-yl)-carbazole-3,6-diyl] -*alt*-[benzo-2,1,3-thiadiazol-4,7-diyl]} **(39)**	216
13	**PL** of Poly{[9-(bis-[4-(2-butyl-octyloxy)-phenyl]-amino-phen-4-yl)-carbazole-3,6-diyl] -*alt*-[benzo-2,1,3-thiadiazol-4,7-diyl]} **(39)**	218
14	**CV** curve for thin films of poly{[9-(bis-[4-(2-butyl-octyloxy)-phenyl]-amino-phen-4-yl)-carbazole-3,6-diyl] -*alt*-[benzo-2,1,3-thiadiazol-4,7-diyl]} **(39)** (single scan rate = 90 mV s^{-1})	220
15	**TGA** of Poly{[9-(bis-[4-(2-butyl-octyloxy)-phenyl]-amino-phen-4-yl)-carbazole-3,6-diyl] -*alt*-[benzo-2,1,3-thiadiazol-4,7-diyl]} **(39)**	222
16	**DSC** of Poly{[9-(bis-[4-(2-butyl-octyloxy)-phenyl]-amino-phen-4-yl)-carbazole-3,6-diyl] -*alt*-[benzo-2,1,3-thiadiazol-4,7-diyl]} **(39)**	222
17	**UV** of Poly-(9,9'-dioctyl-fluorene-2,7-diyls) **(41)**	232
18	**PL** of Poly-(9,9'-dioctyl-fluorene-2,7-diyls) **(41)**	233
19	**TGA** of Poly-(9,9'-dioctyl-fluorene-2,7-diyls) **(41)**	234
20	**DCS** of Poly-(9,9'-dioctyl-fluorene-2,7-diyls) **(41)**	235